Influence of Advanced Coated Tools on Machinability Characteristics of Incoloy 825

Dissertation submitted to the

National Institute of Technology Rourkela

in partial fulfillment of the requirements

of the degree of

Doctor of Philosophy

in

Mechanical Engineering

by

Aruna Thakur
(Roll number: 512ME1040)
under the supervision of
Prof. S. Gangopadhyay
and
Prof. K.P. Maity

January 2016

Department of Mechanical Engineering
National Institute of Technology Rourkela

Mechanical Engineering
National Institute of Technology Rourkela

Certificate of Examination

Roll Number: 512ME1040

Name: Aruna Thakur

Title of Dissertation: Influence of Advanced Coated Tools on Machinability characteristics of Incoloy 825

We the below signed, after checking the dissertation mentioned above and the official record book (s) of the student, hereby state our approval of the dissertation submitted in partial fulfillment of the requirements of the degree of Doctor of Philosophy in Mechanical Engineering at National Institute of Technology Rourkela. We are satisfied with the volume, quality, correctness, and originality of the work.

K.P. Maity
Co-Supervisor

S. Gangopadhyay
Principal Supervisor

S. K. Sahoo
Member (DSC)

M. Masanta
Member (DSC)

B. B. Verma
Member (DSC)

Professor S. K. Choudhury
IIT Kanpur
Examiner

P. K. Ray

Chairman (DSC)

Mechanical Engineering
National Institute of Technology Rourkela

Dr. Soumya Gangopadhyay
Assistant Professor

January 22, 2016

Supervisor's Certificate

This is to certify that the work presented in this dissertation entitled "*Influence of Advanced Coated Tools on Machinability Characteristics of Incoloy 825*" by "*Aruna Thakur*", Roll Number 512ME1040, is a record of original research carried out by him/her under my supervision and guidance in partial fulfillment of the requirements of the degree of *Doctor of Philosophy* in *Mechanical Engineering*. Neither this dissertation nor any part of it has been submitted for any degree or diploma to any institute or university in India or abroad.

Supervisor's Signature
S. Gangopadhyay

Mechanical Engineering
National Institute of Technology Rourkela

January 22, 2016

Supervisors' Certificate

This is to certify that the work presented in this dissertation entitled " *Influence of Advanced Coated Tools on Machinability Characteristics of Incoloy 825*" by "*Aruna Thakur*", Roll Number 512ME1040, is a record of original research carried out by him/her under our supervision and guidance in partial fulfillment of the requirements of the degree of *Doctor of Philosophy* in *Mechanical Engineering*. Neither this dissertation nor any part of it has been submitted for any degree or diploma to any institute or university in India or abroad.

---	---
K.P.Maity	*S. Gangopadhyay*
Co-Supervisor	Principal Supervisor

Declaration of Originality

I, *Aruna Thakur*, Roll Number *512me1040* hereby declare that this dissertation entitled "Influence of Advanced Coated Tools on Machinability Characteristics of Incoloy 825" represents my original work carried out as a doctoral student of NIT Rourkela and, to the best of my knowledge, it contains no material previously published or written by another person, nor any material presented for the award of any other degree or diploma of NIT Rourkela or any other institution. Any contribution made to this research by others, with whom I have worked at NIT Rourkela or elsewhere, is explicitly acknowledged in the dissertation. Works of other authors cited in this dissertation have been duly acknowledged under the section "References". I have also submitted my original research records to the scrutiny committee for evaluation of my dissertation.

I am fully aware that in case of any non-compliance detected in future, the Senate of NIT Rourkela may withdraw the degree awarded to me on the basis of the present dissertation.

January 22, 2016

NIT Rourkela Aruna Thakur

Acknowledgement

I want to express my deepest regards and gratitude to my supervisor **Dr. S. Gangopadhyay** for his invaluable guidance, constant motivation and kind co-operation throughout the period of work which has been instrumental in the success of thesis.

I would like to thank **Prof. K. P. Maity**, co-supervisor who encouraged me a lot for this research.

I am extremely thankful to **Prof. S. S. Mahapatra,** Head of the Department, Mechanical Engineering, for providing invaluable departmental facilities without which experimental work would not have been possible.

I would also like to express my sincere gratitude to **Prof. S.K. Sahoo** and **Dr. M. Masanta** of the Department of Mechanical Engineering and **Prof. S.C. Mishra** of the Department of Metallurgical & Materials Engineering, for their morale support and providing the necessary facilities for my research work.

I would also take this opportunity to thank **Mr. Arabinda Khuntia, Mr. G.S. Reddy and Mr. Kunal Nayak**, Technical Assistants of Production Engineering Laboratory and Department of Mechanical Engineering for carrying out experimental work. I am also grateful to all the staff of Central Workshop for their kind cooperation during my research work. I also express my sincere thanks to the staff members of Mechanical Engineering Department office for their timely help and prompt response.

I must express my sincere thanks to the Ministry of Human Resource and Development, Govt. of India, for providing the necessary grants required for the purchase materials and tools.

I would also like to express my special thanks to my co-researchers **Aveek Mohanty, Arun Jacob, Sabana Azim**, **Gangadharudu Talla** for their constant help and advice throughout the year for successful completion of my experiments and thesis.

Last but not the least, I wish to express my sincere thanks to all those who directly or indirectly helped me at various stages of this work. My little daughter truly deserves a special mention here, since she, even at her tender age, allowed me to pursue my PhD degree. I owe great amount of debt to my parents, family and friends for their inestimable advices and constant encouragement. Without god's grace nothing could have been possible, thanks to almighty for showing me right path.

January 22, 2016 Aruna Thakur

NIT Rourkela Roll Number: 512ME1040

List of symbols

V_c	cutting speed, m/min
F	feed, mm/rev
a_p	depth of cut, mm
t	machining duration, s
H	continuous part of the serrated chip, μm
δ	shear band thickness, μm
F_c	cutting force, N
F_t	thrust force, N
F_f	feed force, N
F_r	radial force, N
f_{ch}	chip segmentation frequency, Hz
L_{ch}	chip-tool contact length, mm
ϒ	orthogonal rake angle
h_{ch}	equivalent chip thickness, μm
Φ_1	saw-tooth angle, degree
P_c	saw-tooth distance, μm
T	temperature, ℃
μ_{app}	apparent coefficient of friction
H	maximum thickness of sawtooth chip, μm
HV	Vickers microhardness
VB	average flank wear, mm
R_a	surface roughness (centre line average), μm
θ	Bragg angle in X-ray diffraction
β_r	integral breadth of the peak, rad
κ	constant (0.9)
λ	wave length of the X-ray radiation (0.15418 nm)
Z	chip reduction coefficient
t_c	cut chip thickness
t_o	uncut chip thickness
ϕ_p	Principal cutting edge angle
Φ	approach angle

Abstract

With vast application of nickel-based super alloys in strategic fields, it has become increasingly necessary to evaluate the performance of advanced cutting tools for machining such alloys. In order to have elementary knowledge on machinability characteristics of Incoloy 825 which was so far unknown, in the initial stage of experiment, tool wear and its mechanism, chip characteristics and surface integrity during dry machining were first studied using uncoated and chemical vapour deposition (CVD) multilayer TiN/TiCN/Al_2O_3/ZrCN coated tool with different cutting speeds. The coated tool could not improve surface finish, but outperformed its uncoated counterpart in terms of other aspects.

In the second stage of the study, the primary objective was to recommend suitable cutting tool for machining Incoloy 825. Detailed study was undertaken using commercially available uncoated, CVD and physical vapour deposition (PVD) coated carbide tools, the performance of which was comparatively evaluated in terms of surface roughness, cutting temperature, cutting force, coefficient of friction, tool wear and its mechanism during dry machining. Effect of cutting speed (V_c) and feed (f) was also studied. Although, CVD coated tool was not useful in decreasing surface roughness and temperature compared to uncoated one, significant decrease in cutting force and tool wear could be achieved with the same coated tool even under high cutting parameters (V_c=124 m/min and f=0.2 mm/rev). On the other hand, PVD coated tool consisting of alternate layers of TiAlN/TiN outperformed the other tools in terms of all machinability characteristics that have been studied. This might be attributed to excellent anti-friction and anti-sticking property of TiN and good toughness which is a salient feature of PVD technique as well as multilayer configuration, in combination with thermally resistant TiAlN phase.

In the final stage of the research work, the feasibility of best performing PVD coated tool was evaluated under environment-friendly dry machining condition in comparison with uncoated tool under conventional flood cooling and minimum quantity lubrication (MQL). Although temperature obtained with PVD coated tool under dry machining has always been significantly more than wet environment, the same coated tool remarkably brought down cutting force, surface roughness and tool wear under dry environment. The results achieved under both rough and finish modes of machining clearly established the use of PVD coated tool under dry environment as a sustainable strategy for achieving green machining of nickel-based super alloys.

Keywords: Machining; Incoloy 825; CVD; PVD; Tool Wear; Chip Characteristics; Surface Integrity; MQL.

Contents

List of tables

List of figures

Chapter 1

Introduction

In recent times, nickel-based super alloys found extensive applications primarily in critical aerospace engine components like gas turbines. Owing to their admirable properties such as fatigue strength, thermal stability and resistance to corrosion under severe environment, in fact, 50% by weight of aerospace engine is made up of nickel-based super alloys (Ezugwu *et al.*, 2003; M'Saoubi *et al.*, 2015; Thakur and Gangopadhyay, 2016). Other areas of applications have been provided in detail in Table 1.1[1,2].

Table 1.1: Application of nickel-based super alloys in different industries[1, 2].

Application	Specific component of nickel-based super alloy
Marine industry	Marine fixtures, marine and industrial gas turbine engine combustors, marine propeller shafts
Nuclear industry	Spent nuclear fuel element recovery, nuclear fuel reprocessing, nuclear reactor springs & bolts.
Chemical industry	Food processing equipment, shipping drums for chemicals, chemical processing equipment, furnace muffles, heat exchanger tubing, petrochemical flares and process piping.

Although advanced processes including precision casting, near net-shape manufacturing have been developed, machining is still considered as one of the final steps of manufacturing process by which desired size, shape, surface finish and other functional features of such components are accomplished by gradual removal of material from the workpiece in the form of chips by shear deformation with the aid of a cutting tool. The machining system comprises of cutting tool, workpiece and machine tool. Evaluation of workpiece-tool interaction is of paramount significance since it directly affects overall performance of machining. At the same time, selection of cutting parameters such as cutting speed (V_c), feed (f) and depth of cut (a_p) largely depends on the material properties of cutting tool and workpiece both. However, some of the major challenges encountered during machining processes include generation of considerable amount of stress and

[1]http://www.hpalloy.com/Alloys/corrosionResistant.html, viewed on 18.Jan.2016.

[2]http://www.specialmetals.com/assets/documents/pcc-8063-sm-quick-reference-guide-v07.pdf, viewed on 18.Jan.2016.

temperature which result in lowering of tool life, increase in power consumption, while adversely affecting surface integrity and thus fatigue durability of the machined component. Situation goes beyond acceptable limit especially when improper cutting parameters are selected. Furthermore, maintenance of clean and hazard-free environment is also difficult since machining processes are often associated with formation of different types of chips and harmful influence of cutting fluid. Therefore, recent research work worldwide is focused on development of advanced strategies for machining of nickel-based super alloys so that superior surface quality can be achieved while maintaining reasonably high productivity and at the same time environmental load can be curtailed. In order to accomplish these objectives, through understanding of the mechanical properties of different grades of nickel-based super alloys along with their chemical composition is essential.

1.1 Nickel-based super alloys

The major advantages of nickel-based super alloys include their resistance to thermal deformation and corrosion. Iron, chromium and cobalt are typically used as major alloying elements. In addition to these, other elements such as molybdenum, niobium, copper, titanium, aluminium and tungsten along with small quantity of carbon, magnesium, zirconium etc. are present in different grades of nickel-based super alloys, the properties and composition of which have been provided in Table 1.2.

Table 1.2: Composition and mechanical properties of different commercial grades of nickel-based super alloy (Thakur and Gangopadhyay, 2016).

Different grades	Composition	Properties
Inconel 718	Ni 54.48, Cr 17.50, Fe 22.3, Nb 4.90, Al 0.66, Ti 0.96.	Precipitation hardenable, high creep-rupture strength at high temperatures to about 700°C and excellent strength. Precipitates of primary niobium carbide (NbC), titanium carbide (TiC) disc-shaped γ′′ precipitates (Ni_3Nb) and needle-like precipitates of δ (Ni_3Nb) present.
Inconel 625	Ni-60.96, Cr-21.7, Fe-3.9, Mo-8.8, Nb-3.9, C-0.05, Mn-0.14, Si-0.15, Al-0.17, Ti-0.23, Co-0.08.	Precipitation hardening in this alloy at high elevated temperatures, mechanical properties has been attributed to the heavy precipitation of intermetallic phases γ′′ and Ni_2(Cr, Mo).

Inconel 100	Ni 60, Cr 10, Co 15, Mo 3, Al 5.5, Ti 4.7, C 0.18, B 0.014, Zr 0.06.	Precipitation hardenable, high rupture strength through 870 ºC. The high percentages of titanium, aluminum and the low refractory metal increase strength to density ratio.
Incoloy 825	Ni 37.1, Fe 32.2, Cr 22.8, Mo 3.24, Cu 2.07, Ti 0.859, C 0.0155.	Good resistance to pitting, inter-granular corrosion, chloride-ion stress-corrosion cracking, and general corrosion in a wide range of oxidizing and reducing environments.
IN-713LC	Ni 74.2, Cr 12.6, Mo 4.9, Nb 1.96, Al 5.7, Zr 0.1, Ti 0.63, C 0.047, B 0.007.	Good combination of tensile and creep-rupture properties as a result of gamma-prime strengthening enhanced by solid solution and grain-boundary strengthening, good castability.
Udimet 720LI	Ni 57.4, Cr 16, Co 15, Mo 3, Ti 5, Al 2.5, W 1, C 0.1.	Solid solution strengthened with tungsten and molybdenum and precipitation-hardened with titanium and aluminum. High strength, excellent impact strength retention at elevated temperatures, good oxidation and corrosion resistance and high degree of work hardening.
FGH95	Ni 62.5, Cr 12.98, Co 8.00, Nb, 3.50, Al 3.48, Ti 2.55, W 3.40 , Mo 3.40, C 0.060, B 0.012.	Precipitation-hardened having higher tensile and yield strength at 650°C. A compact structure after hot isostatic pressing (HIP) consisting of coarse gamma prime phase precipitated along previous particle boundaries (PPB) appear in the grain.
ME-16	Ni 56.3, Cr 10.4, Co 20.5, Al 3.1, Ti 2.6, W 3, Ta 1.4, Mo 1.3, Nb 1.4.	Good strength and creep resistance at high temperatures (600-800°C). Good resistance to fatigue crack initiation at the lower temperatures (300-600°C). Can maintain strength and lower density at elevated temperature.
RR1000	Ni 52.4, Cr 15, Co 18.5, Mo 5, Ti 3.6, Al 3, Ta 2, Hf 0.5, C 0.03.	Solid solution strengthened with chromium, molybdenum and cobalt. Good strength, good toughness, creep resistance, good oxidation and corrosion resistance at high temperature.
Nimonic C-263	Ni 51.0, Cr 20.0, Co 20.0, Mo 5.8, Ti 2.2, Al 0.5.	A readily weldable, age-hardenable superalloy with excellent strength, ductility and corrosion resistance up to around 850°C. Molybdenum for solid-solution strengthening.

Nimonic 105	Ni 54.0, Co 20.0, Cr 15.0, Mo 5.0, Al 4.7, Ti 1.3.	An age-hardenable superalloy with increased aluminum for improved oxidation-resistance and strength, and high creep-rupture properties up to around 950°C. Strengthened by additions of molybdenum, aluminum and titanium.
Nimonic 75	Ni 80.5, Cr 19.5.	Good corrosion, oxidation and heat resistance, high-temperature strength.
Nimonic 80 A	Ni 76.0, Cr 19.5, Ti 2.4, Al 1.4.	An age-hardenable creep-resistant alloy for service at temperatures up to around 815°C.
Hastelloy C-2000	Ni 47, Cr 22, Fe 18, Mo 9, Co 1.5, W 0.6.	Localized corrosion resistance, good resistance to hot acids and stress-corrosion cracking.
Haynes 282	Ni 57 Cr 20 Co 10 Mo 8.5 Ti 2.1 Al 1.5 Fe 1.5 Mn 0.3 Si 0.15 C 0.06 B 0.005	γ′ precipitation strengthened nickel-based super alloy along with excellent creep properties, fabricability and thermal stability.

Careful study of Table 1.2 would reveal some of the common properties which include high resistance to shock and creep at elevated temperature and corrosion, high hot hardness, tensile, fatigue and yield strength. While these properties make nickel-based super alloys highly suitable for a wide domain of applications detailed in Table1.1, on the other hand, the same properties in combination with low thermal conductivity, high rate of strain hardening, presence of hard and abrasive particles in the microstructure and high chemical affinity make such alloys difficult to machine. Therefore, attempts should be made to improve the machinability characteristics of nickel-based super alloys for which role of tool is very important.

1.2 Development in cutting tool materials

During machining nickel-based super alloys, the cutting tools are subjected to extreme level of mechanical and thermal stress leading to accelerated tool wear. Therefore, selection of cutting tool is an important factor when machining nickel-based super alloys. Tool material should possess sufficient wear resistance, thermal stability, good combination of hardness and toughness, chemical stability and thermal shock resistance.

1.2.1 High speed steel (HSS)

HSS is an alloy of higher percentage of carbon and iron along with alloying element like W, Mo, Cr, V and Co. It exhibits 8 to 9 GPa (above 60 HRC) hardness at room temperature, but starts softening beyond temperature at around 600 °C and hardness is reduced to 1.5 to

1.8 GPa at 700 °C. It has excellent fracture toughness, fatigue resistance and can easily be shaped. HSS is inexpensive compared to other tool materials, but it has limitation of cutting parameters. HSS can work at low cutting speed range of 30-50 m/min owing to poor wear resistance along with low thermal and chemical stability.

1.2.2 Cemented carbide

One of the widely used tool materials in the modern industries, cemented carbide tool is manufactured by compacting and sintering hard tungsten carbide (WC) in a powder form mixed with cobalt (Co) binder. Cemented carbide possesses high fatigue and transverse rupture strength, high compressive strength, high stiffness and hot hardness. It exhibits lower friction and is chemically stable. It has strong metallic characteristics with good electrical and thermal conductivities. It can operate at higher cutting speed than HSS, but are more brittle and expensive than HSS. Cemented carbide tools are classified into three grades; P, M and K according to ISO designation. P grade carbide, sometimes called mixed carbide, consists of TiC, TaC and NbC for enhancing resistance to diffusion and stability of WC. These grades are suitable for machining different grades of steel. K grade which comprises of only WC and Co is recommended for machining cast iron and nonferrous alloys. The properties of both P and K grades are included in M grade. Each grade within a group is assigned a number to represent its position from maximum hardness to maximum toughness (higher the number, tougher the tool). P grades are rated from P01 to P50, M grades from M10 to M40 and K grades from K01 to K40. The performance of carbide cutting tool is dependent on the percentage of Co and grain size of carbide particles.

1.2.3 Ceramic

Ceramics are non-metallic materials and can withstand extreme temperature during machining. The capability to retain the stiffness and hardness of the material at elevated temperature as high as 1000 °C is the major advantage of ceramic tools. Basically two types of ceramic tool, available for commercial machining purpose, are given below.

- Alumina-based ceramics
- Silicon nitride-based ceramics

1.2.4 Cermets

Cermets are ceramic materials in a metal binder. It consists of TiC, TiN or TiCN hard particles held together with the help of softer binder like Co and/or Ni, Mo. Different hard phases of Mo_2C, WC and TaC are also found in cermets. It is less susceptible to diffusion wear than WC and has more favourable frictional characteristics. However, they have a

lower resistance to fracture, lower thermal conductivity and a higher thermal expansion coefficient than WC and are more sensitive to feed. It can operate at higher cutting speed than cemented carbide tool. Owing to excellent thermal stability and hot hardness, ceramic and cermets cutting tools have good potential in machining nickel-based super alloys.

1.2.5 Cubic boron nitride (cBN)

Polycrystalline cubic boron nitride (cBN) is a material with excellent hot hardness that can be used at very high cutting speed. It also exhibits good toughness and thermal shock resistance. Modern cBN grades are ceramic composites with a cBN content of 40-65%. The ceramic binder imparts wear resistance to the cBN, which is otherwise prone to chemical wear. Grade with higher content of cBN, with 85% to almost 100%, is also available. These grades may have a metallic binder to improve their toughness.

1.3 Machinability

Machinability which roughly and qualitatively specifies the degree of ease by which a work material can be machined, was quantitatively defined in earlier times in terms of machinability index or rating as follows:

$$Machinability\ index = \frac{\text{Cutting speed of machining work material providing 60 minutes of tool life}}{\text{Cutting speed of machining standard work material providing 60 minutes of tool life}}$$

However, this definition suffers from a great deal of limitations since, it considers only cutting speed and tool life. It has been observed that a particular work material under a constant cutting speed can result in different values of tool life which also depends on initial condition of the workpiece material. This is in turn impacted by its processing routes, prior thermal or mechanical treatments (if any) and resulting change in microstructure, phase, physical and mechanical properties. Moreover, following phenomena also dictate the performance of machining.

- Cutting forces
- Cutting temperature
- Chip morphology
- Surface roughness

In recent times, surface finish is replaced by a broader term called surface integrity which influences functional performance of a machined component such as fatigue durability.

1.3.1 Tool wear

One of the most important and widely used machinability characteristics is tool life for any cutting tool. Much research attention has been directed towards enhancing tool life which can be improved by proper selection of machining parameters, tool material, use of coolant, tool coating etc. It is very important to understand the various mechanisms of tool wear for the improvement of tool life. Tool wear refers to the degradation of cutting or clearance surface, reduction in some of the mechanical properties of the tool and its fracture (Grzesik, 2008; Zhu *et al.*, 2013). Various modes by which tool failure takes place during machining have been shown in Fig. 1.1.

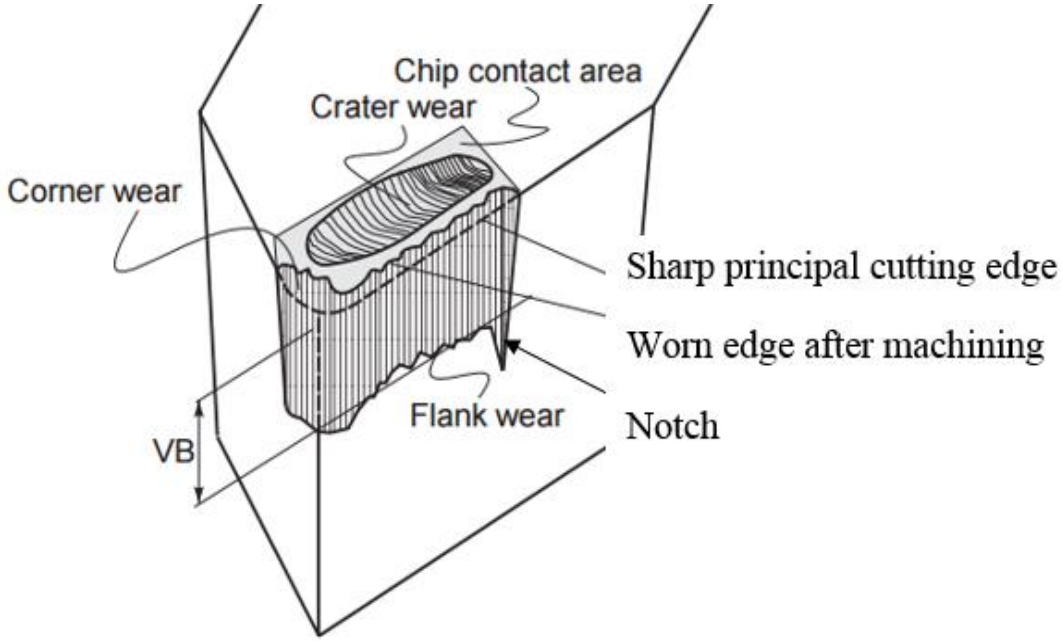

Fig. 1.1: Modes of tool failure[1].

1.3.2 Tool wear mechanism

Different mechanisms of tool wear responsible for such modes of tool failure, shown in Fig.1.2, are discussed as follows.

[1] http://me.emu.edu.tr/me364/ME364_cutting_wear.pdf. Viewed on 21.Jan.2016.

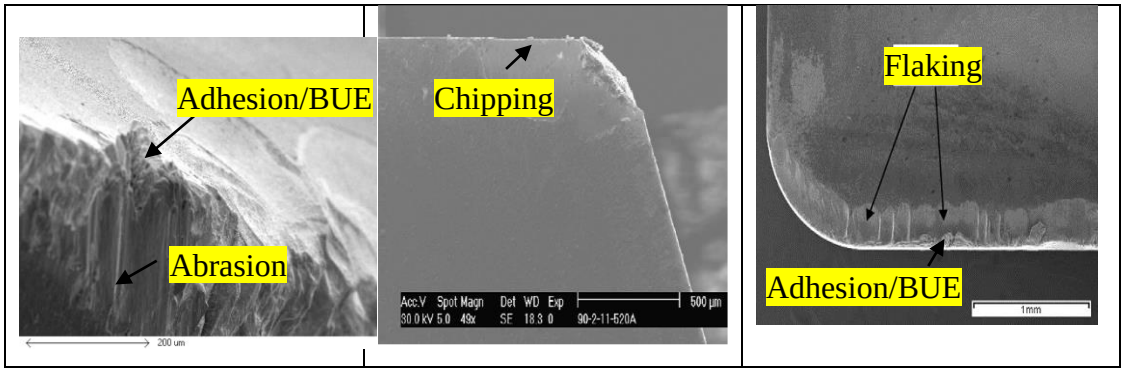

Fig. 1.2: Representative image of various wear mechanism (Biksa *et al.*, 2010; Xue and Chen, 2011; Zhu *et al.*, 2013).

Adhesion and built-up edge (BUE)

High frictional rubbing, pressure and temperature generated at the cutting zone lead to adhesion of workpiece material to the tool surface forming built-up layer (BUL). With progression of machining, growth of adhered layer (BUL) takes place in the form of BUE as shown in Fig. 1.2. This is especially promoted under low cutting speed owing to high chip-tool interface friction. Under the action of machining forces, such BUE gets dislodged from the cutting edge or rake face taking a small chunk of tool material and thus leaves a crater or results in edge chipping. Loss of tool material from the face in an irregular pattern is also termed as attrition wear.

Abrasion

Flank wear is usually caused by abrasion due to frictional rubbing between machined surface and flank face of the tool. Presence of hard abrasive particles in work material is responsible for such wear mechanism. As a result, deep and multiple scratches/scores are perceived on the flank face of the tool as indicated in Fig.1.2.

Diffusion

A smooth cutting edge of tool along with dark burned appearance near to the cutting edge will be characterized as diffusion wear. Machining under very high cutting temperature leads to diffusion wear in which the atoms from harder (either from workpiece or tool materials) diffuse into the softer material. Owing to intimate sliding contact between chips and rake face, temperature at their interface is high. This causes diffusion of metal atoms form harder tool material into softer work material. This leaves a crater at the rake surface. Sometimes, diffusion of work material may also take place into the tool, thus wearing the latter.

Chipping

Chipping is observed on cutting edge and nose in irregular wear pattern which is depicted in Fig.1.2. In addition to dislodgement of BUE, chipping also occurs when the cutting edge is too sharp for the application, cutting pressure (stress) on the edge is very high and significant vibration of machining components or tool fixtures, large tool overhang take place.

Edge depression/bulges

Plastic deformation due to large localized stress at the cutting edge results in edge depression and bulging. It further enhances the deformation and escalation of cutting temperature. As a consequence, the condition of cutting edge further worsens finally leading to edge wipe-out. This mode of tool failure is common for hard and heat resistant alloys and machining under high cutting speeds.

Chemical wear

Chemical wear occurs due to the presence of the active environment at the tool-workpiece interface e.g. oxidation.

Flaking or delamination of uncoated tool

Flaking signifies loss of material from a large area of tool face. This type of tool wear is caused by sudden impact between tool and workpiece or when the tool is suddenly disengaged during heavy duty cut involving large cutting force. Possibility of flaking is typically more for brittle tool material like ceramics.

Flaking or delamination of coated tool

It occurs when coating is peeled off from a relatively large area thus completely exposing the tool substrate as indicated in Fig. 1.2. It is called flaking, delamination or spalling types of wear of coating. This is caused when the interface between coating and substrate is not strong enough to withstand the cutting force.

Fracture

Fracture of the cutting edge occurs due to high cutting force and prolonged use of the tool when wear due to chipping, flaking, deformation or crater is already evident. Tool fracture typically happens because of presence of hard spots on the workpiece or machining at high cutting parameters.

1.3.3 Cutting force

In metal cutting, generation of cutting force is an important index of machinability since cutting force directly or indirectly influences consumption of cutting power, energy loss, distortion of the workpiece and cutting tool. The resultant force can be resolved into three mutually perpendicular components such as F_f, F_r and F_c as shown in Fig. 1.3. F_c is called main cutting force since it acts in the direction of cutting velocity (V_c) vector. F_f and F_r are the feed and radial components due to their direction of action. These three components can be experimentally measured by cutting force dynamometer.

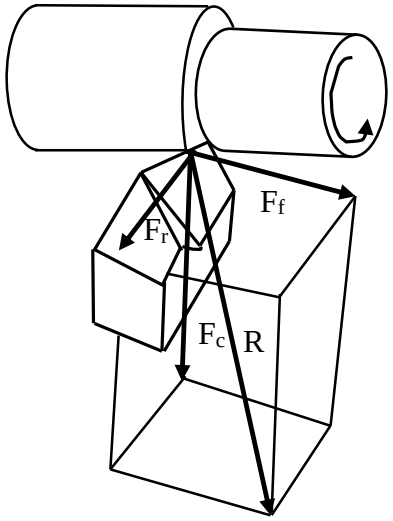

Fig. 1.3: Cutting force in turning (Chattopadhyay, 2011).

Merchant simplified this complex 3D force system into 2D by analysing different forces in orthogonal plane. Accordingly, cutting force applied by the tool against the chip formation is resolved into two components. One which acts against the chip flow is friction force (F) and the acts normal to it (N). Coefficient of friction (μ) can be given by the ratio of these forces as indicated in the following equation,

$$\mu = \frac{F}{N} \tag{1.1}$$

Similarly, the force applied by workpiece can be resolved into shear force (F_s) along the shear plane and normal force (F_n). In addition, thrust (F_t) and main cutting force (F_c) can also be represented in the orthogonal plane. Resultant forces of these individual force components are equal rendering the chips to be under dynamic equilibrium. Merchant's circle diagram is thus constructed and is a useful technique to analyse the forces for orthogonal machining. Therefore, the forces i.e. F, N, F_s and F_n which cannot be directly measured by the dynamometer is expressed by F_c, F_r and F_f. All these forces vary with tool geometry, cutting parameters, properties of cutting tool and workpiece.

1.3.4 Cutting temperature

During machining, high temperature is generated in the vicinity of cutting tool edge. Rise in temperature directly influences the rate of tool wear as well as friction between chip-tool and work-tool interfaces. Therefore, determination of temperature during machining is of considerable importance. Rate of energy consumption or power (P_m) during machining is given by the following equation,

$$P_{m=}\ F_c \times V_c \tag{1.2}$$

During elastic deformation, energy required to deform is stored into the material in the form of strain energy, while, in machining by plastic deformation, most of the energy is converted into heat. Conversion of energy into heat occurs in three different zones as shown in Fig. 1.4. These zones are defined as:

Primary shear zone (zone 1)

Majority of heat generated during machining i.e. about 60-80% of total heat is liberated from primary shear zone with energy of shear deformation being primarily converted to heat.

Secondary deformation zone (zone 2)

Further, heat is generated at the chip-tool interface due to frictional rubbing and shearing. The maximum generation of heat range contributes about 10-15% of total heat.

Work-tool interface (zone 3)

Around 5-10% of total heat is generated at the interface between machined surface and tool flank due to frictional rubbing. Heat generation is particularly prominent with gradual progression of flank wear.

Apportionment of heat during dissipation is also important. Chip is the primary medium to carry away the heat generated at zone 1 and 2, while heat is mainly transferred to workpiece at zone 3. Residual heat is carried to the tool through rake and flank faces.

1.3.5 Chip characteristics

Machining is a process in which removal of excess material takes place in the form of chips. Chip characteristics are primarily specified in terms of shape, size and geometry of chips which in turn are influenced by following aspects during machining:

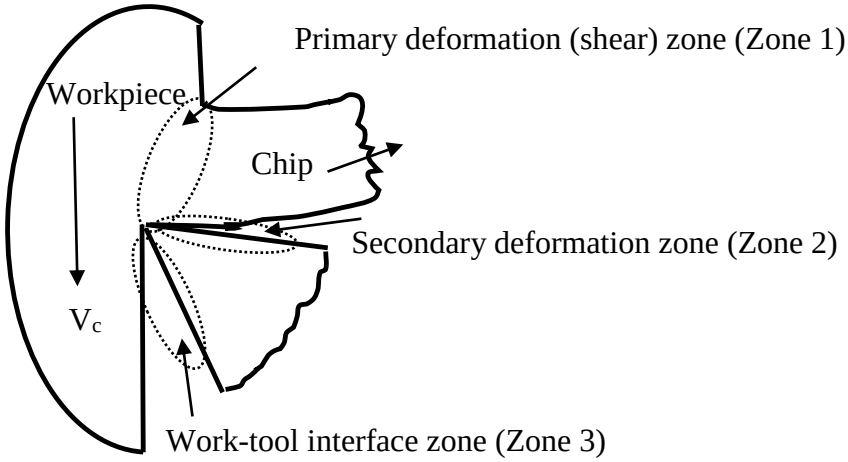

Fig. 1.4: Cutting zones in the chip (Chattopadhyay, 2011).

- Properties of cutting tool and workpiece
- Tool geometry
- Magnitude of cutting temperature
- Nature and degree of tool-chip interaction
- Conditions of the cutting edge of tool
- Cutting parameters
- Cutting environment

Two types of chip formation mechanism depending upon the nature of work material are yielding or shearing for the ductile materials and brittle fracture for the brittle materials. Accordingly, chips can be broadly classified into three types as follows:

Discontinuous chips

Discontinuous chips typically form while machining brittle materials like cast iron or ductile material at very low cutting speed under dry environment. The discontinuous chips may be of both irregular and regular shape and size depending on the cutting condition.

Continuous chips

Machining of ductile material often results in continuous type of chips. This is not desirable since it causes escalation in chip-tool interface friction, hence temperature and formation of built-up layer and/or built-up edge. There is also a greater chance of diffusion wear. Final surface finish might also be adversely affected. Moreover, long and continuous chips pose significant risk to the operator.

Segmented or jointed chips

This type of chips is produced when work material is brittle or machining is performed at a high depth of cut. The different types of chips have been schematically represented in Fig. 1.5.

The type and shape of chip formed have significant role in machining. According to ISO 3685-1977 (E), the type and form of chips can be classified into eight different shapes group given in Fig. 1.6. Short and segmented chips are always desirable rather than long and continuous ones from technical as well as safety point of view.

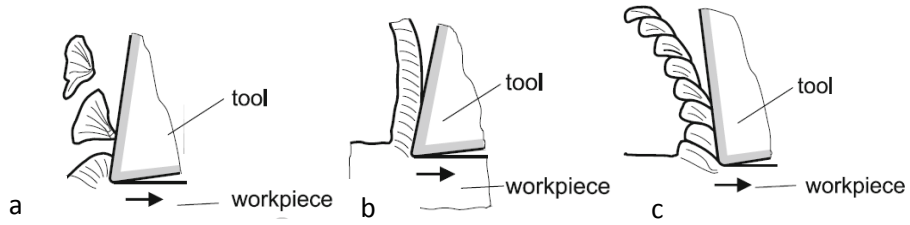

Fig. 1.5: Types of chip (a) discontinuous, (b) continuous and (c) segmented type (Boothroyd and Knight, 2005; Grzesik, 2008).

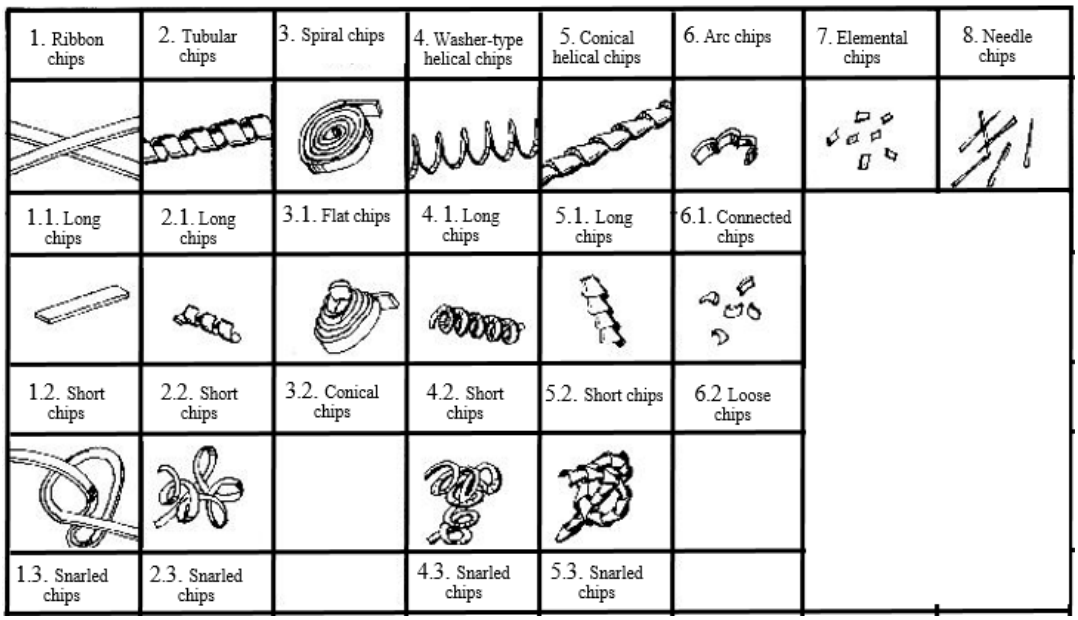

Fig.1.6: Classification of different type of chips (Boothroyd and Knight, 2005).

1.3.6 Surface integrity

Surface integrity can be defined as the combination of mechanical, metallurgical, topographical, thermal and chemical features of surface of a component obtained from a particular manufacturing process. It can be characterised by surface roughness, surface

defects, white layer, strain hardening and residual stress (Field *et al.*, 1972). Therefore, study of these characteristics is very much augmented for fatigue life of a component. Various aspects of surface integrity can be broadly classified under following categories:

Surface topography

It includes surface texture consisting of roughness, waviness and lay combined with other macro morphological features of machined surface usually considered as defects. Surface roughness (mainly arithmetic average, R_a), in particular, is one of the most commonly used characteristics of surface integrity for assessing the quality of machined surface (Ardi *et al.*, 2014; Novovic *et al.*, 2004; Zhang *et al.*, 2015). According to Veldhuis *et al.* (2009), surface roughness refers to high frequency irregularities on the surface caused by the interaction of the material microstructure and the cutting tool action along with repetitive nature of surface defects. Fan *et al.* (2013) observed three major factors to affect the surface roughness. These factors include formation of built up edge, initiation of chip plastic side flow and tool wear equilibrium.

Surface metallurgy

This includes the metallurgical alterations of machined surface and sub-surface layer. During machining of nickel-based super alloys, surface is subjected to high mechanical (high stress and strain) and thermal (high temperature and quenching) load which may cause some microstructural and metallurgical alterations (Bosheh and Mativenga, 2006; Guo and Sahni, 2004; Guo and Schwach, 2005; Kortabarria *et al.*, 2011). They are detrimental to low cycle fatigue life of the machined components under high stress and temperature applications (Herbert *et al.*, 2012a, 2014; Schwach and Guo, 2006). Various researchers (Hardy *et al.*, 2014; Imran *et al.*, 2011, 2012, 2014, 2015; Jawahir *et al.*, 2011; M'Saoubi *et al.*, 2012, 2014; Zhou *et al.*, 2011) have indicated the formation of three distinct zones in sub-surface microstructure of nickel-based super alloys.

Zone 1 is a severely deformed region formed as a result of both mechanical and thermal load produced in the machined region and is characterized by nano crystalline grain structure. Zone 1 has been mostly referred to as white layer in various studies. This white layer was first commented upon by Griffiths (1987).

Zone 2 constitutes partially deformed layer with slip bands and elongated grains.

Zone 3 is characterised by bulk material usually free from any effect of machining induced deformation (Zhou *et al.*, 2011).

Mechanical alteration

Change in mechanical properties of nickel-based super alloys, typically in the form of hardness and residual stress due to machining induced deformation is a common occurrence. During machining, nickel-based super alloys are subjected to high cutting temperature and pressure which result in work hardened layer having hardness value higher than that of bulk material (Ezilarasan *et al.*, 2013a; Sharman *et al.*, 2004a).

Machining induced residual stress for difficult-to-cut nickel-based super alloys is one of the critical aspects of surface integrity. High strain rate accompanied by large plastic deformation as well as thermal energy result in the development of residual stress part of which still persists even after the machined surface is relieved form these thermo-mechanical loads. Mechanically induced plastic deformation results in compressive residual stress while heat generation during machining develops tensile residual stress in machined component (Cao *et al.*, 1994; Doremus *et al.*, 2015; Foss *et al.*, 2013; Herbert *et al.*, 2014; Jang *et al.*, 1996; Jacobus *et al.*, 2000).

1.4 Methods of improving machinability

To improve various machinability characteristics discussed above, different techniques may be employed as follows:

- Suitable variation in the workpiece composition and its mechanical property along with microstructure by the addition of various suitable elements.
- Determination of optimal combination of cutting tool material and its geometry in accordance with workpiece.
- Optimal selection of cutting parameters
- Selection of cutting fluids and techniques of application of the same.
- Judicious choice of coating materials in single or multilayer configuration for cutting tools.
- Application of special techniques such as cryogenic machining, hot machining, plasma enhanced machining (PEM) etc.

1.4.1 Wet machining

One of the beneficial aspects of dry machining is it promotes the concept of environment-friendly manufacturing. On the other hand, escalation in cutting temperature and consequently rapid rate of tool failure as well as deterioration in surface integrity often make the use of cutting fluid essential particular while machining material with low thermal conductivity under adverse machining condition.

1.4.2 Flood cooling

Flood cooling is the system when the machining zone is completely flooded with a coolant with its nozzle adjacent to and directing towards the tool tip. Primary objective of such cooling is to dissipate heat and bring down the friction at chip-tool and work-tool interfaces, thus improving surface integrity, lowering cutting power and increasing tool life. However, this technique leaves deleterious impact on environment and operator because of the hazards associated with disposal and generation of toxic fumes respectively.

1.4.3 Cryogenic cooling

Cryogenics is defined as working with materials at temperatures less than –150 ºC (123K) (Bilstein and Roger, 1996). Liquid nitrogen is the most widely used cryogenic material with its boiling point of –198 ºC. However, liquid CO_2 has also been growing as a viable alternative. Machining in which cryogenic fluid is utilized as a coolant is called cryo machining. Owing to its capability to maintain very low temperature, application of cryogenic fluid is particularly effective when control of machining zone temperature is otherwise a real challenge.

1.4.4 Minimum quantity lubrication (MQL)

MQL can be defined as the application of small amount of cutting fluid with a typical flow rate of 50-500 ml/h by mixing it with compressed air (4-10 bar). Such mixing leads to atomization of cutting fluid so that it can make successful inroads into the narrow zone of chip-tool interface. Major aim of MQL is to reap the benefits of cutting fluids in terms of reduction in friction and temperature while getting rid of its detrimental influences. Since MQL involves significantly lesser amount of cutting fluid, this phenomenon is also popularly referred to as ‘near dry machining’, ‘micro lubrication’ or ‘spatter lubrication’.

1.5 Tool coating

1.5.1 Need of coating

The requirements of materials properties of cutting tool at the core and the top surface are quite different and conflicting. High compressive strength, toughness and thermal conductivity are the desirable properties of core material, while the top surface of the tool needs to be hard, wear resistant with good anti-friction property and low thermal conductivity. It can be realized in actual practice by depositing a well adherent coating of suitable material and thickness over the surface of the tools. Depending on the

requirements, monolayer, multilayer or alternate layers consisting of different coating materials can be deposited.

1.5.2 Beneficial effects of coating on cutting tools

A great deal of benefits can be achieved by virtue of cutting tool coatings. Some of the prominent aspects are included below:

- Coating can reduce cutting force and hence requirement cutting power by 20-50%.
- Tool life can be increased by 100-250% for the cutting speed and can allow to use cutting speed by 50-150% for the same tool life according to the preferable choice of industries for higher productivity.
- Improved surface topography including high surface finish can be achieved with the coated tool.
- Due to anti-friction properties of coating, chip-tool and work-tool interfaces can be substantially reduced leading to reduction in chip-tool contact length and prolonged tool life. At the same time, usage of cutting fluid can also be minimized remarkably. This would definitely promote environment-friendly machining.
- Coated tool can provide resistance to diffusion, chemical attack, adhesion, mechanical abrasion and other forms of wear.
- Thermal stability of the tool can be also be achieved.

1.5.3 Types of coatings

Based upon the requirements, selection of tool coating of suitable nature, structure and composition, selection should be made. Different types of coatings along with typical examples are presented in Table 1.3.

Table 1.3: Different types of coatings and examples.

Type of coating	Example
Conventional hard coating	TiC, TiN, TICN, Al_2O_3
Multi-component coating	TiAlN, TiCrN, TiVN
Multi-layer coating	TiC/TiCN/TiN, TIAlN/AlCrN
Super lattice coating	TiN/NbN, TiN/VN
Super hard coating	Diamond, cBN
Composite coating	Ti+MoS_2, TiN+MoS_2
Soft coatings	MoS_2, WS_2

1.5.4 Coating processes

There are many ways to deposit the coating on a substrate. Coated tool has also been ranked by deposition techniques. There are many ways to deposit the coating such as electro-plating, plasma coating, thermal spraying and vapour deposition. Cutting tools are typically deposited using different vapour deposition techniques which are discussed as follows.

Chemical vapour deposition (CVD)

The chemical reaction between the gaseous species and the substrate is called the CVD process which is usually carried out in the temperature range of 700 to 1100 °C. High density, good stoichiometry and strong chemical bonding of the coating are some of the advantages of CVD coatings. TiC was one of the first CVD coatings for cutting tools followed by the coatings like Al_2O_3, TiCN and TiN. However, high deposition temperature often causes thermal residual stress leading to the formation of eta phase in the interface. This is one of the reasons for the failure of CVD coatings during machining. Moreover, owing to less toughness, CVD coated tools are not used for intermittent machining operations such as milling.

Physical vapour deposition (PVD)

Thin film deposition in PVD process is carried out by the condensation of vaporized form of the film material onto the substrate surface at a particular deposition temperature and pressure. It is a low pressure (10^{-2} to 10^{-3} Torr) process and carried out in a vacuum chamber. In order to maintain contaminants-free environment during deposition, a base is required. This is achieved by combination of vacuum pumps. This method of deposition of thin films consists of mechanical processes such as evaporation, ion sputtering rather than chemical methods. In order to obtain the uniform coating thickness, the substrates are subjected to rotation at a constant speed in all directions. One of the unique advantages of PVD includes better control of film micro-structure, composition variation and growth rate which finally affect the functional characteristics of the coatings. Improvement in structure and property of a PVD coating is also possible by low energy ion bombardment over the film during deposition. Maximum coating thickness of multi-functional PVD coatings is typically limited to 3 µm. The main disadvantages of these coatings are the lower deposition rate, inability to coat a large area of hidden surfaces and difficulty in maintaining the coating stoichiometry and uniformity.

Chapter 2
Literature Review

2.1 Cutting force

Measurement of cutting force is of paramount importance since it is related to power consumption, design of tools and machine parts, vibrations, part accuracy, etc (Ezugwu *et al.*, 2000a; Zębala and Słodki, 2013). Cutting forces are typically high for work material exhibiting work hardening tendency such as nickel-based super alloys (Thakur and Gangopadhyay, 2016; Ulutan and Ozel, 2011). Combination of tool and workpiece, tool geometry, cutting parameters and lubricant's properties have significant influence on cutting force. Fang and Wu *et al.* (2009) showed that influence of tool wear was more significant on feed force than main cutting force. This was attributed to increase in tool edge radius. The study reported by Olovsjö *et al.* (2012) indicated that higher cutting force was required for machining workpiece material with larger grain size as compared to finer grain. When the grain size is of similar order of magnitude that of feed rate or undeformed chip thickness, inhomogeneous or anisotropic deformation takes place during shearing as a result of which cutting force is usually high. On the other hand, homogeneous deformation of material with finer grains resulted in lowering of cutting force.

2.1.1 Effect of tool material including coating

Materials of cutting tool and its coating are also important in influencing the cutting force during machining. While hardness and anti-friction property of such materials are effective in bringing down cutting force, increase in edge radius due to deposition of coating might sometimes diminish the beneficial role of coating. Due to the same reason Chen *et al.* (2012) obtained lower cutting force of TiCN coated tool compared to TiN coated one owing to higher hardness and better anti-friction properties of the former. On the other hand, Bushlya *et al.* (2013a, 2013b) observed rise in cutting force with coated cBN tool than its uncoated counterparts.

Ezugwu *et al.* (2000a) and Ezugwu and Okeke (2002) showed the effectiveness of multilayer (TiN/TiCN/TiN) coated tool compared to single layer (TiAlN) tool in lowering cutting force. This was explained by higher abrasive wear and burr formation for the single layer tool, owing to its insufficient edge support. Similar observation was also observed by Nalbant *et al.* (2007) and Thakur *et al.* (2012a). In a study reported by Ezugwu and Wang (2000a) and Ezuguu *et al.* (2000) it was observed that multilayer TiN/TiCN/TiN coated tool effected less cutting force due to its sharper cutting edge than single layer TiN coated

tool with honed edge. However, role of coating was not exactly understood because of difference in edge preparation for both the coated tools. Thakur *et al.* (2012a) compared the performance of CVD TiN/Al_2O_3/TiCN and PVD TiN/TiAlN coated inserts during machining of Inconel 718 and reported superior performance of CVD coated tool in terms of bringing down the cutting force. Higher thermal stability, resistance to wear and spalling of Al_2O_3 and TiCN layers in CVD coated tool, might have played significant role in lowering cutting force. On the contrary, Thakur *et al.* (2015b) observed lower cutting force with similar PVD coated tool when compared to CVD TiCN /Al_2O_3 coated tool.

2.1.2 Effect of cutting parameters

According to general agreed upon results, reduction in cutting force is caused by increase in cutting speed (Alauddin *et al.*, 1998; Choudhury and El-Baradie, 1998; El-Bestawi *et al.*, 1993; Ezilarasan *et al.*, 2013b; Ezugwu and Bonney, 2004; Fang and Wu. 2009; Hao *et al.*, 2012; Nalbant *et al.*, 2007; Rahman *et al.*, 1997; Samuel and Shin, 2009; Thakur *et al.*, 2012a, 2012b; Thakur *et al.* 2015b). According to Fang and Wu (2009), increases in cutting temperature owing to elevation of cutting speed possibly caused softening of work material thereby facilitating easy deformation. On the contrary, a reverse trend i.e. escalation of cutting force during certain range of cutting speed and feed has also been reported by few researchers (Cai *et al.*, 2014; Nalbant *et al.*, 2007). It was due to the fact that plastic deformation and tool wear have overriding influence in those ranges of cutting parameters (Choudhury and El-Baradie, 1998). It is usually difficult to predict the onset of dominating influence of plastic deformation and tool wear which are closely related to thermomechanical properties of a particular grade of super alloy (Choudhury and El-Baradie, 1998; Cai *et al.*, 2014; Costes *et al.*, 2007; Ezugwu and Bonney, 2004; Ezugwu and Okeke, 2000a, 2002; Nalbant *et al.*, 2007; Soo *et al.*, 2011). Liao *et al.* (2008) explained large impact force during side milling by the contact between tool and workpiece under low cutting speed (11.3 m/min). The force drops to a stable value when the cutting speed was further raised upto 113.1 m/min. Further increase in cutting speed resulted in hike in cutting force which was attributed to the formation of BUE (Alauddin *et al.*, 1998; Choudhury and El-Baradie, 1998; Chen *et al.*, 2012; Ezilarasan *et al.*, 2013b; Fang and Wu, 2009; Liao *et al.*, 2008; Rahman *et al.*, 1997). Alauddin *et al.* (1998) found rise in cutting force with feed due to obvious increase in load on the tool tip. EI-Wardany *et al.* (1996) ascribed reduction in cutting force to the formation of isolated segmented chips under the condition of very high feed (1.25 and 1.76 mm/rev).

Li *et al.* (2006a) observed that as the number of cutting passes increased, peak cutting force component also increased. In order to accomplish minimum cutting force, optimisation of cutting parameters was carried out (Ezilarasan *et al.*, 2013b; Thakur *et al.*,

2009a). Thakur *et al.* (2009a) demonstrated that cutting force was minimum under the highest value of cutting speed of 65 m/min and minimum value of feed of 0.08 mm/rev and depth of cut 0.5 mm. Optimal condition resulted in reduction in cutting force of 235% compared to initial cutting condition.

2.1.3 Effect of cutting environment

Reduction in cutting force is also possible with effective use of coolant. Pusavec *et al.* (2011) noted machining under MQL caused decrease in cutting force than in dry condition. Influence of cutting environment on cutting force is of paramount importance. Since it directly dictates consumption of cutting power. Ezugwu *et al.* (2004) observed that concentration of coolant is also important in this regard. Cutting force was in fact raised with higher concentration of coolant which was attributed to reduced cooling effect. Although this was not explained but logically assumed that it would be increasingly difficult for the coolant to effectively penetrate into the zone with rise in concentration. Similar elevation in coolant pressure to a very high value (beyond 200 bar) during high pressure cooling was also not very effective, since dynamic and reactive force along with temperature increased with coolant pressure. Devillez *et al.* (2011) noted slightly higher cutting force during wet machining than dry condition. It could be attributed to higher cutting temperature during dry machining leading to thermal softening. Decrease in cutting force could also be achieved with the help of PEM. According to Novak *et al.* (1997), softening of workpiece material as a result of plasma heating was the possible explanation.

2.1.4 Effect of tool condition

Geometry and parameters of cutting tools have profound influence on the cutting force. Tool with positive rake exhibited lower cutting force than with negative rake owing to reduction in chip-tool contact length (Ezugwu and Pashby, 1992). According to Rahman *et al.* (1997), cutting force decreases with side cutting edge angle.

Tools with higher edge radius or honed edge are also responsible for increase in cutting force. At the same time, Arunachalam *et al.* (2004a), Fang *et al.* (2013) and Sharman *et al.* (2015) explained effective edge radius also increases, as a result of flank wear, finally leading to escalation in cutting force. Günaya *et al.* (2004) and Huang *et al.* (1999) found increase in cutting force with edge radius could also be related to rake angle being more negative. Furthermore, Bushlya *et al.* (2013a) found that chamfering along with honed edge of whisker-reinforced alumina (WRA) ceramic tool caused higher cutting force using different uncoated and coated PCBN tools without chamfered edge. Cutter orientation and workpiece angle also played a major role during high speed milling of Inconel 718. Aspinwall *et al.* (2007) observed that tilting the workpiece by 45° horizontal direction was

beneficial in reducing the cutting force when compared to machining without tilt. This was attributed to minimising the effect of ploughing with the help of tilting the workpiece.

2.2 Temperature

Owing to low thermal conductivity of nickel-based super alloys, cutting temperature is a critical issue since it has detrimental influence on both and workpeice. According to Hao *et al.* (2012), Jun *et al.* (1997), Kitagawa *et al.* (1997), Narutaki *et al.* (1993), Peng *et al.*, 2012 and Thakur *et al.* (2009a), temperature increased with increase in cutting speed. However, different trend has also been noticed by EI-Wardany *et al.* (1996). Cutting temperature first decreased with increase in cutting speed from 110 to 510 m/min. Further rise in cutting speed caused escalation in cutting temperature. Such variation could be related to thermo-mechanical property of workpiece material. It was reported that thermal conductivity of Inconel 718 increased with temperature. It increases the thermal diffusivity of Inconel 718 and reduces the tool edge temperature since much of the heat was dissipated by workpiece. As cutting speed was further elevated up to 720 m/min, tool edge was covered with BUE due to plastic flow of work material under very high cutting temperature (~1300℃). Consequently, heat dissipation to the tool was aided by BUE formed under such condition. Similar effect was also noted for feed. Cutting force increased with feed, resulting in rise in cutting temperature (Thakur *et al.*, 2009a, 2009b; Xue and Chen, 2011). Thakur *et al.* (2012a) observed lower temperature while adopting CVD TiN/Al_2O_3/TiCN coated tool than PVD TiN/TiAlN coated tool. It could be attributed to higher thermal conductivity of coating layer (Al_2O_3/TiCN) of CVD coated tool along with high edge radius. As a result, ploughing became more dominant mechanism of cutting than shearing leading to decrease in cutting zone temperature. Obikawa *et al.* (2012) observed lower cutting temperature with air assisted jet machining than conventional wet and dry machining owing to high pressure cooling effect associated with the former technique.

2.3 Tool wear

Tool wear is one of the significant criteria for machinability since many performance measures such as cutting force, cutting temperature, chip characteristics, different aspects of surface integrity, tool life along with overall production cost are directly or indirectly influenced by tool wear. During machining of nickel-based super alloys tools suffer from mechanical (abrasion) and chemical (thermochemical, diffusion) types of wear (Ezugwu and Tang, 1995a; Zhu *et al.*, 2013). According to Olovsjö *et al.* (2012), microstructure and mechanical properties of workpiece have dominant role on tool wear mechanism. Reduced flank wear was observed during machining of Waspalloy than Inconel 718 using WC tool.

It was attributed to the formation of W-rich oxide at the chip-tool interface during machining of Waspalloy. Oxide formation was promoted due to higher cutting force and hence temperature during machining of Waspalloy. Higher cutting force was also related to higher ductility of the material. It has been found that flank wear is mainly caused by adhesion between tool and work piece (El-Bestawi *et al.*, 1993; Hao *et al.*, 2012; Song and Zhao, 2008). Mechanism of tool failure may vary with different tools (cemented carbide and ceramic tools with and without coating). Formation of BUE takes place due to adhesion between work material and rake as well as flank faces of the tool. As a result, surface properties of the tool change (Arunachalam and Mannan, 2000; Ezugwu *et al.*, 2003; Zhu *et al.*, 2013). According to Zheng *et al.* (2012), if stress during machining exceeds the cohesive strength of the material, but is less than bond strength of BUE, there is a removal of chunk of material comprising of both BUE and tool material. This obviously leads to reduction in strength of tool material. According to Xue and Chen (2011), depth of cut (DOC) notch is a common problem during machining Ni-based super alloys since DOC region is continuously encountered with work hardened surface layer. Formation of adhering layer at DOC region followed by pull-out of tool material further worsens DOC notch wear. In case of ceramic tool which has low flexural strength and fracture toughness, adhesion propagates in longitudinal as well as lateral direction through cracks. It results in wider crack on the ceramic tool which leads to severe plastic deformation, nose and notch wear (Zhu *et al.*, 2013). Olovsjö *et al.* (2012) observed higher notch wear while machining of larger grain size workpiece than the one with finer grains, since high grain size material requires higher cutting force to deform along shear plane. It is also noted that deformation depends on grain orientation. As a result, higher deformation led to formation of burr and consequently DOC notch.

Diffusion wear is more prominent for carbide tools. The binder phase cobalt in carbide tool is easy to diffuse at elevated temperature. While $_{C}$BN tool is primarily suitable for high speed machining of nickel-based super alloys, adhesion and diffusion get more pronounced when the cutting speed is raised above 300 m/min (Bushlya *et al.*, 2013a). Bushlya *et al.* (2013b) observed two types of notch on the major cutting edge. One is at the DOC extremity (DOC notch) while, the other is located outside the chip area (secondary notch). Attrition by burr on the depth of cut line, thermal and mechanical stress gradient are responsible for DOC notch. On the other hand, adhesion and abrasion caused by chip-curl back effect promote the formation of secondary notch on the rake face outside. Secondary notch can be distinguished by its appearance of fracture and high roughness. Depth of cut notch wear was reduced with increase in feed (Bushlya *et al.*, 2013a). Chen and Liao (2003) described four stages of wear mechanism during drilling of Inconel 718. At the beginning, abrasion of tool faces took place followed by chipping of cutting edge which propagated with growth of micro cracks. This phenomenon gradually led to breakage of cutting edge and finally

complete failure of tool. Similar observation was also reported by Imran *et al.* (2011), Rahim and Sasahara (2011) and Sharman *et al.* (2008a). Appropriate combination of tool materials, tool geometry, cutting parameters and cutting environment for machining of nickel-based super alloys is very much crucial to prevent rapid escalation of tool wear.

2.3.1 Effect of tool material including coating

Tool material should exhibit resistance to different types of wear, good combination of hardness and toughness, thermal and chemical stability and thermal shock resistance (Olovsjö *et al.*, 2010a, 2010b; Zhu *et al.*, 2013). Cemented carbide tool is suitable to machine nickel-based super alloys owing to excellent fracture toughness and reasonably high hardness coupled with fairly good thermal stability (Choudhury and El-Baradie, 1998; Ezugwu *et al.*, 1992, 1999; Liao *et al.*, 2008). Best performance, in terms of reduced and uniform flank wear, was obtained with K20 grade of cemented carbide whereas P40 grade showed more chipping and fracture of cutting edge at a cutting speed of 27 m/min. Amalgamation of different properties like high hardness, thermal conductivity and lower coefficient of thermal expansion possessed by K20 grade was responsible for its superior resistance to tool wear at the existing cutting speed (Ezugwu and Pashby, 1992). The study on wear mechanism of K20 and P20 grades of carbide tool during dry turning of Inconel 718 revealed lower tool life of P grade compared to that of K grade. Due to diffusion wear during machining of nickel-based super alloy, physical separation of carbide particles from the rake surface takes place thus exposing the underlayer. Higher cobalt content in P grade made the surface more prone to wear. Moreover, because of higher solubility of TiC (present in P grade) in nickel compared to WC was also detrimental for tool life of P20 carbide grade insert (Liao and Shiue, 1996). At the same time, best performance of the cemented carbide tool could be achieved at low V_c (less than 50 m/min) (Bhatt *et al.*, 2010; Thakur *et al.*, 2009a, 2009b, 2012a). Nickel-based super alloys can be machined with high cutting speed around 100-400 m/min with the use of ceramic tool owing to its high hot hardness, thus ensuring higher productivity (Altin *et al.*, 2007; Deng *et al.*, 2005; El-Bestawi *et al.*, 1993; Ezilarasan *et al.*, 2013a; Kim, 1994; Kitagawa *et al.*, 1997; Li *et al.*, 2002; Narutaki *et al.*, 1993; Richards and Aspinwall, 1989; Zheng *et al.*, 2012). Dominant wear mechanisms caused by ceramic tools include abrasive, adhesive, microcracks, depth of cut notch, diffusion, cohesive and oxidation (Bhattacharyya *et al.*, 1983; Liu and Zhang, 2014).

Mechanical and chemical properties of ceramic tools also play important role in influencing the wear phenomenon. According to Vigneau *et al.* (1987), performance of SiC whisker reinforced ceramic tool depends on composite properties such as aspect ratio (length/diameter of whiskers) and whiskers volume. Brandt *et al.* (1990) demonstrated that

silicon carbide whisker-reinforced alumina ceramic tool outperformed silicon nitride-based tool in terms of tool life, which can be attributed to higher chemical stability of the former due to presence of stable aluminum-oxide. Ezugwu *et al.* (2004) attributed the worse performance of silicon nitride-based nano ceramic tool owing to poor resistance to abrasion wear leading to nose failure. It is also shown by the same research group that nano ceramic tool (Al_2O_3/TiCN/ZrO_2) with lower edge toughness and hardness offered higher tool life than the one with higher edge toughness and hardness.

Addition of SiC whisker to Al_2O_3/TiB_2 ceramic tool improves resistance to tool breakage at the rake face owing to enhanced resistance to fracture toughness, hardness as well as thermal conductivity (Jianxin and Xing, 1994a, 1994b, 1996, 1997). Owing to excellent wear resistance, thermal conductivity and chemical stability of hot-pressed 25 volume % of SiC_w–Al_2O_3 ceramic tool (JX-1) performed better than other ceramic tools like SG-4 (Al_2O_3–(WTi)C), LT55 (Al_2O_3–TiC–Mo–Ni), Sialon and carbide tool YG6 (WC–Co, equivalent to K10). JX-1 was less susceptible to DOC notch wear than the other, and hence more resistant to flank and nose wear (Jun *et al.*, 1997). Coelho *et al.* (2004) utilised ceramic (Al_2O_3-based, Al_2O_3-based + SiCw) and PCBN tools. Deeper notch and higher flank wear were observed for PCBN than ceramic tools during high speed (500 m/min) turning of Inconel 718.

On the contrary, PCBN demonstrated higher tool life than WRA tool due to less diffusion wear. However, one-to-one comparison was difficult as both the tools had different geometries (Bushlya *et al.*, 2013a). Although ceramic and cBN tools are preferred to carbide tools for high speed machining, the former are more expensive and require dedicated machine tools for high speed machining (finishing mode). On the other hand, coated carbide tools are recommended for low and medium speed machining requiring heavy cut (roughing mode).

From economic and productivity point of view, the machinability of nickel-based alloy can be improved with use of coated tool which tends to improve tool life. Use of coating can mitigate the cost of expensive ceramic tools, elevate tool life even at moderate cutting speed, reduction in chip-tool interface friction and power consumption. Life of uncoated tool could be augmented using coated tool at high cutting speed (upto 150 m/min) (Derrien *et al.*, 2004). Large DOC notch on the rake face and non-uniform flank wear were observed with WC tool whereas uniform flank wear was observed with multilayer coated TiCN/Al_2O_3/TiN tool (Sharman *et al.*, 2004a). According to Sharman *et al.* (2004a, 2006), excellent wear resistance of coating might be the explanation. Use of coated tool was found to be effective in augmenting cutting speed before tool life was reached. This was attributed to formation of more pronounced chip burr (lateral deformation of chips) for uncoated (CNGN-12) tool during machining of Hastelloy C-276. The consequence of chip burr formation was reflected in chipping of edge due to hammering action. Coated (CCMT-12)

tool imparted sufficient edge strength and hence resistance to chipping under such condition (Khidhir and Mohamed, 2010). However, the geometry of uncoated and coated tools was different, the contribution of coating could not be clearly ascertained. For precisely understanding the role of coating, various aspects of machining such as tool geometry, cutting parameters and environment must be identical for both uncoated and coated tools. Nevertheless, there is very little information available in the literature.

Configuration of coating systems and deposition techniques have also prominent role on the performance of coated tools. Ezugwu *et al.* (1999) showed that multilayer (TiN/TiCN/TiN) PVD coated tool outperformed PVD single layer (TiN) and multilayer CVD coated tools. The superiority of TiCN coating over TiN coating can be attributed to its higher hardness, toughness and abrasion resistance along with lower coefficient of friction. Smaller grain size and high density of multilayer PVD coated tool provided high hardness and strength as compared to multilayer CVD coated tool. Similar observation of better performance of PVD than CVD coated tools was found by Habeeb *et al.* (2008), Jindal *et al.* (1999), Kadirgama *et al.* (2011), Li *et al.* (2002), Noor *et al.* (2010), Rahman *et al.* (1997) and Thakur *et al.* (2015b). In contrast, CVD multilayer (TiN/Al_2O_3/TiCN) coated tool performed better than PVD multilayer (TiN/TiAlN) coated tool which showed non uniform tool wear and micro chipping. Owing to stronger bond between coating and substrate and thermal stability (Al_2O_3 coating) of CVD as compared to multilayer PVD coated tools makes the former a superior choice (Thakur *et al.*, 2012a). CVD TiC/N + Al_2O_3 coated tool outclassed PVD TiN coated tool in terms of tool life, owing to higher adhesion strength, except at low cutting speed (50 m/min) and high feed (0.12 mm/rev). Under such condition, premature failure due to flaking (brittle fracture) of CVD coated tool was observed. Chip-tool interface was subjected to high compressive force leading to edge chipping and it was more dominant for PVD coated tool as it has relatively sharper cutting edge (Jawaid *et al.*, 2000). Thicker coating of multilayer TiN/TiCN/TiN coated tool outperformed single layer TiAlN and TiZrN coated tools owing to its greater edge strength (Ezugwu and Okeke, 2000a, 2002). Similar observation was reported by Sharman *et al.* (2001). The performance of TiN+AlTiN+MoS_2 coating was found to be superior to that of TiN+AlTiN and CrN+CrN:C+C coated tools (Settineri *et al.*, 2008). Higher content of aluminium in nanostructured AlTiN coated tool imparted higher resistance to oxidation and hardness at elevated temperature, and hence made it a more suitable option than other coated (nanostructure TiAlN, multilayer lamellar TiAlN + WC/C, TiAlN + MoST (MoS_2 + Ti) and uncoated WC K20 grade tools (Devillez *et al.*, 2007). Fox-Rabinovich *et al.* (2010) found improvement of tool life by 2.3 times by using AlTiN/Cu coated nano multilayer tool in comparison with mono-layer AlTiN coated tool. Improved lubricating properties in combination with lower thermal conductivity of AlTiN/Cu coated nano-composites tool might be the explanation. According to Biksa *et al.* (2010), addition of 5th

and 6^{th} group of elements in the form of nitride in AlTiN coated tool enhanced the tool life. It can be attributed to improved lubrication property due to the formation of tribo-films consisting of lubricious oxide on the surface.

2.3.2 Effect of cutting parameters

Tool wear mechanism is closely related to the range of cutting parameters selected, since cutting parameters (V_c and f in particular) have prominent influence on cutting zone temperature. At low V_c of 20 m/min, BUE formation occurs leading to severe chipping whereas, at high V_c of 45 and 50 m/min diffusion wear takes place and it accelerates the formation and peeling off of wear debris for uncoated carbide tool (Hao *et al.*, 2011). Bhatt *et al.* (2010), Choudhury and El-Baradie (1998), Ezugwu and Pashby (1992), and Jawaid *et al.* (2000) observed that with increase in cutting speed, diffusion of cobalt takes place and brings down the strength of uncoated tool. Higher tool life of uncoated carbide tool was found than that of PVD-TiN coated tool under low cutting speed of 25 m/min and at feed rates of 0.08 and 0.14 mm/tooth. This can be attributed to better resistance to attrition wear of uncoated tool whereas, premature coating removal occurred because of high frictional drag force at low cutting speed. But when speed was further raised upto 50 m/min, the coated tool performed better than uncoated tool owing to its high resistance to wear and low thermal conductivity at high V_c (Jawaid *et al.*, 2001). TiN coated PCBN tool promoted higher tool life than uncoated one at a V_c of 250 m/min. However, there was hardly any benefit of coating when cutting speed was increased upto 350 m/min which was ascribed to oxidation of coating at high temperature. Formation of TiO_2 with higher thermal conductivity resulted in fracture of the tool observed by Bushlya *et al.* (2013a). Similar explanation was also put forward by Zhou *et al.* (2012). In another research work by the same group, formation of an oxide layer named as glassy phase on the rake surface of the WRA tool was observed. During machining, silicon from whisker tool reacted with oxygen to form a layer of SiO_2 which looks like glass with smooth surface. Bhatt *et al.* (2010) exhibited superior resistance of wear of PVD TiAlN coated tool at high V_c of 75 m/min due to formation of thermal stable layer of Al_2O_3. At the same time, its compressive residual stress retarded the abrasive and notch wear. On the other hand, triple layer CVD TiCN/Al_2O_3/TiN coated tool outperformed at higher V_c of 100 m/min owing to stronger bond between coating and substrate. Superior resistance to wear of CVD multilayer coated tool at high cutting speed would also be explained by the synergistic effect of multilayer component coating in arresting crack propagation at high temperature and coating delamination owing to higher coating thickness. High cutting speed is in general detrimental for machining of nickel-based super alloys (low thermal conductivity), since high temperature leads to diffusion (Veldhuis *et. al.*, 2010) and chemical (Bushlya *et al.*, 2013a) wear. Interestingly, DOC notch wear decreases with increase in cutting speed as

work material becomes soft and loses its strength properties (Jun *et al.*, 1997; Kitagawa *et al.*, 1997) Nevertheless, due to higher thermal stability of WRA, effect of cutting speed has been negligible (Bushlya *et al.*, 2013b).

Lower rate of tool wear could be achieved when machining Inconel 718 with ceramic tool at a cutting speed of 100 m/min observed by Aruna *et al.* (2010) and Jianxin *et al.* (2005). Adhesion and diffusion wear became dominant modes with further elevation of cutting speed. This was attributed to the presence of Ni, Cr and Fe with the tendency of adhesion and diffusion (Jianxin *et al.*, 2005; Song and Zhao, 2008). Formation of phases such as FeSi and NiSi has been reported by Song and Zhao (2008) for ceramic tools reinforced with SiC whisker which also contributes to reduction in strength properties of tool materials. Fracture of tool rake surface has also been observed at a very high cutting speed. This can be attributed to alteration in thermomechanical properties at high cutting speed (Jun *et al.*, 1997; Li *et al.*, 2002). SiC WRA ceramic tool performed better at low cutting speed range (100-300 m/min) than Si_3N_4 (Silicon nitride) and TiC added (Al_2O_3 + TiC) ceramic tools. But as cutting speed increases (400 m/min) notch and flank wear increases. In contrast, TiC added ceramic tool outperformed at high cutting speed (upto 500 m/min). It might be due to higher thermal stability of Al_2O_3 + TiC ceramic tool (Narutaki *et al.*, 1993). Ezugwu and Lai (1995b) carried out drilling of Inconel 901 using M35 HSS tool with the split-point 120° (unground) and others ground to different geometries. The unground 120° split-point drills exhibited overall best performance than others, whilst overall worst performance was found with drill with 4 facet and double-angle point. Superior performance unground drill was ascribed to possible formation of ferrous oxide film on the drill lips, unlike other drill geometries where this film was removed during subsequent grinding to the appropriate geometry. This caused rise in friction at the tool-workpiece interface and hence increase in temperature resulting in high wear. At low cutting parameters (325 rpm and feed of 26 mm/min) plucking of carbide particles were observed whereas high cutting parameters (410 rpm and 32 mm/min) led to fracture of cutting edge.

Choudhury and EI Baradie (1998), Ezilarasan *et al.* (2013b) and Thakur *et al.* (2009a, 2010) utilising various optimization techniques found V_c and feed to be the most influential factors affecting tool wear and tool life. It can be claimed that wear mechanism may vary with cutting parameters. Selection of cutting parameters is closely pertained to work-tool material combination. For turning of Inconel 718 with K20 carbide insert, the optimal setting of cutting parameters was found to be cutting speed of 50 m/min, feed rate of 0.05 mm/rev and DOC of 0.5 mm (Thakur *et al.*, 2009a). On the other hand, cutting speed of 210 m/min, with same feed and depth of cut was determined as optimal cutting parameters while adopting whisker reinforced ceramic inserts (Ezilarasan *et al.*, 2013b).

2.3.3 Effect of cutting environment

Cutting fluids for machining processes must be selected to minimize tooling costs, while achieving high quality of the machined surfaces and minimizing environmental impact. Podder and Paul (2008, 2012) demonstrated that high pressure cooling had good potential in curtailing tool wear during machining nickel-based super alloys. Ezugwu and Bonney (2004) noted improvement in tool life with increase in coolant pressure (110, 150 and 203 bar) except for V_c of 20 m/min at high pressure (203 bar) while using carbide tool. It is because of increase in chip-tool contact temperature and consequently tool wear. Similar study was carried out utilising WRA ceramic tool for finish mode machining (V_c of 250, 270 and 300 m/min) and observed the critical pressure of 150 bar (15 MPa). A maximum improvement in tool life of 71% was reported under a condition of V_c of 250 m/min and feed of 0.2 mm/rev while utilising a coolant pressure of 150 bar. Higher coolant pressure of 203 bar was proven to be detrimental under all cutting condition which was due to severe notch wear (Ezugwu and Bonney, 2005). Notch wear at the DOC region is usually the most serious issue when machining nickel-based alloys using ceramic tools under high-pressure cooling whereas, adhesion of workpiece to the tool surface could be prevented. According to the observation of Sharman *et al.* (2008b) and Vagnorius and Sørby (2011), although increase in coolant pressure on flank face caused less flank wear than flood cooling, no improvement in notch wear and hence tool life could be detected. Additionally Sharman *et al.* (2008b) found increase in coolant pressure could be detrimental on rake surface. According to Ezugwu and Bonney (2004), formation of DOC notch could be explained by the hydrodynamic erosion. It has been suggested that when the jet hits the tool there is an instantaneous seizure leading to build up of stagnation pressure. The jet of fluid tries to find an escape route through DOC region to release the pressure. Small abrasive particles contained in the fluid flow at high cutting speed cause significant DOC notch. Increase in fluid pressure further deteriorates the situation (Ezugwu *et al.*, 1990; Machado *et al.*, 1998; Öjmertz and Oskarson, 1999). Lowering of tool life under elevated pressure cooling could also be attributed to reduction in chip-tool contact length without corresponding reduction in cutting force. Increase in cutting force during high pressure cooling is caused by high reactive forces (Ezugwu and Bonney, 2004). Ezugwu *et al.* (2004) also demonstrated that coolant concentration was not effective at low cutting speed (68 m/min). However, medium concentration of cutting fluid (6%) resulted in highest tool life under high V_c of 136 m/min. Further increase in coolant concentration (upto 9%) in fact caused tool failure due to severe chipping. This was attributed to brittleness of cutting tool due to quenching effect caused by high temperature generation and enhanced rate of cooling.

Tool life was increased by using MQL when compared to dry machining due to reduction in frictional rubbing between tool flank and machined surface (Thamizhmanii *et*

al., 2009). Obikawa *et al.* (2008) utilised microliter lubrication (less than 0.1 ml/h) during high speed finish turning of Inconel 718 using multilayer ($TiCN/Al_2O_3/TiN$) CVD coated tool. The cover-type nozzle for oblique spraying exhibited better performance than that for cover-type normal spraying and ordinary nozzle. This can be attributed to control of oil mist flow and shortening of the distance of the nozzle from the tool tip. Cryogenic cooling has deleterious influence on milling of nickel based super alloys (Podder and Paul, 2008, 2012; Shokrani *et al.*, 2012). It was explained by fluctuation of temperature and force typically observed in an intermittent machining process such as milling. Application of liquid nitrogen (LN2) caused dominant thermomechanical fatigue leading to failure of tool by severe edge chipping (Podder and Paul, 2008, 2012). Recent study of Zhuang *et al.* (2015) however, exhibited superior performance of cryogenic cooling compared to conventional wet machining during turning of Inconel 718. This was ascribed to effective scaling down of cutting zone temperature. Zhuang *et al.* (2015) also demonstrated that the performance of plasma enhanced machining (PEM) was superior to dry machining, but inferior to cryogenic machining.

Obikawa *et al.* (2012) developed air jet assisted (AJA) cooling technique which improved tool life by 20-30% in comparison with wet machining for jet angle of cutting fluid of 10-30˚. The study also established that influence of oxygen on wear mechanism was negligible, since no difference in tool life could be detected utilising nitrogen jet assisted (NJA) cooling instead of AJA cooling. Additionally, Kamata and Obikawa (2007) found low specific heat and thermal conductivity of argon gas also contributed to accelerated growth of tool wear. With the help of computation fluid dynamic simulation it was also demonstrated that the onus of air jet was to assist the cutting fluid to effectively penetrate into the narrow cutting zone thereby augmenting heat transfer. Any possibility while utilising AJA technique can be negated by using additional amount of cutting fluid (Obikawa *et al.*, 2012, 2015). Modified nanofluid consisting of water-soluble nano-particle of size 5–23 nm was effective in augmenting the tool life of uncoated and coated tools by 2-3 times compared to traditional cutting fluid during drilling of Inconel 718 (Chen and Liao, 2003).

2.3.4 Effect of tool condition

Positive rake has been found to be beneficial in reducing chip-tool contact length, temperature and pressure and hence, was successful in diminishing tool wear (Ezugwu and Pashby, 1992). Carbide tools with large nose radii generally exhibited lower mechanical stress threshold than those with smaller nose radii in intermittent cutting operations. As a result, tools with larger nose radii rendered lower tool life (Ezugwu and Okeke 2000a; Ezugwu *et al.*, 2000b). Owing to high resistance to notch wear of round insert along with

honed edge, it performed the best in comparison with square (Coelho *et al.*, 2004; El-Bestawi *et al.*, 1993), triangular (Coelho *et al.*, 2004) and rhomboid shape inserts (Ezugwu and Tang, 1995a; Khan *et al.*, 2012). According to Rahman *et al.* (1997), side cutting edge angle (SCEA) plays an important role in determining the tool life during machining of Inconel 718. As SCEA increases tool life increases. With increase in SCEA, distribution of heat covers a larger length of cutting edge and consequently reduces notch wear. Longest tool life was obtained with sharp cutting edge along with SCEA of 45°owing to less notch wear when compared with tools with robust cutting edge and SCEA of 0° (Cantero *et al.*, 2013). Tool with chip breaker induced less abrasion wear at depth of cut region by lifting the chip off the rake face and hence, elevated the tool life of the tool without chip breaker (Sharman *et al.*, 2004a, 2006).

2.4 Chip characteristics

Formation of chips plays a pivotal role in the research in machining as it has close interrelationship with cutting force, temperature, machined surface roughness, tool wear and overall production rate. The production of stringy continuous chips during machining causes not only risk and hazard to the operator but can also result in the deterioration of the machined surface as well as hindrance in machining and chip disposal problems (Machado *et al.*, 1998). During machining, chip should be ideally short. Continuous chips should be broken into short sections by a suitably designed chip breaker and removed from working area in one direction (Wojciech and Słodki, 2013). The chip morphology during machining is not only dependent on tool materials and cutting parameters but others factors like grain size, hardness of the workpiece material, geometry has significance influence on types of chips (Cai *et al.*, 2014; Jin and Liu, 2012; Olovsjö *et al.*, 2010a; Olovsjö and Nyborg, 2012).

Formation of adiabatic shear band occurs due to thermoplastic instability when the rate of thermal softening exceeds the rate of strain hardening (Davies *et al.*, 1997; Hao *et al.*, 2011; Joshi *et al.*, 2013; Komanduri and von Turkovich, 1981; Sun *et al.*, 2009; Wan *et al.*, 2012). This shear band is responsible for generation of segmented or serrated (also known as shear localised) chips during machining of workpiece materials such as titanium and nickel-based super alloys having low thermal conductivity or those with elevated strength like hardened steel (Chen and Liao, 2003; Dong *et al.*, 2011; Hao *et al.*, 2011; Komanduri, *et al.*, 1982; Komanduri and Schroede, 1986; Pawade *et al.*, 2007; Thakur *et al.*, 2012b). Initiation and propagation of cracks inside the primary shear zone are also considered to be responsible for formation of serrated type of chip (Komanduri and Schroede, 1986). According to Olovsjö and Nyborg (2012), serration of chips is more prominent for coarser grain of workpiece as it consumes greater force to deform larger grain than smaller one. According to Lee *et al.* (1979), serration is more prominent in material with strong work

hardening tendency. Formation of segmented or serrated chips leads to fluctuation of cutting force. (Cai and Dai, 2014; Davies *et al.*, 1997; Hao *et al.*, 2011). Barry and Byrne (2002) and Cai and Dai (2014) have demonstrated that both the phenomena of thermal softening and strain hardening responsible for segmented chips depend heavily on cutting parameters, thermo-mechanical properties of workpiece and cutting tool.

2.4.1 Effect of cutting parameters

Cutting parameters, speed in particular, have significant role on formation of different types of chips such as continuous, segmented (or shear localised) and isolated (or separated) during machining of nickel-based super alloys (Komanduri and Schroede, 1986; Pawade and Joshi, 2011). When machining Inconel 718 at low cutting speed of less than 30 m/min, continuous and coiled chips were observed. Beginning of shear localization of chip occurred at the range of 60-90 m/min in the form of long coils (Komanduri and Schroede, 1986). Similar range of cutting speed (40-80 m/min) favourable for segmented chips has also been discussed by Dong *et al.* (2011). Enhanced chip segmentation with rise in cutting speed is typically related to greater size of lamellar structure in terms of width and depth observed on free surface of the chips. Formation of such lamellar structure is a clear evidence of segmented chips (Zheng *et al.*, 2013). Higher degree of thermoplastic instability as a result of rise in strain rate and thermal deformation might be the possible explanation for increase in chip segmentation. According to Komanduri and Schroede (1986), more severe shear localization is caused by poorer thermal conductivity of workpiece material due to higher heat accumulation in narrow zone (shear band) and also by high resistance to deformation of individual chip segments. Therefore, elevation of cutting speed to a high value (typically more than 150 m/min) might lead to an actual separation of individual chip segments, termed as isolated chips. Different observation was also made by Ezugwu and Tang (1995a). Long and continuous type of chips were obtained when machining at cutting speed of 152 m/min, at feed of 0.25 mm/rev and depth of cut of 2 mm. Although it was not mentioned, difference in cutting environment i.e. dry or wet machining might be the plausible cause for such contradiction. Formation of different types of chips also depends on thermomechanical properties of workpiece material (El-bestawi *et al.*, 1993).

Thakur *et al.* (2009b, 2012a) demonstrated that increase in cutting speed resulted in decrease in chip thickness, whereas increase in the feed rate increased in chip thickness. Similarly, increase in the chip-tool contact area also resulted in thicker chip at higher depth of cut (Thakur *et al.*, 2009c). There was a change in shape of chip burr from triangle to square due to increase in cutting speed during turning of Hastelloy C-276 with uncoated tool owing to more lateral deformation causing side flow (Khidhir and Mohamed, 2010). Segmented chips for a particular work material can be characterised by different means.

These include shear band thickness, saw-tooth distance, equivalent chip thickness, saw-tooth angle, shear angle and chip segmentation frequency (Wang *et al.*, 2014). Most of these aspects of serrated chips are primarily influenced by shear deformation, strain hardening and thermal deformation. However, there is no clear agreement among researchers on characteristics of segmented chips of nickel-based super alloys. Dong *et al.* (2011) reported a fall in saw-tooth distance (distance between the successive teeth) with cutting speed, hence the frequency of serrated chip (reciprocal to the saw-tooth distance) increased. On the contrary, Zhang *et al.* (2013) reported that the frequency of segmentation of saw-tooth type of chip decreased with increase in cutting speed. However, the saw-tooth became more prominent under the condition of high cutting speed (50 m/min). The degree of chip segmentation was more at higher speed of 180 m/min with segments being closer than that at lower cutting speed (Lorentzon *et al.*, 2009). The frequency of serrated chip initially decreased upto feed rate of 0.16 mm/rev but increased thereafter, while saw-tooth distance obviously followed the reverse trend (Dong *et al.*, 2011). Arunachalam and Mannan (2000) and Gatto and Iuliano (1997) noted an increase in size of chip segments with elevation of feed owing to larger undeformed chip thickness.

2.4.2 Effect of cutting environment

The formation of chip is influenced by cutting conditions as well as coolant pressure. The use of high pressure coolant led to effective chip segmentation due to reduction in tool-chip contact length/area. The tendency of the chip to lift off increased because of high pressure causing early fracture of chip. Long, continuous and spiral chips were obtained when machining Inconel 718 at low coolant pressure of 150 bar whereas at high coolant pressure of 250 bar, there was a fall in chip curl radius resulting in the formation of segmented chips (Ezugwu and Bonney, 2004; Machado and Wallbank, 1994). Similar observation was reported by Courbon *et al.* (2009) and Ezugwu and Bonney (2005). Dry machining of Inconel 718 resulted in generation of long and only slightly curled type chip, while short and tightly curled chips were obtained when machining under high jet pressure (Ojmertz and Oskarson, 1999). Elevation of jet pressure was also beneficial in reducing the chip thickness.

2.4.3 Effect of tool condition

The geometry and shape of the cutting insert also play a major role (Ezugwu and Pashby, 1992). Increase in SCEA affected a rise in width and thickness of deformed chip owing to decrease in true feed and undeformed chip (Rahman *et al.*, 1997). Pawade *et al.* (2007) observed reduction in chip thickness ratio by the use of chamfered and honed edge tool owing to higher plastic deformation.

2.5 Surface integrity

The surface integrity characteristics affect the functional performance by controlling tribological phenomena in terms of friction and wear behavior of contacting bodies, lubrication efficiency, stress corrosion, growth of fatigue cracks etc. (Guo *et al.*, 2009; M'Saoubi *et al.*, 2008; Pervaiz *et al.*, 2014; Ulutan and Ozel, 2011). Different aspects of surface integrity have been discussed in section 1.3.6.

During machining some visual defects have detrimental influence on surface integrity. Different types of surface defects during machining of nickel-based super alloys are detailed in Table 2.1.

Table 2.1: Different surface defects after machining nickel-based super alloys (Thakur and Gangopadhyay, 2016).

Defects	Different grades	Description
Tearing surface	Inconel 718 (Chang *et al.*, 2015), FGH95 (Jin and Liu, 2013), Inconel 825 (Thakur *et al.*, 2015a), Hastelloy C-2000 (Razak *et al.*, 2014).	Any surface defect except natural defects like feed marks can be termed as tearing surface. These are described below.
Surface cavities/ crack/ micro void	Inconel 718 (Chang *et al.*, 2015; Sharman *et al.*, 2004a; Zhou *et al.*, 2012), FGH95 (Jin and Liu, 2013), NiCr20TiAl (Zou *et al.*, 2009), Inconel 825 (Thakur *et al.*, 2015a).	Cavities may arise due to workpiece material's inhomogeneity and tool wear. Machining with worn tool might induce severe plastic deformation resulting in lateral displacement or material side flow and hence fine groves. Portion of the material might be removed leaving cavity. Nickel-based super alloys are often characterised by non-uniform distribution of hard and abrasive particles (γ′ and γ′′ phases) including carbides. These particles resist plastic deformation and lead to crack initiation to relieve strain.

Grooves	Inconel 718 (Arunachalam *et al.*, 2004a; Chang *et al.*, 2015; Sharman *et al.*, 2004a; Zhou *et al.*, 2012), RR1000 (Axinte *et al.*, 2006), Inconel 825 (Thakur *et al.*, 2014b), Nimonic C-263 (Ezilarasan *et al.*, 2013a), Hastelloy C-2000 (Razak *et al.*, 2012).	In addition to feed mark ridges which are natural surface defects, grooves can also be formed due to dragging by chipped off materials of tools or ploughing by chips bonded to the tools.
Metal debris	Inconel 718 (Arunachalam *et al.*, 2004a; Sharman *et al.*, 2004a), RR1000 (Axinte *et al.*, 2006), Inconel 825 (Thakur *et al.*, 2014b), Nimonic C-263 (Ezilarasan *et al.*, 2013a), Hastelloy C-2000 (Razak *et al.*, 2012).	Material debris of around 1–2 mm of size is deposited on the machined surface produced at high cutting condition. Chipping of tool edge or nose and micro fragmentation of chips are primary source.
Smeared material	Inconel 718 (Arunachalam *et al.*, 2004a; Axinte *et al.*, 2004; Pawade and Joshi, 2012), RR1000 (Axinte *et al.*, 2006; Soo *et al.*, 2011), FGH95 (Jin and Liu, 2013), NiCr20TiAl (Zou *et al.*, 2009), Inconel 825 (Thakur *et al.*, 2015a), Hastelloy C-2000 (Razak *et al.*, 2014), Haynes 282 (Hood *et al.*, 2012).	Smearing takes place due to severe plastic deformation caused due to squeezing action between auxiliary flank and machined surface during progression of tool. This is similar to material side flow.
Plucking	Inconel 718 (Marinescu and Axinte, 2008, 2009, 2011; Shi *et al.*, 2007), NiCr20TiAl (Zou *et al.*, 2009), Inconel 825 (Thakur *et al.*, 2014a), Hastelloy C-2000 (Razak *et al.*, 2014), RR-X (Axinte *et al.*, 2006).	Material may be plucked of machined surface due to dragging by harder carbide particles of worn or micro fractured tool thus causing material pile-up.
Laps	RR-X (Axinte *et al.*, 2006), Inconel 718 (Axinte *et al.*, 2004; Marinescu and Axinte, 2008, 2009).	Material folded onto the surface.
Redeposited material	RR-X (Axinte *et al.*, 2006), Inconel 825 (Thakur *et al.*, 2014b), NiCr20TiAl (Zou *et al.*, 2009).	Adhesion of foreign particles consisting of chip fragments or chipped off tool materials over the machined surface.

Ezugwu and Tang (1995a), Ezugwu *et al.* (1999), Pawade *et al.* (2008), Sharman *et al.* (2004a, 2004b) and Umbrello (2013) found higher hardness of surface and sub-surface than the bulk material. Ezilarasan *et al.* (2013a), Sharman *et al.* (2004a, 2004b), Thakur *et al.* (2014b, 2014c) on the other hand, reported microhardness at surface region to be less than that at sub-surface region. One of the possible mechanisms is predominant thermal softening (Che-Haron and Jawaid, 2005; Ginting and Nouari, 2009; Sun and Gou, 2009). The studies of Outeiro *et al.* (2008), Peng *et al.* (2013a, 2013b), Sharman *et al.* (2004b) and Zhou *et al.* (2014) indicated that residual stress on surface was primarily tensile in nature which gradually became compressive at the sub-surface region during machining of nickel-alloys. On the contrary, Bushlya *et al.* (2012) and Coelho *et al.* (2004) have also noted compressive residual stresses throughout. This deviation in result can be attributed to the competing influences arising from both thermal and mechanical deformation under a particular machining condition.

2.5.1 Effect of tool material including coating

Mechanical and thermo-physical properties of tool materials contribute to modification of surface integrity characteristics of nickel-based super alloys. Akhtar *et al.* (2014) reported superior surface integrity with carbide tool than ceramic tool. According to Ezugwu *et al.* (1999), types of tool coating also have some influences on surface roughness. Single layer TiN coated carbide insert registered lower surface roughness than multilayer coating (Ezugwu *et al.*, 1999; Nalbant *et al.*, 2007) owing to honed edge and uniform flank wear of the former. It was found that excessive chipping of sharp edges in PVD multilayer (TiN/TiCN/TiN) coated insert and notching of edges in CVD multilayer coated insert resulted in poor surface finish. CVD multilayer (TiN/TiCN/Al_2O_3/ZrCN) coated tool resulted in poor surface finish than its uncoated counterpart. This was explained by rougher surface morphology of CVD coating along with larger edge radius compared to the uncoated tool (Thakur *et al.*, 2014a, 2014b). Similar observation was also noted by other researchers who studied surface roughness using uncoated and TiN coated cBN tool (Bushlya *et al.*, 2012; Zhou *et al.*, 2012). However, different observation has also been reported (Motorcu *et al.*, 2014). Performance of the coated tool in modifying surface roughness during machining of nickel-based super alloys seems to have been primarily evaluated in terms of either edge preparation prior to coating or alternation of edge radius due to deposition process. Actual role of coating materials or coating architectures (i.e. single, bilayer or multilayer configuration) could be studied by maintaining the identical condition of cutting edge.

Effect of multilayer coating (TiN/TiCN/Al_2O_3/ZrCN) was also studied on micro morphology of the surface. It was seen that the evidence of dynamic recrystallization

(DRX) at cutting speed of 124 m/min was observed during machining of nickel-based super alloy. Uncoated tool exhibited formation of new undeformed recrystallized grains due to high cutting temperature. On the other hand, in the absence of high cutting temperature which was required for grain growth, coated tool resulted in machined surface with micromorphology which was pre stage of grain growth. The surface revealed large number of nucleation sites which is responsible for grain refinement. Due to the capability of the coated tool to circumvent detrimental thermal influence, it is also possible to decrease white layer thickness under different cutting condition (Thakur *et al.*, 2014b).

Due to reduction in deformed layer thickness, coated tool also has a potential to arrest the tendency of work hardening (Thakur *et al.*, 2014b). Since the phenomena is related to mechanical deformation factored by tool wear among other parameters, superior resistance to tool wear of coated tool compared to that of its uncoated counter part is also significant point to be noted. However, if the thermal conductivity of the coated tool is less, then prominent thermal effect may again be expected leading to possibility of more work hardening than the unoated tool. This might be the reason why Zhou *et al.* (2012) observed slightly higher value of microhardness with coated cBN tool than uncoated cBN during machining of Inconel 718.

The same thermal conductivity of cutting tool might be the deciding factor for residual stress as well. Lower thermal conductivity of the tool would cause dominance of the thermal influence resulting in residual stress to be more tensile. Due to this fact, mixed alumina ceramic insert effected higher tensile stress than cBN or PCBN tools during machining Inconel 718 (Arunachalam *et al.*, 2004a; Coelho *et al.*, 2004; Zhou *et al.*, 2014). Surface compressive stress obtained with PCBN tool was ascribed to its higher thermal conductivity responsible for effective dissipation of heat from the cutting zone (Zhou *et al.*, 2014). Similar results on higher surface tensile stress have also been reported with tool having lower thermal conductivity coating material (Bushlya *et al.*, 2012; Sharman *et al.*, 2004b). Moreover, higher deformation depth obtained with coated tool than the uncoated one might be related to greater mechanical-induced deformation caused by higher edge radius of the coated tool (Bushlya *et al.*, 2012). Similar observation has also been reported by Outerio *et al.* (2008). However, the contribution of tool coating in influencing the residual stress was not free from contradiction. Different observation was noted with uncoated tool showing higher surface tensile stress than that of coated tool during machining RR1000 nickel-based super alloy (Li *et al.*, 2006b, 2009). Although coating composition was not known, the contradiction was apparently related to either difference in properties of tool coating, workpiece materials or different machining conditions used.

2.5.2 Effect of cutting parameters

According to general agreed upon results for different grades of nickel-based super alloys, there is a decrease in surface roughness with increase in cutting speed (Devillez *et al.*, 2011; Ezilarasan *et al.*, 2013a, 2013b; Fan *et al.*, 2013; Habeeb *et al.*, 2010; Hood, *et al.*, 2012; Nalbant *et al.*, 2007; Pawade *et al.*, 2008; Sharman *et al.*, 2004a, 2004b; Umbrello, 2013). Fan *et al.* (2013) explained this phenomenon by the reduction in BUE, cutting force along with vibration. On the contrary, studies of Habeeb *et al.* (2008), Motorcu *et al.* (2014) and Thakur *et al.* (2014a, 2014b) also reported increase in surface roughness with cutting speed particularly when tool wear becomes a decisive factor (Thakur *et al.*, 2014a, 2014b). Selected range of cutting speed is also important in the discussion of surface roughness (Jin and Liu, 2012, Thakur *et al.*, 2015b). In a separate study, Ezilarasan *et al.* (2013a) attributed decrease in surface roughness in the initial range of cutting speed to thermal softening phenomenon, while subsequent increase in surface roughness at higher range of cutting speed was related to tool wear. The results are, however, in contradiction with those reported by Cai *et al.* (2014). In fact, no clear trend of variation between cutting speed and surface roughness could be found (Ezilarasan *et al.*, 2011, 2013a; Habeeb *et al.*, 2008; Jin and Liu, 2012). These apparent contradictions can be explained if key phenomena e.g. formation of BUE, friction, tool wear and temperature are taken into consideration. Feed rate has been found to be the most dominant factor for surface roughness. Many researchers have noted increase in surface roughness with feed rate (Cai *et al.*, 2014; Darwish, 2000; Ezugwu *et al.*, 1999; Ezilarasan *et al.*, 2011, 2013a; Habeeb *et al.*, 2010; Joshi *et al.*, 2008; Sharman *et al.*, 2004a; Umbrello, 2013). Ezugwu *et al.* (1999) and Umbrello (2013) explained by either increased feed marks or generation of enhanced cutting load at the edge of the tool inducing more plastic deformation resulting in higher surface roughness. Ezilarasan *et al.* (2011, 2013b) further observed that depth of cut could also influence surface roughness. It was seen that as depth of cut increased, surface roughness decreased. On the contrary, Darwish (2000) reported increasing trend of surface roughness with depth of cut with variable feed of 0.075 and 0.3 mm/rev and cutting speed of 32 and 125 m/min, while Arunachalam *et al.* (2004a) noticed the same using feed of 0.15 mm/rev along with V_c of 225 m/min. Ezilarasan *et al.* (2011) determined optimal cutting parameters of V_c of 54 m/min, feed of 0.051 mm/rev and a_p of 1mm for good surface finish during machining of Nimonic C-263 with PVD coated carbide tool.

The depth of deformed layers in the sub-surface region increases with elevation in cutting parameters owing to increase in cutting temperature (Bushlya *et al.*, 2011; Ezilarasan *et al.*, 2012; Imran *et al.*, 2011; Jin *et al.*, 2011; Jin and Liu, 2012, 2013, Jin and Shaoyu, 2014; Umbrello, 2013; Zhou *et al.*, 2011). According to Imran *et al.* (2011), strain rate in cutting region also increases resulting in higher amount of plastic deformation and hence rise in thickness of white layer. However, Jin and Liu, (2012, 2013) and Jin and Shaoyu (2014) could not establish consistent trend of variation of white layer with cutting

speed. Decrease in white layer thickness with increase in V_c was also observed by Klocke *et al.* (2013), Sadat (1987) and Veldhuis *et al.* (2010). One of the possible explanations might be lower residence time of moving heat source leading to reduced level of thermal energy transferred to machined surface although temperature of cutting edge is higher.

Few investigations have conveyed occurrence of phase change in the white layer region. Veldhuis *et al.* (2010) utilised XRD data of white layer at cutting speed of 50 m/min to reveal formation of γ-alumina phase which was believed to be brittle, abrasive and thermally resistant ceramic layer which prevented heat to be evenly absorbed by core of machined surface. This undesirable phase was absent during machining with cutting speeds of 30 and 40 m/min indicating that phase change is thermal phenomenon. Umbrello (2013) studied the influence of cutting speed and feed on grain size and microstuructural alteration. However, cutting speed of 70 m/min and feed of 0.1 mm/rev resulted in formation of an extra phase of γ'' which was the outcome of nucleation and coarsening of γ' particles. The precipitated γ'' phase along with γ' is responsible for enhancing heat resistance property of Inconel 718. Phase change during machining of super alloy is a debatable issue since Herbert *et al.* (2012a, 2012b), Jin and Shaoyu (2014) and Thakur *et al.* (2014b) could not detect any change of phase.

According to general observation, hardness of surface and sub-surface layer increases with cutting speed (Ezugwu and Tang, 1995a; Ezugwu *et al.*, 1999; Ezilarasan *et al.*, 2013a; Jin and Liu, 2012, 2013; Madariaga *et al.*, 2014; Pawade *et al.*, 2008; Wusatowska-Sarnek *et al.*, 2011; Thakur *et al.*, 2014b; Umbrello, 2013; Vincent *et al.*, 2010;). Increase in V_c usually results in high strain rate and increase in cutting temperature. The combined effect causes the thickness of both thermally affected layer and plastic deformation zone to increase leading to strain hardening of super alloys (Sharman *et al.*, 2004a, 2004b). Work hardening demonstrates increasing trend with feed (Ezugwu *et al.*, 1999; Ezilarasan *et al.*, 2013a) and depth of cut (Ezugwu *et al.*, 1999; Pawade *et al.*, 2008) owing to high cutting force during turning of Inconel 718. On the other hand, Hood *et al.* (2012) could not detect any significant variation with cutting parameters during milling of Haynes 282. Degree of work hardening can be reduced by optimal cutting parameters. Pawade *et al.* (2008) obtained minimum degree of work hardening (DWH) with optimal combination of cutting parameters consisting of V_c of 300 m/min, high feed of 0.15 mm/rev and low a_p of 0.5 mm during machining of Inconel 718 with 20° chamfered edge insert.

Like other aspects of surface integrity the residual stress also depends on cutting parameters. Some investigators found that with increase in the cutting speed, the residual stress tended to shift from compressive to tensile. This can be attributed to the rise in temperature of the machined surface, indicating thermal dominance at higher cutting speed (Arunachalam *et al.*, 2004a; Ezilarasan *et al.*, 2013a). It was also observed that residual stress progressively became more tensile when cutting speed was increased during facing

(Arunachalam *et al.*, 2004a), turning (Berruti *et al.*, 2009; Darwish, 2000; Ezugwu *et al.*, 1999; Sadat *et al.*, 1991; Schlauer *et al.*, 2002), milling (Cai *et al.*, 2014; Guerville *et al.*, 2004; Peng *et al.*, 2013a) of Inconel 718. On the other hand, different result can be expected if worn tools are used. According to Sharman *et al.* (2004b), increase in cutting speed possibly induces strain hardening which causes surface tensile stress to increase and compressive stress to be deeper. In another study of Pawade *et al.* (2008), apart from usual hike in tensile residual stress with elevation of cutting speed in the range of 125-300 m/min, deviation in trend was also noted at a V_c of 475 m/min. In addition to considerable strain hardening at such a high V_c, there can be faster dissipation of heat by the chips, thus not allowing significant heat to be diffused into the work material. Similar decrease in surface tensile stress with increase in V_c (40-80 m/min) has also been reported and explained similarly by Devillez *et al.* (2011). Similar competing mechanism of mechanical and thermal induced deformation has also been found on the influence of feed on residual stress. Most of the researchers observed increase in tensile residual stress at the surface with increase in feed (Berruti *et al.*, 2009; Pawade *et al.*, 2008; Sharman *et al.*, 2004b, 2015; Thakur *et al.*, 2014b) and attributed to increase in heat generation caused due to greater work done to remove larger volume of chips. On one hand, Arunachalam *et al.* (2004a) observed decrease in compressive stress was reported when depth of cut increased from 0.05 to 0.5 mm during face turning of age hardened Inconel 718, whereas Pawade *et al.* (2008) reported increase in compressive residual stress with depth of cut (from 0.5 to 1 mm) during turning of Inconel 718. Due to directional characteristics of stress, different trend is perhaps not unexpected for straight and face turning operations. Moreover, during machining of age hardened workpiece, more pronounced thermal effect might cause decrease in compressive residual stress (Arunachalam *et al.*, 2004a).

2.5.3 Effect of cutting environment

Since temperature has major influence on surface integrity particularly for nickel-based super alloys, use of cutting fluids and their modes of application needs to be critically evaluated. Some of the researchers studied the effect of coolants and their modes of application on machined surface roughness of Inconel 718. Superior surface finish in wet machining was attributed to the ability of coolant to prevent adhesion wear leading to reduction in BUE formation (Arunachalam *et al.*, 2004a, 2004b; Cantero *et al.*, 2013; Kaynak, 2014). Podder and Paul (2008, 2012) utilised different cooling techniques like conventional, cryogenic and high pressure cooling (50 bar) during machining of Nimonic C-263. It was found that cryogenic and high pressure cooling resulted in lower surface roughness than conventional cooling. Beneficial effect of high pressure cooling in diminishing surface roughness has also been discussed by Ezugwu *et al.* (1990), Ezugwu

and Bonney (2005) and Machado and Wallbank (1994). Owing to effective penetration of cutting fluid into the interface between flank and machined surface, frictional rubbing and hence tool wear can be brought down, leading to reduction in surface roughness. On the other hand, in the work reported by Obikawa *et al.* (2012) different cooling techniques such as conventional wet machining, air jet assisted (AJA) and nitrogen jet assisted (NJA) machining in comparison with dry machining could not show any improvement of surface finish.

Nevertheless, application of MQL can improve surface finish with relation to that obtained by dry machining owing to better cooling and lubrication efficiency at the chip-tool and work-tool interface. Furthermore, reduction in surface roughness with increase in flow rate of MQL might be associated with less tool wear (Behera *et al.*, 2014; Thamizhmanii *et al.*, 2009; Yazid *et al.*, 2011). Yazid *et al.* (2011) recommended to increase flow rate of MQL proportionally with cutting speed in order to achieve same beneficial effect in terms of reduction in surface roughness. Superior surface finish was obtained with cryo MQL compared to dry machining and flood cooling with cryogenic (Pusavec *et al.*, 2011). Shokrani *et al.* (2012) attributed to the fact that cryogenic cooling affected the surface area of the workpiece making it harder, requiring additional force to cut and consequently resulted in rougher surface (Aramcharoen and Chuan, 2014). Pusavec *et al.* (2011) explained that cryo MQL being directed to the narrower region of chip-tool contact helped to get rid of this influence and obtain better surface finish. However, the beneficial effect of cryogenic machining was superseded by the higher rate of tool wear with progression of machining. In fact, dry machining recorded lower surface roughness after longer machining length, since more severe chipping occurred during cryogenic machining resulting in shorter tool life (Shokrani *et al.*, 2012).

Dry machining induces more sub-surface damage and microstructural deformation as compared to machining carried out under conventional wet (Devillez *et al.*, 2011) and MQL mode (Yazid *et al.*, 2011). Although cryogenic cooling leads to surface hardening, depth of work hardened layer is less and no significant microstructural alteration may be detected with respect to that of bulk material (Pusavec *et al.*, 2011; Aramcharoen and Chuan, 2014). At the same time, use of cryogenic cooling also has potential to decrease thickness of plastic deformation zone compared to dry and conventional cooling (Pusavec *et al.*, 2011; Aramcharoen and Chuan, 2014; Yildiz and Nalbant, 2008). Interestingly, different observation on influence of cutting fluid was noted during micro drilling of Inconel 718 by Imran *et al.* (2014). Less depth of both deformation layers in dry machining in comparison with those under wet environment can be possibly explained by the increased difficulty of penetration of cutting fluid into the machining zone during micro drilling operation resulting in non-uniform heat transfer.

Machined surface hardness is significantly influenced by cutting environment. Dry machining resulted in higher hardness value than both MQL (Yazid *et al.*, 2011) as well as wet (Devillez *et al.*, 2011) machining. MQL or wet machining reduces friction between tool-work interface thereby bringing down severity of plastic deformation and also temperature (Yazid *et al.*, 2011). Effective hardening of surface layer of Inconel 718 could also be achieved with the help of cryo machining (in conventional or MQL mode). Rapid heating and cooling might be responsible for high hardness in cryogenic cooling. Pusavec *et al.* (2011) further recommended to carry out pre-cooling of tool and workpiece which would bring down their temperature in order to achieve high surface hardness. Similar observation of higher hardness with cryo cooling in comparison with other modes (conventional and high pressure cooling) has also been reported during milling of Nimonic C-263 by Podder and Paul (2008, 2012). Viscosity of cutting fluid also has some role in modifying work hardening phenomena. Rahim and Sasahara (2011) observed that palm oil owing to lower viscosity than synthetic ester reduced the microhardness by providing effective lubrication and cooling. Imran *et al.* (2014) could not establish, significant difference of nanohardness on surface and sub-surface region using dry and wet environment.

Use of coolant can lower friction as well as cutting temperature. As a result, it has the capability of negating thermal dominance resulting in reduction in tensile residual stress when compared to dry machining. However, this trend is prominent under lower range of V_c (40-60 m/min). Cutting fluid may not maintain its effectiveness at higher cutting speed particularly under flood cooling mode, resulting in no significant difference in residual stress under dry and wet condition (Devillez *et al.*, 2011). Pusavec *et al.* (2011) observed that deeper compressive residual stress developed with cryo machining in comparison with machining under dry and MQL mode. Sharman *et al.* (2008b) demonstrated that ultra-high-pressure (450 bar) coolant was more helpful in reducing surface tensile residual stress than flood cooling owing to the capability of the coolant to effectively penetrate into the tool flank-work interface.

2.5.4 Effect of tool condition

Shape and condition of cutting edge also have great deal of influence on machined surface roughness of nickel-based super alloys. Arunachalam *et al.* (2004a, 2004b), Coelho *et al.* (2004) and Nalbant *et al.* (2007) utilised round insert with large nose radius to produce better surface finish than square insert, due to large contact length of the tool. According to Arunachalam *et al.* (2004a), sharp cutting edge with lower resistance to chipping produces higher surface roughness than honed cutting edges. Axinte and Andrews *et al.* (2007) established that if rough drilling was followed by plunge milling without any chamfer

angle, the same could result in superior finish than reaming. The performance of reaming could, however, be enhanced by reducing chamfer angle owing to less contact area between machined surface and tool. Cutting orientation and tilt angle should also be considered especially during milling of nickel-based super alloys. Aspinwall *et al.* (2007) showed that minimum surface roughness was obtained for horizontal downward movement of the cutter with workpiece tilted at an angle of 45˚.

Arunachalam *et al.* (2004b), Beera *et al.* (2014) and Pawade *et al.* (2008) found that the degree of work hardening was largely influenced by the geometry of cutting edge. In study of Ezugwu *et al.* (1999), sharp edged PVD multilayer (TiN/TiCN/TiN) coated carbide insert showed higher amount of hardness than honed edge PVD (TiN) single layer and CVD multilayer (TiC/Al_2O_3/TiN) coated carbide tools. Sharman *et al.* (2004a) used tool with complex chip breaker geometry which caused high curling of chip generating considerable amount of stress at the cutting region leading to high degree of strain hardening. Madariaga *et al.* (2014) exhibited that hardness was also measurably influenced by large nose radius during face turning of Inconel 718 under variable cutting speed of 30-70 m/min, feed rate of 0.15-0.25 mm/rev and constant depth of cut of 0.15 mm. Deep work hardening layer (100 µm) was obtained with large nose radius (4 mm). Although no specific explanation was provided, it is possible that rubbing and ploughing, caused due to increase in nose radius (Arunachalam *et al.*, 2004b; Madariaga *et al.*, 2014), might be responsible for work hardening tendency.

Cutting edge preparation and shape of the tool have significant influence on residual stress during machining nickel-based super alloys. Effect of chamfered tool and that with modified honed edge with 13–38 µm radius were measured on residual stress. It was found that due to negative chamfer on the edge and negative rake angle on the tool holder, all values of residual stress were compressive (Coelho *et al.*, 2004; Muthu *et al.*, 2012). Coelho *et al.* (2004) showed that modified (honed) tool with higher edge radius needed larger cutting force resulting in higher compressive residual stress compared to that of commercial tool without honing. Round insert (Bushlya *et al.*, 2012) or insert with large nose radius (Sharman *et al.*, 2015) can lead to thinning of chips at the trailing edge and formation of chips on round edge. This situation depicts a tool with negative rake angle requiring larger cutting force and increases tendency of ploughing. As a result, compressive stress at sub-surface layer increases with nose radius. It is interesting to note that round inserts demonstrate compressive residual stress at both surface and sub-surface region during machining of nickel-based super alloys (Arunachalam *et al.*, 2004b; Bushlya *et al.*, 2012; Coelho *et al.*, 2004; Zhou *et al.*, 2014). Round and square shaped cBN tool having different edge preparations were utilised in face turning of Inconel 718. Residual stress was measured at a different distance from the periphery of the workpiece. Round tool resulted in compressive stress up to a distance of 15 mm from the periphery and then after tensile

whereas, the square inserts produced tensile stress throughout. However, Arunachalam *et al.* (2004b) clarified that specific comparison was not possible due to difference in edge preparation for both round and square inserts. In contradiction to previous finding, Li *et al.* (2009) observed round insert generated slightly higher amount of tensile stress than the rhombic insert.

2.5.5 Effect of tool wear

Tool wear also plays a prominent role in modifying surface roughness. Chen *et al.* (2014) and Sharman *et al.* (2004a) reported lower surface roughness with worn tool. It was explained by the position of wear scars on flank surface which tended to shift the trailing edge away from it and the same trailing edge acted as wiper to curtail the peaks height of the machined surface. Nevertheless, their argument was valid only when uniform flank wear could be ascertained. Different other modes of tool failure such as chipping of cutting edge and nose, delamination, adhesion and attrition wear might have overriding influence causing surface roughness to increase (Ezilarasan *et al.*, 2013a, 2013b; Jafarian *et al.*, 2014; Motorcu *et al.*, 2014; Shokrani *et al.*, 2012).

Increase in white layer with tool wear was also observed by Jin and Liu (2012) and Zhou *et al.* (2011). The mechanical load is encountered due to the plastic flow of material ahead of the tool resulting in the shear stress and strain produced in the material. According to Zhou *et al.* (2011), thermal effect produced is due to the higher amount of friction caused due to rubbing action at the chip-tool and tool-workpiece interface. The characteristics of deformed layers found during drilling are somewhat different from other processes. Herbert *et al.* (2012a) and Sharman *et al.* (2008a) found an uneven white layer thickness along axial direction during drilling of Inconel 718. This was probably owing to an increase in contact between the workpiece surface and the worn primary and secondary cutting edges causing pull-out/fracture of the white layer when the drill advanced down into the workpiece, while it was of continuous in hoop direction. Moreover, the thickness of white layer (observed hoop direction) decreased with depth down the hole (Herbert *et al.*, 2012a; Kwong *et al.*, 2009). However, Sharman *et al.* (2008a) could not detect white layer on holes produced by milling, boring, reaming, while Axinte and Andrews (2007) got rid of such layer by drilling hole followed by plunge milling (without any chamfer angle) and special reaming with reduced chamfer angle. Similarly Herbert *et al.* (2012a) could not locate any material drag/plastic deformation zone along axial direction irrespective of the condition of the drill bit (fresh or worn). On the other hand, more intense material drag could be observed with worn out drill bit compared to new drills at the hoop direction while drilling RR 1000 alloy. Similar observation was also reported by Popa *et al.* (2010).

Condition of the cutting tool is another influencing factor for work hardening. General trend indicates that microhardness increases with tool wear (Ezugwu *et al.*, 1999; Ezugwu and Tang, 1995a; Ezilarasan *et al.*, 2013a; Li *et al.*, 2014; Sharman *et al.*, 2004a, 2004b, 2015; Soo *et al.*, 2011; Thakur *et al.*, 2012b). Jin and Liu (2012, 2013) explained increase in work hardening tendency by severe plastic deformation, friction between tool flank and machined surface and extrusion of nose. Madariaga *et al.* (2014) also related the same to generation of high pressure, temperature and dislocation density due to plastic deformation. According to Sharman *et al.* (2004a, 2004b, 2015), turning Inconel 718 with worn tool causes larger contact between flank and machined surface along with severe frictional rubbing which in turn lead to escalation in force, plastic deformation and temperature. As a consequence, more work hardening is expected in worn tool compared to that for fresh tool. Similarly, it was also shown that prolonged machining led to rise in friction at tool-workpiece interface, generation of high temperature and pressure contributing to hardening of the surface layer (Ezugwu and Tang, 1995a; Ezugwu *et al.*, 1999; Ezilarasan *et al.*, 2013a; Li *et al.*, 2014). Hardness depth profile obtained with a tool under different flank wear condition. According to Zhuang *et al.* (2014), formation of work hardening layer takes place mainly due to notch wear during dry machining of Inconel 718. However, same mechanism may not be valid for drilling, since no significant difference on micro hardness with new and worn tools could be observed after drilling Inconel 718 (Sharman *et al.*, 2008a). It was explained by the fact that flute of the drill being primarily responsible for generation of hole surface did not undergo significant wear compared to the cutting edges.

According to general observance, use of worn tool makes surface residual stress to be more tensile in nature particularly along cutting direction (Cantero *et al.*, 2013; Li *et al.*, 2009; Outeiro *et al.*, 2008; Sharman *et al.*, 2004b, 2015). At the same time, worn tool also resulted in higher compressive residual stress beneath heat affected layer as well as deeper peak of compressive stress. Increase in tensile residual stress at machined surface was attributed to higher cutting temperature caused due to rubbing and ploughing of the machined surface by the worn flank of the tool. The same effect also causes higher degree of plastic deformation of the workpiece which in turn increases compressive stress beneath thermally affected surface layer. It was interesting to note that the observation of deeper compressive stress peak was more prominent with escalation of cutting speed (Schlauer and Oden, 2005). Residual stress is found to be anisotropic in nature due to difference in stress values along cutting and feed directions. It is evident that this anisotropy is more pronounced for worn out tool with significant differences in residual stress values on the machined surface and sub-surface region along different directions. This anisotropy particularly for worn out tool was attributed to dominance of mechanical effect. This phenomenon was further explained by the fact that tool wear increased radial and feed force components more prominently compared to cutting force component. Similar observation

on anisotropic nature on residual stress was also made during turning of Inconel 718 (Peng *et al.*, 2013a; Sharman *et al.*, 2004b) and drilling of RR1000 super alloy (Kwong *et al.*, 2009a, 2009b). Li *et al.* (2009) observed large compressive radial residual stress during face turning of RR1000 Ni-based super alloy using chipped tool. Herbert *et al.* (2012a) further demonstrated that large tensile stress obtained in abusive drilling can be successfully negated with the use of finishing operation like plunge milling.

2.6 Motivation and objective of research work

From the extensive review of past literature, it is evident that resistance to tool wear could be achieved with the help of few coated tools during machining of nickel-based super alloys. Although considerable work on tool wear during machining of nickel-based super alloys with major focus on Inconel 718 has been investigated, similar work on different other grades is relatively scarce. It is known that machining characteristics of a particular workpiece material depend primarily on its composition, microstructure and thermomechanical properties. Therefore, it is also important to evaluate the machinability characteristics of other grades with prominent engineering applications.

Although coated tools have been used in the past, detailed wear mechanism of the same has hardly been explored. Effect of tool coating on chip characteristics and surface integrity is also not evident from the past research work. Moreover, previous studies could not establish potential of coated tool in dry machining in comparison with wet machining. The above issues were never addressed for any of the grades of nickel-based super alloy. Therefore, a different grade of nickel-based super alloys may be chosen for which complete machinability characteristics can be evaluated addressing all such issues.

It is also evident that different coated tools have been utilized during machining of super alloys. However, role of CVD and PVD coating techniques on tool wear mechanism and other aspects of machinability is still not clear. Furthermore, potential of the applied coated tools was evaluated primarily in terms of tool life. Nevertheless, there was hardly any endeavour to critically analyse the wear of different coating layers deposited by CVD and PVD techniques. Moreover, clear agreement on the suitability of different coating systems during machining of nickel-based super alloy is still lacking. cBN and ceramic tools are highly expensive and essentially require high cutting speed and dedicated machine tools. Cemented carbide-based tools, on the other hand, are more versatile and economical However, significant difference in opinion exists as far as the suitable composition of cutting tool is concerned.

Machinability of Incoloy 825 with sizeable difference in chemical composition and properties from other grades is so far unknown. Incoloy 825, in particular, works remarkably well under corrosive environment and hence is widely used in chemical and

marine industries. Therefore, the major objective of the current research work is to investigate the capabilities of advanced coated tools in improving various machinability aspects during machining of Incoloy 825. Different grades of uncoated carbide tool have been used. Different coated tools obtained with CVD and PVD techniques have also been utilized. While, all the cutting tools considered for the current study are commercially available, logical selection of the same is of utmost significance. The specific objectives of the present research work are described as follows.

1. To investigate the effect of cutting speed and comparatively evaluate the performance of uncoated and CVD coated cemented carbide tools on three important characteristics such as tool wear, chip characteristics and surface integrity.
2. To study the influences of coating techniques (CVD and PVD), cutting speed and feed on some machinability characteristics such as cutting force, cutting temperature and tool wear.
3. To investigate the effect of environment (dry, conventional flood cooling and MQL) on various machining characteristics to determine if usage of cutting fluid can be completely eliminated with the help of best performing coated tool under different cutting condition (roughing and finishing).
4. To evaluate the variation of tool wear, chip characteristics, surface roughness, cutting force and temperature with progression of machining.

2.7 Organization of the thesis

Entire research work has been divided into following three stages.

During the first phase of the work, ISO P grade of uncoated cemented carbide and CVD coated tools consisting of TiN/TiCN/Al_2O_3/ZrCN with an insert designation of SCMT 12 04 08 was selected. Purpose of using multilayer coating was to achieve synergistic influence of different layers on the properties of the cutting tools primarily in terms of hardness, antifriction, wear resistance and thermal stability. Three important characteristics in the forms of tool wear, chip characteristics and surface integrity which were investigated in detail have been discussed in three different sub-chapters.

In the second phase, different grade of tool material i.e. ISO K grade has been utilized and accordingly minor modification had to be incorporated in terms of tool geometry and composition of CVD coating, since previous combination of geometry and composition could not be maintained in the commercially available K grade of carbide tool. This time bilayer CVD coated tool consisting of TiCN/Al_2O_3 with an insert designation of SNMG 12 04 08 was considered. Additionally, a PVD coated tool with identical tool geometry consisting of alternate layer of TiAlN/TiN was chosen with an aim to determine and

recommend best cutting tool (cemented carbide-based) for machining nickel-based super alloys. Various machinability characteristics such as cutting force, cutting temperature and tool wear were investigated with these types of tools. This study has been included in the fourth sub-chapter of Results and Discussion (Chapter 4).

In the final phase, the best performing coated tool has been utilised under dry machining, while its uncoated counterpart was employed under conventional flood cooling and MQL environments. Different machining characteristics such as cutting force, temperature, tool wear, chip characteristics and surface integrity were comparatively evaluated under rough and finish modes of machining with an aim to judge the suitability of a coated tool under environment-friendly dry machining condition.

Chapter 3

Experimental Methods and Conditions

In this section, experimental methodology, the details of equipment facilities, machine tools used, cutting tool, workpiece material, machining parameters and experimental set-up have been described.

3.1 Workpiece material

Incoloy 825 is a precipitation-hardenable nickel-chromium-iron alloy, and its chemical composition has been given in Table 3.1. Detailed properties of Incoloy 825 are provided in Table 3.2. Selection of Incoloy 825 as the work material has been motivated by its great deal of advantages and industrial applications.

Table 3.1: Chemical composition of Incoloy 825 (Thakur *et al.*, 2014a, 2014b).

Element	Ni	Fe	Cr	Mo	Cu	Ti
Content %	38-46	22-37.9	19.5-23.5	1.5-3.5	1.5-3	0.6-1.2

Table. 3.2: Properties of Incoloy 825[1].

Density, g/cm^3	8.36
Specific Heat (J/kg)	461
Thermal expansion co-efficient (μm/m°C)	10.3
Thermal conductivity (W/mK)	11.7
Poisson's ratio	0.28-0.35
Elastic modulus (GPa)	196
Vickers hardness (HV)	200

3.1.1 Advantages of Incoloy 825

Incoloy 825 possesses excellent combination of different properties such as high mechanical strength, resistance to oxidation and corrosion at elevated temperature, good precipitation hardening ability and remarkable capability to with stand chemical attack especially under sulphuric acid, phosphoric acid and marine (chloride) environments.

[1]http://www.specialmetals.com/documents/Incoloy%20alloy%20925.pdf, viewed on 21.Jan.2016.

Nickel, which is the major alloying element, has excellent resistance to chloride ion stress corrosion cracking. Chromium resists to oxidizing substances such as nitric acid, nitrates and oxidizing salt. It reacts with the atmospheric oxygen to form a protective scale layer of chromium oxide (Cr_2O_3).This layer prevents outward diffusion of metallic element. Molybdenum has resistance to pitting and crevice corrosion. Combination of Ni, Cr, Mo and Cu provides outstanding resistance to reducing environment.

3.1.2 Application of Incoloy 825

Application of Incoloy 825 has wide domain of industrial applications which are provided below (Aytekin and Akcin, 2013; Prabhu and Vinayagam, 2011).

- Sulphuric acid plant
- Pickling equipment
- Compounding of industrial furnace
- Food processing equipment
- Submarine and chemical industries
- Nuclear power plant
- Oil and gas recovery
- Handling of radioactive wastes
- Pollution control, Heat exchanger
- Petrochemical plant

Before experiment, one rod of 75 mm diameter and 390 mm length and three rods, each of diameter of 75 mm and length of 650 mm were procured from the same manufacturer (Narendra Steel, India). Entire research work was carried out in three stages during which different tools, cutting parameters and environments were considered. These are discussed below.

3.2 Experimental details

3.2.1 First stage of experiment

A round bar of 75 mm diameter and 390 mm length was first cut for machining. Dry turning operation was performed in a heavy duty lathe machine (Make: Tussor Machine Tools India (P) LTD., India and model: 180 x 750) as depicted in Fig.3.1.

Experimental condition is provided in Table 3.3. The trial runs were carried out under varying cutting condition at the initial stage of the study. Lower values of cutting speed than those selected in the study resulted in insignificant tool wear. Productivity in terms of

material removal rate was also less. On the other hand, catastrophic tool failure was noted under elevated cutting speed particularly for uncoated tool. Accordingly, the cutting parameters range has been selected for the entire study.

Table 3.3: Experimental conditions during first stage of research.

Cutting tools	• Uncoated ISO P30 grade cemented carbide tool • CVD multilayer coated tool consisting of TiN/TiCN/Al_2O_3/ZrCN
Tool designation	ISO designation of SCMT 120408
Tool holder designation	ISO designation of SSBCR 2020K12
Tool geometry	0°, 0°, 7°, 6°, 15°, 75°, 0.8 (mm)
Cutting speed (V_c), m/min	51, 84 and 124
Feed (f), mm/rev	0.198
Depth of cut (a_p), mm	1
Environment	Dry
Machining duration	300 s of machining or up to tool failure with an interval of 60 s

Fig. 3.1: Photograph of experimental setup for turning of Incoloy 825.

3.2.2 Second stage of experiment

During the experiments, a round bar of Incoloy 825 with same diameter as before and 650 mm length was machined in the same industrial scale lathe machine. The experimental set up clearly showing four-component piezoelectric dynamometer (Model: 9272 Make: Kistler, Switzerland) in combination with a charge amplifier (Make: Kistler Instrumente AG, CH-8408 Winterthur, Switzerland; Model: 5070A10100) and tool-work thermocouple (K-type) for measuring cutting force and temperature is also depicted in Fig. 3.2 along with

data acquisition system (DAQ system of National Instruments, India) for measurement of cutting force and temperature. Detailed experimental condition is presented in Table 3.4.

Table 3.4: Experimental condition during second stage of research.

Cutting tools	•Uncoated ISO K20 grade cemented carbide tool •CVD bilayer coating consisting of TiCN/Al_2O_3 •PVD multilayer coating of TiAlN/TiN
Tool designation	ISO designation of SNMG 120408
Tool holder designation	ISO designation of PSBNR2020K12
Tool geometry	−6°, −6°, 6°, 6°, 15°, 75°, 0.8 (mm)
V_c, m/min	51, 84 and 124
f, mm/rev	0.08, 0.14 and 0.2
a_p, mm	1
Environment	Dry
Machining duration	300 s of machining in general. However, under the most adverse condition (V_c= 124 m/min and f= 0.2 mm/rev) machining was continued till tool failure. Different intervals (duration of each trial after which the tool was disengaged) of 30 s, 60 s and 5 min were employed.

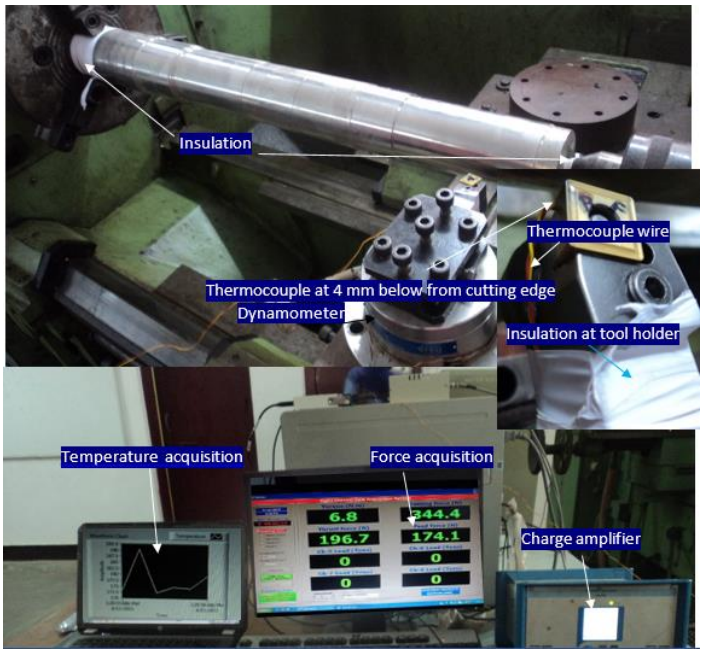

Fig. 3.2: Photograph of experimental setup for turning of Incoloy 825.

3.2.3 Third stage of experiment

During the experiments, a round bar of Incoloy 825 with same dimension as in previous stage was machined in the same lathe machine. The experimental photograph showing MQL set up is demonstrated in Fig. 3.3. Table 3.5 presents experimental condition adopted during the current stage of study. For better statistical accuracy, each cutting experiment was repeated twice in all stages of the work.

Table 3.5: Experimental condition during third stage of research.

Cutting tools	• Uncoated ISO K20 grade cemented carbide tool • PVD multilayer coating of TiAlN/TiN
Roughing mode of machining	V_c=51 m/min, f=0.2 mm/rev and a_p=1.5 mm
Finishing mode of machining	V_c=124 m/min, f=0.08 mm/rev and a_p=0.5 mm
Environment	Dry (PVD coated tool), flood (uncoated tool) and MQL (uncoated tool)
MQL supply Air flow rate Quantity of oil consumed Spraying direction of MQL nozzle	Through external nozzle with oil (water soluble) to water ratio of 1:5. 0.5 MPa 50 ml/h Rake face
Machining duration	30, 90, 150, 210, 300 and 480 s

3.3 Evaluation methodology of different characteristics in machining

3.3.1 Characterization of workpiece and tool materials

Field emission scanning electron microscopy (FESEM) (Make: NOVA NANO SEM-450) in combination with energy dispersive spectroscopy (EDS) through X-ray was used to reveal the microstructure of Incoloy 825 and surface morphology of tools before machining. The photographic image of the system is shown in Fig. 3.4 (a). With an aim to evaluate various phases of work material (Incoloy 825) and uncoated tools, X-ray diffraction (XRD) (Make: Regaku, Ultima IV) utilized in Bragg-Branteno mode. The same technique was also employed to assess possible modification in material structure and give size. A 2θ scan range of 30°- 80°, step size of 0.05° and count time of 2 s per

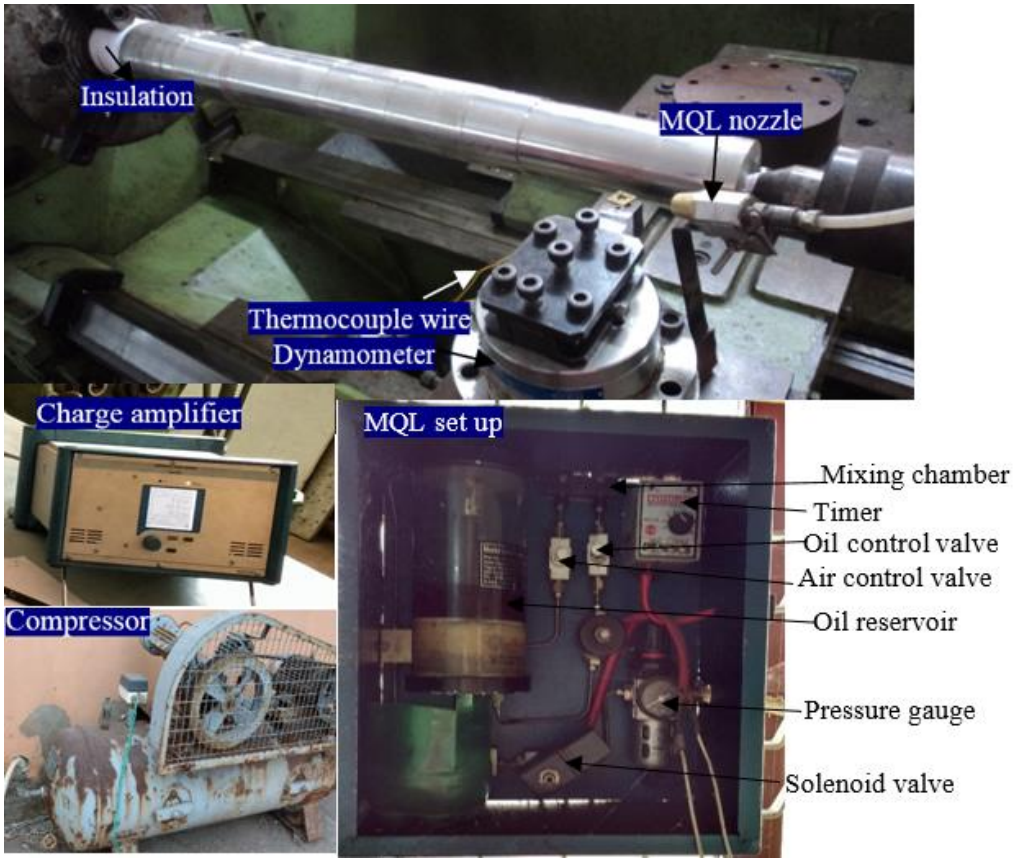

Fig. 3.3: Photograph of the experimental setup for turning Incoloy 825.

step were considered. Fig. 3.4 (b) shows the photographic view of XRD system. In order to identify various phases of different layers of coating, the same was studied using grazing incidence XRD (GIXRD) technique with a grazing incidence angle of 2°. A 2θ scan range of 30°- 90°, step size of 0.05° and a count time of 2 s per step were considered.

(a) (b)

Fig. 3.4: Photographic images of the machine for (a) FESEM and (b) XRD system.

3.3.2 Tool wear

A stereo zoom microscope (Make: Radical Instruments, India) was used to capture the image of the tools (both rake and flank surfaces) after each duration of machining. Fig. 3.5 (a) shows photograph of the microscope. Scanning electron microscopy (SEM-JEOL- JSM-6480 LV) shown in Fig. 3.5 (b) in combination with EDS were further used to detect if there was any material transfer from the workpiece to the tools.

(a) (b)

Fig. 3.5: Photographic images of the machine for (a) stereo zoom microscope and (b) scanning electron microscopy.

3.3.3 Chip characteristics

After each experimental run, chip was collected for further analysis. Chip thickness was measured with the help of a micrometer (Make: Mitutoyo, Japan). Micro morphology of the chips involving both free and under surfaces were investigated using SEM in combination with EDS for analysing wear debris. For studying the different characteristics of serrated chips, cross section of chips were prepared by embedding the chips inside epoxy resin moulds (cold mounting). The specimens were initially polished with different grades of polishing paper having SiC grits with decreasing size. Final surface finish was obtained by polishing with diamond paste before etching. The polished surfaces were then etched with 2% (by volume) of diluted (40%) hydrofluoric acid, 40% of concentrated hydrochloric acid, 50% of de-ionised water and 8% hydrogen per oxide. The macro morphology of chip and micro-features of the chip's cross section was studied using AxioCam ERc 5s optical microscope (Make: Carl Zeiss, Germany) coupled with image processing software

(exhibition release 4.8.2). Hardness of the chip samples was measured on the transverse plane using a Vickers microhardness tester (LECO, USA) with 100 g. photographic images of optical microscope and microhardness tester are shown in Fig.3.6. XRD was used to reveal any phase transformation and modification of grain size.

(a) (b)

Fig. 3.6: Photographic images of the machine for (a) optical microscope and (b) Vickers microhardness tester.

3.3.4 Surface integrity

Surface roughness of machined surface was determined with Talysurf (Make:Taylor Hobson, Model: Surtronic 3+) shown in Fig. 3.7. In order to carry out the surface integrity study, the samples were first cut along a plane perpendicular to the axis of rotation. The specimens were then prepared metallographically by polishing as discussed above. The prepared samples were then analysed under FESEM to reveal the formation of white layers and micro morphology of machined surface. Macro machined surface topography was analysed with the help of SEM. To identify any phase transformation and grain refinement taking place at the altered layers of the machined surface, XRD technique was used. Vickers microhardness measurement was employed to get machined surface and sub-surface microhardness, measured on the cross sectional surfaces along a straight line from the edge (corresponding to the circumference of the machined work piece) towards the centre. Each indent was separated from the next one by 20 µm. The tests were carried out at 25 g load for a dwell time of 10 s. PANalytical high resolution XRD machine was used to measure the residual stress. The stress was measured for (1 1 1) peak which is observed at $2\theta = 42.75°$ using Cu ($\lambda = 1.5418$ Å) radiation. The lattice spacing measurement was performed

in 7ψ tilts. The Lorentz polarization, Kα-2 splitting and background corrections were performed for the measured intensities. Peaks were identified using the Gaussian curve fit.

Fig. 3.7: Photographic image of the surface measurement set-up.

3.3.5 Cutting temperature

A tool-work thermocouple was used to approximately measure cutting temperature. For measuring temperature the probe having diameter of 0.5 mm was placed at the interface of insert and shim at the place below tool tip. Proper insulation was provided (Teflon tape) for reducing heat transfer on the head stock, tail stock and tool holder. Prior to machining operation, calibration of K-type thermocouple was carried out by putting the same inside water which was heated to boiling point from room temperature. Such technique is a common practice to measure cutting temperature and has been adopted by many researchers (Herbert, 1926; Shaw, 1984; Shiva and Wallbank, 1999). Data acquisition was used for cutting temperature shown in Fig. 3.2.

3.3.6 Cutting force

Cutting force was measured using a four-component piezoelectric dynamometer. Data acquisition system of National Instruments, India was used to acquire the signals of cutting force. Dynamometer along with charge amplifier and DAQ are indicated in Fig. 3.2.

Chapter 4

Results and Discussion

4.1 Effects of CVD tool coating and cutting speed on tool wear during dry machining of Incoloy 825

4.1.1 Characterisation of workpiece material (Incoloy 825)

Majority of the mechanical properties of nickel-based super alloys is directly or indirectly related to their microstructure which in turn impacts the machinability characteristics in significant way. Therefore, prior study of microstructure of a particular grade of nickel-based super alloy i.e. Incoloy 825, is of utmost relevance. Microstructure of as-received Incoloy 825 has been investigated using FESEM while, chemical composition and phases have been evaluated using EDS and XRD respectively. Microstructure shown in Fig. 4.1 (a) reveals grains, grain boundaries and its distribution in the alloy. Clear segregation of particles along the grain boundaries can also be captured from the figure. EDS (Fig. 4.1 b) and subsequent analysis using XRD (Fig. 4.1 c) revealed these particles to be possibly consisting of carbides of various metals like Cr, Mo and Ti. According to Thakur *et al.* (2015b), their general formula is $M_{23}C_6$ (primarily Cr-rich phase) which has also been conformed from XRD analysis (Fig. 4.1 c). Additionally, Mo_2C might have been formed. However, the microstructure of Incoloy 825 primarily constitutes of Ni_2 (Cr, Mo) i.e. ϒ phase as evident from XRD spectrum. Similar phases have also been found in other grades of nickel-based super alloy by Pan *et al.* (2000), Raymond (1968), Rai *et al.* (2004) and Thakur *et al.* (2015c). These phases are primarily responsible for superior thermomechanical properties such as high strength, high temperature stability and resistance to corrosion. At the same time such microstructure also renders the material with poor machinability characteristics.

4.1.2 Characterisation of uncoated and CVD coated carbide tools

Prior to carrying out the machining experiments, both uncoated and coated carbide tools were characterised using SEM, whereas EDS was utilised to identify the composition of the tools. Fig. 4.2 shows SEM micrographs of surface morphology and corresponding EDS spectra of uncoated and coated tools in as-received condition. Since, ISO P grade cemented carbide insert has been utilised as uncoated tool, elements like Ti, Ta and Ti

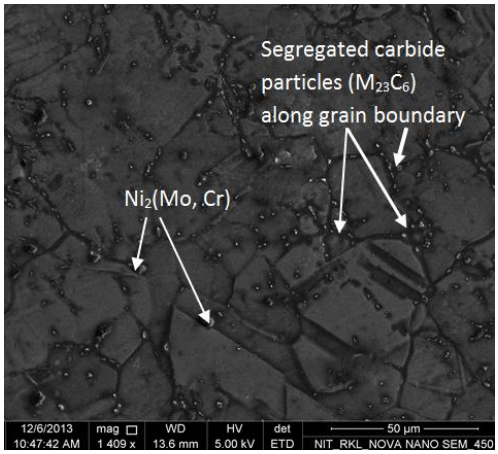

(a)

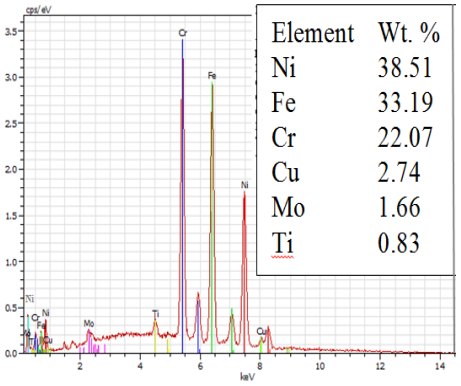

(b)

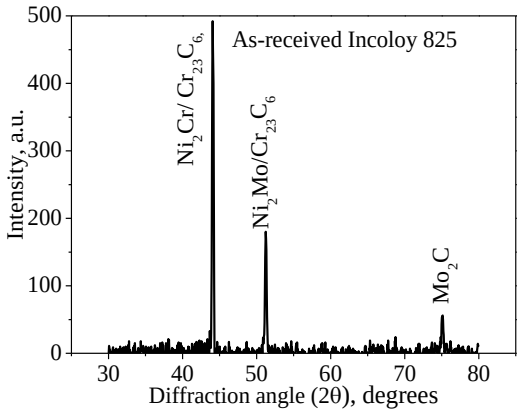

(c)

Fig. 4.1: (a) FESEM image of microstructure, (b) corresponding EDS spectrum and (c) XRD spectrum, of as-received Incoloy 825.

(present in the form of carbides) could also be detected from the EDS spectrum (Fig. 4.2 a). Since, top layer of coated tool consists of ZrCN, it is obvious that the surface morphology also corresponds to same.

X-ray diffraction was carried out to identify different phases of uncoated and coated inserts. Fig. 4.3 (a) shows the presence of different phases like WC, Co, TiC and TaC which are the constituents of ISO P grade cemented carbide insert. The composition of multilayer coating of the coated tool is depicted in Fig. 4.3 (b). It may be noted that in addition to the coating materials, some phases of the substrate material are also revealed in the same figure.

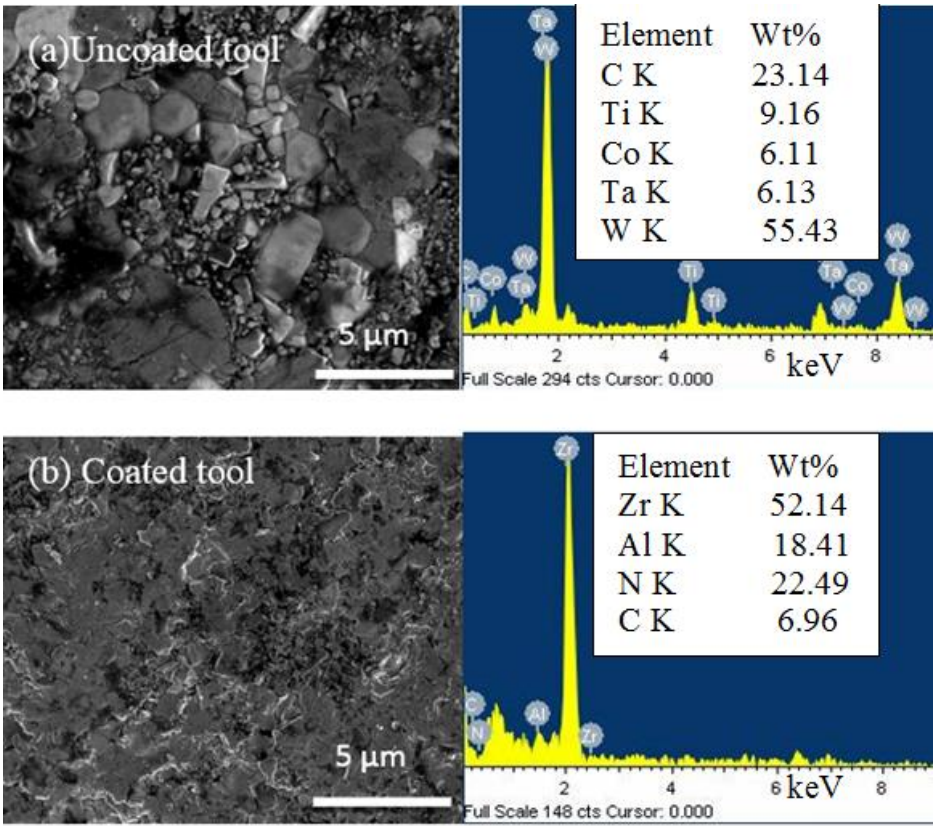

Fig. 4.2: FESEM images along with the EDS spectra of (a) uncoated (ISO P grade cemented carbide) and (b) CVD coated tools before machining.

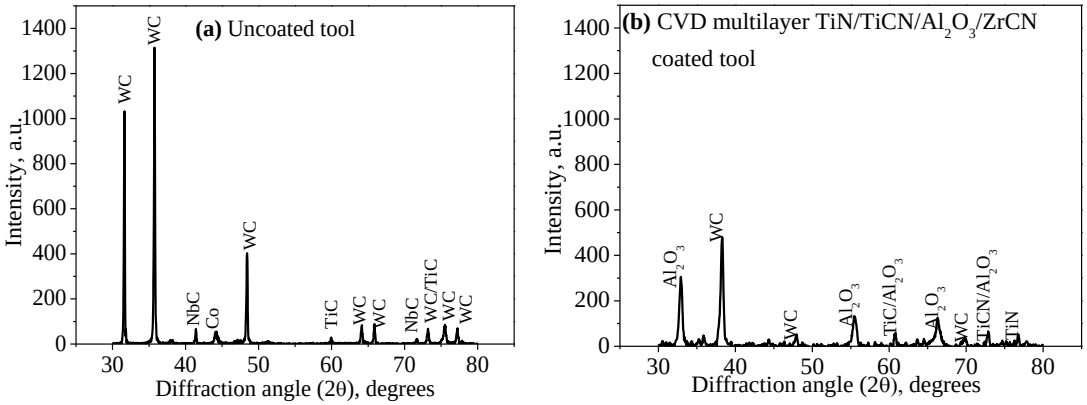

Fig. 4.3: XRD spectrum for (a) uncoated and (b) GIXRD spectrum of CVD multilayer TiN/TiCN/Al_2O_3/ZrCN coated inserts.

Further, the EDS dot mapping of the cross-section of the CVD multilayer coated tool ascertains the true composition of the tool as shown in Fig. 4.4. The top layer consists of ZrCN coating followed by thin layer of Al_2O_3. Bottom layers of TiCN and TiN could not be individually discerned. Total thickness of around 4 µm may be observed from the same figure. WC substrate over which coating layers were deposited is also revealed from Fig. 4.4.

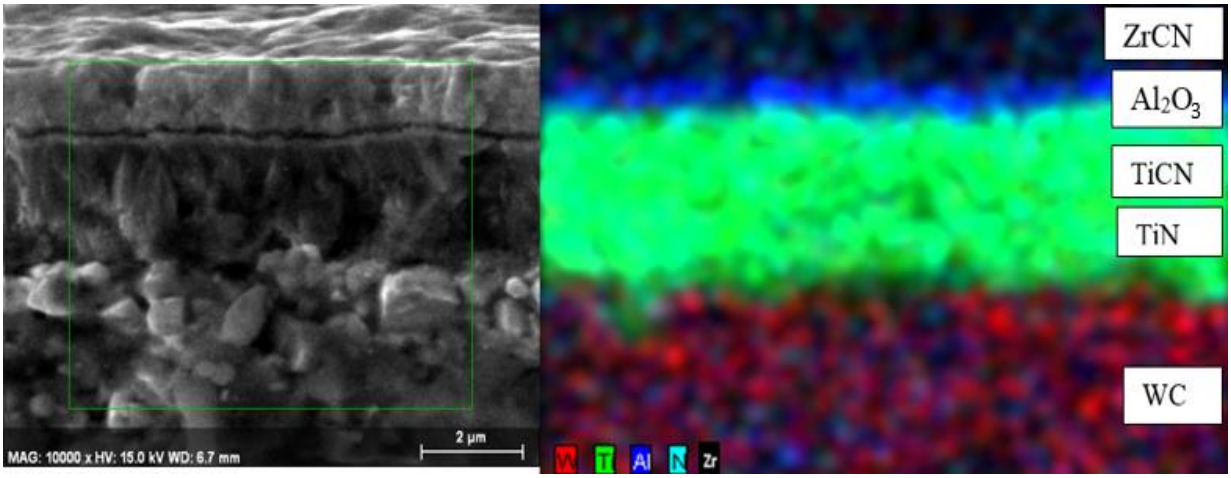

Fig. 4.4: (a) Coating fractograph and (b) EDS dot mapping of CVD multilayer TiN/TiCN/Al_2O_3/ZrCN coated insert.

4.1.3 Effect of CVD coated tool and cutting speed on tool wear

Flank wear

Tool wear during dry turning of Incoloy 825 with both uncoated and coated carbide inserts was characterised by crater and flank wear which were investigated using optical microscopy and SEM. Fig. 4.5 demonstrates the optical microscopic images of flank surface depicting the growth of wear of the uncoated and coated carbide inserts with the machining duration and for different cutting speeds. It is evident that increase of both cutting speed and machining duration increased average flank wear of both uncoated and coated tools. It can also be observed from the same figure that there was no significant difference in wear pattern of uncoated and coated tools initially up to 90 s of machining. However, the superiority of coated tool was more prominently visible with the progression of machining due to higher resistance to abrasion of multilayer coated tool. Catastrophic failure mode could be visible in the flank surface of the uncoated insert after 150 s of machining at high cutting speed (124 m/min). On the other hand, CVD coated tool survived for 300 s, establishing the capability of multilayer coated tool in enhancing the resistance to flank wear particularly at high cutting speed. This is also evident from Fig. 4.6 which shows evolution of average flank wear graphically with machining duration for different cutting speeds. Sharman *et al.* (2004a) observed similar tool life using CVD coated tool with similar cutting speed (120 m/min) and feed (0.15 and 0.25 mm/rev), but with less depth of cut (0.25 mm) while machining Inconel 718. However, no experiment was carried out with uncoated tool using such high cutting speed.

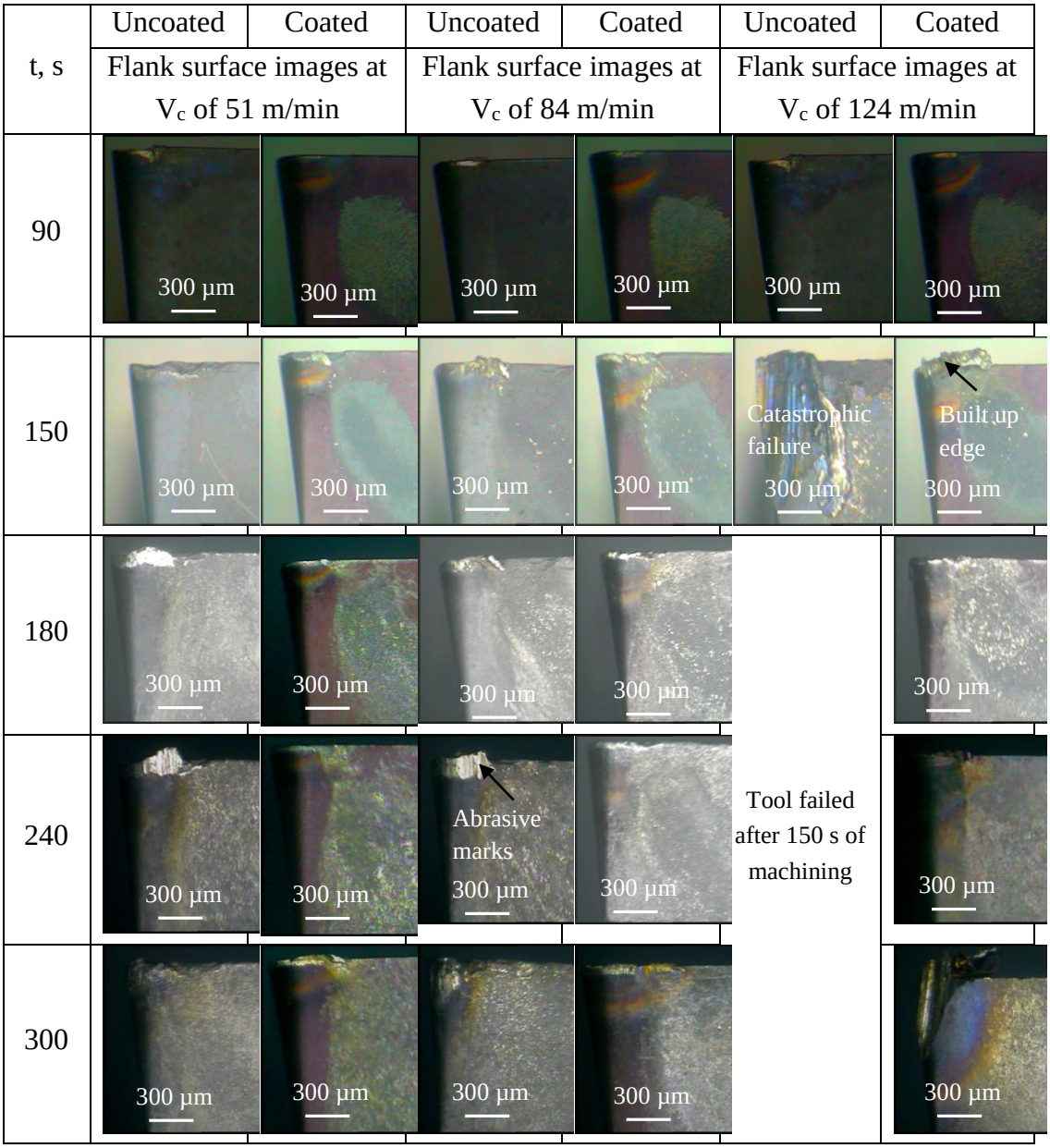

Fig. 4.5: Optical microscopic images of flank surface of inserts with machining duration and V_c for uncoated and coated inserts at constant f = 0.198 mm/rev and a_p = 1 mm.

Crater wear mechanism

Crater wear of tool while machining nickel-based super alloys is primarily governed by the contact mechanics at chip-tool interface region. High contact pressure, high chip-tool interface temperature and stickiness of the work material cause adhesion and diffusion types of wear (Zhu *et al.*, 2013). Fig. 4.7 shows the SEM images of rake surface of uncoated and coated inserts after 150 s of machining. Due to high chemical affinity of

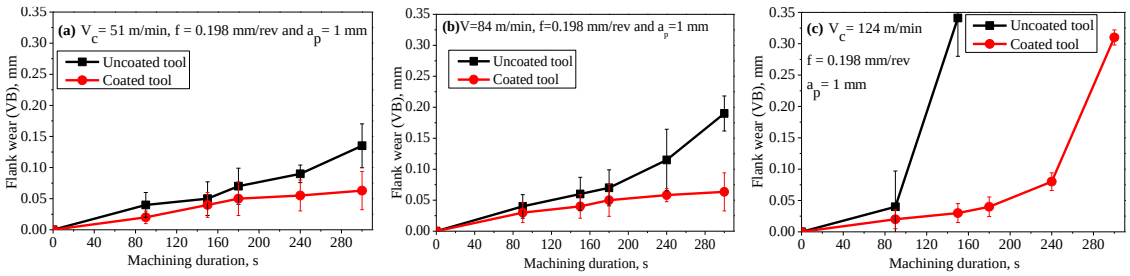

Fig. 4.6: Variation of flank wear with machining duration for different cutting speeds of (a) 51, (b) 84 and (c) 124 m/min, while using uncoated and CVD coated inserts at constant feed and depth of cut.

nickel-based super alloys, material adhesion on the rake surface of the tool has been one of the major issues in machining. This results in the formation of BUE which not only deteriorates the surface finish of workpiece, but also promotes adhesive wear thus lowering tool life. It is evident from Fig. 4.7 that tendency of formation of BUE is more for uncoated tool compared to that for multilayer coated tool. Due to anti-sticking properties of the coating materials, the coated tool caused a reduction in material adhesion. However, removal of coating particular under low cutting speed condition, led to the formation of localised material build-up. Higher drag force at low cutting speed reduces the beneficial effect of coating in combating crater wear (Thakur *et al.*, 2014a, 2015a). Partial removal of coating while machining at cutting speed of 51 m/min, as seen in Fig. 4.7, corroborates the fact. However, with increase in cutting speed the coating not only acts as a diffusion barrier but also imparts sufficient protection to the cutting edge. After 150 s of machining with high cutting speed (i.e. V_c = 124 m/min), there was severe plastic deformation of the cutting edge of uncoated tool resulting in catastrophic failure and therefore machining was discontinued.

Comparison between uncoated and coated tools particularly under 84 m/min (in Fig. 4.7) clearly revealed formation of smoother surface of the coated tool with apparently less transfer of materials denoted by the lighter regions. This phenomenon might be attributed to the BUE formation over the rake face of the uncoated tool owing to the higher degree of chemical affinity of Incoloy 825. However, coated tool restricted the formation of BUE, due to the chemical inertness and anti-friction properties of the coatings, resulting in the very less material transfer between tool and the workpiece (Thakur *et al.*, 2014b, 2015a). These regions were later magnified and probed with EDS to verify the phenomenon of transfer of workpiece material in Fig. 4.8. Fig. 4.8 clearly reveals that significant amount of material transfer took place from workpiece to the cutting tool. Significant presence of coating materials like Zr, Al, Ti and N in the EDS results (Fig. 4.8) pertaining to machining with V_c = 84 m/min, indicates that removal of coating might not have taken place. This can be attributed to the fact that the condition of medium cutting speed is more favourable for the coated tools, since coating is more prone to failure under low cutting speed and

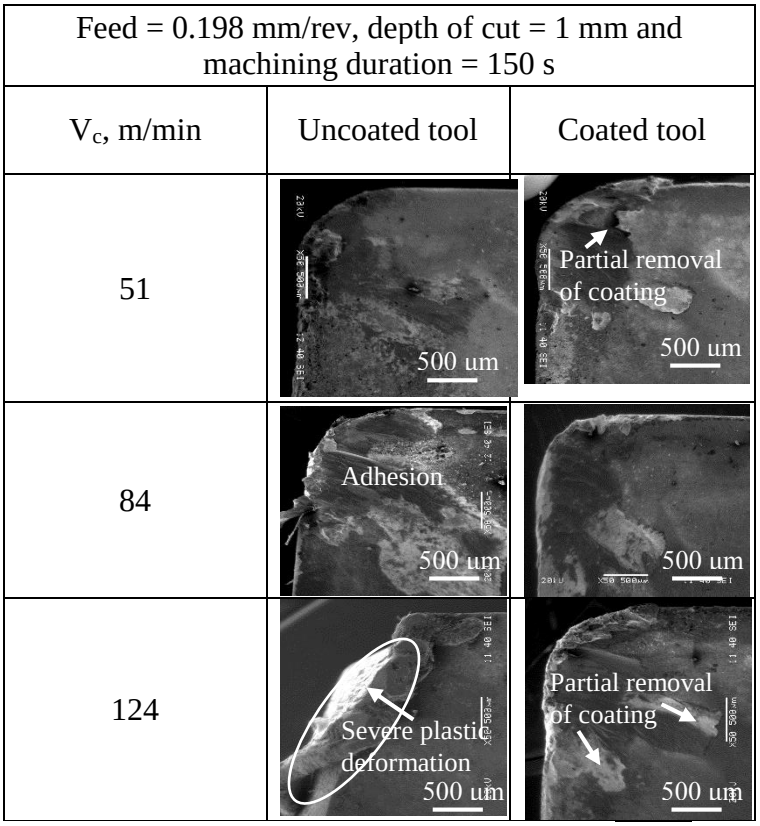

Fig. 4.7: SEM images of rake surface of tool for uncoated and CVD coated inserts using variable cutting speeds.

subjected to high thermo-mechanical load under very high cutting speed. This is effect is prominent particularly during machining nickel-based super alloys.

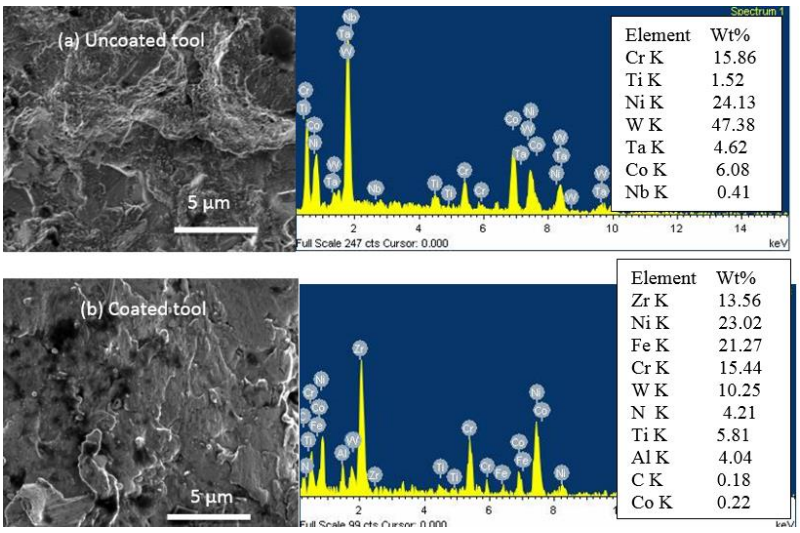

Fig. 4.8: FESEM images of rake surface and corresponding EDS spectra of (a) uncoated and (b) CVD coated tools after machining of 180 s with V_c of 84 m/min constant feed (0.198 mm/rev) and depth of cut (1 mm).

4.2 Effects of CVD tool coating and cutting speed on chip characteristics during dry machining of Incoloy 825

4.2.1 Macro morphology of chip

Chip formation which is dictated by energy of shear deformation, is of utmost importance in machining of nickel-based super alloys since the process plays a pivotal role in controlling the cutting force, tool wear and surface roughness. Fig. 4.9 shows a gradual change of macro morphology of chips with duration of machining obtained while turning of Incoloy 825 with uncoated and coated inserts under different cutting speeds. It is evident from Fig. 4.9 that the shape gradually transforms from loose arc and connected arc type to continuous snarled ribbon type chip with progression of machining. Careful investigation of Fig. 4.9 would also reveal that the tendency of formation of serrated chip increased as cutting speed increases and this effect got more pronounced as duration of machining increased (Jin and Liu, 2012).

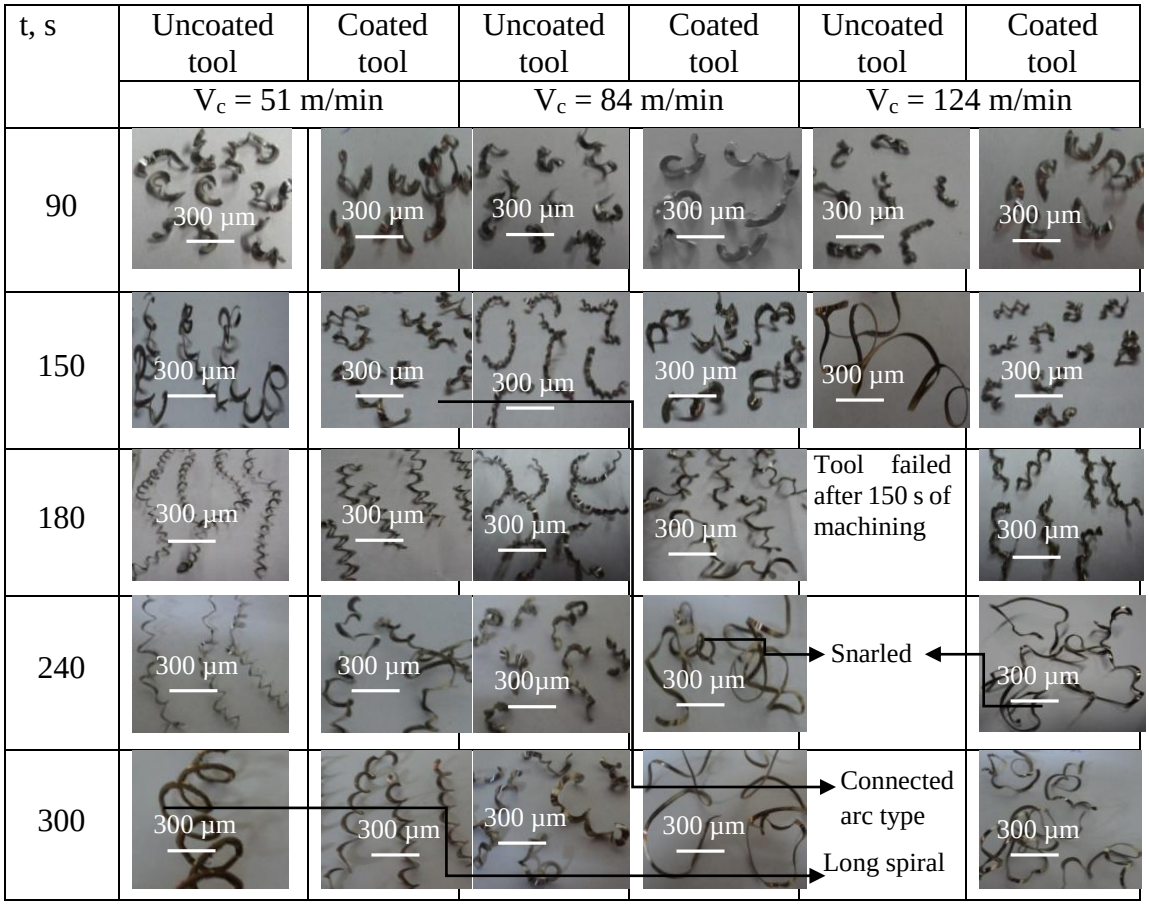

Fig. 4.9: Optical microscopy images of chips with progression of machining for different cutting speeds while using uncoated and coated carbide inserts.

4.2.2 Formation of shear band of serrated chips

Shear band is an important aspect of chip characteristics as it may also cause fluctuation of cutting force (Komanduri and Schroeder, 1986; Wan *et al.*, 2012; Zhang *et al.*, 2013). Both the phenomena of thermal softening and strain hardening responsible for segmented chips depend heavily on cutting parameters, thermomechanical properties of workpiece and cutting tool. Although chip formation mechanism of nickel-based super alloy like Inconel 718 has been studied, it would be also interesting to investigate the same for other grades having different thermomechanical properties. Representative optical microscopic images of segmented chips of Incoloy 825 along with shear band obtained with uncoated and coated tools are indicated in Fig. 4.10 (a, b). Micro fracture at the tip might be related to strain hardening tendency of Incoloy 825. Fig. 4.11 represents the variation of shear band thickness with cutting speed using uncoated and coated tools during machining of Incoloy 825. Gradual increase in shear band thickness is revealed with cutting speed for both the tools. According to Wan *et al.* (2012), such trend of variation with cutting speed can be explained by higher degree of thermal softening. Increase in shear band thickness as a result of thermal softening has also been discussed by Barry and Byrne (2002). Steep increase in shear band thickness with cutting speed for uncoated tool is ascribed to escalation in cutting temperature owing to high tool wear (Fig. 4.5) and consequently thermal softening. On the other hand, smaller slope of curve for the coated tool might be explained by mechanical deformation leading to grain refinement particularly at high cutting speed which would be discussed in the following section. According to Komanduri and Schroeder (1986), more severe shear localization is caused by poorer thermal conductivity of workpiece material due to higher heat accumulation in narrow zone (shear band) and also by high resistance to deformation of individual chip segments. Comparing the mechanism of chip formation of Inconel 718 with that of Incoloy 825 under similar cutting speed it is evident that more intense shear localisation can be expected in Inconel 718.

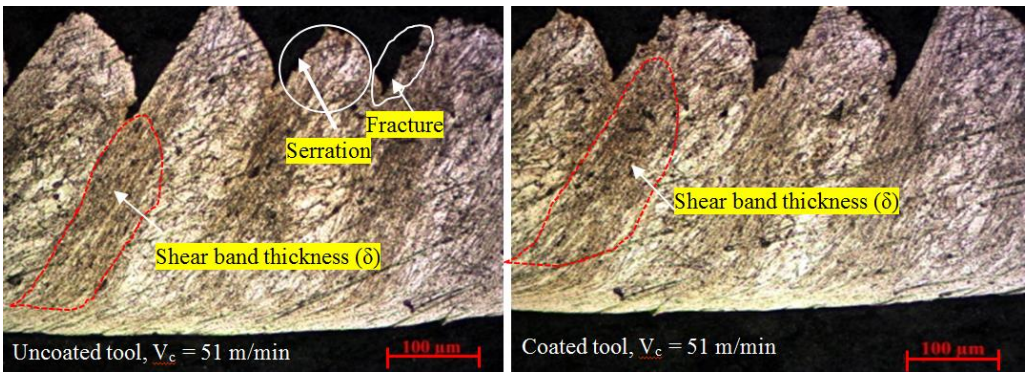

(a)

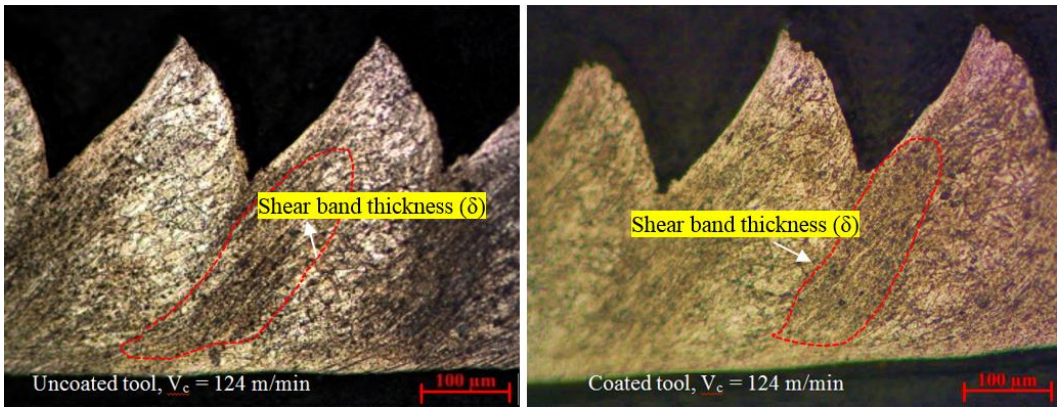

(b)

Fig. 4.10: Representative optical microscopic images of cross section of chips showing serration and shear band thickness while adopting uncoated and coated carbide inserts at (a) low (V_c = 51 m/min) and (b) high (V_c =124 m/min) cutting speeds.

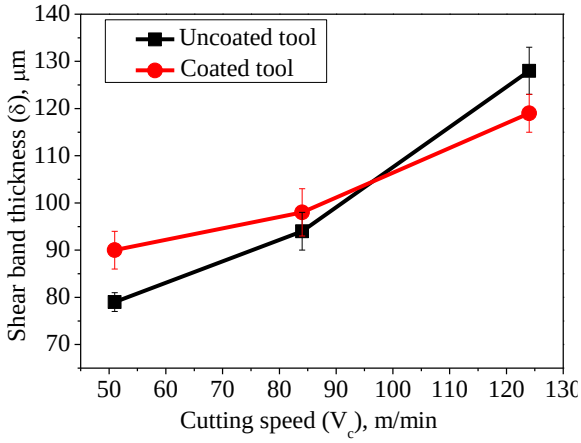

Fig. 4.11: Variation of shear band thickness with cutting speed while adopting uncoated and coated carbide inserts.

4.2.3 Influence of cutting condition on characteristics of saw-tooth chip

Micro morphology of chip

According to Hou and Komanduri (1997), formation of serrated chip during machining of nickel-based super alloys occurs due to shear localization in primary deformation zone. Cutting speed plays an important role in deciding whether thermal softening or strain hardening would govern mechanism of chip formation during machining of nickel-based super alloys. A representative SEM image of the cross section of a serrated chip revealing various characteristics of chip serrations obtained after machining Incoloy 825 has been indicated in Fig. 4.12. The various features include maximum thickness of saw-tooth chip (H), continuous part of the serrated chip (h), saw-tooth distance (P_c) and saw-tooth angle (ϕ_1) as indicated in the Fig. 4.12. Additionally, some material adhered on the back surface

of the chips, has been noticed. EDS point analysis reveals that wear debris primarily consists of adhered work material on rake face (BUE) with minor trace of tungsten from cutting tool. Such re-deposited material can be subsequently transferred to the machined surface thus deteriorating surface integrity (Thakur *et al.*, 2015a).

Fig. 4.13 shows SEM images of free surface and corresponding optical images of its cross section of chip depicting gradual transformation with the progression of machining during turning of Incoloy 825 with both uncoated and CVD multilayer coated tools at different cutting speeds. Different features of free surface of the chips can be detected from the SEM images. Primary serrated teeth, as indicated in Fig. 4.13, are formed due to primary shear deformation, whereas secondary serrated teeth are generated at the corner of chip owing to side flow of material i.e. secondary deformation. SEM micrographs also depict undeformed and slipping surfaces of the serrated chips (Patwari *et al.*, 2011). It is quite evident from the figure that cutting speed, machining duration and tool coating do have some influence on the chip morphology and characteristics of chip serration. Difference in sharpness of segment of the tip has also been noted. According to Barry and Byrne (2002), roundness is the result of upsetting of developing segment of chips prior to catastrophic failure, whereas segment becomes more pointed for harder materials and also when cutting speed is increased. General trend in the current work also indicates sharpening of tips with increase in cutting speed particularly for coated tool, whereas prominent tool wear for its uncoated counterpart as clearly indicated in Fig. 4.5 and 4.6 might have led to rounding of tips. It is evident from the same figure that chips with truncated saw-tooth profile can be obtained at lower cutting speed (51 m/min) particularly with the progression of machining. This can be explained by higher chip-tool interface friction at lower cutting speed while using uncoated tool. Degree of deformation of chip as well as tool wear increase with machining duration leading to gradual flattening of saw tooth. Both of these aspects could be improved with the application of coated tool as evident from the figure. From Fig. 4.12, various characteristics of segmented chip such as saw-tooth distance, equivalent chip thickness, saw-tooth angle and chip segmentation frequency have been calculated and analysed.

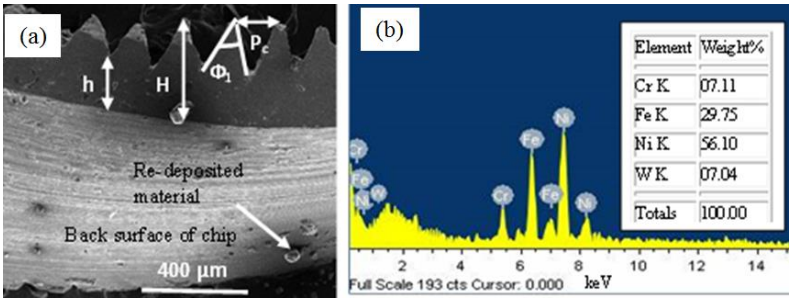

Fig. 4.12: (a) Representative SEM image of chip showing different features and (b) EDS spectrum of re-deposite material.

V_c, m/min	Uncoated tool	CVD coated tool
Feed = 0 .198 mm/rev, depth of cut = 1 mm and machining duration = 90 s		
51	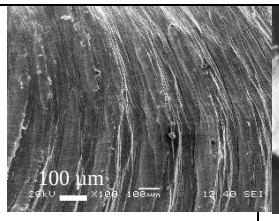 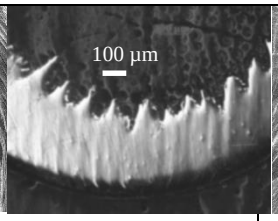	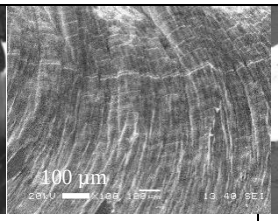 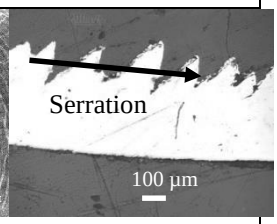
84	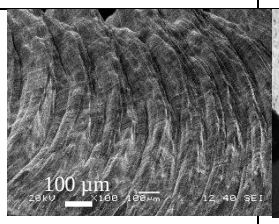 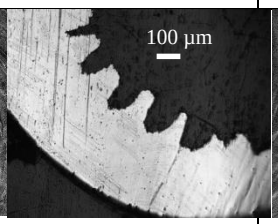	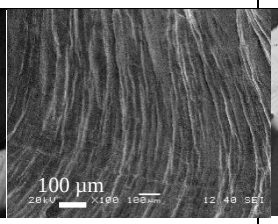 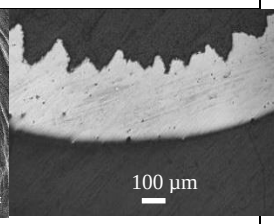
124	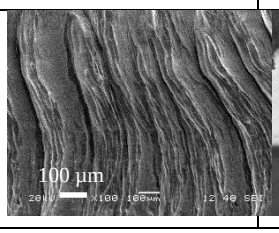 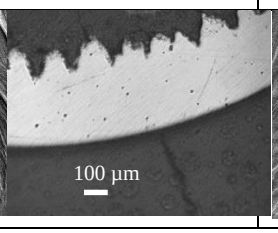	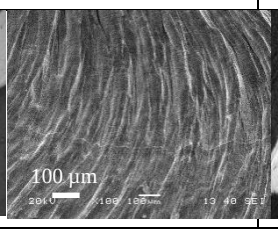 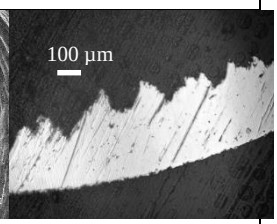
Feed = 0 .198 mm/rev, depth of cut = 1 mm and machining duration = 180 s		
51	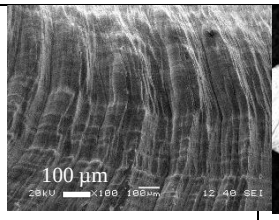 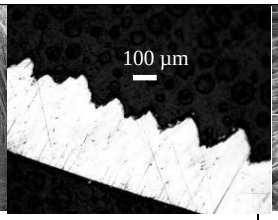	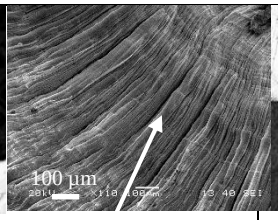 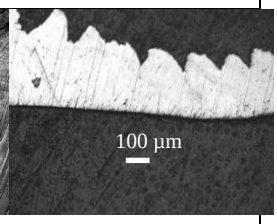
84	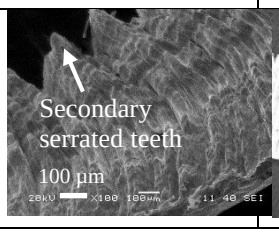 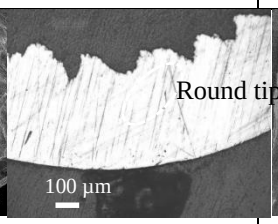	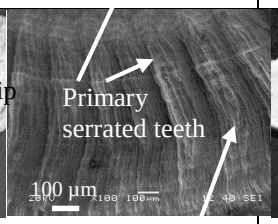 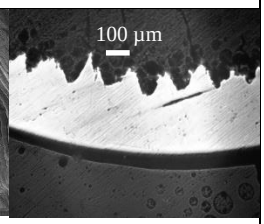
124	Tool failed after 150 s of machining	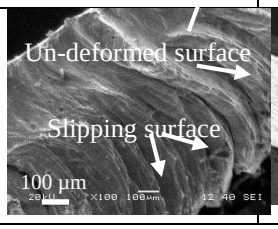 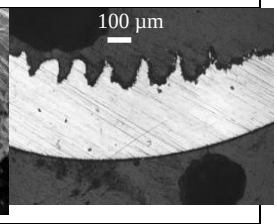
Feed = 0 .198 mm/rev, depth of cut = 1 mm and machining duration = 240 s		

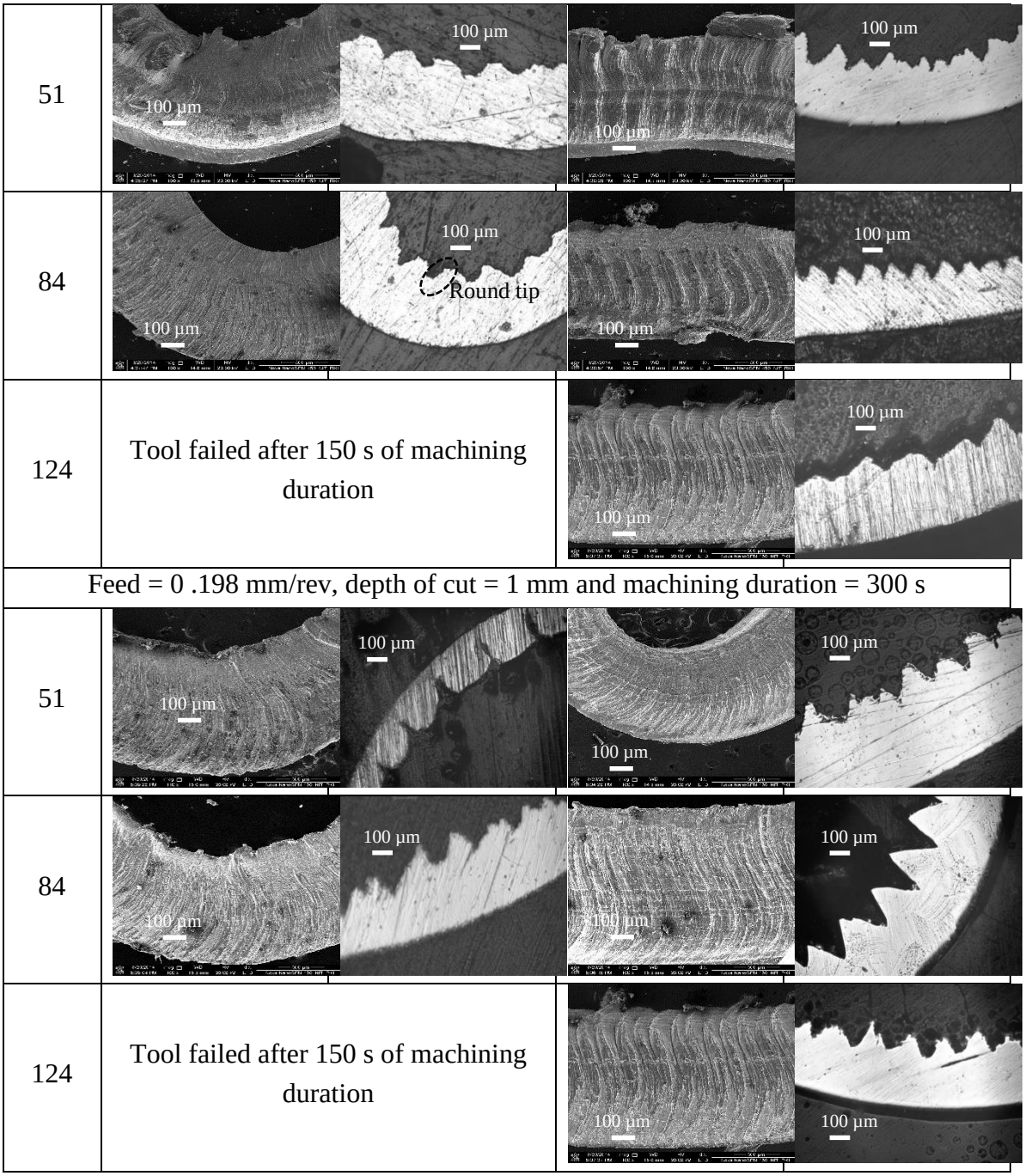

Fig. 4.13: SEM and corresponding optical images of chips with machining duration and cutting speed while using uncoated and CVD multilayer coated tools.

Saw-tooth distance (P_c) and chip segmentation frequency (f_{ch})

Two important aspects of chip serration include saw-tooth distance and chip segmentation frequency. These two characteristics of serrated chip are primarily influenced by shear deformation, strain hardening, strain rate and thermal softening. Saw-tooth distance was

calculated from the micro morphology of the chips whereas frequency of chip segmentation was calculated from equation (4.1) (Dong *et al.*, 2011).

$$f_{ch} = \frac{Vc\, f sin\phi_p}{Pc \times H} Hz \tag{4.1}$$

where ϕ_p is the principal cutting edge angle and its value is 75°. However, there is no clear agreement among the trend reported by various researchers. Kouadri *et al.* (2008) did not find any clear trend with cutting speed. Wang *et al.* (2014) reported rise in saw-tooth distance with cutting speed, whereas the observation made by Dong *et al.* (2011) was the exactly opposite. Variation of saw-tooth distance in the current study has been shown in Fig. 4.14. Increase in saw-tooth distance with cutting speed or machining duration may be attributed to the degree of deformation (strain rate) as well as tool wear, where fall can be explained by the effect of thermal softening. According to Katuku et al. (2009), thermal softening during machining of nickel-based super alloys causes formation of streaks and micro pores at the under surface of the chips. This in turn results in higher frequency of segmentation (*i.e.* shear banding) and reduction in saw-tooth distance. This phenomenon is pre dominant when the machining duration is higher. Since coated tool has the capability to restrict degree of deformation which in turn leads to less flank wear, saw-tooth distance could be reduced with the use of coated tool. Most prominent decrease can be noted at medium cutting speed. Since both the effects of strain hardening or thermal softening are less dominant at low cutting speed compared to those at medium and high cutting speed, coated tool did not cause substantial reduction in saw-tooth distance at low cutting speed. In fact, uncoated tool failed after 150 s under high cutting speed (Fig. 4.6) and therefore was discontinued (Thakur *et al.*, 2014a, 2015a). Steady increase in saw-tooth distance for coated tool at high cutting speed was due to increase in flank wear (Fig. 4.6) and increase in degree of deformation or strain hardening.

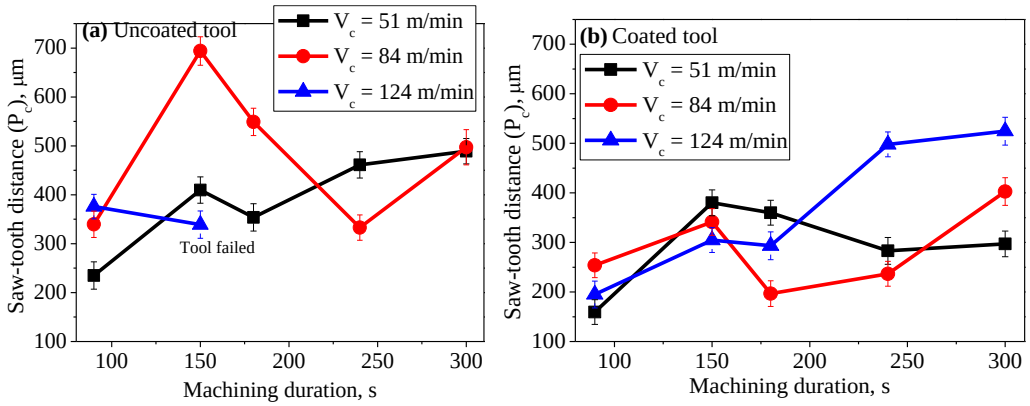

Fig. 4.14: Variation of saw-tooth distance with machining duration and cutting speed while using (a) uncoated and (b) CVD multilayer coated carbide inserts.

Fig. 4.15 depicts the effect of cutting speed, machining duration and CVD multilayer coated carbide tool on chip segmentation frequency. Chip segmentation frequency is dictated by two competing phenomena namely strain hardening or degree of deformation and thermal softening. The figure clearly reveals that increase in chip segmentation frequency with cutting speed took place for the fresh tools, both uncoated and coated. Moreover, the same for coated tool was significantly more than its uncoated counterpart. Increase in chip segmentation frequency might be related to reduction in chip-tool interface friction and rise in cutting temperature, improvement in overall machinability associated with enhanced cutting speed (resulting in rise in cutting temperature and consequent material softening) and with the application of coated tool. According to various researchers such as Atlati *et al.* (2011), Gente *et al.* (2001) and Ning *et al.* (2008), tool wear plays a major role in decreasing chip segmentation frequency. Tool wear causes plastic deformation in the primary shear zone to be more and large variation in cutting force. A further increase of the flank wear leads to an intensification of the chip segmentation. Plastic deformation of the material in the primary cutting zone becomes more pronounced with a distinctive border between the formed segments. The current work, in addition to bolstering their claims, shows an interesting feature of increase in chip segmentation frequency with coated tool by virtue of reduced flank wear. Recent study of the authors indicated that multilayer coated tool restricted tool wear significantly during dry machining of Incoloy 825 at high cutting speed i.e. 124 m/min (Thakur *et al.*, 2014a). Therefore, coated tool has caused higher chip segmentation frequency. It is interesting to note that the degree of increase also expanded when the cutting speed was elevated from 51-124 m/min. This is due to more effectiveness of the coated tool in augmenting resistance to wear at high cutting speed compared to that at lower cutting speed. This has already been established in the preceding section and presented graphically in Fig. 4.6. No consistent trend of variation of chip segmentation frequency with machining duration could be revealed.

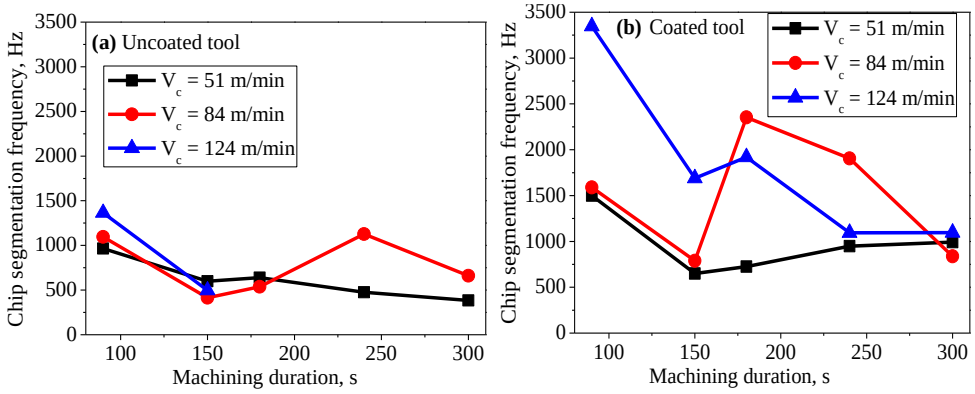

Fig. 4.15: Variation of chip segmentation frequency with machining duration and cutting speed while using (a) uncoated and (b) CVD multilayer coated carbide inserts.

Equivalent chip thickness (h_{ch})

Another important characteristic of serrated chip is equivalent chip thickness which is expressed by the following equation (Wang *et al.*, 2014),

$$h_{ch} = h + \frac{H-h}{2} \tag{4.2}$$

Increase in cutting speed led to decrease in equivalent chip thickness for uncoated tool (except at the initial condition) as evident from Fig. 4.16 owing to increase in flow velocity and consequent reduction in tendency in chip stagnation over rake surface of the tool. On the other hand, there is no uniform trend of variation of h_{ch} with V_c for coated tool. The behaviour for the coated tool is taken into consideration, as such the trend is not very consistent with machining duration. However, at the beginning (i.e. after 60 s of machining) values were same for the coated tool irrespective of cutting speed. Variation of h_{ch} typically depends on chip-tool interface friction, fluctuation of force and tool wear. Since none of these effects is pre-dominant for the fresh coated tool, cutting speed hardly has any impact on h_{ch}. Increase in h_{ch} till 150 s followed by reduction may be attributed to formation and subsequent removal of BUE and edge rounding due to tool wear. Higher edge rounding would tend to decrease effective deformed layer thickness and consequently result in lower chip thickness. Increasing trend of equivalent chip thickness for coated tool under high cutting speed can be explained by higher chip-tool interface friction and tool wear due to partial removal of coating which is demonstrated in Fig. 4.7. Due to the same explanation of tool wear being more predominant for the uncoated tool under high cutting speed, higher edge rounding would effect a reduction in equivalent chip thickness. Due to the same reason, there is always a drooping nature of the curve towards the end i.e. after 240 s of machining. Interestingly, due to the same explanation, drooping nature of chip segmentation frequency (Fig. 4.15) and increasing trend of equivalent chip thickness (Fig. 4.16) seemed to be correlated.

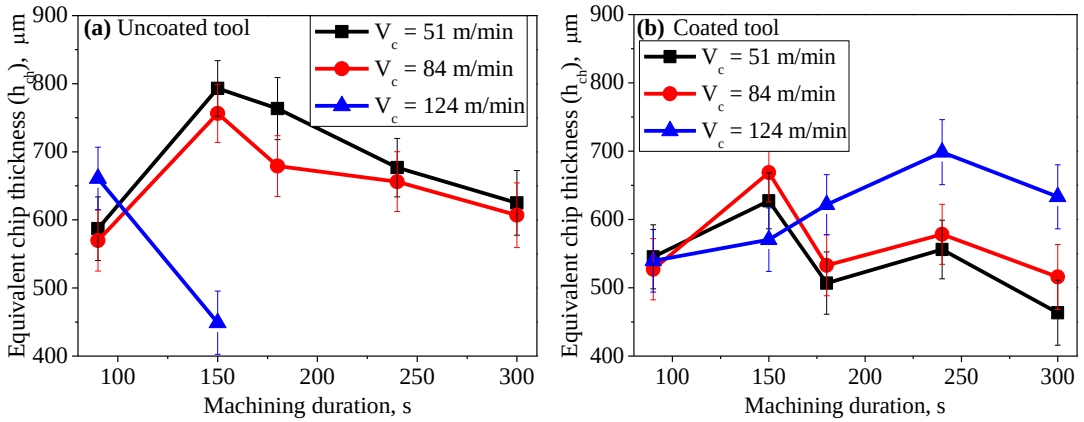

Fig. 4.16: Variation of the equivalent chip thickness with progression of machining and cutting speeds while using (a) uncoated and (b) CVD multilayer coated carbide inserts.

Saw-tooth chip angle (ϕ_1)

Saw-tooth chip angle is influenced by degree of shear deformation, strain hardening and thermal softening (Cotterell and Byrne, 2008; Gente *et al.*, 2001). Therefore, the trend of variation of the same with cutting speed and machining duration, shown in Fig. 4.17, is basically by the competitive influence of these mechanisms which are difficult to predict. It is evident that rise in cutting speed causes ϕ_1 to increase (except for two machining durations using coated tool) which is primarily related to higher rate of deformation. Interestingly, increase in cutting temperature resulting from elevation in cutting speed and machining duration can lead to both thermal softening as well as strengthening of work material in the form of dynamic recrystallization with or without grain growth (Thakur *et al.*, 2014b). Accordingly, decreasing trend of ϕ_1 is related to thermal softening, whereas increasing trend can be explained by strain hardening for both uncoated and coated tools (Joshi *et al.*, 2013). General increasing trend after 180 s of machining with the coated tool can therefore be explained by thermal softening due to prominent increase in temperature caused both by deformation as well as tool wear (Fig. 4.6) (Thakur *et al.*, 2014a, 2015a).

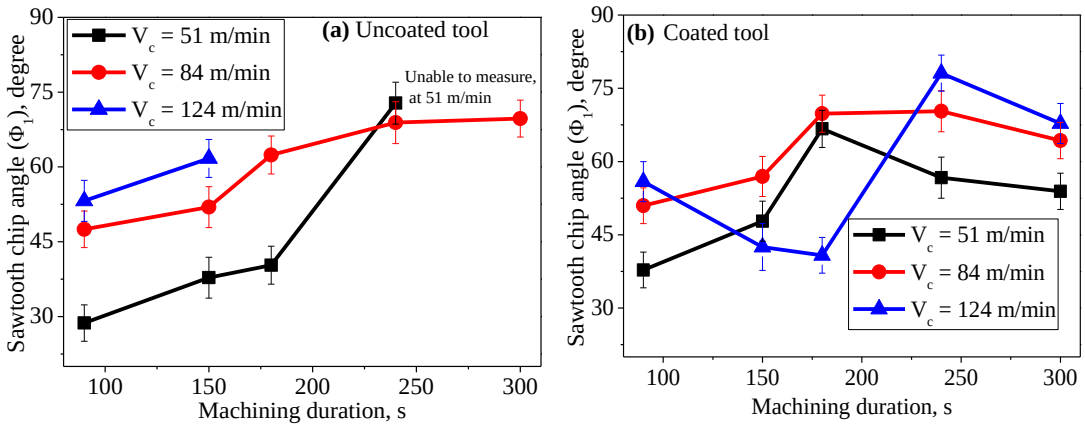

Fig. 4.17: Variation of saw tooth chip angle with machining duration and cutting speed while using (a) uncoated and (b) CVD multilayer coated carbide inserts.

4.2.4 Study of chip-tool contact length (L_{ch})

Chip-tool contact length is one of the important aspects deciding the mechanism of chip formation during machining. This has been measured from the SEM micrographs of the rake surface of the tool. Representative image of chip-tool contact length is depicted in Fig. 4.18. Fig. 4.19 represents variation of chip-tool contact length with progression of machining duration and cutting speed while using both uncoated and coated tools. It is evident from the figure that chip-tool contact length gradually decreased with machining duration till 240 s and subsequently increased when machining with cutting speeds of 51

and 84 m/min. Decrease in chip-tool contact length with elevation in cutting speed was observed by Kouadri *et al.* (2008). Chip-tool contact length is primarily governed by chip-tool interface friction and tool wear. The observed phenomena might be attributed to the initial formation of BUL or BUE which got reduced as the machining operation progressed. After a machining duration of 240 s, the role of tool wear became more predominant which led to rise in contact length. The figure also clearly demonstrated two more aspects with relation to chip-tool contact length. Increase in cutting speed for both the tools resulted in decrease in contact length (Atlati *et al.*, 2011; Kouadri *et al.*, 2008) except under high cutting speed for uncoated insert. Coated tool was found to be beneficial in reducing chip-tool contact length during dry machining of Incoloy 825. Application of high cutting speed or use of coated tool contributed to drop in chip-tool interface friction and consequent decrease in chip-tool contact length. However, tool wear played a predominant role at high cutting speed (124 m/min) for uncoated tool (Fig.4.6) leading to rapid increase in contact length.

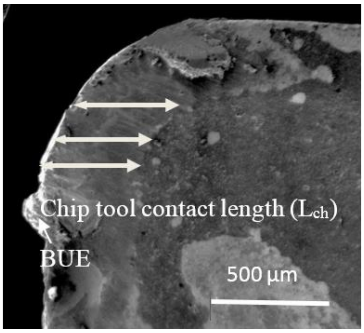

Fig. 4.18: Representative SEM image of rake surface indicating measurement of L_{ch}.

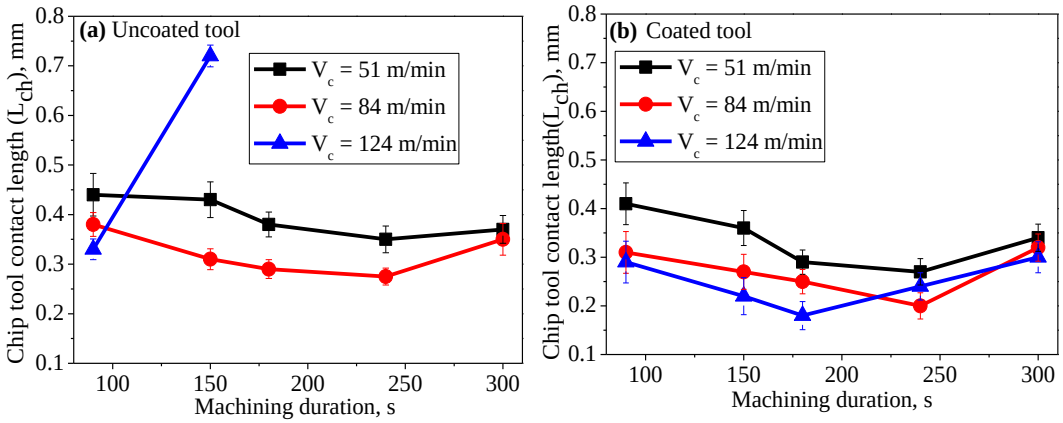

Fig. 4.19: Variation of chip tool contact length with machining duration and cutting speed while using (a) uncoated and (b) CVD multilayer coated carbide inserts.

4.2.5 Microhardness of chip

Microhardness of chip is primarily influenced by deformation due to thermal softening and shear strain reported by Velásquez *et al.* (2007). Measurement of microhardness was carried out in the matrix of chips as shown in Fig. 4.20. Variation of chip hardness with progression of machining for different cutting speeds using both uncoated and CVD coated inserts is presented in Fig. 4.21. It clearly indicates that there is a rise in microhardness of chip with increase in cutting speed which might be attributed to mechanical deformation associated with high cutting speed. With increase in cutting speed, combination of both mechanical and thermal deformation results in increase in dislocation density, thereby causing grain refinement (Thakur *et al.*, 2014b). This might be responsible for increase in microhardness of chip during machining. However, when machining was carried out progressively, there was hardly any uniform variation of microhardness of chip with machining duration. However, increase in microhardness is attributed to mechanical induced deformation leading to dynamic recrystallization. On the hand, thermal induced deformation leads to material softening. These two competing mechanisms are essentially responsible for variation of results. Application of multilayer coating appeared to bring down chip hardness particularly at low and medium cutting speed. Beneficial effect of coating in reducing chip microhardness may be explained by decrease in strain hardening. This result is in good agreement with influence of tool coating on saw-tooth distance (Fig. 4.14).

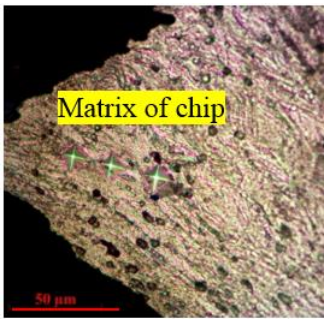

Fig. 4.20: Representative optical microscopic image of Vickers indents on matrix of chip.

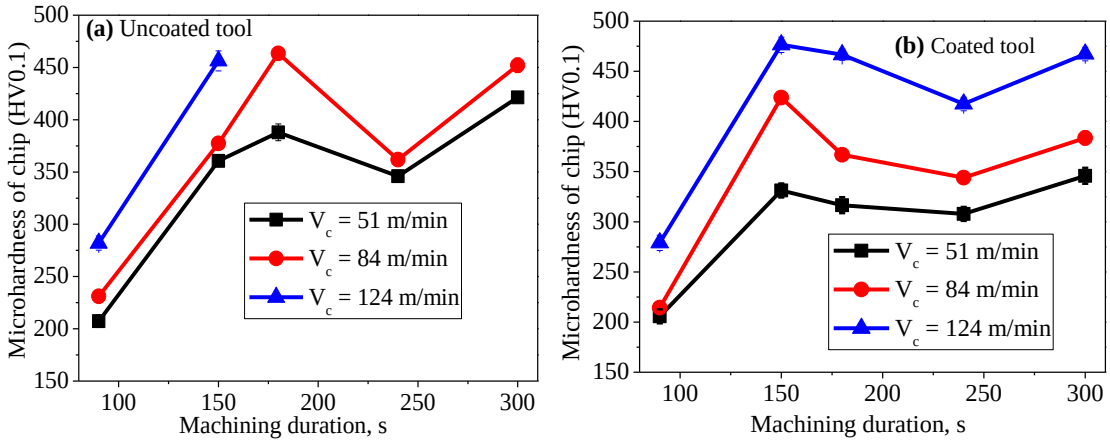

Fig. 4.21: Variation of microhardness of chip measured at the matrix of chip with machining duration and cutting speed while using (a) uncoated and (b) CVD coated carbide inserts.

4.2.6 X-ray diffraction of chip

X-ray diffraction was carried out on chips to investigate if there was any phase transformation, modification of grain size or lattice strain due to machining under different cutting speeds while using uncoated and coated tools. Fig. 4.22 indicates XRD spectra of chips obtained during dry turning of Incoloy 825 with cutting speed of 84 m/min using both uncoated and CVD coated tools. The figure reveals there was neither change in phase nor prominent shifting of peaks in the deformed chips due to application of coated tool. On the other hand, uncoated tool effected noticeable broadening of peaks indicating that grain size of the chips obtained with the uncoated tool was less compared to its coated counterpart as depicted in Fig. 4.22.

The result is indicative of higher amount of plastic deformation and chip-tool interface friction (Velásquez *et al.*, 2007) resulting in strain hardening taking place during machining with uncoated carbide insert which could be reduced with the application of coated tool. It is known that peak broadening i.e. increase in full width half maxima (FWHM) is related to grain refinement which in turn is responsible for rise in hardness according to Hall-Petch effect (Gangopadhyay *et al.*, 2010). The XRD result can therefore, explain the harder chip obtained with uncoated tool in comparison with the coated one while machining with a cutting speed of 84 m/min.

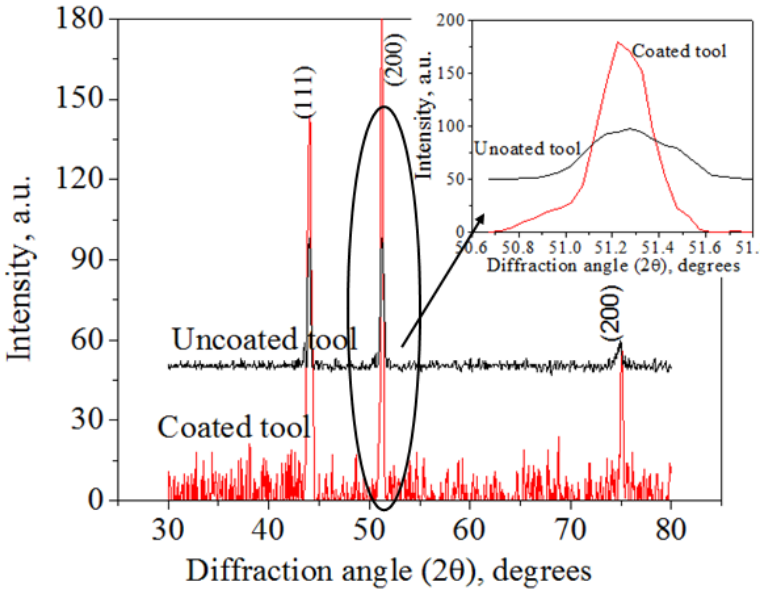

Fig. 4.22: XRD spectra of chips obtained using uncoated and CVD multilayer coated inserts.

4.3 Effects of CVD tool coating and cutting speed on surface integrity during dry machining of Incoloy 825

4.3.1 Surface roughness

Surface roughness of the machined component is one of the most significant indices indicating surface quality or integrity of the same. Fig. 4.23 shows the variation of surface roughness with cutting speed after 150 s machining of Incoloy 825 using uncoated and CVD multilayer coated tools. Fig. 4.23 clearly shows gradual deterioration of surface finish with increase in cutting speed. Severe frictional rubbing combined with formation of BUE within the specified cutting range was responsible for worsening surface finish. It is also evident that the CVD multilayer coated tool could not improve the surface quality compared to its uncoated counterpart. It may be noted that the surface roughness of uncoated insert is usually lower than CVD coated insert as shown in Table 4.1. In addition to this, the rounding of cutting edge due to edge treatment (like honing) typically done prior to CVD and presence of several layers of coating for CVD multilayer coated tool can also be attributed to higher machined surface roughness as compared to its uncoated counterpart. Similar observation has been made by other researchers such as Narasimhan and Russell (2001) and Zhou *et al.* (2012). High surface roughness at cutting speed of 124 m/min obtained with uncoated tool can be explained by complete failure of the same tool after 150 s of machining (Fig. 4.5).

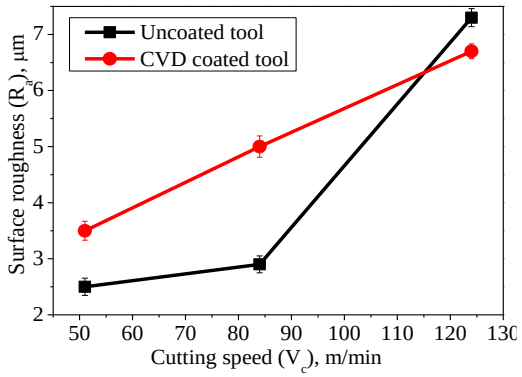

Fig. 4.23: Variation of surface roughness with V_c while using uncoated and CVD coated inserts.

Table. 4.1: Surface roughness of uncoated and CVD coated tools.

Tools	R_a on flank face (µm)	R_a on rake face (µm)
Uncoated tool	0.6	0.7
CVD coated tool	1.2	1.4

4.3.2 Macro morphology of machined surface

Surface quality is often characterised by morphology of the machined surface which remains one of the areas of concern for nickel-based super alloys. Fig. 4.24 shows FESEM images of the morphology of machined surface of Incoloy 825 using uncoated and coated carbide inserts after machining duration of 150 s. Smeared materials, feed marks, debris and re-deposited material were observed on the machined surface. Feed marks were more prominent under lower cutting speed (51 m/min). With increase in cutting speed, cutting temperature increases resulting in more plastic deformation of the workpiece surface. As a consequence, gradual deformation of the feed mark took place on the surface machined with both uncoated and coated tools. However, under the condition of high cutting speed (124 m/min), characteristics or quality of the machined surface deteriorated with the evidence of surface plucking, chip debris and re-deposited materials. This might be explained by high cutting temperature, severe deformation and failure of the uncoated tool (Thakur *et al.*, 2014a). It may be further noted that the coated tool could not significantly improve the machined surface morphology, since presence of debris and material re-deposition could be detected. This might be attributed to the lower thermal conductivity of Al_2O_3 coating which caused a rise in temperature of the machined workpiece compared to that obtained using uncoated carbide insert. The observation is in good agreement with the result of surface roughness (Fig. 4.23).

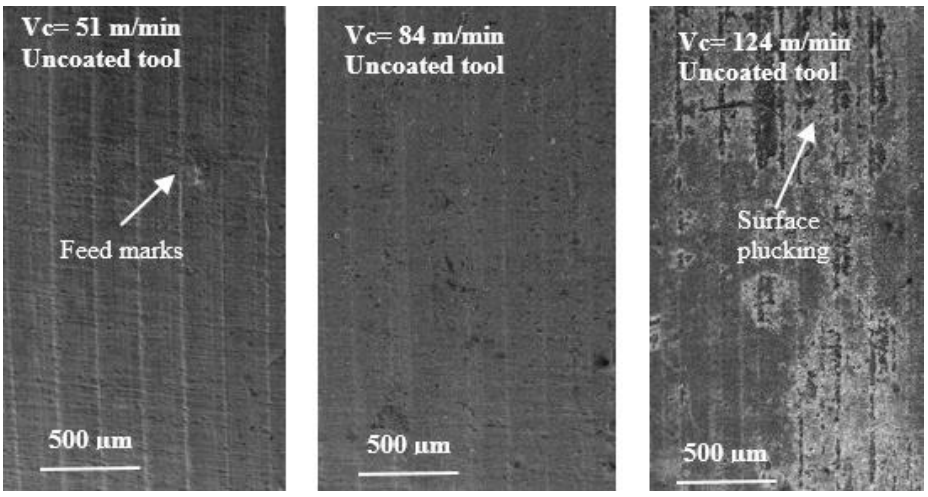

(a)

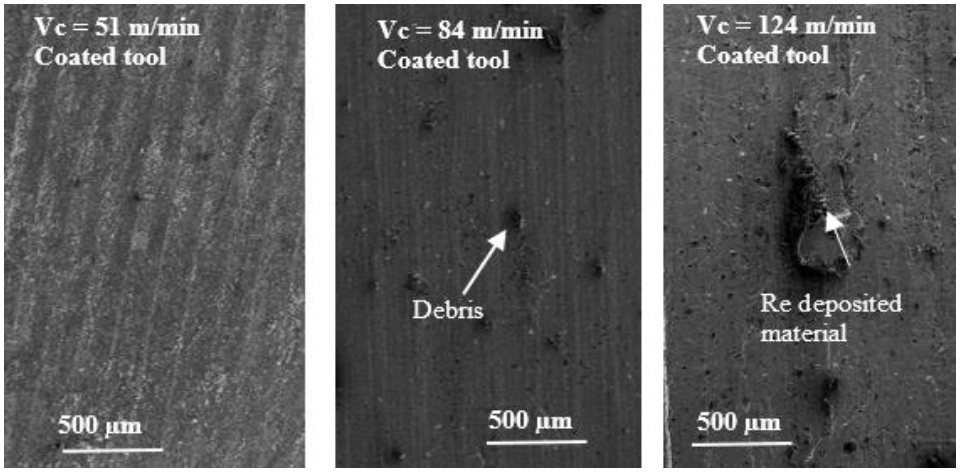

(b)

Fig. 4.24: Various features on workpiece surface after machining with different cutting speeds while using (a) uncoated and (b) CVD multilayer coated tools.

4.3.3 X-ray diffraction analysis

XRD spectra for as-received and machined surface of Incoloy 825 using uncoated and coated tools at various cutting speeds are presented in Fig. 4.25. XRD was carried out for determination of any metallurgical changes taking place such as phase transformation or any modification in grain size. Crystal structure and phase change can be established primarily through position of the peaks, whereas the crystallite size can be determined through FWHM. The XRD patterns of all the test samples show similar sequence of peaks in terms of the intensity. Since similar position of peaks as that of bulk material were obtained for all test samples it can be concluded that no phase change took place during the machining under various cutting condition with both the types of tools. Broadening (FWHM) of the peaks divulges the variation in the crystallite size. Comparing the XRD spectra of the bulk material to that of machined surface obtained using uncoated and coated tools, clear difference in the intensity and width of the peaks could be observed. Therefore, it can be concluded that machining process induced grain refinement of the workpiece material while using different cutting tools. The grain refinement due to machining process can be explained by severe plastic deformation of the machined surface due to thermomechanical effect which in turn causes metallurgical modification of the surface. Severe deformation during machining of nickel-based super alloy also leads to dynamic recrystallization involving nucleation of new grains resulting in grain refinement (Chou *et al.*, 1999; Mondelin *et al.*, 2013; Pawade *et al.*, 2008; Umbrello, 2013).

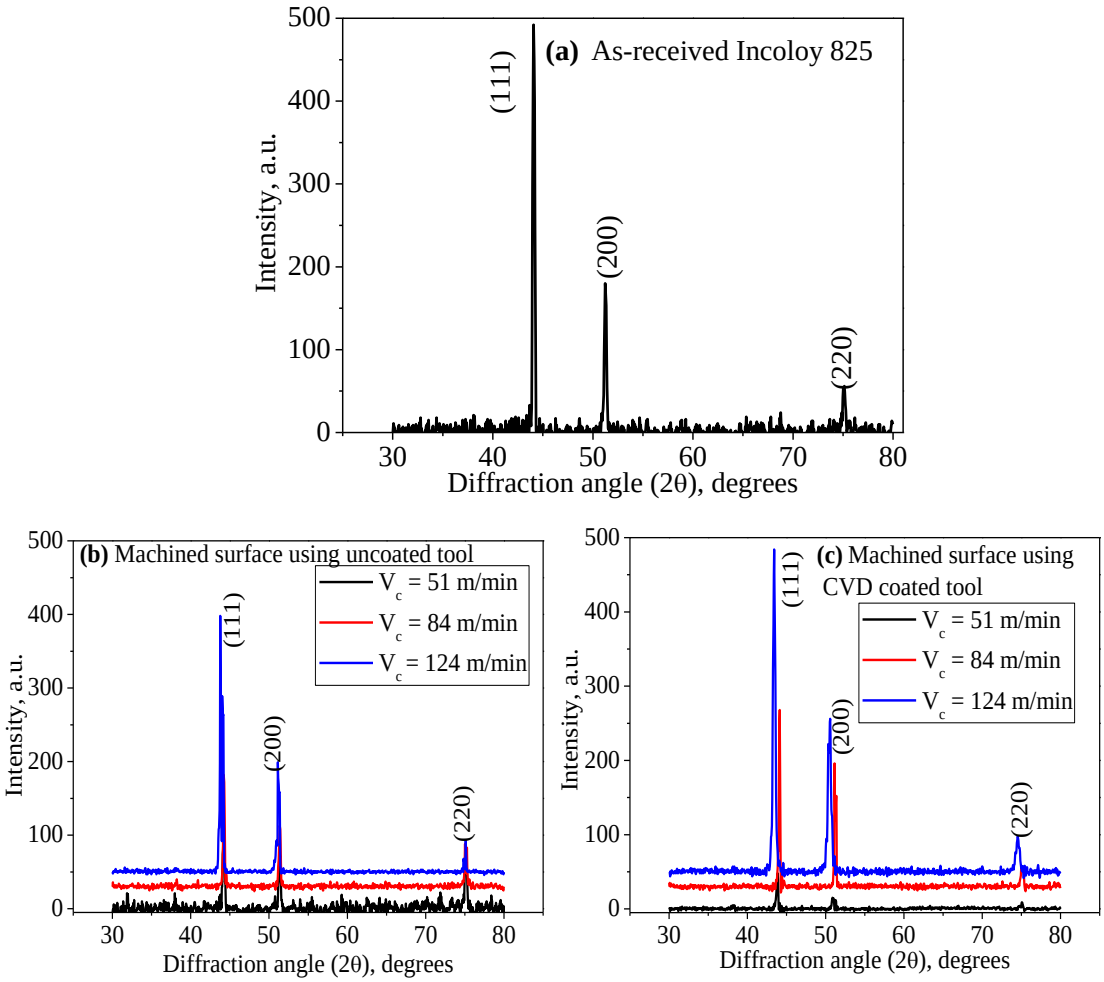

Fig.4.25: XRD spectra for (a) as-received and machined surface using (b) uncoated and (c) CVD multilayer coated tools.

4.3.4 Grain size analysis

It can be observed from Fig. 4.26 that the grain size as calculated from Scherrer's formulae given by equation (4.3) (Joshi *et al.*, 2014) for surface machined with uncoated and coated tools, followed a decreasing trend with increase in cutting speed.

$$\tau = \frac{K\lambda}{\beta cos\theta} \tag{4.3}$$

where, τ is the crystallite size (Å), K is a dimensionless constant generally close to one but approximately taken as 0.9, λ (Cu- Kα radiation, 1.5418 Å) is the wavelength of incident radiation, β is the line broadening at half the maximum and 2θ is the diffraction angle. Initially, with increase in cutting speed decrement in crystallite size was observed for both uncoated and coated inserts. Similar findings were noted by Mondelin *et al.* (2013) and

Umbrello (2013). Degree of shear deformation and consequently the plastic deformation enhance when cutting speed is elevated. Rate of tool wear also becomes faster at higher cutting speed contributing to further increase of deformation. The combined effect results in severe deformation of grains i.e. increasing dislocation density which when reaches a critical value results in nucleation of new undeformed grains. The change in the crystallite size when machining with uncoated and coated carbide inserts is responsible for variation in the hardness of machined surface and sub-surface region which has been further discussed. It is also evident from Fig. 4.26 that the machining with uncoated tool at low (V_c = 51 m/min) and medium cutting speeds (V_c= 84 m/min) led to more grain refinement than that with coated carbide insert. This can be attributed to poor wear resistance of uncoated carbide insert than the CVD multilayer coated insert (Fig. 4.5). However, at higher cutting speed of 124 m/min, grain size for the uncoated carbide tool was more than that for coated carbide tool. Uncoated insert resulted in higher cutting temperature due to high cutting speed as well as severe tool wear. This possibly caused prominent grain growth during dynamic recrystallization (DRX).

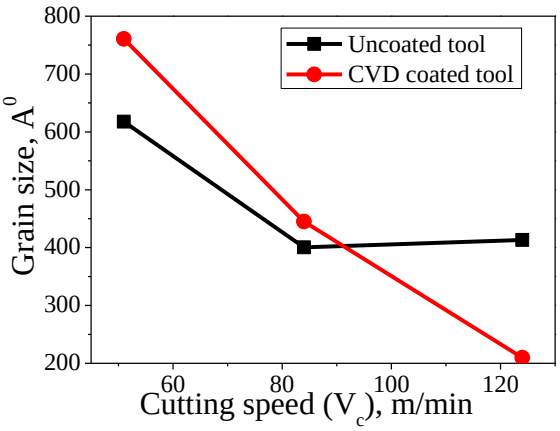

Fig. 4.26: Variation of grain size of machined samples with cutting speed while using uncoated and CVD multilayer coated tools.

4.3.5 Micromorphology of machined surface

Imran *et al.* (2011, 2014) carried out in depth analysis of microstructure in the sub-surface region of machined surface using SEM, EBSD and TEM techniques, the modification of crystal structure has so far been investigated only using XRD technique. Moreover, many researchers (Jin and Shaoyu, 2014; Thakur *et al.*, 2014b; Umbrello, 2013) have pointed out that DRX involving grain refinement, nucleation of grains and grain growth plays a pivotal role on generation of modified surface during machining of nickel-based super alloy. Therefore, it is also equally essential to study micromorphology of machined surface using high resolution SEM with an aim to provide direct evidence of DRX. Fig. 4.27 depicts

micro features of the machined surface of Incoloy 825 obtained during machining with uncoated and CVD coated carbide inserts under varying cutting speeds. It can be observed that at lower cutting speed of 51 m/min some micro surface textures of deformation due to machining are visible on the machined surface for uncoated and coated inserts. However, coated tool resulted in a smoother micromorphology having less evidence of plastic flow than its uncoated counterpart. Nevertheless, no evidence of nucleation or recrystallization could be revealed at this stage. But with increase in cutting speed to 84 m/min generation of early nucleation sites occurred, although due to poor crystallinity the nucleation sites were not very prominent. Therefore, no undeformed recrystallized grains could be visible. Higher degree of deformation associated with more dislocation density at higher cutting speed of 124 m/min led to generation of more nucleation sites or grain refinement on machined surface as a consequence of DRX during machining with coated carbide tool as clearly depicted in Fig. 4.27.

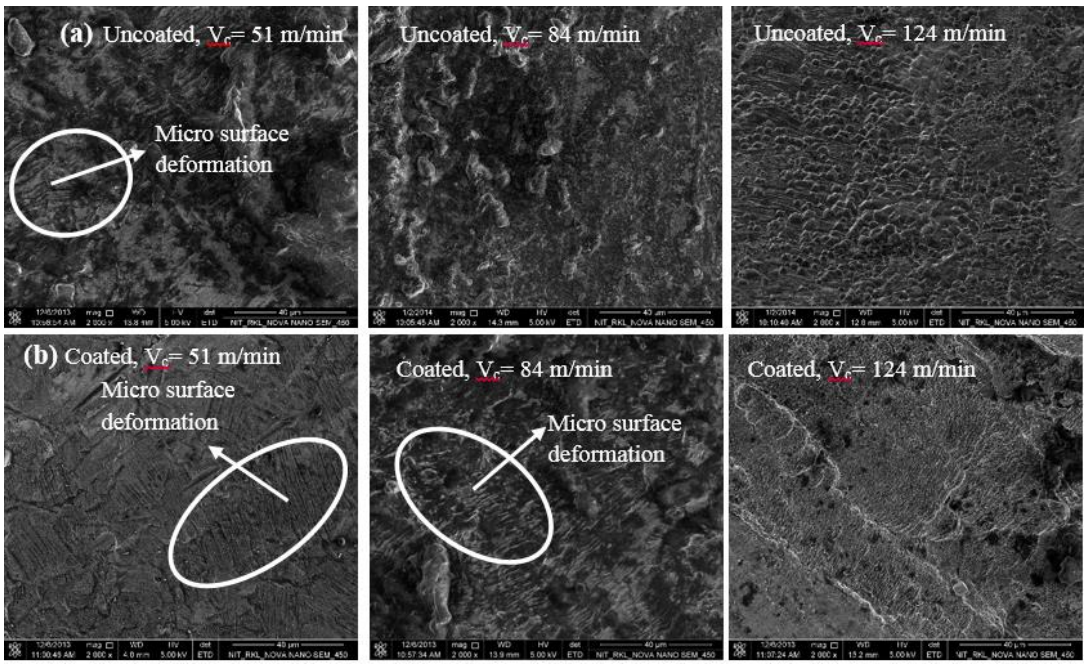

Fig. 4.27: Variation of micro features of the machined surface of Incoloy 825 obtained after machining with different cutting speeds while using (a) uncoated and (b) CVD coated tools.

It is very interesting to note different stages of nucleation of new recrystallized grains during DRX while machining with uncoated tool. The detailed features of the machined surface obtained at higher cutting speed was further magnified and has been depicted in Fig. 4.28. The figure clearly demonstrates the formation of nucleation or incubation sites wherein large number of new undeformed recrystallized grains grow during DRX. The grain growth observed during machining with uncoated tool was facilitated by high cutting temperature due to combined effect of severe plastic deformation as well as tool wear taking

place at high cutting speed. This observation also clearly establishes results obtained by XRD (Fig. 4.25) which indicated larger grain size obtained with the uncoated tool compared to that with coated tool at higher cutting speed. Lower cutting temperature as a result of lower deformation and tool wear did not promote formation of recrystallized grains. With increase in further deformation the incubation sites would have been resulted into formation of fully grown recrystallized grains. Therefore, the surface shown in Fig. 4.28 (a) is considered to be the pre stage for the formation of the surface obtained with uncoated tool Fig. 4.28 (b).

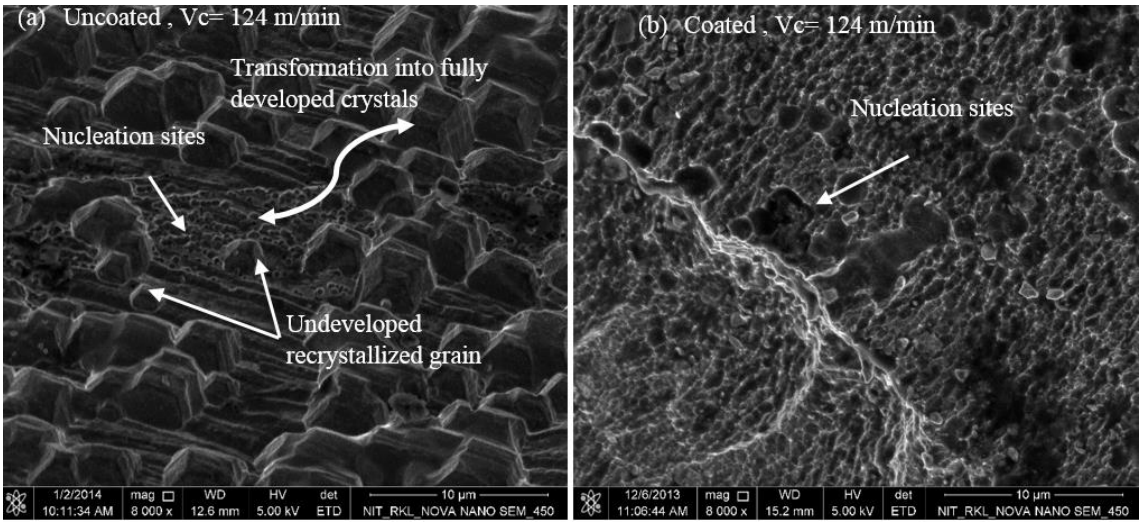

Fig. 4.28: Magnified view of micro features of the machined surface of Incoloy 825 obtained during machining at 124 m/min cutting speed using (a) uncoated and (b) CVD coated inserts.

4.3.6 Surface and sub-surface analysis

Three mechanisms namely rapid heating and quenching, plastic deformation and surface reaction are responsible for the formation of white layer during machining (Alexandre *et al.*, 2011; Jin and Shaoyu, 2014). The white layer is known to be detrimental to the low cycle fatigue life of the machined components under high stress and temperature applications (Alexandre, 2004; Ranganath *et al.*, 2009). Fig. 4.29 demonstrates FESEM images of surface and sub-surface regions after machining with uncoated and coated tools for duration of 150 s under different cutting speeds. Severe shear deformation accompanied by rise in temperature in the cutting zone with increase in cutting speed may be attributed to the increase in the thickness of white layer. The lower thermal conductivity of Incoloy 825 results in poor dissipation of heat to the surroundings. This phenomenon was more pronounced at higher cutting speed (124 m/min). With progression of cutting speed, tool wear for both uncoated and CVD coated inserts gradually increase, with more dominant for uncoated carbide insert (Thakur *et al.*, 2014a). The benefits of using CVD multilayer coated

tool over its uncoated counterpart in the formation of the white layer are clearly visible for the cutting speeds of 51 and 84 m/min. Under this cutting condition, the anti-friction property of CVD coated insert was able to restrict mechanically and thermally induced deformation, hence, resulting in formation of thinner white layer as well as deformed layer at surface and sub-surface region than its uncoated counterpart. When machining under low cutting speed with CVD coated tool, either white layer could not be visible or very thin white layer could be detected. However, thickness of white layer obtained for coated insert under high cutting speed of 124 m/min was observed to be comparable with that of uncoated insert. This phenomenon can be attributed to lower thermal conductivity of the coating layers of coated tool, particularly Al_2O_3, which prevented heat to dissipate into the tool substrate leading to generation of higher temperature at tool-workpiece interface and hence presence of greater heat affected region.

4.3.7 Hardness depth profile

Work hardening tendency of the nickel-based super alloy poses a major problem during machining. The degree of work hardening of the machined surface is primarily influenced by cutting parameters. The current research work investigates the influence of cutting speed and CVD multilayer coating on the hardness of the machined surface and sub-surface layers. Fig. 4.30 depicts the variation of micro hardness with distance from the edge towards the centre of machined sample with different cutting speeds using uncoated and coated carbide inserts for machining duration of 150 s. It is evident from the figure that there is significant difference in hardness between the machined surface and sub-surface layers to that of bulk material. This can be attributed to variation in the grain or crystallite size between the machined surface and bulk material. SEM images of the microstructure obtained at two different depths clearly show increase in grain size with depth from the top surface. Microhardness as usual showed a decreasing trend till bulk material at all cutting speeds when machining with both uncoated and coated tools, implying work hardening of material during machining. It is also evident that hardness increased with cutting speed for all the tools. This might be attributed to fact that tool wear progressed simultaneously with cutting speed (Fig. 4.6) (Thakur *et al.*, 2014a) including high friction at tool-workpiece interface leading to higher plastic deformation and hence the hardness. However, it can be observed from Fig. 4.30 that hardness of machined surface with the uncoated carbide insert happened to be lower than that found for low and medium cutting speeds. This can be attributed to the thermal softening of the

V_c, m/min	Uncoated tool	CVD coated tool

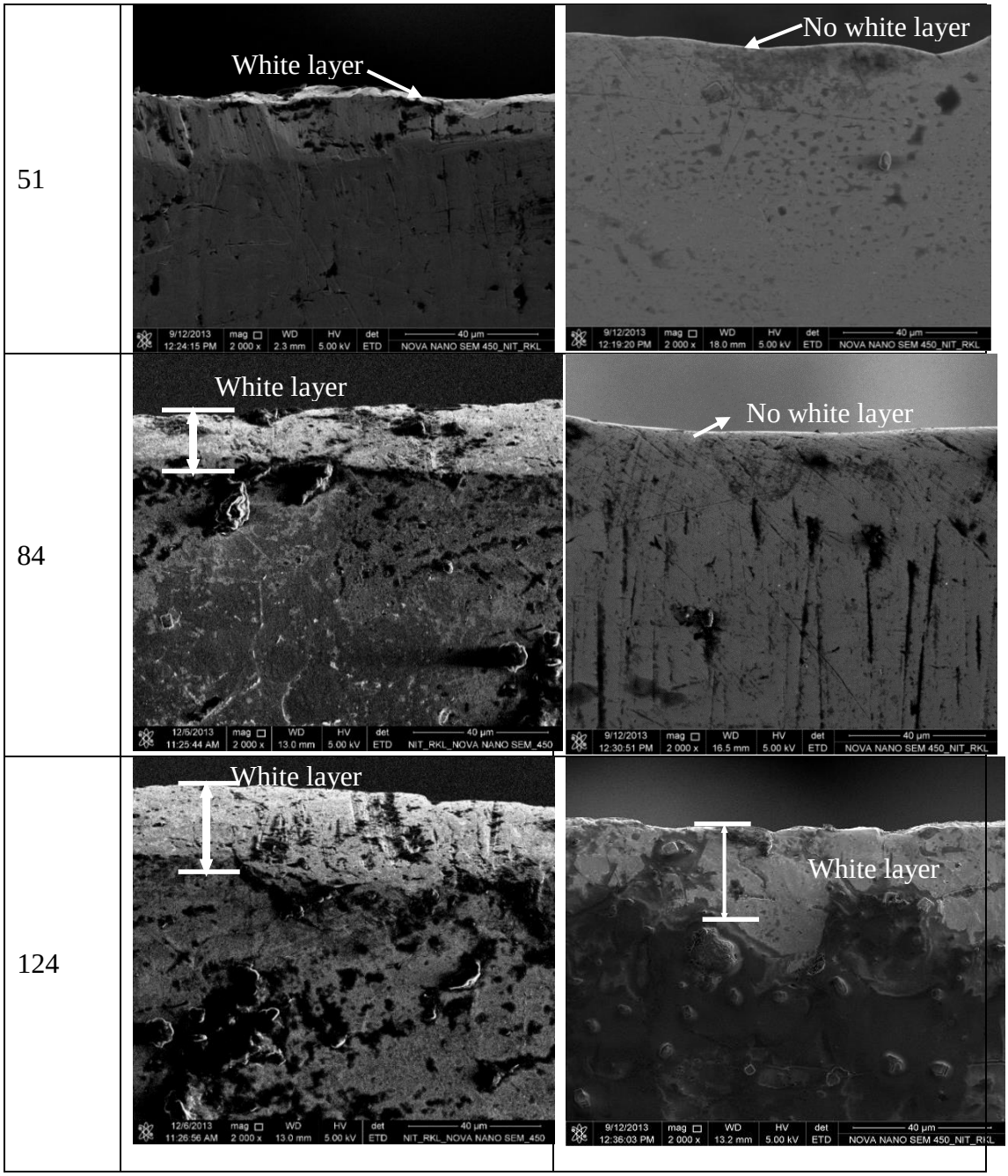

Fig. 4.29: FESEM images of surface and sub-surface region of cross section of machined part for different cutting speeds after machining with uncoated and CVD multilayer coated carbide tools.

machined surface at such high cutting speed of 124 m/min for the uncoated carbide insert. Lower hardness value can also be ascertained to the larger grain size due to grain growth occurring particularly at cutting speed of 124 m/min for uncoated carbide insert. The variation of the hardness between uncoated and CVD multilayer coated tools can be attributed to difference in friction characteristics of the tool materials. Low coefficient of friction of coating layers restricted rapid escalation of temperature at chip-tool interface

and consequently resulted in lower tool wear. This phenomenon led to decrease in both thermally and mechanically induced plastic deformation causing lower hardness of the machined surface compared to its uncoated counterpart.

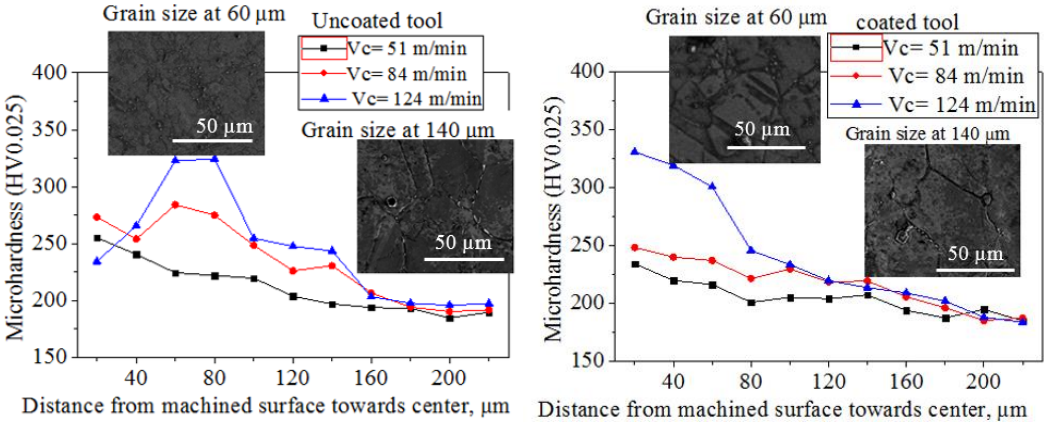

Fig. 4.30: Variation of micro hardness with distance from edge towards centre of machined surface for variable cutting speeds while using (a) uncoated and (b) CVD coated carbide inserts.

4.3.8 Residual stress

Machining induced residual stress for difficult-to-cut nickel-based super alloys is one of the critical aspects of surface integrity. Different characteristics of the machined components such as dimensional instability or distortion, resistance to corrosion and fatigue life are primarily influenced by residual stress. Therefore, the study of the same for better understanding the mechanism of formation and controlling the residual stress is of utmost importance. Fig. 4.31 depicts the variation of machined surface residual stress with cutting speed while using uncoated and coated tools. Tensile residual stress was found for the entire range of cutting speed while using uncoated tool, whereas coated tool resulted in compressive stress under high cutting speed. Significant variation of residual stress was noticed at high V_c. It can be attributed to higher tool wear (Fig. 4.5) which leads to thermally induced tensile residual stress for uncoated tool. On the other hand, excellent thermomechanical properties of CVD coated tool helped restrict tool wear. Abrupt decrease in residual stress under higher cutting speed (124 m/min) is explained by grain refinement while using CVD coated tool (Fig. 4.28). Low value of compressive residual stress owing to plastic deformation rather than thermal effect led to grain refinement which was also confirmed from XRD results (Fig. 4.25 and 4.26). Outeiro *et al.* (2008) also demonstrated that surface residual stress was slightly higher during dry turning of Inconel 718 using uncoated (1100 MPa) and coated (700 MPa) carbide tools at cutting speed of 70 m/min, feed of 0.2 mm/rev and depth of cut of 0.5 mm.

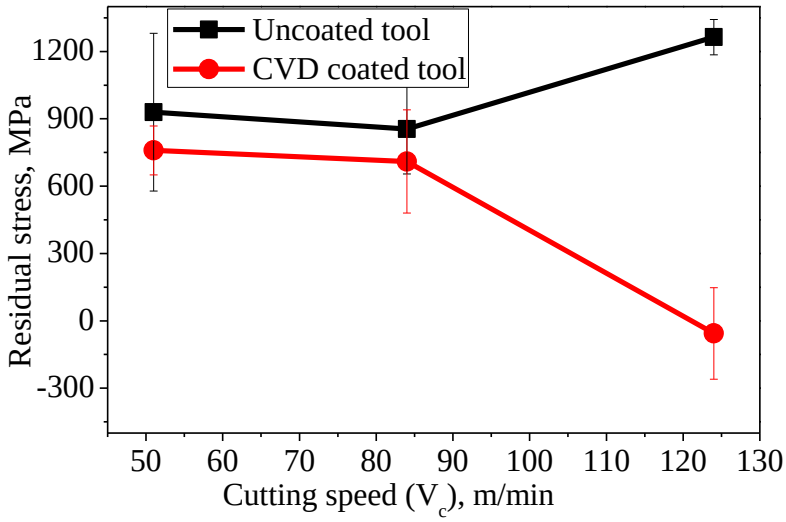

Fig. 4.31: Variation of residual stress with cutting speed while using uncoated and CVD multilayer coated carbide inserts.

4.4 Effects of deposition techniques, cutting speed and feed on some machinability aspects of Incoloy 825

4.4.1 Characterisation of cutting tools

Prior to evaluating the performance of different cutting tools, it is necessary to understand physical properties of the tools in terms of microstructure and chemical composition. Fig. 4.32 (a) shows a typical surface morphology of a microstructure of K20 grade of uncoated carbide insert. The performance of the uncoated tool has been compared with CVD TiCN/Al_2O_3 bilayer and PVD TiAlN/TiN multilayer coated tools, the morphology of which is indicated in Fig. 4.32 (b, c). Both the coated tools revealed quite uniform and smoother morphology which is important for good tribological properties. During machining, non-uniform coating would cause delamination finally leading to premature failure of coated tools.

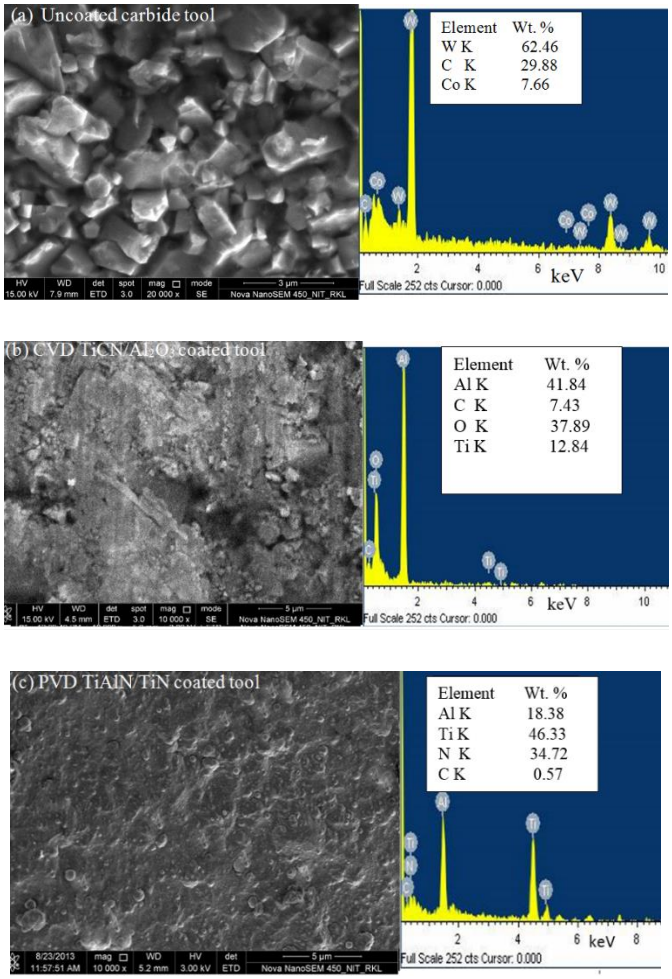

Fig.4.32: FESEM images of morphology along with EDS spectra of (a) uncoated, (b) CVD coated and (c) PVD coated tools.

Further, fractured surface of coated tools indicating thickness of coating layers has been depicted in Fig. 4.33. It indicates that CVD coated tool is thicker than the PVD coated tool. A base layer of TiCN with a thickness of approximately 5 µm and top layer consisting of Al_2O_3 with a thickness of approximately 3 µm is clearly visible from the coating fractograph of CVD coated tool. However, it is difficult to distinguish the nano-multilayer configuration of TiAlN/TiN for which ultra-high magnification possibly utilising TEM would be required. A thin layer of 1.7 µm thickness could only be detected.

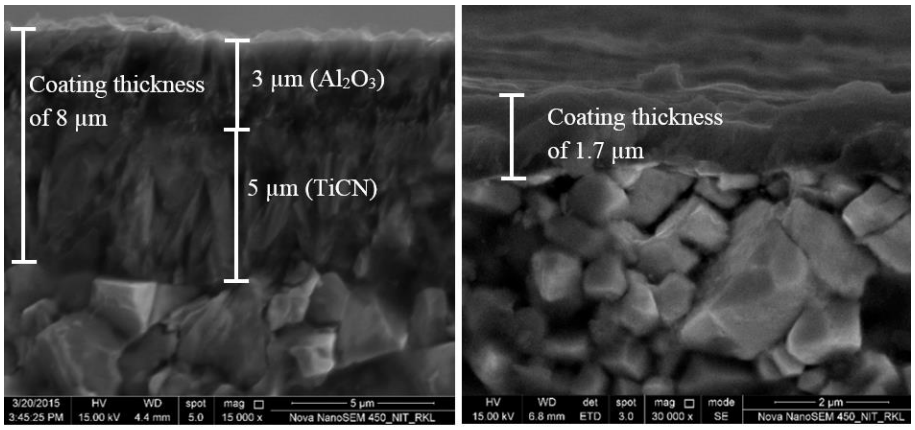

Fig. 4.33: Coating fractographs of (a) TiCN/Al_2O_3 bilayer coated and (b) TiAlN/TiN multilayer coated tools.

Various phases of uncoated tool has been determined and verified using XRD as shown in Fig. 4.34(a). In order to extract more information from the coated surface, GIXRD was carried out Fig. 4.34(b, c). While XRD spectrum of uncoated tool reveals the presence of WC and Co, coated tools clearly indicate the presence of Al_2O_3, TiCN for CVD and TiAlN, TiN for PVD coated tools.

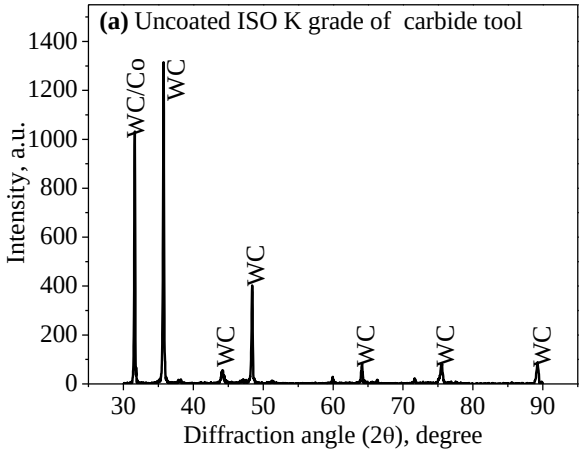

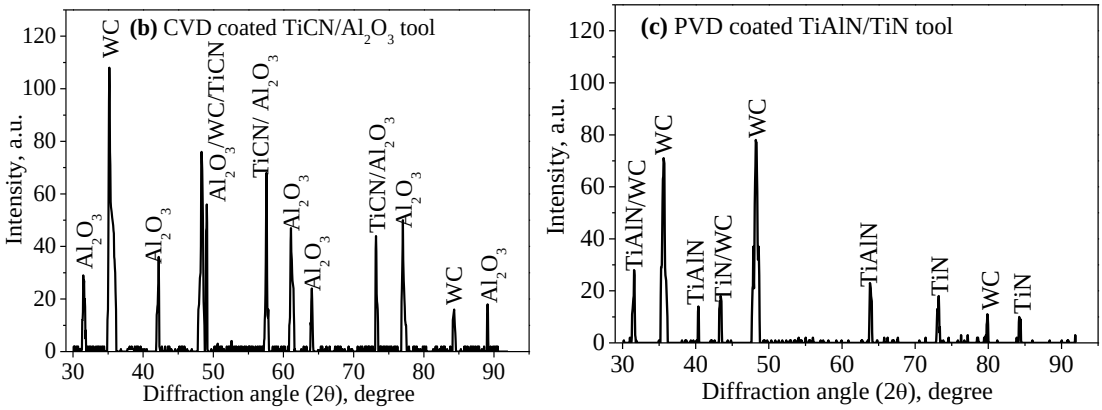

Fig. 4.34: XRD spectrum of (a) uncoated tool, GIXRD spectra for (b) $TiCN/Al_2O_3$ bilayer and (c) TiAlN/TiN multilayer coated tools.

4.4.2 Cutting temperature (T)

Owing to low thermal conductivity of Incoloy 825, cutting temperature is a critical issue and hence, should be studied. Fig. 4.35 demonstrates variation of temperature with variable cutting speed and feed at a constant depth of cut of 1 mm using uncoated, CVD and PVD coated tools after 30 s of machining. The temperature of the CVD coated tool was found to be higher than that of uncoated and PVD coated tools. Thermal conductivity has significant influence on both tribological and mechanical properties of the cutting tool with respect to machinability aspects. The thermal conductivity of the CVD coated tool is less than others which can be attributed to the presence of Al_2O_3 layer on CVD coated tool. Hence, other tools (uncoated and PVD coated tools) have greater ability to dissipate heat to the surrounding resulting in less temperature. Aslantas *et al.* (2012) and Samani *et al.* (2015) demonstrated that thermal conductivity of Al_2O_3 decreased with increase in temperature, while that of TiN increased with temperature. The cutting temperature increased with cutting speed for all the tools. This is related to increase in strain rate and deformation leading to higher tool wear (Kitagawa *et al.*, 1997; Thakur *et al.*, 2012b). It was also noticed that higher value of cutting temperature was noticed while using uncoated tool at high cutting speed. Lower resistance to wear of uncoated tool is responsible for higher temperature at high cutting speed (124 m/min) and feed (0.2 mm/rev). Under the same machining condition, temperature of uncoated tool reached the highest value of around 490℃. Similar results pertaining to higher temperature for uncoated tool than its coated counterpart have also been reported by Grzesik (2000) and M'Saoubi and Chandrasekaran (2004). On the other hand, PVD coated tool was found to be effective in decreasing cutting zone temperature. This is primarily due to the fact that TiN layer significantly contributed

to reduction in chip-tool and flank-work interface friction, while considerable wear resistance was imparted by TiAlN layer.

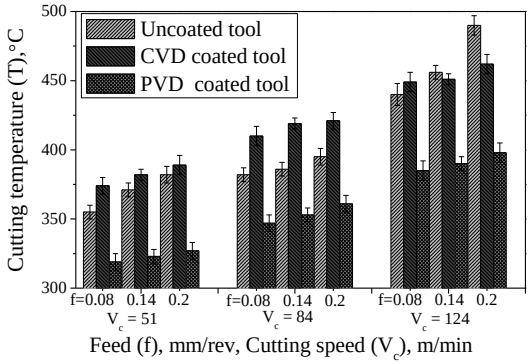

Fig. 4.35: Variations of cutting temperature with variable cutting speed and feed using uncoated, CVD coated and PVD coated tools.

4.4.3 Cutting force (F_c)

Role of tool coating on cutting force during machining of nickel-based super alloy would be of particular interest owing to strain hardening tendency of work material and also since it is directly related to requirement of cutting power. However, such information is relatively scarce in literature. While both CVD and PVD coated tools are used in the industries, the relative merits and demerits of such coated tools in terms of cutting force or power are also unknown. The current part of the research work which compared the performance of uncoated, CVD and PVD coated tools established interesting phenomena during dry machining of Incoloy 825. Fig. 4.36 (a) shows variation of cutting force with cutting speed while adopting constant feed of 0.08 mm/rev and depth of cut of 1 mm after 30 s of machining. Results clearly indicate that the magnitude of cutting force can be brought down with the use of coated tools. More interestingly, PVD coated tool consisting of TiAlN/TiN multi-layer coating showed more remarkable reduction in the magnitude as well as dynamic component Fig. 4.36 (b) compared to CVD coated tool in the entire range of cutting speed. A maximum reduction in cutting force of 58% compared to uncoated tool and 31% compared to CVD coated tool have been noted with PVD coated tool. It is also evident from the same figure that there was hardly any difference in dynamic component between uncoated and CVD coated tools. It may be noted that Al_2O_3 and TiCN coatings are known for their hardness rather than toughness which can be provided only with the help of PVD technique (Grzesik, 2000; Samani *et al.*, 2015). Moreover, good balance of hardness and toughness is also possible by the use of TiAlN and TiN layers in their alternate multilayer architecture deposited by PVD technique (Barshiliaa and Rajam, 2004; Dobrzanski and Pakuła, 2005). Prominent dynamic fluctuation in Incoloy 825 might be

attributed to the presence of non-uniform distribution of hard and abrasive ϒ′ phase consisting of precipitate of Ni_3Ti along with metal carbides such as $Cr_{23}C_6$, Mo_2C etc. (Pan *et al.*, 2000; Rai *et al.*, 2004). It is also important to note from Fig. 4.36 that more significant reduction in cutting force took place when cutting speed was elevated to 124 m/min. This might be ascribed to decrease in contact surface area with high cutting speed and also possible softening of work material due to rise in temperature (Fig. 4.35) (Ezilarasan *et al.*, 2013; Nalbant *et al.*, 2007). Additionally, prominent reduction by around 43% in cutting force was also possible with CVD coated tool when compared with uncoated tool. Obvious trend of increase in cutting force with feed has also been observed, as shown in Fig. 36 (c). Much higher cutting force was observed with Inconel 718 in the study of Devillez *et al.* (2007). It may be therefore inferred that overall machinability of Incoloy 825 is higher than Inconel 718.

4.4.4 Apparent coefficient of friction (μ_{app})

Friction at the chip-tool interface is an important mechanism governing several aspects of machining like cutting force, temperature, chip formation and tool wear and is typically expressed by apparent coefficient of friction. The value of apparent coefficient of friction has been calculated by equation (4.4). Apparent coefficient of friction using same formulae was also used by Bouchnak *et al.* (2015).

$$\mu_{app} = \frac{F_c \, sin\gamma + F_t \cos\gamma}{F_c \cos\gamma - F_t \sin\gamma} \tag{4.4}$$

Where, γ is orthogonal rake angle with a value of $-6°$ and F_t is thrust force given by the following equation,

$$F_t = \sqrt{{F_r}^2 + {F_f}^2} \tag{4.5}$$

The variation of the same with feed and cutting speed for different tools has been presented in Fig. 4.37. The beneficial aspect of PVD coating, in terms of reduction in cutting force and temperature, was also reflected in the results of apparent coefficient of friction. It is evident that while CVD coated tool could not significantly reduce friction coefficient, particularly under low and medium cutting speeds, PVD coated tool was more effective in bringing down friction due to the presence of TiN phase and smoother coating morphology. Decrease in friction with cutting speed might be explained by dynamic friction associated with higher flow velocity of chip i.e. less residence time (Ojolo and Awe, 2011; Radwan, 1985) and shrinkage of chip-tool contact length (Noordin, 2004;

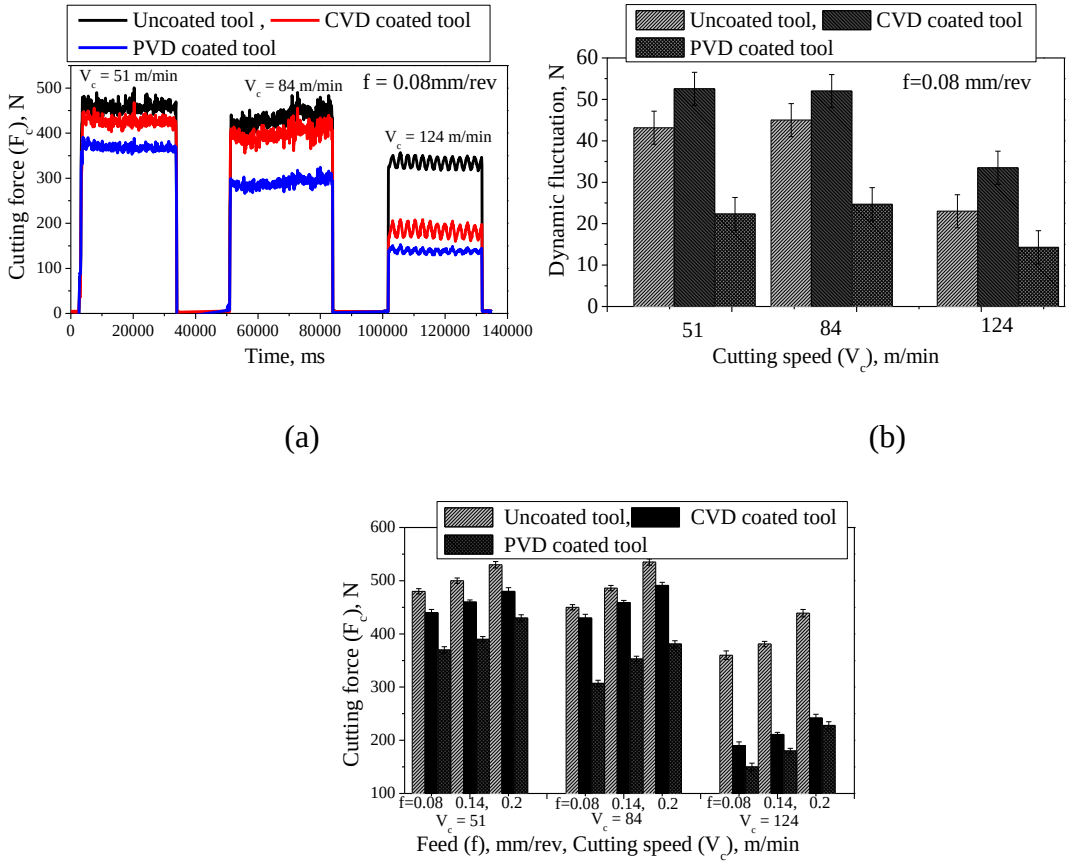

Fig. 4.36: Variation of (a) cutting force, (b) dynamic fluctuation, with V_c at feed of 0.08 mm/rev and (c) variation of F_c with cutting speed and feed using uncoated, CVD and PVD coated tools.

Sadik and LindstrSm,1993). Increase in feed would make undeformed chip to be thicker, increasing the area of shear zone. This would in turn make the deformed chip thinner. As a result, sticking area (tool seizure effect) would be less and chip-tool interface friction would be mitigated (Alkali *et al.*, 2013; Noordin, 2004; Thakur *et al.*, 2015b).

4.4.5 Study of tool wear

Flank wear and its mechanism

Fig. 4.38 (a) shows the condition of flank wear under three different cutting speeds. It is evident that tool wear under low cutting speed is governed by adhesion, while abrasion wear is the prominent mode under high cutting speed. The same figure also indicates

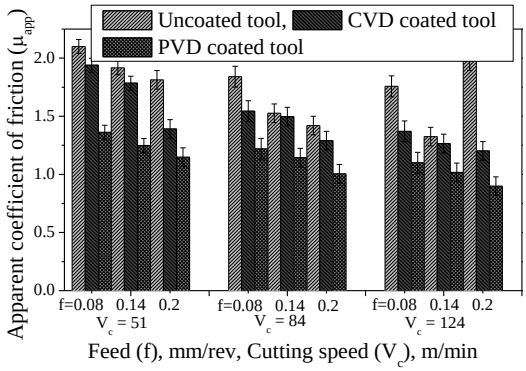

Fig. 4.37: Variation of apparent coefficient of friction with cutting speed and feed using uncoated, CVD coated and PVD coated tools.

chipping of cutting edge of uncoated tool which is attributed to adhesion of work material and subsequent removal. It is worth to underline that formation of BUE with considerable size onto CVD coated tool (indicated in Fig. 4.38). On the other hand, PVD coated tool demonstrates diminished effect of material adhesion. Chipping of cutting edge usually takes place when the bonding strength of BUE with the tool exceeds the cohesive strength of the latter. When such lower cohesive strength of tool material is superseded by the stress acting during cutting, removal of BUE along with tool material occurs, finally leading to edge chipping. The results clearly indicate two important roles of coating in combating such adhesion wear under the condition of low cutting speed and feed. First, coating material by virtue of its anti-sticking and anti-friction properties should ideally resist material adhesion or formation of BUE, which is the case with the PVD coated tool having TiAlN/TiN multilayer system. On the other hand, despite having BUE, chipping of tool could be prevented due to sufficient resistance to tool wear imparted by TiCN/Al_2O_3 bilayer coating. Similarly, under a cutting speed of 124 m/min prominent abrasion marks are visible on uncoated tool which could be effectively brought down with the superior wear resistance properties of both CVD and PVD coated tools. It is important to note that increase in feed up to 0.2 mm/rev significantly increased adhesion of work material on the tools in the form of BUE and sticking of chips as demonstrated in Fig. 4.38 (b). Even the coated tools were not very effective probably due to higher rate of coating removal under higher cutting force (Fig. 4.36). Excessive rise in cutting zone temperature (Fig. 4.35) might be another contributing factor behind higher degree of material adhesion under high feed rate. Interestingly, such observation might explain more random fluctuation of cutting force under higher feed (Fig. 4.38 b). Similar edge chipping and more severe abrasion wear were also noted for uncoated inserts while adopting high feed of 0.2 mm/rev. Such severe abrasive wear can be explained by the presence of hard and heat resistant phase such as Ni_2(Cr/Mo) present in Incoloy 825. Interestingly, both CVD and PVD coatings as well as adhered layer on the flank face imparted effective resistance to abrasion to the tool

substrate. According to Devillez *et al.* (2007), similar abrasive marks also visible due to different phases present in Inconel 718, BUE and BUL are the dominant wear mechanism Moreover, Ezugwu *et al.* (1999) showed that PVD coated tool outperformed CVD coated one while machining of Inconel 718.

V_c, m/min	Uncoated tool	$TiCN/Al_2O_3$ coated tool	TiAlN/TiN coated tool
	Feed = 0.08 mm/rev and depth of cut = 1 mm		
51	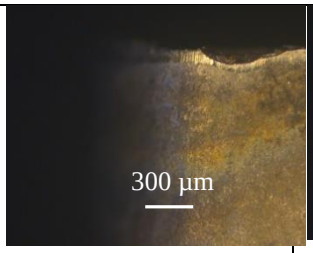	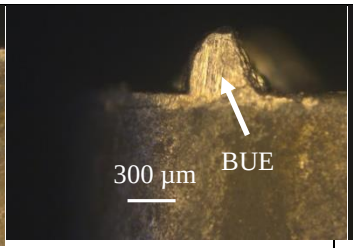	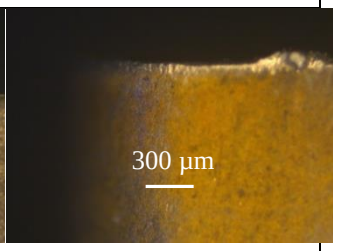
84	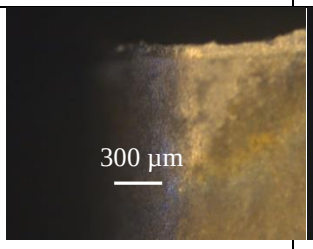	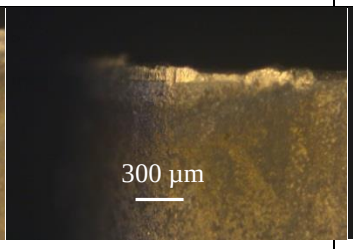	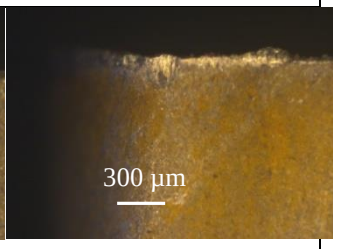
124	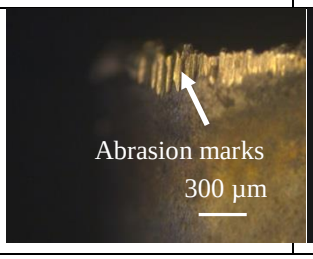	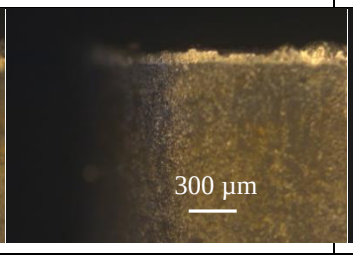	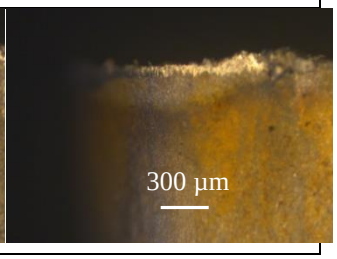

(a)

V_c, m/min	Uncoated tool	$TiCN/Al_2O_3$ coated tool	TiAlN/TiN coated tool
	Feed = 0.14 mm/rev and depth of cut = 1 mm		
51	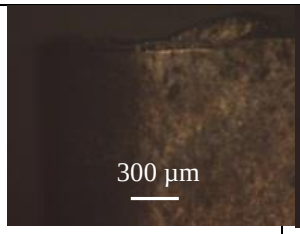	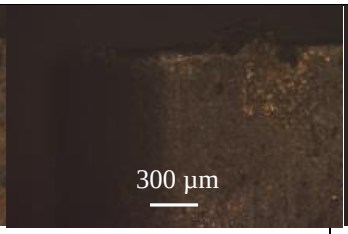	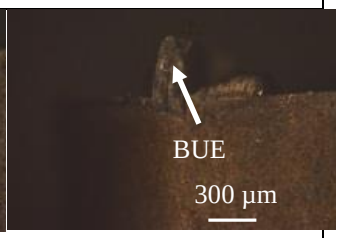
84	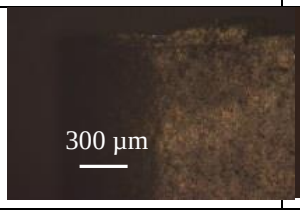	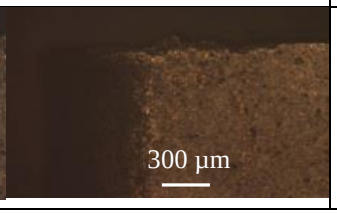	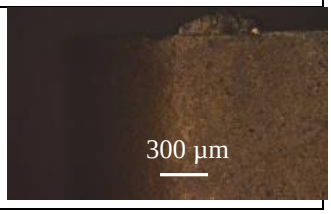

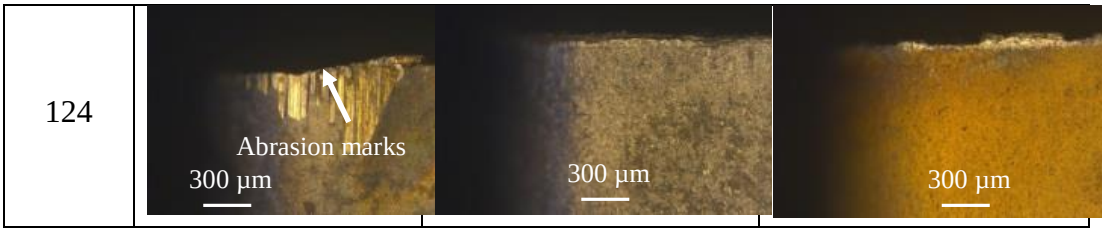

(b)

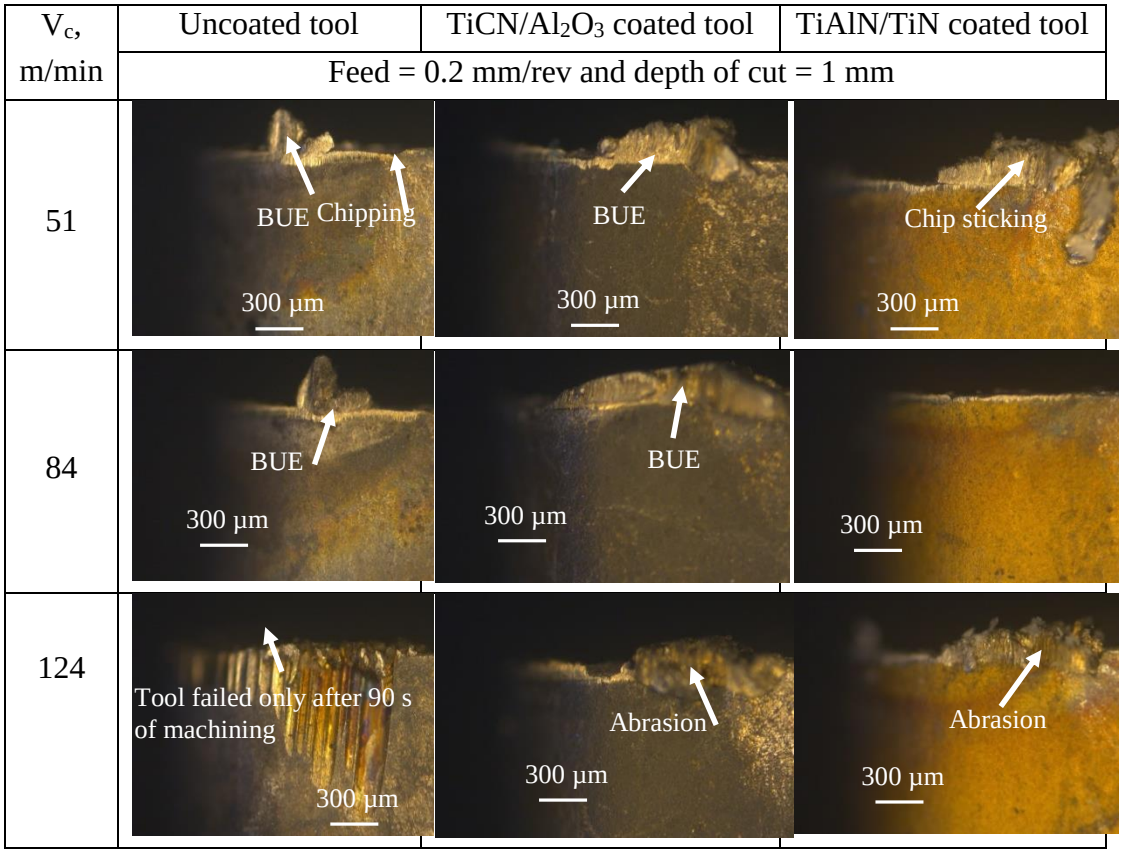

(c)

Fig. 4.38: Optical microscopic images of flank surface of different tools under varying cutting speeds and feeds of (a) 0.08, (b) 0.14 and (c) 0.2 mm/rev after 270 s of machining.

Wear at flank face under the condition of high cutting speed (124 m/min) and feed (0.2 mm/rev) using SEM and EDS analyses is shown in Fig. 4.39. It clearly depicts the formation of deep abrasive marks almost resembling micro grooves. EDS spectra captured in that region revealed the formation of a thin layer of work material along with formation of BUL. The SEM image further reveals formation of depth of cut notch on the flank face of uncoated tool. SEM images of coated tools demonstrated beneficial influence of adhered layer in protecting the cutting edge of tool substrate. Clear abrasive marks are visible on the adhered layer itself, formation of which has been further confirmed using EDS spectra shown in the same figure. Interestingly, Fig. 4.39 (c) exhibits the build-up of adhering layer in the form of stacks on to the cutting edge extending up to flank face. This also shows the

formation of cracks within the BUE which would finally lead to separation of growing layers from the tool surface. Graphical representation of flank wear with machining duration for variable cutting speeds and feeds is shown in Fig. 4.40.

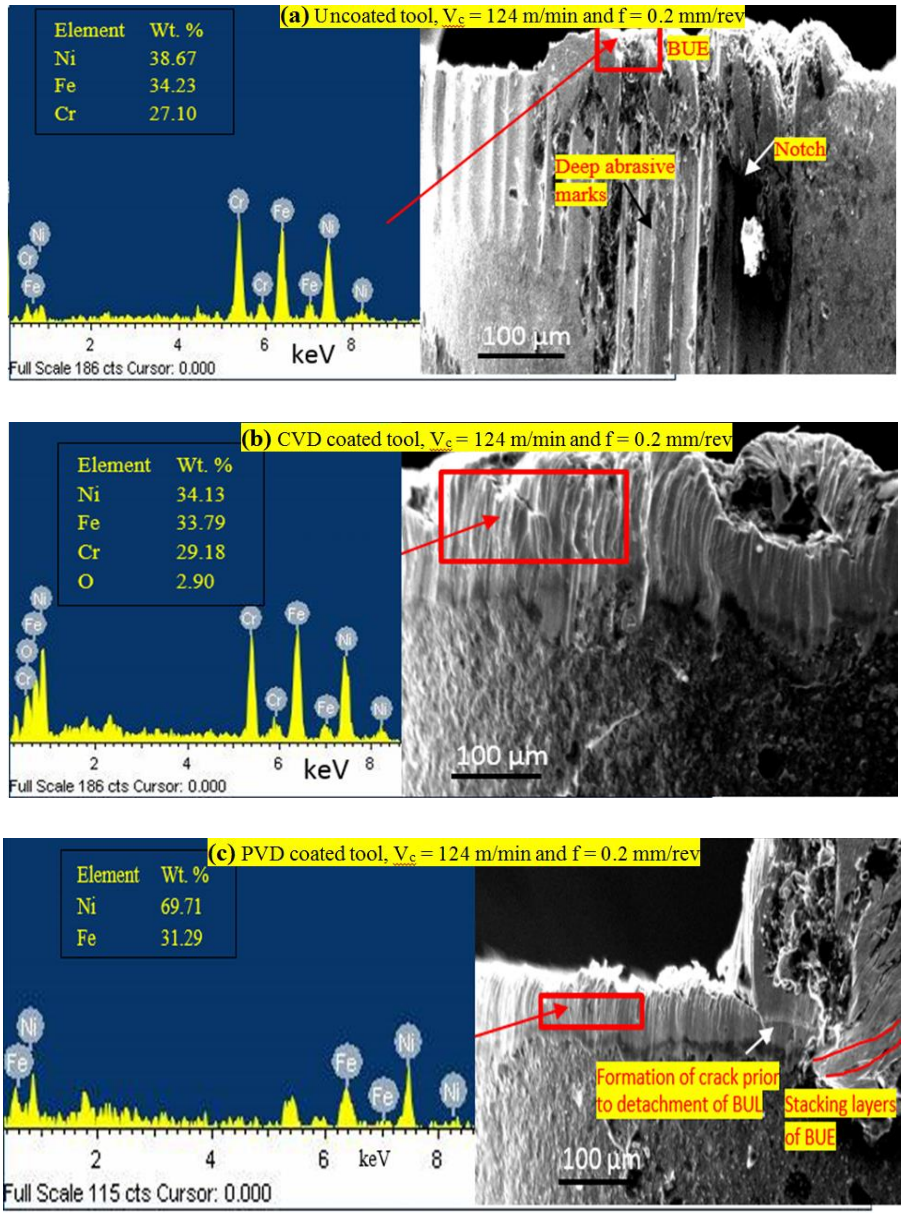

Fig. 4.39: SEM images and corresponding EDS analysis of flank surface of (a) uncoated tool after 90 s of machining, (b) CVD and (c) PVD coated tools, after 300 s of machining at cutting speed of 124 m/min and feed of 0.2 mm/rev.

Crater wear mechanism

The knowledge of tool wear characteristics plays a pivotal role in judicious selection of cutting tool for machining difficult-to-cut materials like nickel-based super alloys. This

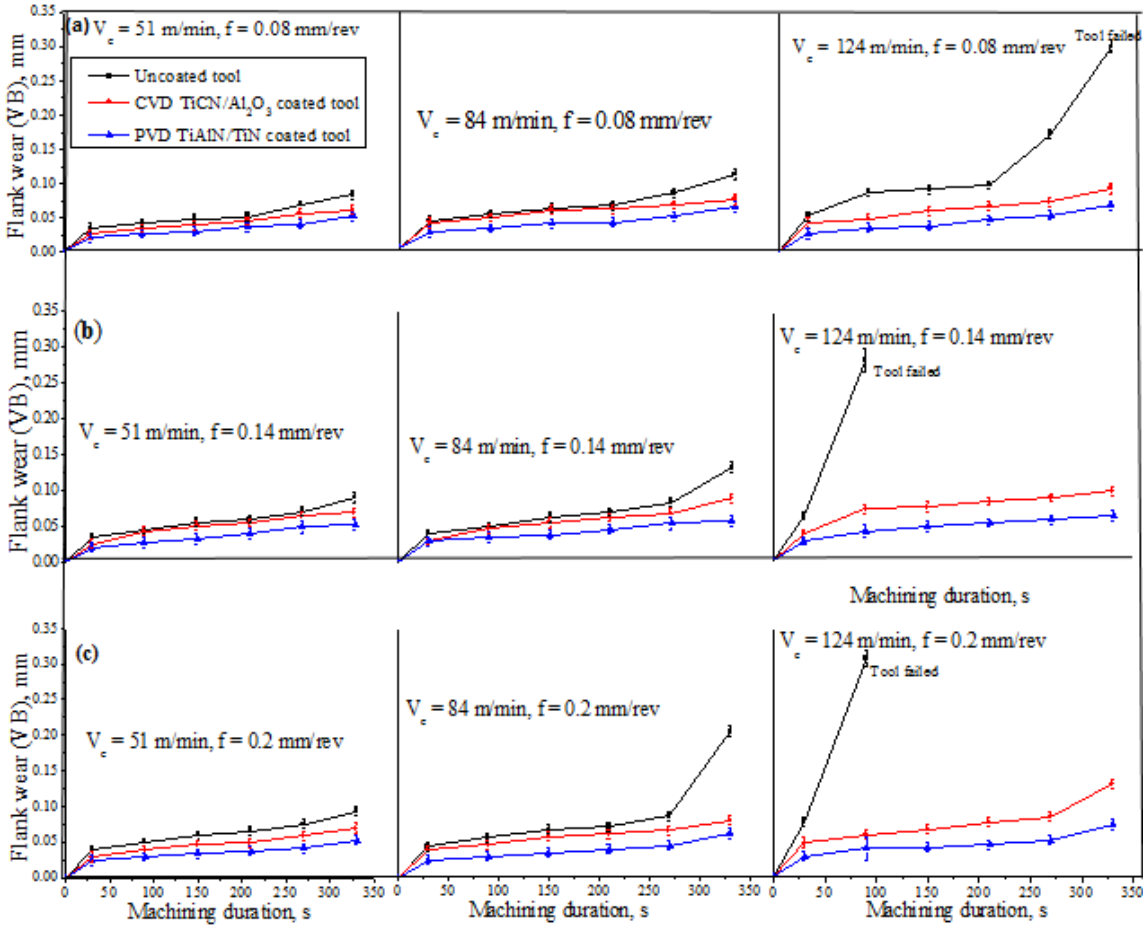

Fig. 4.40: Variation of flank wear of all tools at different feeds of (a) 0.08, (b) 0.14 and (c) 0.2 mm/rev with machining duration and cutting speed.

is particularly significant since comparative evaluation of wear characteristics of CVD and PVD coated tools with reference to uncoated insert is not so well documented. Therefore, current study investigates detailed tool wear mechanism under various cutting condition. Fig. 4.41 shows the SEM images of rake face of uncoated and different coated tools under varying cutting speeds and high feed rate of 0.2 mm/rev. Careful investigation would reveal the formation of three distinct zones on the rake face which have also been reported by Bordin *et al.* (2015). Zone 1, very adjacent to the tool nose and principal cutting edge, indicates the region of extreme adhesion in the form of sticking and seizure of chips which were also confirmed from EDS spectra as shown in Fig. 4.42. This area has been bounded by red dotted line. Higher magnification image of the same region (Fig. 4.43) also demonstrates BUE and chip sliding marks. This is caused by high level of stress during machining. Formation of Zone 2 is primarily dictated by abrasion and attrition which lead to formation of crater on uncoated tool and removal of coating in the form of gradual wear, chipping or delamination. This region has been delimitated by blue dotted line. Fragments of chips are also visible when Zone 2 was magnified and shown in Fig. 4.43. The region

beyond Zone 2 which practically remains unaffected during machining is termed as Zone 3. After carefully examining the SEM images, it is understood that increase in cutting speed led to thinning of region where BUE formation and seizure (zone 1) were evident. However, application of tool coating did not cause significant change in the area of zone 1. Application of coating clearly resulted in shrinkage of zone 2, which is more prominent in PVD coated tool under medium (84 m/min) and high (124 m/min) cutting speed compared to the CVD coated tool. Such contraction of a region in which attrition and tearing are the dominant wear mechanism might be logically ascribed to reduction in friction at the chip-tool interface. This beneficial influence of coating could decelerate the propagation of crater wear during machining.

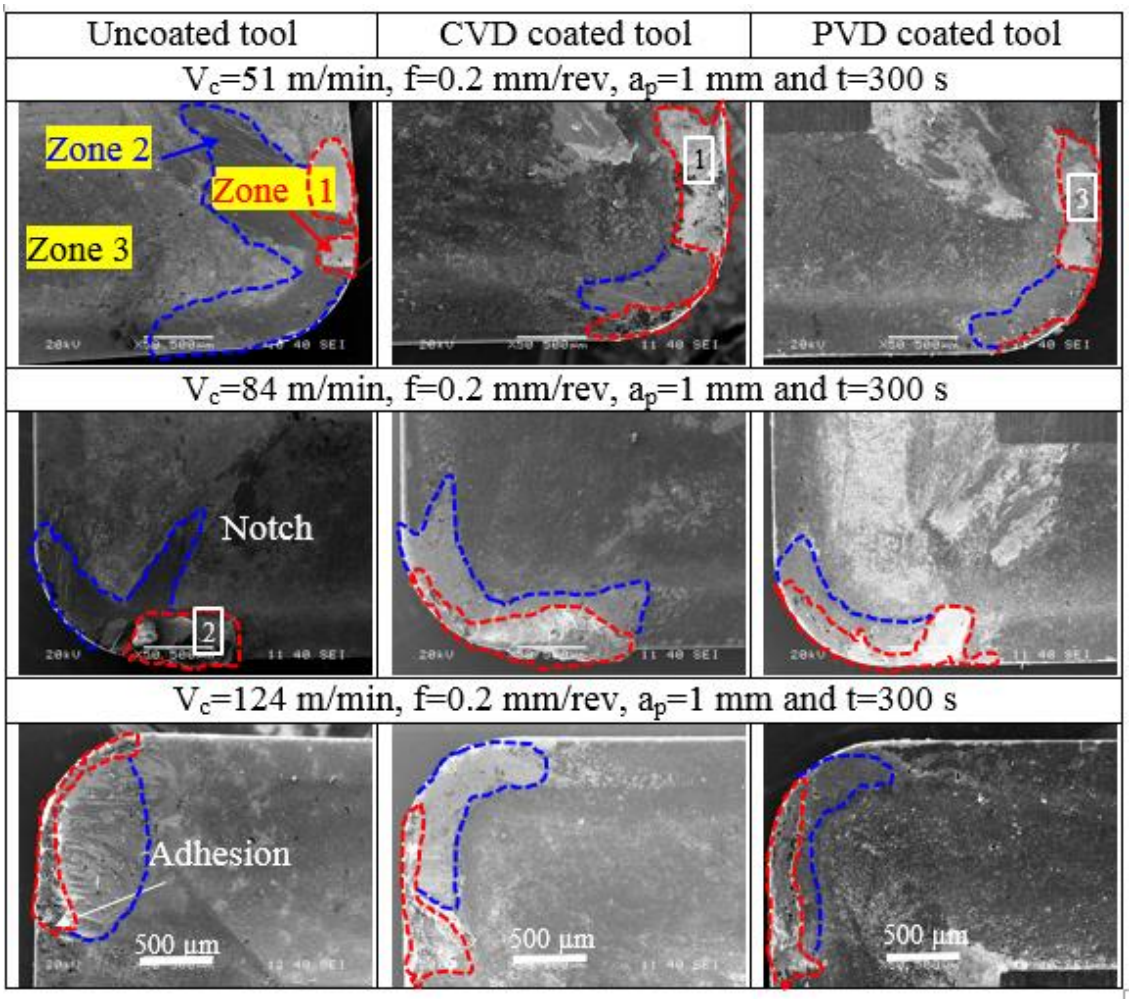

Fig. 4.41: SEM images of rake surface for different cutting speeds while using uncoated and coated tools after 300 s of machining.

Fig. 4.43 also reveals morphology of worn surface. Primary features include lamellar wear debris caused as a result of chip flow, plastic deformation, attrition and oxidation on

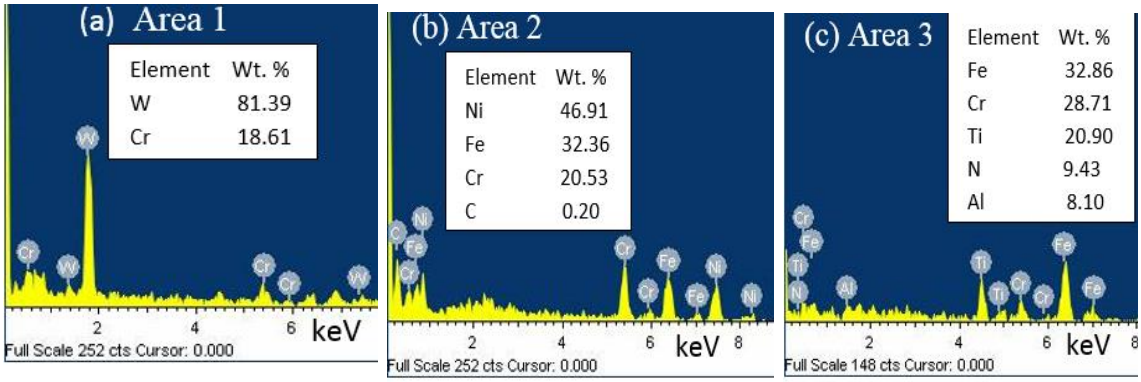

Fig. 4.42: EDS analysis of marked areas (a) 1, (b) 2 and (c) 3, on SEM images shown in Fig. 4.41.

the tool surface. This lamellar debris has the tendency of getting peeled off leaving groove marks or crater. Such delamination of lamellar wear debris on tool rake face during machining of Inconel 718 has also been demonstrated by Hou *et al.* (2011). Fig 4.43 depicts interesting mechanism of how material adhesion takes place on uncoated and coated tools surface. While material adhered and grew randomly on the area where coating has been flaked off which is also depicted in the figure, the coated surface exhibited a general trend of non-wettability which can be evident with the help of formation of micro sphere on the PVD coated surface (Fig. 4.43). EDS analysis of such micro sphere as indicates in Fig. 4.44, the possible formation of copper rich phase. However, it requires further investigation into the spherical micro features on coated surface.

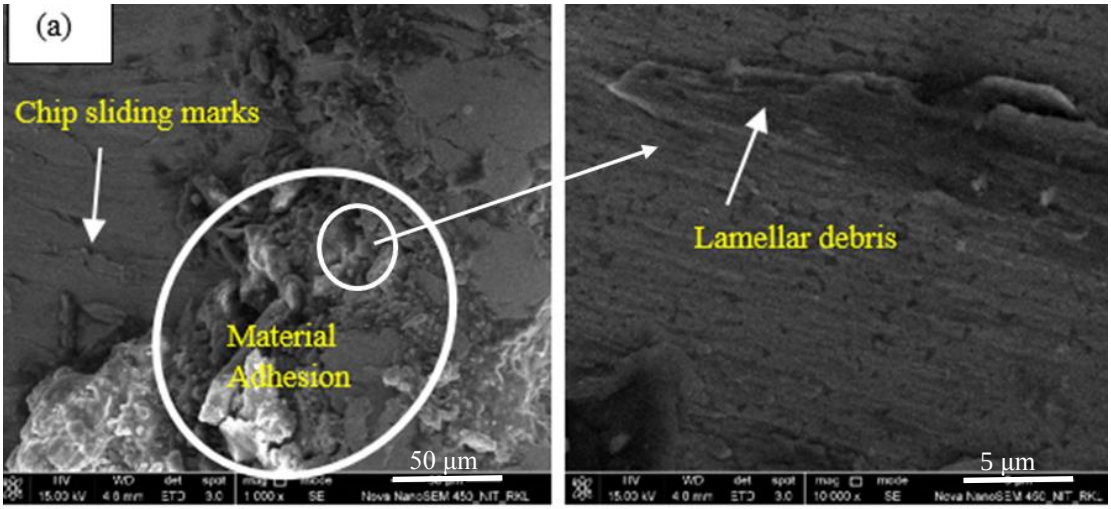

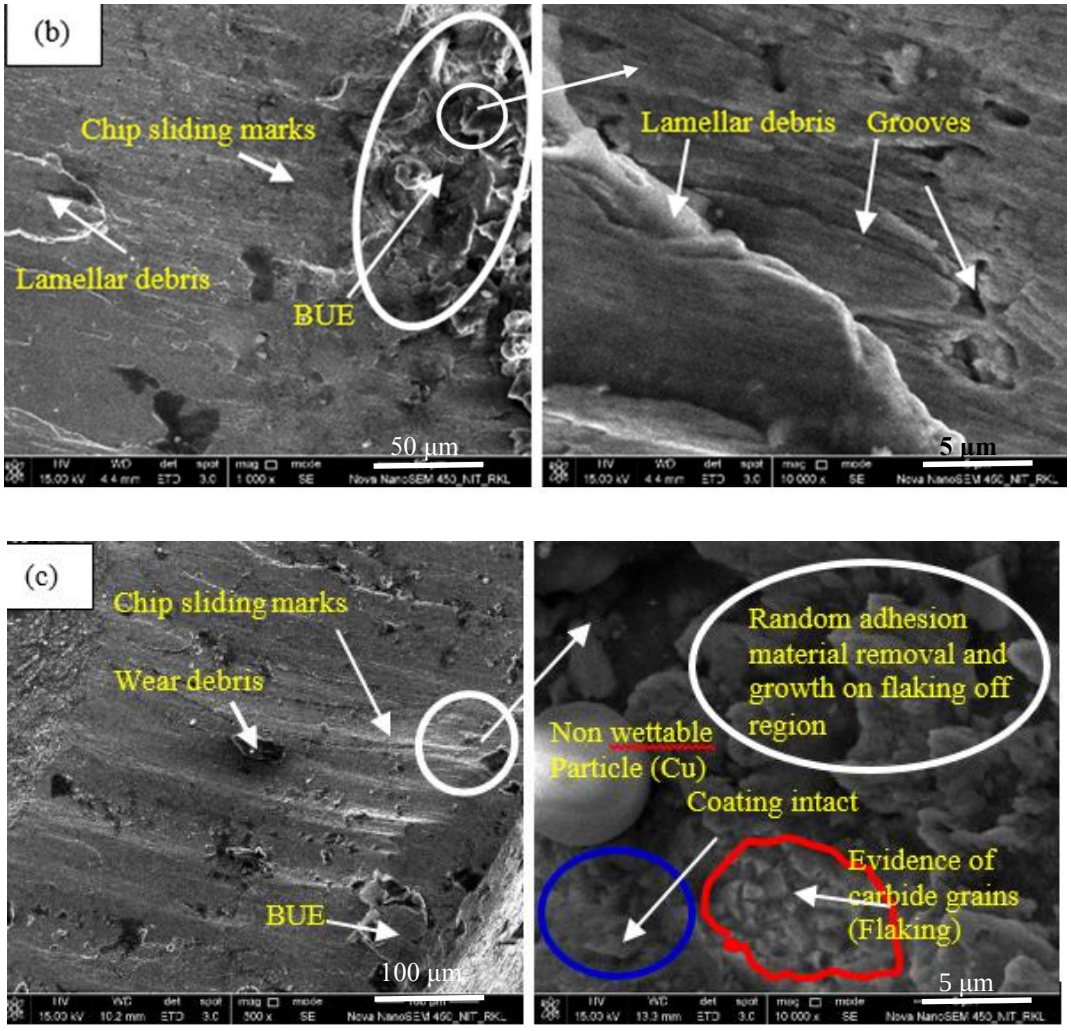

Fig. 4.43: Magnified FESEM images of rake surface of (a) uncoated, (b) CVD and (c) PVD coated tools.

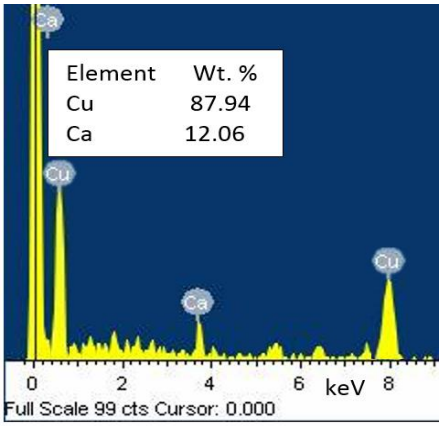

Fig. 4.44: EDS spectrum of spherical particle shown in Fig. 4.43.

Tool life

After evaluating the mechanism of wear of uncoated and different coated tools, it will be naturally important to know how this wear phenomena affect their tool life. Therefore, cutting was prolonged under most adverse cutting condition (V_c of 124 m/min and f of 0.2 mm/rev) till tool failure took place as indicated in Fig. 4.45. The criteria of tool failure was adopted according to ISO 3685. It was already observed that tool life for uncoated tool was only 90 s. On the other hand, CVD TiCN/Al_2O_3 coated tool sustained for 28 min and PVD TiAlN/TiN coated tool continued as long as 40 min. Therefore, improvement in tool life up to 18.67 times could be achieved with CVD coated tool whereas the same for PVD coated tool was as high as 26.67 times. Comparison between both the coated tools resulted in increase in tool life of 1.43 times of PVD compared to CVD coated tools. It is also worth to underline, that the slope of increase in flank wear under steady zone, was higher for the CVD coated tool compared to its PVD coated counterpart.

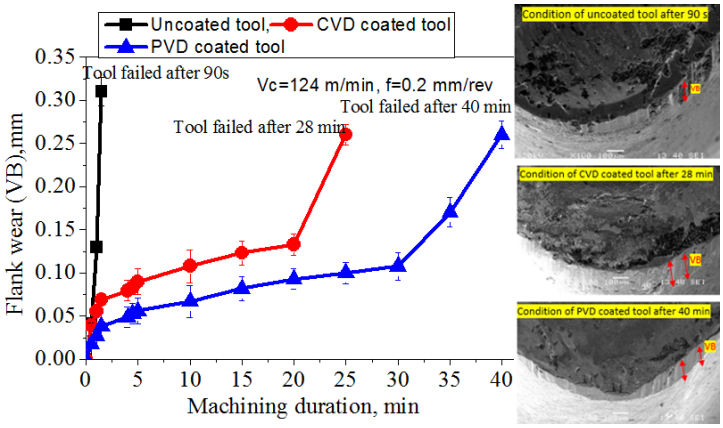

Fig.4.45: Tool life of uncoated and different coated tools under adverse machining condition (V_c = 124 m/min and f = 0.2 mm/rev).

4.4.6 Surface roughness (R_a)

Fig. 4.46 shows the variation of surface roughness of Incoloy 825 with variable cutting speed and feed using uncoated, CVD coated and PVD coated tools. According to general trend, gradual increase followed by decrease in surface roughness with increase in cutting speed was observed. Severe frictional rubbing combined with formation of BUE under low and medium cutting speed was responsible for worsening surface finish (Ezilarasan *et al.*, 2013; Fan *et al.*, 2013). Slightly different trend was observed under the condition of low cutting speed and feed particularly for the coated tools as well as high cutting speed and feed for the uncoated tool. This might be explained by the fact that elevation in cutting speed is more effective for the coated tools in reducing the formation of BUE which is the

major factor in the absence of significant tool wear of the coated tools. On the other hand, continuous increase in surface roughness with cutting speed for uncoated tool under high feed condition might be the consequence of excessive tool wear. Formation of BUE is one of the major challenges during machining of nickel-based super alloys. Therefore, anti-friction coating is expected to be of particular advantage in this context. It may be noted that CVD coated tool could not provide any benefit under the given operating condition. On the other hand, PVD TiAlN/TiN multilayer coating showed immense promise in improving surface finish possibly due to anti-adhesion tendency of TiN phase (Thakur *et al.*, 2012b). Higher surface roughness with CVD coated tool compared to even uncoated tool may be attributed to rougher surface morphology of CVD coating along with high edge radius (Thakur *et al.*, 2014a, 2014b). Surface roughness value was also measured for all the tools and it can be noticed that CVD coated tool has higher value of surface roughness than uncoated and PVD coated tools as indicated in Table 4.2. It is also evident from the figure that superior surface finish was achieved under higher cutting speed, since tendency of material adhesion could be restricted combined with the tendency of thermal softening (Ezilarasan *et al.*, 2013; Pawade *et al.*, 2008). While surface roughness obviously increased with feed (Ezilarasan *et al.*, 2013; Umbrello, 2013), PVD coated tool all along resulted in better surface finish compared to the other two types of tools.

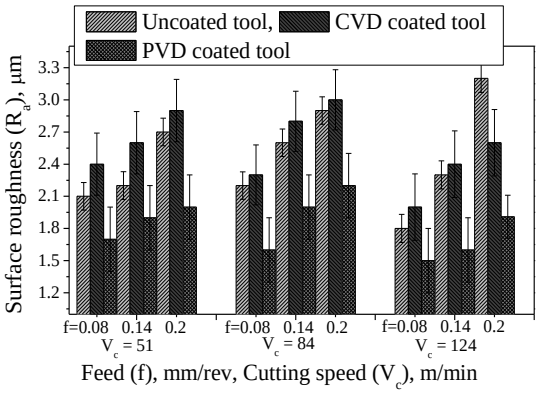

Fig. 4.46: Variation of surface roughness with cutting speed and feed using uncoated, CVD and PVD coated tools.

Table 4.2: Surface roughness uncoated and coated tools.

Tool	R_a of rake surface, µm	R_a of flank surface, µm
Uncoated	0.7	0.8
CVD coated	1.6	1.8
PVD coated	0.8	0.8

4.5 Effect of cutting environment as well as condition on some machinability aspects of Incoloy 825

4.5.1 Cutting temperature

One of the primary objectives for resorting to cutting fluid (CF) is to bring down in cutting temperature. Variation of cutting temperature as obtained by tool-work thermocouple technique during rough and finish modes of machining under both dry (TiN/TiAlN coated tool) and wet (uncoated carbide tool) environment has been illustrated in Fig. 4.47. Temperature using coated tool under dry machining was always found to be higher compared to that in wet machining (both for flood and MQL). It is also evident from Fig. 4.46 that cutting temperature during roughing mode was higher than that in finishing mode while using PVD coated tool. This might be attributed to inability of coating to resist very high frictional drag force under rough cut leading to coating failure. While wet machining remarkably reduces cutting temperature during both rough (around 30%) as well as rough (around 19%) condition. Moreover, MQL outperformed flood cooling during finish mode machining. This can be explained by improved capability of atomised coolant to effectively penetrate into the machining zone under finish mode.

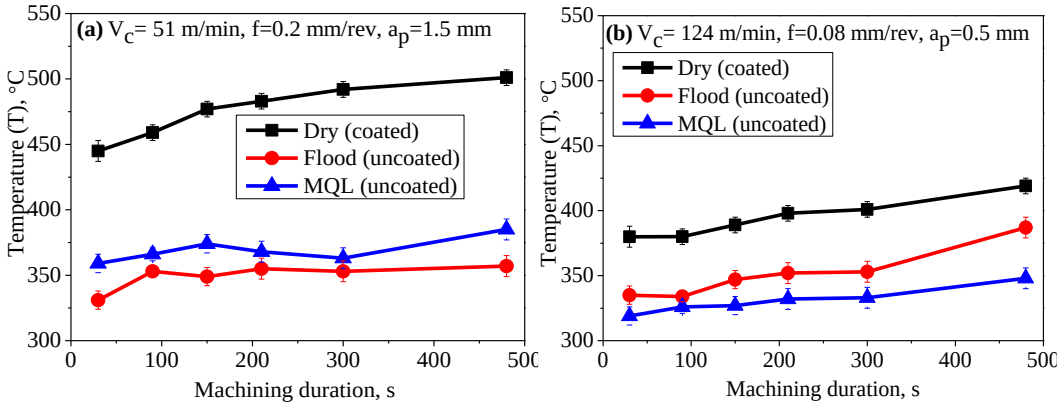

Fig. 4.47: Variation in cutting temperature with machining duration under (a) roughing and (b) finishing modes of machining.

4.5.2 Cutting force

Influence of cutting environment and tool coating on cutting force is of paramount importance. Since the latter directly dictates consumption of cutting power and therefore environmental impact. Fig. 4.48 depicts actual variation of cutting force components (F_c, F_r and F_f,) obtained under dry (using PVD TiN/TiAlN multilayer coated tool), flood and MQL (both using uncoated carbide tool) environments. Interestingly, coated tool under

both finishing and roughing modes resulted in remarkable reduction in cutting force around 40% and 16% in comparison with those under flood and MQL condition respectively. The same figure also indicates that forces are evidently steadier for coated tool whereas that for wet machining shows increasing trend with time. It may also be noted that dynamic fluctuation of main cutting force (F_c), as shown in Fig.4.48 (c), could also be mitigated using coated tool.

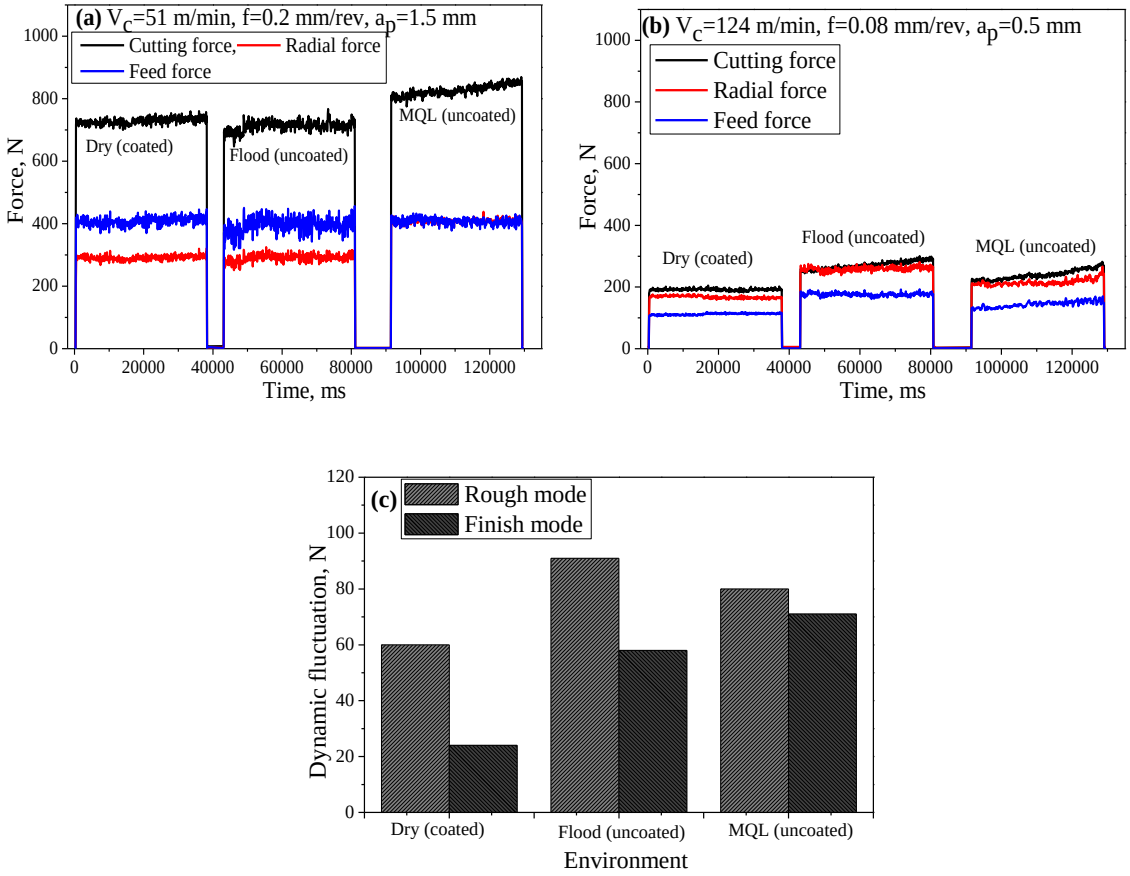

Fig. 4.48: Actual variation of cutting force components under dry, flood and MQL environment using (a) roughing, (b) finishing modes of machining and (c) variation of dynamic fluctuation of cutting force (F_c).

Furthermore, variation in cutting force (F_c) with progression of machining has also been shown in Fig. 4.49. While, the figure does not indicate any significant change in cutting force with machining duration, maximum reduction of up to 21 % (rough mode) and 47 % (finish mode) was obtained with coated tool under dry machining environment in comparison with MQL and flood cooling respectively. These results clearly established the superiority of TiN/TiAlN coated tool over its uncoated counterpart even when the PVD coated tool is utilised without a single drop of CF, while the uncoated one is used under wet machining environment.

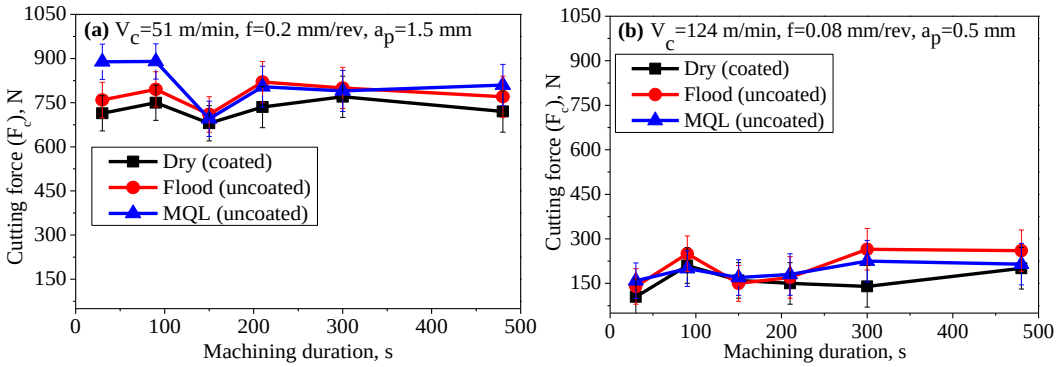

Fig. 4.49: Development of F_c with progression of machining under (a) roughing and (b) finishing modes of machining.

4.5.3 Apparent coefficient of friction

Apparent coefficient of friction at chip-tool interface is governed by environment as well as tool wear and subsequently plotted against machining duration under different machining environments (dry, flood and MQL) in Fig. 4.50.

It is interesting to note that apparent coefficient of friction under flood (uncoated carbide tool) cooling was minimum during rough machining, while that under dry (TiN/TiAlN coated tool) and MQL (uncoated carbide tool) modes were almost similar in both condition. However, beneficial role of coating gradually got more prominent with progression of machining and at the end of test i.e. after 480 s of machining. PVD coated tool exhibited lowest friction even under dry condition. On the other hand, flood cooling, particularly for finish mode machining, friction was considerably high owing to increased difficulty of cutting fluid to penetrate into the machining zone thereby causing non-uniformity as well as fluctuation in result as evident from Fig. 4.50 (b).

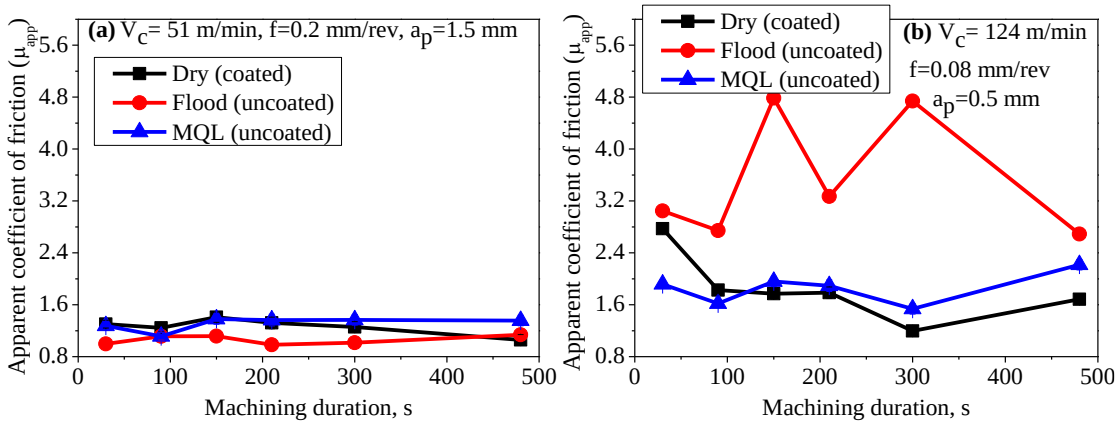

Fig. 4.50: Variation in apparent coefficient of friction under (a) roughing and (b) finishing modes of machining.

4.5.4 Tool wear

Flank wear and its mechanism

One of the basic purposes to utilise cutting fluid in machining is to restrict tool wear and thus increase tool life by virtue of minimising friction, temperature and cutting forces during machining. Therefore, study of tool wear is of considerable significance for justifying the quantity of CF to be used. It is particularly so because, CF has adverse impact on operator as well as environment in general. Therefore, detailed study has been undertaken to investigate tool wear under conventional wet machining and MQL using uncoated insert in comparison with that under dry condition using PVD TiN/TiAlN multilayer coated tool.

Progression of flank wear with duration both under dry (PVD coated tool) and wet (flood and MQL using uncoated tool) conditions has been illustrated in Fig. 4.51 which clearly demonstrates formation of BUE for rough machining both under dry as well as wet environment. This phenomenon which is obviously attributed to higher friction could not be avoided using different modes of coolant or coating. Uncoated tool failed after 480 s of machining both under flood cooling and MQL modes while employing finish condition, whereas further machining was still possible with PVD coated tool without using a single drop of coolant, since flank wear of only around 0.09 mm was noted. Excellent anti friction property and wear resistance of TiN in combination with superior thermal stability of TiAlN coating are responsible for outstanding performance of PVD coated tool even during machining at such high cutting speed (124 m/min). Fig. 4.52 represents graphical variation of average flank wear with machining duration under both roughing and finishing modes of machining. It is also evident that PVD coated tool under dry condition is more effective for finish mode as far as the capability to restrict tool wear is concerned.

Crater wear mechanism

Wear mechanism on rake and flank surfaces can be illustrated by SEM images along with EDS spectra. Wear on rake face while machining nickel-based super alloys is primarily governed by the contact mechanism at chip-tool interface region. Due to high chemical affinity of nickel-based super alloys, material adhesion on the rake surface of the tool has been one of the major issues in machining super alloys (Thakur *et al.* 2012, 2014a, b). Fig. 4.53 shows the representative SEM images of rake and flank surfaces after 480 s of machining for finish and rough modes of experiment. More prominent damage to rake face is visible with flood cooling under finish mode, whereas in rough machining no significant difference among the tools could be noted.

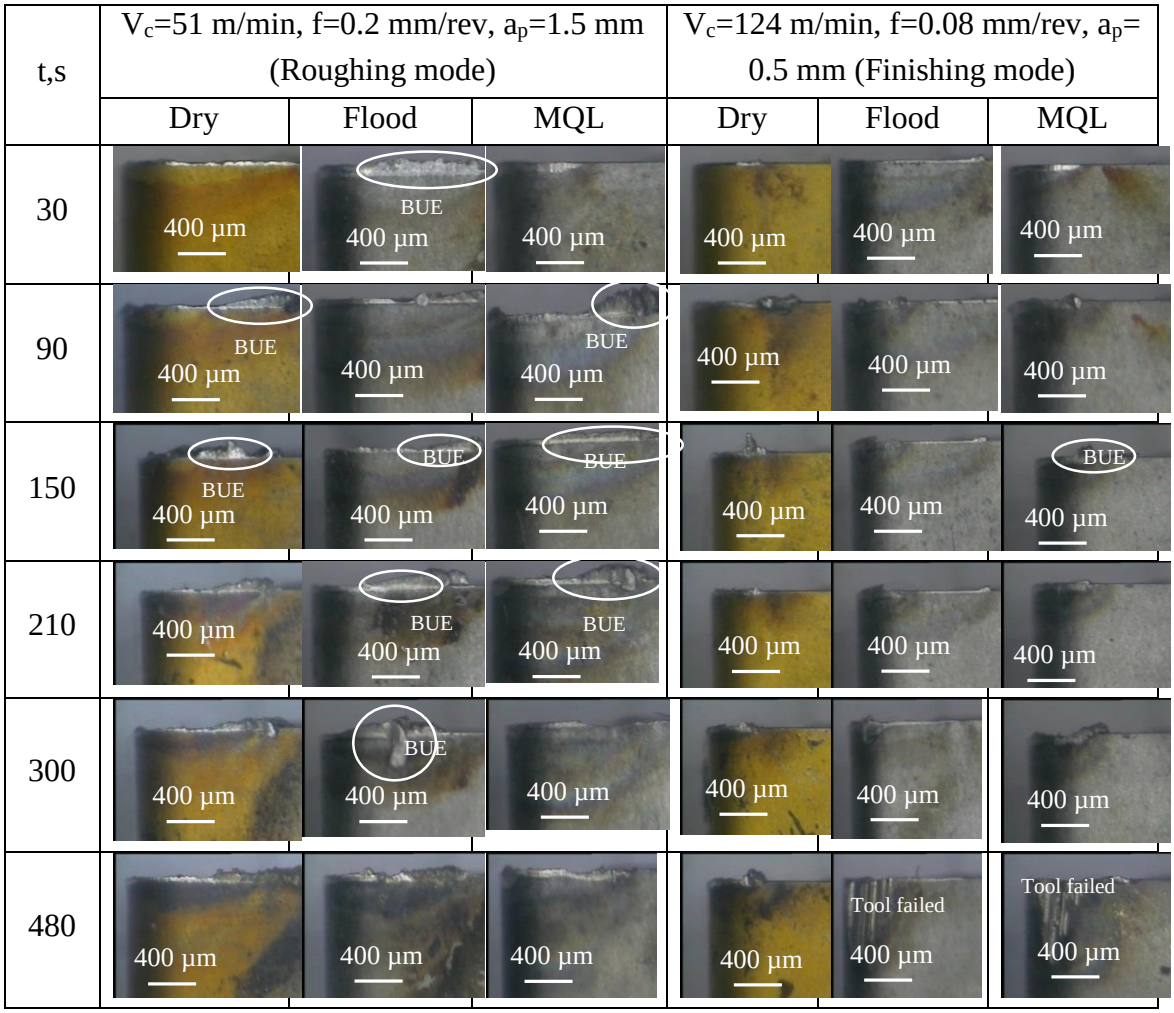

Fig. 4.51: Optical microscopic images showing development of flank wear with progression of machining under roughing and finishing modes of machining.

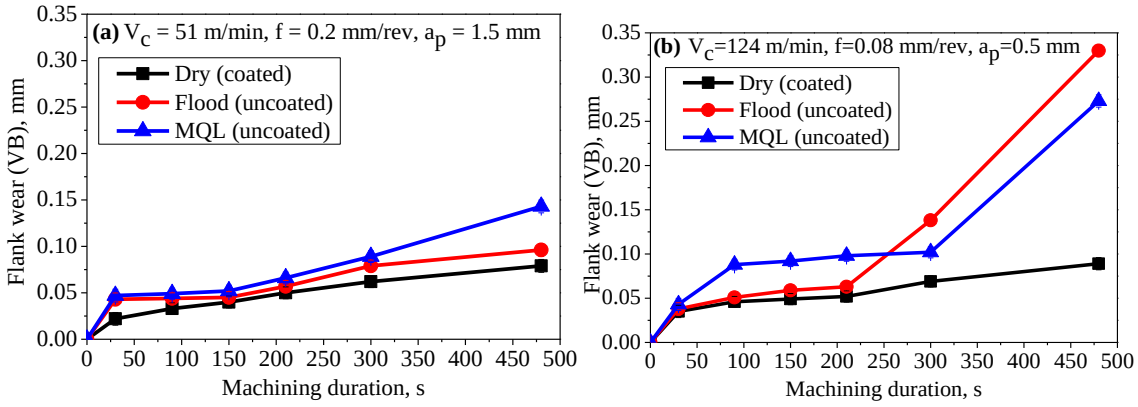

Fig. 4.52: Variation of tool flank wear during (a) roughing and (b) finishing mode of machining with progression of machining under dry, flood and MQL environment.

BUE and nose damage were found with uncoated carbide tool both under flood and MQL machining in finishing mode. Partial removal of coating was observed in dry machining using PVD multilayer coated tool under roughing condition. This shows better capability of retention of coating under high speed using finish mode. Evidence of formation of BUE and coating removal was further confirmed by compositional analysis in the marked regions using EDS which is presented in Fig. 4.54. While it is true that performance of TiN/TiAlN coated tool under finish mode has been superior compared to in roughing mode, the same coated tool under dry condition also outperformed its uncoated counterpart during its use in wet and MQL modes even when roughing mode was adopted. Although cutting temperature was clearly higher, it is the effective thermal stability i.e. capability to withstand high temperature and maintaining high hardness and excellent tribological properties even under elevated temperature, that makes the advanced multilayer coated tool a promising candidate for high speed machining of nickel-based super alloys under dry or near dry environment.

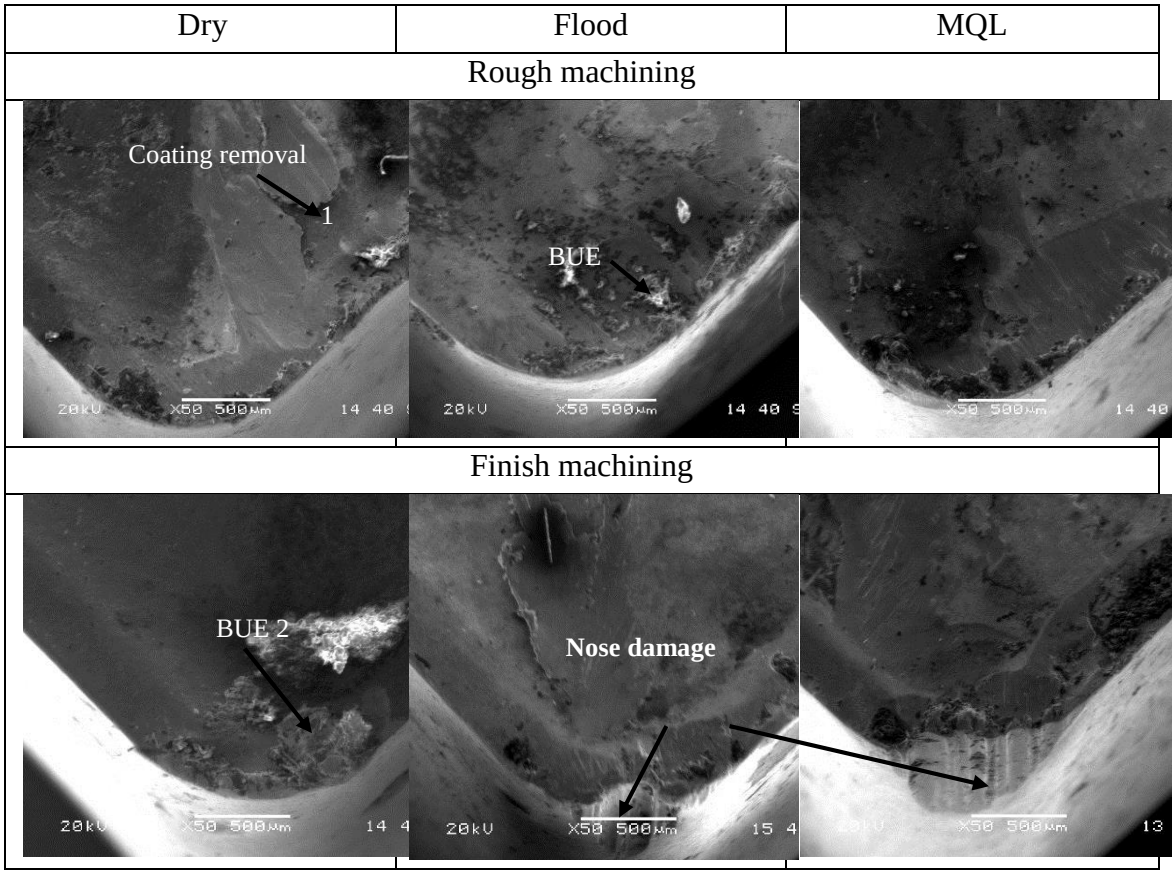

Fig. 4.53: SEM images of nose area of tools after 480 s of machining with finishing and roughing mode under dry, flood and MQL environment.

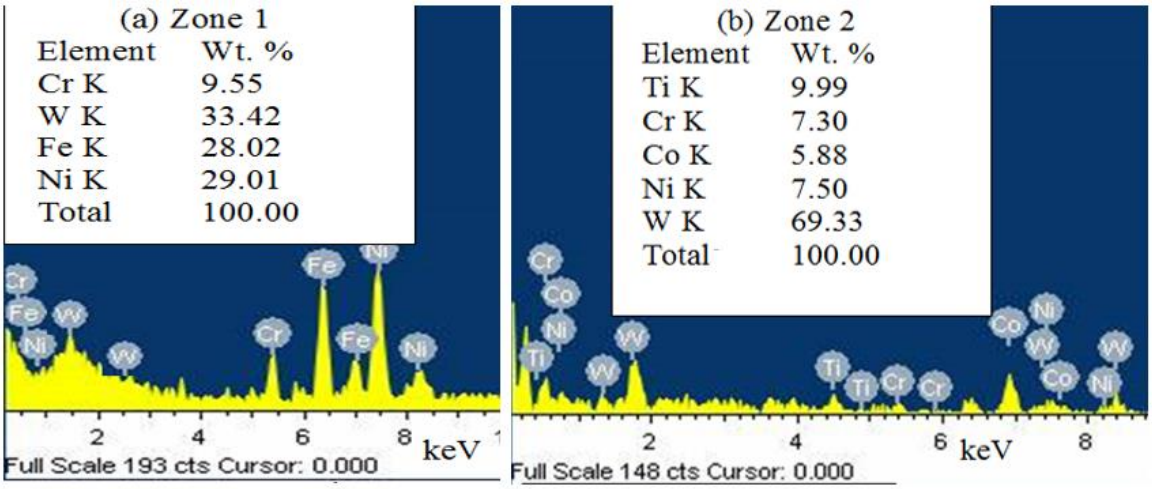

Fig. 4.54: EDS spectra of (a) zone 1 and (b) zone 2 shown in Fig. 4.53.

4.5.5 Chip morphology

Fig. 4.55 shows a gradual change of macro morphology of chips obtained while roughing and finishing modes of machining. Loose arc and connected arc types of chips were observed with roughing mode of machining owing to high shear strain and plastic deformation as depth of cut and feed both were high. On the other hand, continuous snarled ribbon chips were found with finishing modes of machining. No further variation was revealed with progression of machining. It can be concluded that depth of cut and feed have significant impact on the shape of chip.

Free surface of the chips produced during machining was examined using SEM as shown in Fig. 4.56. Nickel-based super alloys are usually characterised by serrated chips which are clearly indicated in the same figure for both the modes of machining. Chip serration is primarily attributed to plastic deformation and shear localisation. Higher degree of serration for rough cutting mode might be explained by high feed and depth of cut which caused higher amount of plastic deformation in combination with more chip-tool interface friction compared to finish mode of machining. Degree of serration was also found to be more under dry condition when compared with that under flood and MQL environment. This phenomenon can be explained by high temperature, evident from Fig. 4.47, leading to enhanced plasticity of work material and reduction in cutting force as discussed previously in Fig. 4.48. This also caused higher amount of deformation energy to be accumulated and subsequently increased shear localisation (Hou and Komanduri, 1997). Obviously, deformation under wet condition (both flood and MQL) was less. While TiN/TiAlN multilayer coated tool caused easy deformation, it also resisted deformation to the tool itself. This is also indirect evidence of less tool wear for coated tool, since higher tool wear could have caused less cutting deformation which has not been observed for the present case. Prominent side flow of chip material (Fig. 4.56 a), particularly under flood cooling

condition, was due to higher chip-tool interface friction which has been already obtained under finish mode (Fig. 4.51 b).

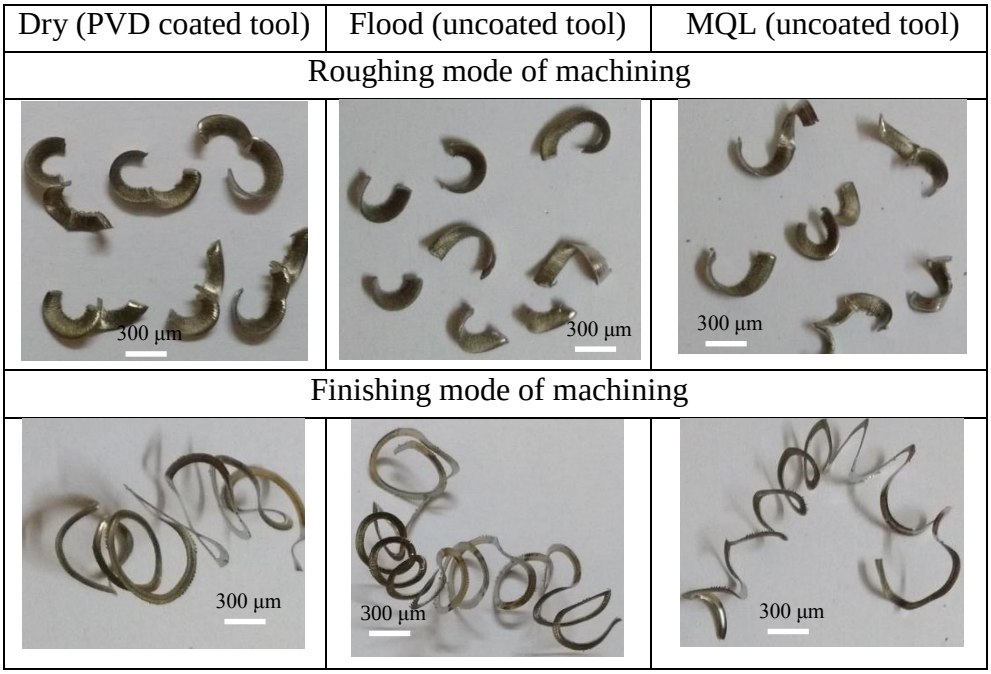

Fig. 4.55: Optical microscopy images of chips under roughing and finishing modes of machining.

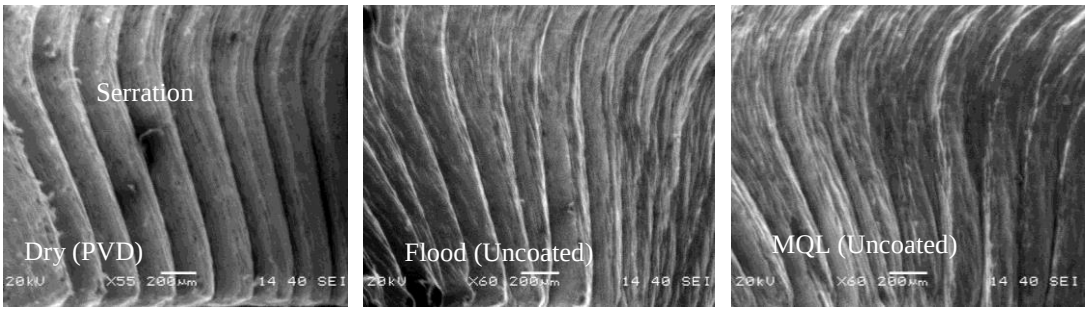

(a)

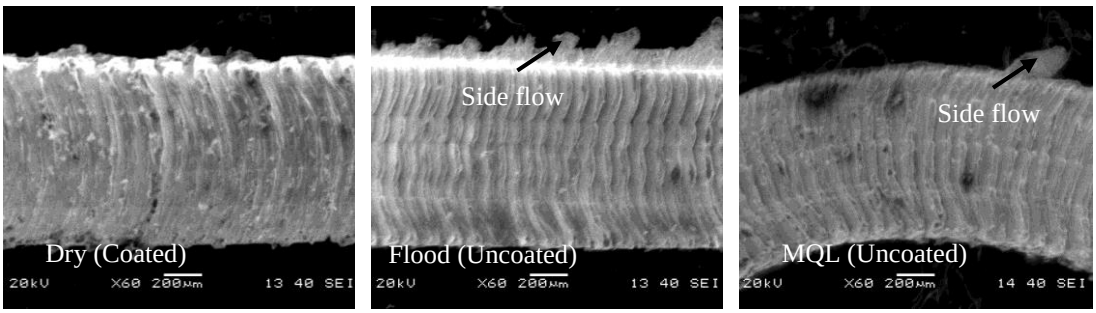

(b)

Fig. 4.56: SEM images of free surface of chips under finish and rough modes of machining.

4.5.6 Chip reduction coefficient (ζ)

Chip reduction coefficient which is a measure of deformation of work material is mainly influenced by chip-tool interface friction, BUE and tool wear. Chip reduction coefficient is measured by equation (4.6), which is ratio of chip thickness (t_c) to uncut chip thickness (t_o).

$$\zeta = \frac{t_c}{t_o} \tag{4.6}$$

where $to = f\,sin\phi$ and ϕ is the approach angle of the tool and its value is 75°.

Effect of machining environment on chip reduction coefficient under rough and finish modes has been shown in Fig. 4.57. Evidently, roughing condition resulted in higher chip reduction coefficient compared to finish mode owing to more friction. The figure also clearly indicates the effectiveness of flood cooling during roughing and MQL under finish mode of machining. It should also be noted that apparent coefficient of friction for PVD coated tool was particularly higher in rough mode due to obvious damage of coating particularly under dry condition. Decrease in dynamic friction during finish mode was responsible for significant fall in chip reduction coefficient.

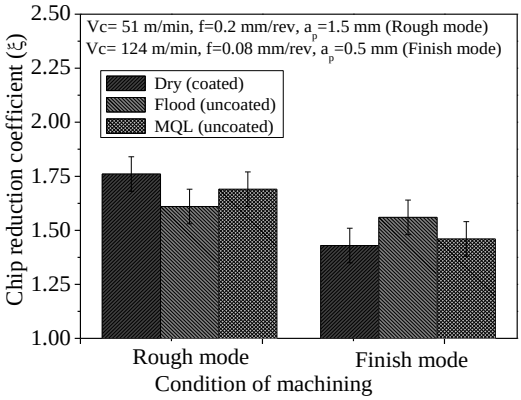

Fig. 4.57: Variation in chip reduction coefficient after 480 s of machining under rough and finish modes of machining.

4.5.7 Surface roughness

Influence of coolants under different environments (flood and MQL) and PVD coating has been investigated on surface roughness and which is plotted against machining duration for rough as well as finish modes and indicated in Fig. 4.58. Both the graphs clearly point out interesting phenomena. Surface roughness obtained with TiN/TiAlN coated tool under dry condition has all along been minimum irrespective with machining condition. On the other hand, surface finish after conventional wet machining happened to be the worst. MQL,

however, demonstrated superior performance to that of flood cooling. Little consideration will also indicate that the difference in surface roughness under different environments is more prominent for rough mode in comparison with finish mode of machining. General trend also indicates that there is gradual reduction in surface roughness in finish mode while increasing trend has been observed during rough machining. This can be attributed to greater dominance of thermal effect under finish mode and consequent smoothing of surface peaks and feed marks. This can also be related to gradual wear of tool particularly at flank surface. Increasing trend during roughing condition is possibly associated with higher friction at chip-tool interface (Fig. 4.50) resulting in enhanced tendency of BUE formation with progression of machining. Obviously due to the same reason, surface roughness for roughing mode has always been higher compared to that in finish mode.

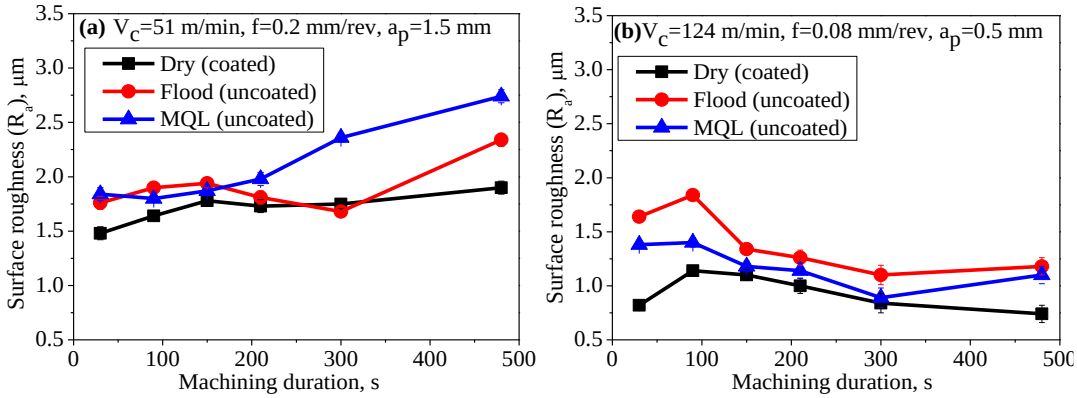

Fig. 4.58: Variation of surface roughness with machining duration under (a) roughing and (b) finishing modes of machining.

4.5.8 Surface and sub-surface analysis

Fig. 4.59 demonstrates FESEM images of surface and sub-surface regions after dry machining using PVD coated tool in addition to flood and MQL modes of machining with uncoated tool after 480 s under roughing and finishing condition. It has been found that white layer formation is more dominant for uncoated tool under roughing mode than in finish mode of machining. It is essentially attributed to higher cutting force (Fig. 4.49) leading to more mechanically induced deformation apart from higher cutting temperature associated with roughing operation (Fig. 4.47). It is interesting to note that PVD coated tool even under dry condition not only resulted in lower white layer thickness than uncoated tool (under both flood and MQL modes), but also formation of white layer obtained with the coated tool is independent of roughing and finishing conditions. According to various researchers Bushlya *et al.* (2011) and Thakur *et al.* (2014b), formation of white layer is cumulative consequence of thermally and mechanically induced deformation. Although

cutting temperature recorded with the coated tool was higher, its outstanding contribution towards minimising chip-tool interface friction, cutting force and tool wear, as evident from the foregoing discussion, led to diminished influence of mechanically induced deformation. As a consequence, white layer thickness was less.

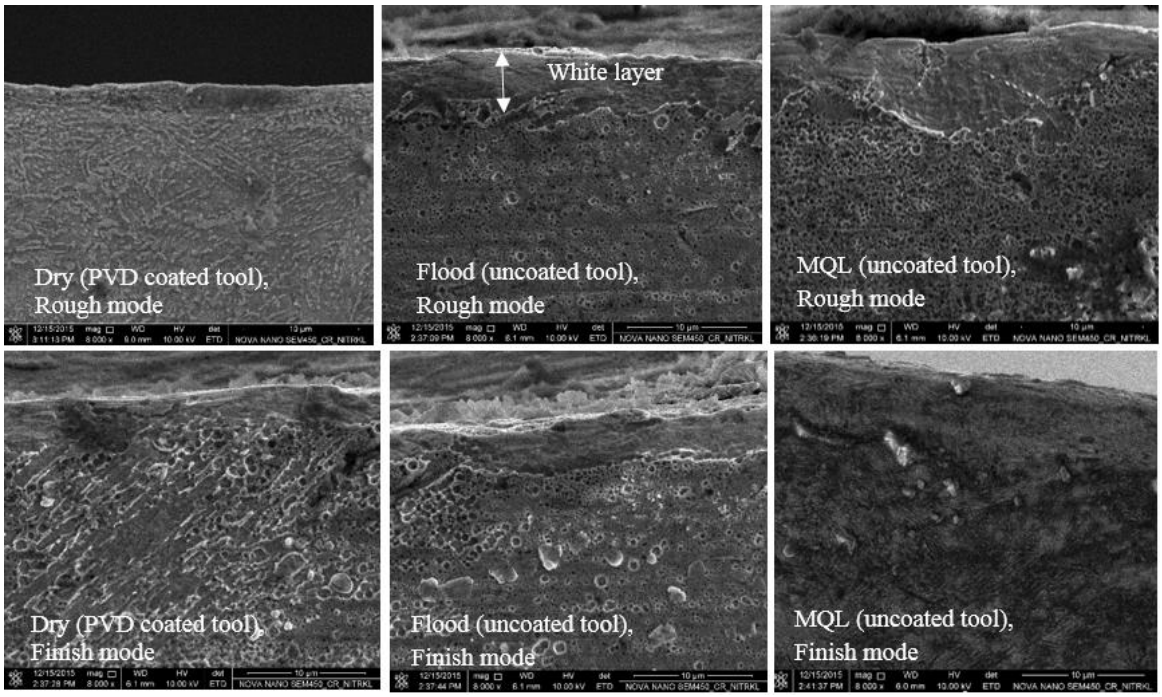

Fig. 4.59: FESEM images of surface and sub-surface region of cross section of machined part using dry and wet (flood and MQL) machining under roughing and finishing modes of machining.

4.5.9 Hardness depth profile

Fig. 4.60 depicts the variation of micro hardness with distance from the edge towards the centre of machined sample with different condition using dry (PVD coated tool), flood and MQL (uncoated tool) modes of machining after 480 s. It is evident from the figure that work hardening obtained with PVD coated tool under dry condition lies between those under flood cooling and MQL condition. Moreover, microhardness close to surface region for dry (coated tool) and MQL conditions was higher under roughing mode. Different modes of machining (roughing and finishing) did not have significant influence in altering near-surface microhardness during flood cooling. During roughing mode of machining, steeper gradient of microhardness with decreasing trend was noticed. On the other hand, hardened layer was obtained at the sub-surface region for both the wet machining conditions under finish mode. Further, gradient of microhardness was also shallower in finish mode compared to roughing mode. Such difference in depth profile of microhardness could be closely related to generation of cutting temperature along with cooling techniques.

Thermal and mechanical deformation under roughing condition were higher causing steeper gradient of hardness. Flood cooling resulted in more prominent quenching effect under roughing mode causing considerable work hardening. On the other hand, cutting force and temperature were less under finish mode. Therefore, shallower gradient was obtained. Moreover, temperature of workpiece surface might be more under high cutting speed (124 m/min) since less heat would be carried away by the chip flowing at high velocity and the cooling ability of CF would be also less (Devillez *et al.*, 2011; Veldhuis *et al.*, 2010). Therefore, wet machining under finish mode caused softer surface than sub-surface. Harder sub-surface particularly under higher cutting speed was also reported and discussed in the previous studies (Che-Haron and Jawaid, 2005; Ginting and Nouari, 2009; Sun and Gou, 2009; Thakur *et al.*, 2014b).

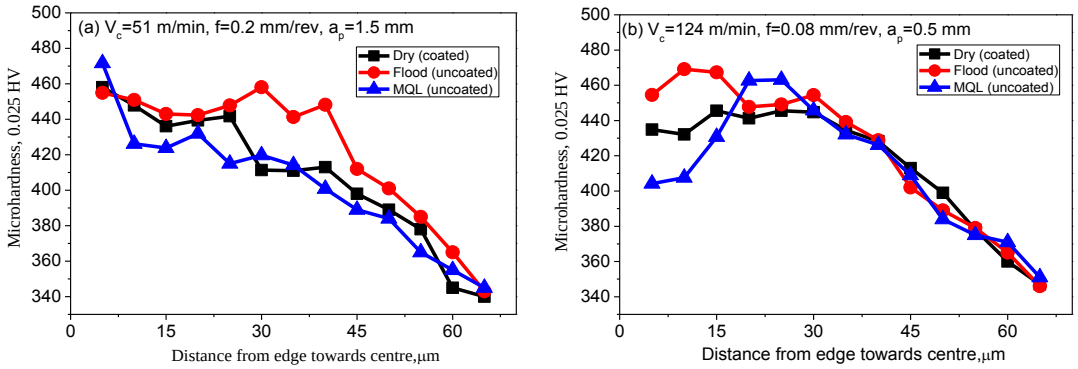

Fig. 4.60: Variation of microhardness with distance from edge towards centre of machined surface under (a) roughing and (b) finishing modes of machining.

Chapter 5

Conclusions, major contributions and future scope of work

5.1 Conclusions

Following are the major conclusions which can be drawn from the present research work:

(a) Effect of CVD coated tool, cutting speed and machining duration on tool wear, chip characteristics and surface integrity

1. Tool wear during dry machining of Incoloy 825 was characterized by adhesion, plastic deformation, diffusion and catastrophic failure. The average flank wear increased with both cutting speed due to rise in both plastic deformation and temperature.
2. CVD multilayer coating consisting of TiN/TiCN/Al_2O_3/ZrCN plays a major role in improving resistance to wear particularly at higher cutting velocity. The uncoated tool suffered catastrophic failure at high cutting speed (i.e. Vc= 124 m/min) only after 150 s of machining. The same uncoated cemented carbide insert resulted in favourable machinability characteristics in terms of chip formation and tool wear at 51 m/min.
3. Steeper increase in shear band thickness with cutting speed has been found with uncoated tool due to prominent influence of tool wear and thermal softening.
4. General trend of variation of saw-tooth distance indicated that it increased with both cutting speed as well as machining duration. Coated tool helped in bringing down the saw-tooth distance. However, this improvement got more noticeable as cutting speed was increased. Saw-tooth angle followed almost similar pattern of variation.
5. Chip segmentation frequency appeared to increase with cutting speed and decrease with progression of machining. This has been primarily related to tool wear and consequent severity in plastic deformation. Multilayer coated tool brought an increase in chip segmentation frequency due to its effective resistance to tool wear. Due to the same mechanism, equivalent chip thickness decreased with cutting speed and coated tool.
6. Chip-tool contact length decreased with cutting speed and machining duration. Reduction in chip-tool contact length was found by the application of CVD coated tool.
7. Hardness of chip increased when cutting speed was enhanced from 51 to 124 m/min. Application of multilayer coated tool was found to be beneficial in decreasing hardness of chip.
8. Although no phase transformation has been recorded, broadening of peaks in XRD for uncoated carbide inserts was correlated with larger deformation in the chips compared to that with coated tool.

9. Surface roughness obtained with CVD multilayer coated tool was higher than that of uncoated carbide insert while machining at low (V_c = 51 m/min) and medium (V_c = 84 m/min) cutting speed. However, at high cutting speed (V_c = 124 m/min), the uncoated carbide resulted in poor surface finish when machining Incoloy 825. Macro morphology of machined surface revealed surface plucking, chip debris and re-deposited materials defects.
10. Machining using both uncoated and coated tools could not induce any phase transformation. It only resulted in the formation of white layer with finer grains. Increase in cutting speed caused grains to become finer for both uncoated and coated tools. The grain size obtained with uncoated tool at low and medium cutting speeds was smaller than that for coated tools. However, coated tool caused significant grain refinement at high cutting speed whereas uncoated insert promoted grain growth during recrystallization. Coated tool resulted in the formation of large number of nucleation sites which corresponded to the stage just prior to the nucleation and grain growth.
11. Use of CVD multilayer coated insert at lower and medium cutting speeds prevented the formation of white layer. However, at high cutting speed the thickness of white layer obtained with both uncoated and CVD multilayer coated tools was comparable.
12. Machining with coated tool resulted in less degree of work hardening in surface and sub-surface regions than that of uncoated counterpart.
13. Coated tool successfully reduced tensile residual stress with cutting speed while it became compressive at high cutting speed. Residual stress using uncoated tool was all along tensile in nature irrespective of cutting speed.

(b) Effect of coating deposition techniques and cutting parameters on different machinability characteristics

1. Significant reduction in cutting force was obtained with PVD coated tool for all cutting speeds in comparison with others with a maximum of 58 and 31 % compared to uncoated and CVD coated tools respectively. On the other hand, prominent decrease in cutting force for CVD coated tool than the uncoated one was noted only under high cutting speed of 124 m/min.
2. Cutting temperature increased with cutting speed and feed for all the tools. Low thermal conductivity of Al_2O_3 coating corresponded to higher cutting temperature than others.
3. Adhesion wear, chipping of cutting edge and notching were more dominant wear mechanisms for uncoated tool while, such modes of wear could be more significantly restricted with the application of PVD coated tool. Increase in feed rate clearly resulted in higher degree of adhesion for all tools. Owing to superior anti-friction properties, TiAlN/TiN coating sufficiently resisted material adhesion from the coated surface.

However, random formation and growth of BUE took place onto the revealed tool substrate. Non-wetting characteristics of such coating towards work material has also been evidenced.

4. Formation of three distinct zones could be established on the rake face of all the cutting tools, while elevation of cutting speed caused shrinkage of zone 1 for all the tools. No noticeable alteration could be observed with the application of tool coating. On the other hand, there was clear reduction in the area of zone 2 when coated tools were employed. Such contraction was, however, more pronounced for the PVD coated tool particularly under medium (84 m/min) and high (124 m/min) cutting speeds. In addition to attrition and tearing of tool materials, lamellar wear debris and grooves have also been detected in zone 2.
5. Uncoated K grade of cemented carbide insert failed only after 90 s of machining at high cutting speed of 124 m/min and feed of 0.2 mm/rev. Since P grade of carbide tool sustained for 150 s of machining, it may be inferred that the latter is the better option for machining nickel-based super alloy while employing only uncoated carbide tool. On the other hand, CVD coated tool sustained the same cutting condition for 28 min, while the maximum tool life of 40 min was achieved with PVD coated tool. Therefore, outstanding resistance to flank wear could be established with the TiAlN/TiN multilayer coated tool.
6. Surface roughness increased with cutting speed for both uncoated and coated tools. Anti-friction and anti-sticking properties of TiAlN/TiN enabled the PVD coated tool to bring down apparent co-efficient of friction, BUE formation and hence surface roughness compared to uncoated and CVD coated tools. Surface roughness of CVD coated tool was even higher than its uncoated counterpart. Reduction in chip thickness was obtained with PVD followed by CVD coated tools.

(c) Effect of cutting environment

1. Use of cutting fluid was more effective in bringing down cutting zone temperature. MQL, in particular, resulted in minimum cutting temperature under finish mode while, there was hardly any variation in result under roughing mode. Temperature obtained with PVD coated tool under dry machining has always been significantly more than in flood cooling and MQL environments. However, the same coated tool caused reduction in temperature when roughing mode was changed over to finish mode.

2. Interestingly, TiN/TiAlN coated tool remarkably diminished cutting force around 40% and 16% in comparison with those under flood and MQL condition respectively. This did not only ensure consumption of less cutting power, but also would promote environment-friendly dry machining.

3. Outstanding improvement in resistance to tool wear and chip reduction coefficient indicative of superior machinability was consistently obtained with PVD multilayer coated tool under dry machining and was particularly more prominent under finish mode.
4. Overall superior machined surface integrity of Incoloy 825 could be achieved with the TiN/TiAlN multilayer coated tool even under dry condition. Best surface finish was obtained using coated tool even under dry machining condition in comparison with that under flood cooling and MQL environment. Maximum reduction up to around 40 % is noted for finish mode machining. Surface finish obtained under MQL was, however, better than for conventional wet machining. Moreover, thinner white layer could be attained with the PVD coated tool consistently under dry machining compared to those with uncoated tool under wet machining for both rough and finish modes. As such, wet machining caused higher thickness under roughing operation. Steeper gradient of microhardness was obtained under roughing condition. Overall hardening effect at the surface and sub-surface regions under dry condition was in between those under flood cooling and MQL environments.

5.2 Major contributions

The current research work was undertaken in order to accomplish deeper insight into the role of coated tool in machining nickel-based super alloys, so that suitable recommendation may be made. It is claimed that following issues have been successfully addressed for the first time.

- Effect of tool coating on surface integrity of nickel-based super alloy has been established.
- Effect of tool coating on chip characteristics of nickel-based super alloy has been established.
- Various mechanisms of wear of coated tool during dry machining have been significantly done.
- The research work clearly demonstrated that the PVD coated tool has enormous potential in minimising or eliminating the usage of cutting fluid and thus promoting environment-conscious machining concept.

Therefore, the information generated from present research work would be of considerable significance and interest for academia, aerospace and relevant industries, machining industries and cutting tool manufacturers.

5.3 Future scope of work

Future research work may be undertaken in the following areas:

- Application of other advanced strategies to improve machinability characteristics of Incoloy 825.
- Use of different cooling techniques
  - Cryogenic (flood cooling and MQL)
  - High pressure cooling
  - Nano-fluid lubrication
- Use of other advanced cutting tool material such as ceramic and cBN tools during high speed machining characteristics of Incoloy 825.
- Modelling and simulation of various machinability characteristics such as cutting force, cutting temperature, tool wear and surface integrity.
- Determination of optimal cutting condition during machining of Incoloy 825.

References

Akhtar, W., Sun, J., Chen, W. (2014), Effect of machining parameters on surface integrity in high speed milling of super alloy GH4169/Inconel 718, Materials and Manufacturing Processes, DOI:10.1080/10426914.2014.994769.

Alauddin, M., Mazid, M. A., EI Baradi, M. A., Hashmi, M. S. J. (1998), Cutting forces in the end milling of Inconel 718, Journal of Materials Processing Technology, Vol. 77, Issue 1, pp. 153-159.

Alexandre, F. (2004), Modeling the optimum grain size on the low cycle fatigue life of a Ni based superalloy in the presence of two possible crack initiation sites, Scripta Materialia, Vol. 50, Issue 1, pp. 25–30.

Alexandre, F., Valiorgue, F., Coret, M., Feulvarcha, E., Recha, J. (2011), Surface integrity prediction in finish turning of 15-5PH stainless steel, Procedia Engineering, Vol. 19, pp. 270 – 275.

Alkali, A.U., Yusof, N.M., Elmunafi, M.H.S., Fawad, H. (2013), Influence of cutting conditions on chip formation when turning ASSAB DF-3 hardened tool steel, International Journal of Materials, Mechanics and Manufacturing, Vol. 1, pp. 1.

Altin, A., Nalbant, M., Taskesen, A. (2007), The effects of cutting speed on tool wear and tool life when machining Inconel 718 with ceramic tools, Materials and Design, Vol. 28, pp. 2518–2522.

Aramcharoen, A., Chuan, S. K. (2014), An experimental investigation on cryogenic milling of Inconel 718 and its sustainability assessment, Procedia CIRP, Vol. 14, pp. 529 – 534.

Ardi, D.T., Li, Y.G., Chan, K.H.K., Bache, M.R. (2014), Surface Roughness, Areal topographic measurement, and correlation to lcf behavior in a nickel-based superalloy, Journal of Materials Engineering and Performance, Vol. 23, pp. 3657–3665.

Aruna, M., Dhanalakshmi, V., Mohan, S. (2010), Wear analysis of ceramic cutting tools in finish turning of Inconel 718, International Journal of Engineering Science and Technology, Vol. 2, Issue 9, pp. 4253–4262.

Arunachalam, R., Mannan, M. A. (2000), Machinability of nickel-based high temperature alloys, Machining Science and Technology, Vol. 4, Issue 1, pp.127-168.

Arunachalam, R.M., Mannan, M. A., Spowage, A. C. (2004a), Residual stress and surface roughness when facing age hardened Inconel 718 with cBN and ceramic cutting tools, International Journal of Machine Tools Manufacture, Vol. 44, Issue 9, pp. 879-887.

Arunachalam, R.M., Mannan, M. A., Spowage, A. C. (2004b), Surface integrity when machining age hardened Inconel 718 with coated carbide cutting tools, International Journal of Machine Tools Manufacture, Vol. 44, Issue 14, pp. 1481-1491.

Aslantas, K., Ucunb, I., C¢icek, A. (2012), Tool life and wear mechanism of coated and uncoated Al_2O_3/TiCN mixed ceramic tools in turning hardened alloy steel, Wear, Vol. 274–275, pp. 442– 451.

Aspinwall, D.K., Dewes, R.C., Ng, E.G., Sage, C., Soo, S.L. (2007), The influence of cutter orientation and workpiece angle on machinability when high-speed milling Inconel

718 under finishing conditions, International Journal of Machine Tools Manufacture, Vol. 47, pp. 1839–1846.

Atlati, S., Haddag, B., Nouari, M., Zenasni, M. (2011), Analysis of a new Segmentation Intensity Ratio ‘‘SIR’’ to characterize the chip segmentation process in machining ductile metals, International Journal of Machine Tools Manufacture, Vol. 51, pp. 687–700.

Axinte, D. A., Gindy, N., Fox, K., Unanue, I. (2004), Process monitoring to assist the workpiece surface quality in machining, International Journal of Advanced Manufacturing Technology, Vol. 44, pp. 1091–1108.

Axinte, D.A., Andrews, P., Li, W., Gindy, N., Withers, P.J. (2006), Turning of advanced Ni based alloys obtained via powder metallurgy route, CIRP Annals, Vol. 55, Issue 1, pp.117–120.

Axinte, D.A., Andrews, P. (2007), Some considerations on tool wear and workpiece surface quality of holes finished by reaming or milling in a nickel-base superalloy, Proceedings of the Institution of Mechanical Engineers, Part B, Vol. 221, pp. 591–603.

Aytekin, H., Akcin, Y. (2013), Characterization of borided Incoloy 825 alloy, Materials & Design, Vol. 50, pp. 515–521.

Barry, J., Byrne, G. (2002), The mechanisms of chip formation in machining hardened steels, Journal of Manufacturing Science and Engineering - ASME, Vol. 528, pp. 124.

Beera, N., Özkayaa, E., Biermann, D. (2014), Drilling of Inconel 718 with geometry-modified twist drills, Procedia CIRP, Vol. 24, pp. 49 – 55.

Behera, B. C., Chetan, Ghosh, S., Rao, P. V. (2014), Effects on forces and surface roughness during machining Inconel 718 alloy using minimum quantity lubrication, 5th International and 26th All India Manufacturing Technology, Design and Research Conference (AIMTDR 2014) December 12th–14th, IIT Guwahati, Assam, India.

Berruti, T., Lavella, M., Gola, M.M. (2009), Residual stresses on Inconel 718 turbine shaft after turning, Machining Science and Technology An International Journal, Vol. 13, Issue 4, pp. 543–560.

Bhattacharyya, S.K., Jawaid, A., Lewis, M.H., Wallbank, J. (1983), Wear mechanisms of Syalon ceramic tools when machining nickel-based materials, Metals Technology, Vol. 10, pp. 482–489.

Bhatt, A., Attia, H., Vargas, R., Thomson, V. (2010), Wear mechanisms of WC coated and uncoated tools in finish turning of Inconel 718, Tribology International, Vol. 43, pp.1113–1121.

Biksa, A., Yamamoto, K., Dosbaeva, G., Veldhuis, S.C., Fox-Rabinovich, G.S., Elfizy, A., Wagga, T., Shuster, L.S. (2010), Wear behaviour of adaptive nano-multilayered AlTiN/MexN PVD coatings during machining of aerospace alloys, Tribology International, Vol. 43, pp.1491–1499.

Bilstein, Roger, E. (1996), Stages to saturn: a technological history of the apollo/saturn launch vehicles (NASA SP-4206) (The NASA History Series), NASA History Office, pp. 89–91, ISBN 0-7881-8186-6.

Boothroyd, G., Knight, W.A. (2005), Fundamentals of Machining and Machine Tools, CRC Press, Edition.

Bordin, A., Bruschi, S., Ghiotti, A., Bariani, P.F. (2015), Analysis of tool wear in cryogenic machining of additive manufactured Ti6Al4V alloy, Wear, Vols. 328-329, pp. 89–99.

Bosheh, S.S., Mativenga, P.T. (2006), White layer formation in hard turning of H13 tool steel at high cutting speeds using CBN tooling, International Journal of Machine Tools Manufacture, Vol. 46, pp. 225–233.

Braham-Bouchnak, T., Germain, G., Morel, A., Furet, B. (2015), Influence of high-pressure coolant assistance on the machinability of the titanium alloy Ti555–3, Machining Science and Technology, Vol. 19, Issue 1, pp. 134-151.

Brandt, G., Gerendas, A., Mikus, M. (1990), Wear mechanisms of ceramic cutting tools machining ferrous and non-ferrous alloys, Journal of the European Ceramic Society, Vol. 6, pp. 273-290.

Bushlya, V., Zhou, J.M., Lenrick, F., Avdovic, P., Stahl, J.E. (2011), Characterization of white layer generated when turning aged Inconel 718, Procedia Engineering, Vol. 19, pp. 60-66.

Bushlya, V., Zhou, J., Stahl, J.E. (2012), Effect of cutting conditions on machinability of superalloy Inconel 718 during high speed turning with coated and uncoated PCBN tools, Procedia CIRP, Vol. 3, pp. 370-375.

Bushlya, V., Zhou, J., Avdovic, P., Ståhl, J.E. (2013a), Performance and wear mechanisms of whisker-reinforced alumina, coated and uncoated PCBN tools when high-speed turning aged Inconel 718, International Journal of Advanced Manufacturing Technology, Vol. 66, pp. 2013–2021.

Bushlya, V., Zhou, J., Avdovic, P., Ståhl, J.E. (2013b), Wear mechanisms of silicon carbide-whisker-reinforced, alumina (Al_2O_3–SiCw) cutting tools when high-speed machining aged Alloy 718, International Journal of Advanced Manufacturing Technology, Vol. 68, pp.1083–1093.

Cai, S.L., Dai, L.H. (2014), Suppression of repeated adiabatic shear banding by dynamic large strain extrusion machining, Journal of the Mechanics and Physics of Solids, Vol. 73, pp. 84-102.

Cai, X., Qin, S., Li, J., An, Q., Chen, M. (2014), Experimental investigation on surface integrity of end milling nickel-based alloy Inconel 718, Machining Science and Technology An International Journal, Vol. 18, Issue 1, pp. 31-46.

Cantero, J. L., Dıaz, J., lvarez, A., Miguelez, M. H., Marın, N.C. (2013), Analysis of tool wear patterns in finishing turning of Inconel 718, Wear, Vol. 297, pp. 885–894.

Cao, W., Khadhraoui, M., Brenier, B., Guedou, J.Y., Castex, L. (1994), Thermomechanical relaxation of residual-stress in shot peened nickel-base superalloy, Mechanical Science & Technology, Vol. 10, pp. 947–954.

Chang, L., Chengzu, R., Guofeng, W., Yinwei, Y., Lu, Z. (2015), Study on surface defects in milling Inconel 718 super alloy, Journal of Mechanical Science and Technology, Vol. 29, Issue 4, pp. 1723-1730.

Chattopadhyay, A.B. (2011), Machining and Machine Tools, Wiley India Private Limited, Edition.

Che-Haron, C. H., Jawaid, A. (2005), The effect of machining on surface integrity of titanium alloy Ti6Al4V, Journal of Materials Processing Technology, Vol. 166, pp. 188–192.

Chen, Y.C., Liao, Y.S. (2003), Study on wear mechanisms in drilling of Inconel 718 superalloy, Journal of Materials Processing Technology, Vol. 140, pp. 269–273.

Chen, S.H., Su, S.C., Kuo, C.P., Chang, P.C. (2012), Determination of stress state in chip formation zone when orthogonal machining nickel-based superalloy Inconel 718, Journal of the Chinese Institute of Engineers, Vol. 35, Issue 6, pp.747-754.

Chen, Z., Lin Peng, R., Avdovic, P., Moverare, J., Karlsson, F., Zhou, J.M., Johansson, S. (2014), Analysis of thermal effect on the residual stresses of broached Inconel 718, Advanced Materials Research, Vol. 966, pp. 574-579.

Chou, Y., Kevin, Y., Chris, J. E. (1999), White layers and thermal modeling of hard turned surfaces, International Journal of Machine Tools and Manufacture, Vol. 39, Issue 12, pp. 1863-1881.

Choudhury, I.A., El-Baradie, M.A. (1998), Machinability of nickel-base super alloys: a general review, Journal of Materials Processing Technology, Vol. 77, Issue 1, pp.278-284.

Coelho, R.T., Silva, L.R., Braghini, A., Bezerra, A.A. (2004), Some effects of cutting edge preparation and geometric modifications when turning Inconel 718 (TM) at high cutting speeds, Journal of Materials Processing Technology, Vol. 148, pp.147–153.

Cotterell, M., Byrne, G. (2008), Dynamics of chip formation during orthogonal cutting of titanium alloy Ti–6Al–4V, CIRP Annals - Manufacturing Technology, Vol. 57, pp. 93–96.

Courbon, C., Kramar, D., Krajnik, P., Pusavec, F., Rech, J., Kopac, J. (2009), Investigation of machining performance in high-pressure jet assisted turning of Inconel 718: an experimental study, International Journal of Machine Tools Manufacture, Vol. 49, pp. 1114–1125.

Darwish, S.M. (2000), The impact of tool material and the cutting parameters on surface roughness of supermet 718 nickel superalloy, Journal of Materials Processing Technology, Vol. 97, pp. 10–18.

Davies, A., Burns, T., Evans, C. (1997), On the dynamics of chip formation in machining hard metals, CIRP Annals - Manufacturing Technology, Vol. 46, Issue 1, pp. 25–30.

Deng, J., Liu, L., Liu, J., Zhao, J., Yang, X. (2005), Failure mechanisms of TiB2 particle and SiC whisker reinforced Al_2O_3 ceramic cutting tools when machining nickel-based alloys, International Journal of Machine Tools and Manufacture, Vol. 45, pp. 1393–1401.

Derrien, S., Vigneau, J., Dudzinski, D., Devillez, A., Moufki, A., Larrouquerre, D., Zerrouki, V., Vigneau, J. (2004), High speed milling of difficult to machine alloys, in: A review of developments towards dry and high speed machining of Inconel 718 alloy, International Journal of Machine Tools Manufacture, Vol. 44, pp. 439–456.

Devillez, A., Schneider, F., Dominiak, S., Dudzinski, D., Larrouquere, D. (2007), Cutting forces and wear in dry machining of Inconel 718 with coated carbide tools, Wear, Vol. 262, pp. 931-942.

Devillez, A., Le Coz, G., Dominiak, S., Dudzinski, D. (2011), Dry machining of Inconel 718, workpiece surface integrity, Journal of Materials Processing Technology, Vol. 211, pp. 1590–1598.

Dong, G., Zhaopeng, H., Rongdi, H., Yanli, C., Muguthu, J.N. (2011), Study of cutting deformation in machining nickel-based alloy Inconel 718, International Journal of Machine Tools Manufacture, Vol. 51, Issue 6, pp. 520-527.

Doremus, L., Cormier, J.,Villechaise, P., Henaff, G., Nadot, Y., Pierret, S. (2015), Influence of residual stresses on the fatigue crack growth from surface anomalies in a nickel-based superalloy, Materials Science and Engineering A, Vol. 644, pp. 234–246.

El-Bestawi, M.A., El-Wardany, T.I., Di, Y., Min, T. (1993), Performance of whisker-reinforced ceramic tools in milling nickel-based alloy, Annals of the CIRP, Vol. 42, Issue 1, pp. 99–102.

Ezilarasan, C., Zhu, K., Velayudham, A., Palanikumar, K. (2011), Assessment of factors influencing tool wear on the machining of Nimonic C-263 alloy with PVD coated carbide inserts, Advanced Materials Research, Vol. 291, pp.794-799.

Ezilarasan, C., Senthil kumar, V.S. (2012), Effect of machining parameters on micro hardness and residual stresses, International Review of Mechanical Engineering, Vol. l.6, Issue 3, pp. 91-97.

Ezilarasan, C., Senthil kumar, V.S., Velayudham, A. (2013a), Effect of machining parameters on surface integrity in machining nimonic c-263 super alloy using whisker-reinforced ceramic insert, Journal of Materials Engineering and Performance, Vol. 22, pp. 1619–1628.

Ezilarasan, C., Senthil kumar, V.S., Velayudham, A. (2013b), An experimental analysis and measurement of process performances in machining of nimonic C-263 super alloy, Measurement, Vol. 46, pp. 185–199.

Ezugwu, E.O., Machado, A.R., Pashby, I.R., Wallbank, J. (1990), The effect of high-pressure coolant supply when machining a heat-resistant nickel-based superalloy, Lubrication engineering, Vol. 47, Issue 9, pp. 751– 757.

Ezugwu, E.O., Pashby, I.R. (1992), High speed milling of nickel-based superalloys, Journal of Materials Processing Technology, Vol. 3, pp. 429–437.

Ezugwu, E.O., Tang, S.H. (1995a), Surface abuse when machining cast iron (G-17) and nickel-base superalloy (Inconel 718) with ceramic tools, Journal of Materials Processing Technology, Vol. 55, pp. 63–69.

Ezugwu, E.O., Lai, C.J. (1995b), Failure modes and wear mechanisms of M35 high-speed steel drills when machining inconel 901, Journal of Materials Processing Technology, Vol. 49, pp. 295-312.

Ezugwu, E. O., Wang, Z. M., Machado, A. R. (1999), The machinability of nickel-based alloys: a review, Journal of Materials Processing Technology, Vol. 86, pp. 1–16.

Ezugwu, E. O., Wang, Z. M., Machado, A. R. (2000), Wear of coated carbide tools when machining nickel (Inconel 718) and Titanium Base (Ti-6A1-4V) alloys, Tribology Transactions, Vol. 43, Issue 2, pp. 263-268.

Ezugwu, E.O., Okeke, C.I. (2000a), Effects of coating materials on the machinability of a nickel base, C-263, alloy, Tribology Transactions, Vol. 43, Issue 3, pp. 549-553.

Ezugwu, E.O., Okeke. C.I. (2000b), Performance of PVD coated carbide inserts when machining a Nimonic (C-263) alloy at high speed conditions, Tribology transactions, Vol. 43, Issue 2, pp. 332-336.

Ezugwu, E.O., Okeke, C.I. (2002), Behavior of coated carbide tools in high speed machining of a nickel-based alloy, Tribology Transactions, Vol. 45, Issue 1, pp.122-126.

Ezugwu, E.O., Bonney, J. Yamane, Y. (2003), An overview of the machinability of aeroengine alloys, Journal of Materials Processing Technology, Vol. 134, Issue 2, pp. 233-253.

Ezugwu, E.O., Bonney, J. (2004), Effect of high-pressure coolant supply when machining nickel-base, Inconel 718, alloy with coated carbide tools, Journal of Materials Processing Technology, Vol. 153–154, pp.1045–1050.

Ezugwu, E.O., Bonney, J., Olajire, K.A. (2004), The effect of coolant concentration on the machinability of nickel-base, Nimonic C-263 alloy, Tribology Letters, Vol. 16, Issue 4, pp. 311-316.

Ezugwu, E. O., Bonney, J. (2005), Finish machining of nickel-base Inconel 718 alloy with coated carbide tool under conventional and high-pressure coolant supplies, Tribology Transactions, Vol. 48, Issue 1, pp. 76-81.

Fan, Y., Hao, Z., Zheng, M., Sun, F., Yang, S. (2013), Study of surface quality in machining nickel-based alloy Inconel 718, International Journal of Advanced Manufacturing Technology, Vol. 69, Issues 9-12, pp. 2659-2667.

Fang, N., Srinivasa, P.P., Edwards, N. (2013), A comparative study of high-speed machining of Ti–6Al–4V and Inconel 718 - part I: effect of dynamic tool edge wear on cutting forces, International Journal of Advanced Manufacturing Technology, Vol. 68, pp. 1839–1849.

Fang, N., Wu, Q. (2009), A comparative study of the cutting forces in high speed machining of Ti.6Al.4V and Inconel 718 with a round cutting edge tool, Journal of Materials Processing Technology, Vol. 209, pp. 4385–4389.

Field, M., Kahles, J. F., Cammett, J.T. (1972), Review of measuring methods for surface integrity, Annals of CIRP, Vol. 21, pp. 219–238.

Foss, B.J., Gray, S., Hardy, M.C., Stekovic, S., McPhail, D.S., Shollock, B.A. (2013), Analysis of shot-peening and residual stress relaxation in the nickel-based superalloy RR1000, Acta Materialia, Vol. 61, pp. 2548–2559.

Fox-Rabinovich, G.S., Yamamoto, K, Aguirre, M.H., Cahill, D.G., Veldhuis, S.C., Biksa, A., Dosbaeva, G., Shuster, L.S. (2010), Multi-functional nano-multilayered AlTiN/Cu PVD coating for machining of Inconel 718 superalloy, Surface & Coatings Technology, Vol. 204, pp. 2465–2471.

Gangopadhyay, S., Acharya, R., Chattopadhyay, A.K., Paul, S. (2010), Effect of substrate bias voltage on structural and mechanical properties of pulsed DC magnetron sputtered TiN-MoSx composite coatings, Vacuum, Vol. 84, pp. 843-850.

Gatto, A., Iuliano, L. (1997), Advanced coated ceramic tools for machining superalloys, International Journal of Machine Tools Manufacture, Vol. 37, Issue 5, pp. 591-605.

Gente, A., Hoffmeister, H.W., Evans, C.J. (2001), Chip formation in machining Ti6Al4V at extremely high cutting speeds, CIRP Annals - Manufacturing Technology, Vol. 50, pp.(49–52.

Ginting, A., Nouari, M. (2009), Surface integrity of dry machined titanium alloys, International Journal of Machine Tools Manufacture, Vol. 49, pp. 352–332.

Griffiths, B. J., (1987), Mechanisms of white layer generation with reference to machining and deformation processes, ASME Journal of Tribology, Vol. 109, pp. 523-530.

Grzesik, W. (2000), The influence of thin hard coatings on frictional behaviour in the orthogonal cutting process, Tribology International, Vol. 33, pp. 131–140.

Grzesik, W. (2008), Advanced Machining Process of Metallic Materials: Theory, Modelling and Applications, Oxford, U.K, Elsevier, First edition.

Guerville, L., Vigneau, J. Dudzinski, D., Devillez, A., Moufki, A., Larrouquerre, D., Zerrouki, V., Vigneau (Eds.), J. (2004), Influence of machining conditions on residual

stresses, in: A review of developments towards dry and high speed machining of Inconel 718 alloy, International Journal of Machine Tools Manufacture, Vol. 44, pp. 439–456.

Günaya, M., Aslanb, E., Korkuta, I., Ulvi, (2004), Investigation of the effect of rake angle on main cutting force, International Journal of Machine Tools and Manufacture, Vol. 44, Issue 9, PP. 953–959.

Guo, Y.B., Sahni, J. (2004), A comparative study of hard turned and cylindrically grounded white layers, International Journal of Machine Tools Manufacture, Vol. 44, Issue 2, pp. 135–145.

Guo, Y.B., Schwach, D.W. (2005), An experimental investigation of white layer on rolling contact fatigue using acoustic emission technique, International Journal of Fatigue, Vol. 27, Issue 9, pp. 1051–1061.

Guo, Y.B., Li, W., Jawahir, I.S. (2009), Surface integrity characterization and prediction in machining of hardened and difficult-to-machine alloys; a state-of-the-art research review and analysis, Machining Science and Technology An International Journal, Vol. 13, pp. 437–470.

Habeeb, H.H., Abou-El-Hossein, K.A., Mohammad, B., Kadirgama, K. (2008), Effect of tool holder geometry and cutting condition when milling nickel-based alloy 242, Journal of Materials Processing Technology, Vol. 201, pp. 483–485.

Habeeb, H.H., Kadirgama, K., Noor, M.M., Rahman, M.M., Mohammad, B., Bakar, R.A., Abouel Hossein, K.A. (2010), Machining of nickel alloy 242 with cubic boron nitride tools, Journal of Applied Science, Vol. 10, pp. 2322-2327.

Hao, Z., Gao, D., Fan, Y., Han, R. (2011), New observations on tool wear mechanism in dry machining Inconel 718, International Journal of Machine Tools & Manufacture, Vol. 51, pp. 973–979.

Hao, Z.P., Lu, Y., Gao, D., Fan, Y.H., Chang, Y.L. (2012), Cutting parameter optimization based on optimal cutting temperature in machining Inconel718, Materials and Manufacturing Processes, Vol. 27, Issue 10, pp. 1084-1089

Hardy, M.C., Herbert, C.R.J., Kwong, J., Li, W., Axinte, D.A., Sharman, A.R.C., Oropesa, E., Withers, P.J. (2014), Characterising the integrity of machined surfaces in a powder nickel alloy used in aircraft engines, Procedia CIRP, Vol. 13, pp. 411 – 416.

Herbert, E.G. (1926), The measurement of cutting temperatures, Proceedings of the Institution of Mechanical Engineers, Part B: Journal of Engineering Manufacture Vol. 1, pp. 289–329.

Herbert, C.R.J., Axinte, D.A., Hardy, M.C., Brown, P.D. (2012b), Investigation into the characteristics of white layers produced in a nickel-based super alloy from drilling operations, Machining Science and Technology An International Journal, Vol. 16, Issue 4, pp. 40-52.

Herbert, C.R.J., Kwong, J., Kong, M.C., Axinte, D.A., Hardy, M.C., Withers, P.J. (2012a), An evaluation of the evolution of workpiece surface integrity in hole making operations for a nickel-based super alloy, Journal of Materials Processing Technology, Vol. 212, pp. 1723– 1730.

Herbert, C., Axinte, D. A., Hardy, M., Withers, P. (2014), Influence of surface anomalies following hole making operations on the fatigue performance for a nickel-based superalloy, Journal of Manufacturing Science and Engineering - ASME, Vol. 136, pp. 051016-1.

Hood, R., Soo, S. L., Aspinwall, D. K., Andrews, P., Sage, C. (2012), Radius end milling of Haynes 282 nickel based superalloy, Proceedings of the Institution of Mechanical Engineers, Part B: Journal of Engineering Manufacture, Vol. 226, Issue 10, pp. 1745–1753.

Hou, Z. B., Komanduri, R. (1997), Modeling of thermo mechanical shear instability in machining, International Journal of Mechanical Science, Vol. 39, Issue 11, pp. 1273-1314.

Huang, L., Chen, J.C., Chang, T. (1999), Effect of tool/chip contact length on orthogonal turning performance, Journal of Industrial Technology, Vol. 15, Issue 2, pp. 1-5.

Imran, M., Mativenga, P.T., Gholinia, A., Withers, P.J. (2011), Evaluation of surface integrity in micro drilling process for nickel-based super alloy, International Journal of Advanced Manufacturing Technology, Vol. 55, Issues 5-8, pp. 465-476.

Imran, M., Mativenga, P.T., Kannan, S. (2012), Evaluation of the effects of tool geometry on tool wear and surface integrity in the micro drilling process for Inconel 718 alloy, International Journal of Machining and Machinability of Materials, Vol. 11, pp. 3.

Imran, M., Mativenga, P.T., Gholinia, A., Withers, P.J. (2014), Comparison of tool wear mechanisms and surface integrity for dry and wet micro-drilling of nickel-base superalloys, International Journal of Machine Tools Manufacture, Vol. 76, pp. 49-60.

Imran, M., Mativenga, P.T., Gholinia, A., Withers, P.J. (2015), Assessment of surface integrity of Ni superalloy after electrical-discharge, laser and mechanical micro-drilling processes, International Journal of Advanced Manufacturing Technology, Vol. 79, pp. 1303–1311.

Jacobus, K., Devor, R.E., Kapoor, S.G. (2000), Machining-induced residual stress; experimentation and modelling, Transaction of the ASME, Vol. 122, pp. 20–31.

Jafarian, F., Amirabadi, H., Fattahi, M. (2013), Improving surface integrity in finish machining of Inconel 718 alloy using intelligent systems, International Journal of Advanced Manufacturing Technology, Vol. 71, Issue 5, pp. 817-827.

Jang, D.Y., Watkins, T.R., Kozaczek, K.J., Hubbard, C.R. (1996), Surface residual stress in machined austenitic stainless steel, Wear, Vol. 194, pp.168–173.

Jawahir, I.S., Brinksmeier, E., M'Saoubi, R., Aspinwall, D.K., Outeiro, J.C., Meyer, D., Umbrello, D., Jayal, A.D. (2011), Surface integrity in material removal processes: Recent advances, CIRP Annals - Manufacturing Technology, Vol. 60, pp. 603–626.

Jawaid, A., Koksal, S., Sharif, S. (2000), Wear behavior of PVD and CVD coated carbide tools when face milling Inconel 718, Tribology Transactions, Vol. 43, pp. 325-331.

Jawaid, A., Koksal, S., Sharif, S. (2001), Cutting performance and wear characteristics of PVD coated and uncoated carbide tools in face milling Inconel 718 aerospace alloy, Journal of Materials Processing Technology, Vol. 116, pp. 2–9.

Jianxin, D., Xing, A. (1994a), Development of a new ceramic tool Al2O3/TiB2 and study on its wear resistance, Advanced Ceramic, Vol. 15, Issue 2, pp. 8–14.

Jianxin, D., Xing, A. (1994b), Study on the cutting performance of Al2O3/TiB2 ceramic cutting tools, Cemented Carbide, Vol. 11, Issue 4, pp. 222–226.

Jianxin, D., Xing, A. (1996), Effect of whisker orientation on the friction and wear behaviour of $Al_2O_3/TiB_2/SiC_w$ composite in sliding wear tests and in cutting process, Wear, Vol. 201, pp. 178–185.

Jianxin, D., Xing, A. (1997), Wear behavior and mechanisms of alumina-based ceramic tools in machining of ferrous and nonferrous alloys, Tribology International, Vol. 30, Issue 11, pp. 807–813.

Jianxin, D., Lili, L., Jianhua, L., Jinlong, Z., Xuefeng, Y. (2005), Failure mechanisms of TiB_2 particle and SiC whisker reinforced Al_2O_3 ceramic cutting tools when machining nickel-based alloys, International Journal of Machine Tools & Manufacture, Vol. 45, pp. 1393–1401.

Jin, D., Liu, Z., Yi, W., Su, G. (2011), Influence of cutting speed on surface integrity for powder metallurgy nickel-based superalloy FGH95, International Journal of Advanced Manufacturing Technology, Vol. 56, pp. 553–559.

Jin, D., Liu, Z. (2012), Effect of cutting speed on surface integrity and chip morphology in high-speed machining of PM nickel-based super alloy FGH95, International Journal of Advanced Manufacturing Technology, Vol. 60, pp. 893–899.

Jin, D., Liu, Z. (2013), Damage of the machined surface and subsurface in orthogonal milling of FGH95 superalloy, International Journal of Advanced Manufacturing Technology, Vol. 68, pp. 1573–1581.

Jin, D., Shaoyu, L. (2014), Deformation-phase transformation coupling mechanism of white layer formation in high speed machining of FGH95 Ni-based superalloys, Applied Surface Science, Vol. 292, pp. 197-203.

Joshi, R.S., Srivastava, S., Singh, H. (2014), Microstructural analysis of nanostructured aluminum alloy strips created from machining based deformation process, Procedia CIRP, Vol. 14, pp. 130–135.

Joshi, S., Tewari, A., Joshi, S. (2013), Influence of preheating on chip segmentation and microstructure in orthogonal machining of Ti6Al4V, Journal of Manufacturing Science and Engineering – ASME, Vol. 135, pp. 061017-1.

Jun, Z., Jianxin, D., Jianhua, Z., Xing, A. (1997), Failure mechanisms of a whisker-reinforced ceramic tool when, machining nickel-based alloys, Wear, Vol. 208, pp. 220–225.

Kadirgama, K., Abou-El-Hossein, K.A., Noor, M.M., Sharma, K.V., Mohammad, B. (2011), Tool life and wear mechanism when machining Hastelloy C-22HS, Wear, Vol. 270, Issue 3–4, pp. 258–268.

Kamata, Y., Obikawa, T. (2007), High speed MQL finish-turning of Inconel 718 with different coated tools, Journal of Materials Processing Technology, Vol. 192, pp. 281-286.

Kaynak, Y. (2014), Evaluation of machining performance in cryogenic machining of Inconel 718 and comparison with dry and MQL machining, International Journal of Advanced Manufacturing Technology, Vol. 72, pp. 919–933.

Khan, S.A., Soo, S.L., Aspinwall, D.K., Sage, C., Hardend, P., Fleminge, M., White, A., M'Saoubi, R. (2012), Tool wear/life evaluation when finish turning Inconel 718 using PCBN tooling, Procedia CIRP, Vol. 1, pp. 283 – 288.

Khidhir, B.A., Mohamed, B. (2010), Machining of nickel based alloys using different cemented carbide tools, Journal of Engineering Science and Technology, Vol. 5, pp. 264–271.

Kim, S. (1994), Material properties of ceramic cutting tools, Key Engineering Materials, Trans Tech Publications, Switzerland, Vol. 96, pp. 3380.

Kitagawa, T., Kubo, A., Maekawa, K. (1997), Temperature and wear of cutting tools in high-speed machining of Inconel 718 and Ti–6Al–6V–2Sn, Wear, Vol. 202, pp. 142–148.

Klocke, F., Vogtel, P., Gierlings, S., Lung, D., Veselovac, D. (2013), Broaching of Inconel 718 with cemented carbide, Production Engineering, Vol. 7, pp. 593-600.

Komanduri, R., von Turkovich, B. F. (1981), New observations on the mechanism of chip formation when machining titanium alloys, Wear, Vol. 69, pp. 179–188.

Komanduri, R., Schroeder, T., Hazra, J., von Turkovich, B. F., and Flom, D. G. (1982), On the catastrophic shear instability in high-speed machining of an AISI 4340 Steel, Journal of Engineering for Industry, Vol. 104, pp. 121–131.

Komanduri, R., Schroeder, T. A. (1986), On shear instability in machining a nickel-iron base superalloy, Journal of Engineering for Industry, Vol. 108, pp. 93.

Kortabarria, A., Madariaga, A., Fernandez, E., Esnaola, J.A., Arrazola, P.J. (2011), A comparative study of residual stress profiles on Inconel 718 induced by dry face turning, Procedia Engineering, Vol. 19, pp. 228–234.

Kwong, J., Axinte, D.A., Withers, P.J., Hardy, M.C. (2009a), Minor cutting edge–workpiece interactions in drilling of an advanced nickel-based superalloy, International Journal of Machine Tools Manufacture, Vol. 49, pp. 645–658.

Kwong, J., Axinte, D.A., Withers, P.J. (2009b), The sensitivity of Ni-based superalloy to hole making operations: Influence of process parameters on subsurface damage and residual stress, Journal of Materials Processing Technology, Vol. 209, pp. 3968–3977.

Lee, M., Horne, J.G., Tabor, D. (1979), The mechanism of notch formation at the depth of cut line of ceramic tools machining nickel base superalloys, Electric Power Research Institute (Report) EPRI EL, pp. 460-469.

Li, L., He, N., Wang, M., Wang, Z.W. (2002), High speed cutting of Inconel 718 with coated carbide and ceramic inserts, Journal of Materials Processing Technology, Vol. 129, pp. 127–130.

Li, H.Z., Zeng, H., Chen, X.Q. (2006a), An experimental study of tool wear and cutting force variation in the end milling of Inconel 718 with coated carbide inserts, Journal of Materials Processing Technology, Vol. 180, pp. 296–304.

Li, W., Preuss, M., Withers, P. J., Axinte, D., Andrews, P. (2006b), Characterisation of residual stresses in machined surfaces of a high strength nickel-base superalloy, Materials Science Forum, Vol. 587, pp. 524-525.

Li, W., Withers, P. J., Axinte, D., Preuss, M. Andrews, P. (2009), Residual stresses in face finish turning of high strength nickel-based superalloy, Journal of Materials Processing Technology, Vol. 209, Issue 10, pp. 4896-4902.

Li, W., Guo, Y.B., Barkey, M.E., Jordon, J.B. (2014), Effect tool wear during end milling on the surface integrity and fatigue life of Inconel 718, Procedia CIRP, Vol. 14, pp. 546 – 551.

Liao, Y.S., Shiue, R.H. (1996), Carbide tool wear mechanism in turning of Inconel 718 superalloy, Wear, Vol. 193, pp. 16-24.

Liao, Y.S., Linb, H.M., Wanga, J.H. (2008), Behaviors of end milling Inconel 718 superalloy by cemented carbide tools, Journal of Materials Processing Technology, Vol. 201, pp. 460–465.

Liu, Y., Zhang, Y. (2014), Research on the wear mechanism of ceramic tool in turning of nickel-based superalloy GH4169, International Journal of Control and Automation, Vol. 7, Issue 12, pp. 407-414.

Lorentzon, J., Jarvstrat, N., Josefson, B.L. (2009), Modelling chip formation of alloy 718, Journal of Materials Processing Technology, Vol. 209, Issue 10, pp. 4645-4653.

M'Saoubi, R., Chandrasekaran, H. (2004), Investigation of the effects of tool micro-geometry and coating on tool temperature during orthogonal turning of quenched and tempered steel, International Journal of Machine Tools & Manufacture, Vol. 44, pp. 213–224.

M’Saoubi, R., Outeiro, J.C., Chandrasekaran, H., DillonJr, O.W., Jawahir, I.S. (2008), A Review of surface integrity in machining and its impact on functional performance and life of machined products, International Journal of Sustainable Manufacturing, Vol. 1–2, pp. 203–236.

M'Saoubi, R., Larsson, T., Outeiro, J., Guo, Y., Suslov, S., Saldana, C., Chandrasekar, S. (2012), Surface integrity analysis of machined Inconel 718 over multiple length scales, CIRP Annals - Manufacturing Technology, Vol. 61, Issue 1, pp. 99-102.

M’Saoubi, R., Axinte, D., Herbert, C., Hardy, M., Salmon, P. (2014), Surface integrity of nickel-based alloys subjected to severe plastic deformation by abusive drilling, CIRP Annals - Manufacturing Technology, Vol. 63, pp. 61–64.

M’Saoubi, R., Axinte, D., Soo, S. L., Nobel, C., Attia, H., Kappmeyer, G., Engin, S., Sim, W. M. (2015), High performance cutting of advanced aerospace alloys and composite materials, CIRP Annals - Manufacturing Technology, Vol. 64, Issue 2, pp. 557–580.

Machado, A. R., Wallbank, J. (1994), The effect of high-pressure jet on machining, Proceedings of the Institution of Mechanical Engineers, Part B: Journal of Engineering Manufacture, Vol. 208, pp. 29-38.

Machado, A. R., Wallbank, J., Pashby, I. R., Ezugwu, E. O. (1998), Tool performance and chip control when machining Ti6A14V and Inconel 901 using high pressure coolant supply, Machining Science and Technology, Vol. 2, Issue 1, pp.1-12

Madariaga, A., Esnaola, J. A., Fernandez, E., Arrazola, P. J., Garay, A., Morel, F. (2014), Analysis of residual stress and work-hardened profiles on Inconel 718 when face turning with large-nose radius tools, International Journal of Advanced Manufacturing Technology, Vol. 71, pp. 1587–1598.

Marinescu, I., Axinte, D.A. (2008), A critical analysis of effectiveness of acoustic emission signals to detect tool and workpiece malfunctions in milling operations, International Journal of Machine Tools Manufacture, Vol. 48, pp. 1148–1160.

Marinescu, I., Axinte, D.A. (2009), A time–frequency acoustic emission-based monitoring technique to identify workpiece surface malfunctions in milling with multiple teeth cutting simultaneously, International Journal of Machine Tools Manufacture, Vol. 49, pp. 53–65.

Marinescu, I., Axinte, D., Herbert, C., McGourlay, J., Withers, P.J. (2011), Assessment of thread-cutting strategies to enable damage-tolerant surfaces on an advanced Ni-based aerospace superalloy, Proceedings of the Institution of Mechanical Engineers, Part B: Journal of Engineering Manufacture, Vol. 225, Issue 1, pp. 12-24.

Mondelin, A., Valiorgue, F., Rech, J., Coret, M., Feulvarch, E. (2013), Modeling of surface dynamic recrystallisation during the finish turning of the 15-5PH Steel, Procedia CIRP, Vol. 8, pp. 310-314.

Motorcu, A. R., Kus, A., Durgun, I. (2014), The evaluation of the effects of control factors on surface roughness in the drilling of Waspaloy superalloy, Measurement, Vol. 58, pp. 394–408.

Muthu, E., Senthamarai, K., Jayabal, S. (2012), Finite element simulation in machining of Inconel 718 nickel based super alloy, International journal of advanced engineering application, Vol. 5, Issue 3, pp. 22-27.

Nalbant, M., Altm, A., Gokkaya, H. (2007), The effect of cutting speed and cutting tool geometry on machinability properties of nickel-base Inconel 718 super alloys, Materials & Design, Vol. 28, pp. 1334–1338.

Narasimhan, K., Russell, W.C. (2001), Multilayer CVD coated article and process for producing same, US Patent 20010016273 A1.

Narutaki, N., Yamane, Y. (1993), High speed machining of Inconel 718 with ceramic tools, Annals of CIRP, Vol. 42, pp. 103–106.

Ning, L, Veldhuis, S. C., Yamamoto, K. (2008), Investigation of wear behavior and chip formation for cutting tools with nano-multilayered TiAlCrN/NbN PVD coating, International Journal of Machine Tools & Manufacture, Vol. 48, Issue 6, pp. 656-665.

Noor, M.M., Kadirgama, K., Habeeb, H.H., Rahman, M.M., Mohammad, B. (2010), Performance of carbide cutting tools when machining of nickel based alloy, International Journal of Material Forming, Vol. 3, pp. 475– 478.

Noordin, M. Y. (2004), Performance evaluation of coated carbide and coated cermet tools when turning hardened tool steel, Ph.D. dissertation, Department of Mechanical Engineering, Universiti Teknologi Malaysia.

Novak, W., Shin, Y. C., lncropera, F. P. (1997), Assessment of plasma enhanced machining for improved machinability of Inconel 718, Journal of Manufacturing Science and Engineering, Vol. 1, pp. 125-129.

Novovic, D., Dewes, R.C., Aspinwall, D.K., Voice, W.E., Bowen, P. (2004), The effect of machined topography and integrity on fatigue life, International Journal of Machine Tools Manufacture, Vol. 44, Issues 2–3, pp. 125–134.

Obikawa, T., Kamata, Y., Asano, Y., Nakayama, K., Otieno, A.W. (2008), Micro-liter lubrication machining of Inconel 718, International Journal of Machine Tools & Manufacture, Vol. 48, pp. 1605–1612.

Obikawa, T., Yamaguchi, M., Funai, K., Kamata, Y., Yamada, S. (2012), Air jet assisted machining of nickel-base super alloy, International Journal of Machine Tools Manufacture, Vol. 61, pp. 20–26.

Obikawa, T., Yamaguchi, M. (2015), Suppression of notch wear of a whisker reinforced ceramic tool in air-jet-assisted high-speed machining of Inconel 718, Precision Engineering, Vol. 39, pp. 143–151.

Öjmertz, K., Oskarson, H.B. (1999), Wear on SiC-whiskers reinforced ceramic inserts when cutting Inconel with waterjet assistance, Tribology Transactions, Vol. 42, Issue 3, pp. 471–478.

Ojolo, S.J., Awe, O. (2011), Investigation into the effect of tool-chip contact length on cutting stability, Journal of Emerging Trends in Engineering and Applied Sciences, Vol. 2 Issue 4, pp. 626-630.

Olovsjö, S., Wretland, A., Sjöberg, G. (2010a), The effect of grain size and hardness of wrought Alloy 718 on the wear of cemented carbide tools, Wear, Vol. 268, Issues 9–10, pp. 1045–1052.

Olovsjö, S., Wretland, A., Sjöberg, G. (2010b), The effect of grain size and hardness of waspaloy on the wear of cemented carbide tools, The International Journal of Advanced Manufacturing Technology, Vol. 50, Issues 9-12, pp. 907-915.

Olovsjö, S., Nyborg, L. (2012), Influence of microstructure on wear behaviour of uncoated WC tools in turning of Alloy 718 and Waspaloy, Wear, Vol. 282–283, pp. 12–21.

Outeiro, J. C., Pina, J.C., M'Saoubi, R., Pusavec, F., Jawahir, I.S. (2008), Analysis of residual stresses induced by dry turning of difficult-to-machine materials, CIRP Annals - Manufacturing Technology, Vol. 57, pp. 77–80.

Pan, Y.M., Dunn, D.S., Cragnolino, G.A., Sridhar, N. (2000), Grain-boundary chemistry and intergranular corrosion in alloy 825, Metallurgical and Materials Transactions A, Vol. 31, pp 1163.

Patwari, M. A. U., Amin, A. N., Faris, W. F. (2011), Influence of chip serration frequency on chatter formation during end milling of Ti6Al4V, Journal of Manufacturing Science and Engineering: ASME, Vol. 133, Issue 1, pp. 011-013.

Pawade, R.S., Joshi, S.S., Brahmankar, P.K., Rahman, M. (2007), An investigation of cutting forces and surface damage in high-speed turning of Inconel 718, Journal of Materials Processing Technology, Vol. 192, pp. 139-146.

Pawade, R.S., Joshi, S.S., Brahmankar, P.K. (2008), Effect of machining parameters and cutting edge geometry on surface integrity of high-speed turned Inconel 718, International Journal of Machine Tools Manufacture, Vol. 48, pp. 15–28.

Pawade, R.S., Joshi, S.S. (2011), Mechanism of chip formation in high-speed turning of Inconel 718, Machining Science and Technology An International Journal, Vol. 15, pp. 132–152.

Pawade, R.S., Joshi, S. S. (2012), Analysis of acoustic emission signals and surface integrity in the high-speed turning of Inconel 718, Proceedings of the Institution of Mechanical Engineers, Part B: Journal of Engineering Manufacture, Vol. 226, Issue 1, pp. 3-27.

Peng, H.Z., Lu, Y., Gao, D., Fan, Y.H., Chang, Y.L. (2012), Cutting parameter optimization based on optimal cutting temperature in machining Inconel 718, Materials and Manufacturing Processes, Vol. 27, Issue 10, pp. 1084-1089.

Peng, R. L., Zhou, J., Johansson, S., Billenius, A., Bushlya, V., Stahl, J. E. (2013a), Surface integrity and the influence of tool wear in high speed machining of Inconel 718, 13th International Conference on Fracture June 16–21, Beijing, China.

Peng, R. L., Zhou, J.M., Johansson, S., Billenius, A., Bushlya, V., Stahl, J.E. (2013b), Influence of dry cut and tool wear on residual stresses in high speed machining of nickel-based superalloy, Materials Science Forum, Vols. 768-769, pp. 470-477.

Pervaiz, S., Rashid, A., Deiab, I., Nicolescu, M. (2014), Influence of tool materials on machinability of Titanium- and Nickel-Based Alloys: A Review, Materials and Manufacturing Processes, Vol. 29, Issue 3, pp. 219-252.

Podder, B., Paul, S. (2008), Effect of machining environment on machinability of Nimonic 263 during end milling with uncoated carbide tool, International Journal of Machining and Machinability of Materials, Vol. 3, Issue 1, pp.104-119.

Podder, B., Paul, S. (2012), Improvement of machinability in end milling of Nimonic C–263 by application of high pressure coolant, International Journal of Machining and Machinability of Materials, Vol. 11, Issue 4, pp. 418-433.

Popa, A., Dutilh, V., Baili, M., Dessein, G., Perrin, G. (2010), Identification of influent factors on surface integrity in nickel-based superalloy drilling, Journal of Production Manufacturing Systems, Vol. 5, Issue 4, pp. 231-236.

Prabhu, S., Vinayagam, B.K. (2011), AFM surface investigation of Inconel 825 with multi wall carbon nano tube in electrical discharge machining process using Taguchi analysis, Archives of Civil and Mechanical Engineering, Vol. 6, Issue 1, pp. 149–170.

Pusavec, F., Hamdi, H., Kopac, J., Jawahir, I.S. (2011), Surface integrity in cryogenic machining of nickel-based alloy Inconel 718, Journal of Materials Processing Technology, Vol. 211, pp. 773–783.

Radwan, A. A. (1985), Investigation of secondary deformation zone and mean coefficient of friction during the machining of 5083-H34 aluminum alloy, Wear, Vol. 101, pp. 191–204.

Rahim, E. A., Sasahara, H. (2011), An analysis of surface integrity when drilling Inconel 718 using palm oil and synthetic ester under MQL condition, Machining Science and Technology An International Journal, Vol. 15, Issue 1, pp. 76-90.

Rahman, M., Seah, W.K.H., Teo, T.T. (1997), The machinability of Inconel 718, Journal of Materials Processing Technology, Vol. 63, pp. 199–204.

Rai, S. K., Kumar, A., Shankar, V., Jayakumar, T., Rao, K. B.S., Raj, B. (2004), Characterization of microstructures in Inconel 625 using X-ray diffraction peak broadening and lattice parameter measurements, Scripta Materialia, Vol. 51, pp. 59–63.

Ranganath, S. Guo, C., Hegde, P. (2009), A finite element modeling approach to predicting white layer formation in nickel superalloys, CIRP Annals - Manufacturing Technology, Vol. 58, pp. 77–80.

Raymond, E.L. (1968), Mechanisms of sensitization and stabilization of incoloy nickel-iron-chromium alloy 825, Tradenames of international nickel Co, Vol. 24, Issue 6, pp. 180-188.

Razak, N.H., Rahman, M. M., Kadirgama, K. (2012), Response surface design model to predict surface roughness when machining Hastelloy C-2000 using uncoated carbide insert, IOP Conference Series Material Science Engineering, Vol. 36, pp. 012-022.

Razak, N. H., Rahman, M. M., Kadirgama, K. (2014), Experimental study on surface integrity in end milling of Hastelloy C-2000 superalloy, Journal of Automotive and Mechanical Engineering, Vol. 9, pp. 1578-1587.

Richards, N., Aspinwall, D. (1989), Use of cceramic tools for machining nickel-based alloys, International Journal of Machine Tools and Manufacture, Vol. 29, Issue 4, 575-588.

Sadat, A.B. (1987), Surface region damage of machined Inconel 718 nickel base superalloy using natural and controlled contact length tools, Wear, Vol. 119, pp. 225–235.

Sadat, A.B., Reddy, M.Y., Wang, B.P. (1991), Plastic deformation analysis in machining of Inconel 718 nickel base superalloy using both experimental and numerical methods, International Journal of Mechanical Science, Vol. 33, Issue 10, pp. 829–842.

Sadik, M.I., LindstrSm, B. (1993), The role of tool-chip contact length in metal cutting, Journal of Materials Processing Technology, Vol. 37, pp. 613-627.

Samani, M.K., Ding, X.Z., Khosravian, N., Amin-Ahmadi, B., Yang, Y., Chene, G., Neyts, E.C., Bogaerts, A., Tay, B.K. (2015), Thermal conductivity of titanium nitride/titanium aluminum nitride multilayer coatings deposited by lateral rotating cathode arc, Thin Solid Films, Vol. 578, pp. 133–138.

Samuel, L., Truesdale, Shin, Y.C. (2009), Microstructural analysis and machinability improvement of udimet 720 via cryogenic milling, Machining Science and Technology: An International Journal, Vol. 13, Issue 1, pp. 1-19.

Schlauer, C., Peng, R.L., Oden, M. (2002), Residual stresses in a nickel-based superalloy introduced by turning, Materials Science Forum, Vols. 404–407, pp. 173–178.

Schlauer, C., Oden, M. (2005), Residual stress evolution and near surface microstructure after turning of the nickel-based superalloy Inconel 718, Zeitschrift für Metallkunde, Vol. 96, Issue 4, pp. 385-392.

Schwach, D.W., Guo, Y.B. (2006), A fundamental study on the impact of surface integrity by hard turning on rolling contact fatigue, International Journal of Fatigue, Vol. 28, Issue 12, pp. 1838-1844.

Settineria, L., Fagab, M.G., Lerga, B. (2008), Properties and performances of innovative coated tools for turning Inconel 718, International Journal of Machine Tools & Manufacture, Vol. 48, pp. 815–823.

Sharman, A., Dewes, R.C., Aspinwall, K.D. (2001), Tool life when high speed ball nose end milling Inconel 718, Journal of Materials Processing Technology, Vol.118, pp. 29–35

Sharman, A. R. C., Hughes, J. I., Ridgway, K. (2004a), Workpiece surface integrity and tool life issues when turning Inconel 718™ nickel based superalloy, Machining Science and Technology An International Journal, Vol. 8, pp. 399–414.

Sharman, A. R. C., Hughes, J. I., Ridgway, K. (2004b), An analysis of the residual stresses generated in Inconel 718 when turning, Journal of Materials Processing Technology, Vol. 173, pp. 359–367.

Sharman, A.R.C, Amarashighe, A., Ridgway, K. (2008a), Tool life and surface integrity aspects when drilling and hole making in Inconel 718, Journal of Materials Processing Technology, Vol. 200, Issue 1, pp. 424–432.

Sharman, A. R. C., Hughes, J. I., Ridgway, K. (2008b), Surface integrity and tool life when turning Inconel 718 using ultra-high pressure and flood coolant systems, The Institution of Mechanical Engineers-Journal of Engineering Manufacture, Vol. 222, Issue 6, pp. 653-664.

Sharman, A. R. C., Hughes, J. I., Ridgway, K. (2015), The effect of tool nose radius on surface integrity and residual stresses when turning Inconel 718TM, Journal of Materials Processing Technology, Vol. 216, pp. 123–132.

Shaw, M.C. (1984), Metal Cutting Principles, Oxford University Press, London, ISBN 0-19-859002-4, pp. 594.

Shi, D., Axinte, D.A., Gindy, N.N. (2007), Development of an online machining process monitoring system: a case study of the broaching process, International Journal of Advanced Manufacturing Technology, Vol. 34, pp. 34–46.

Shiva, M.B.D., Wallbank, J. (1999), Cutting temperature: prediction and measurement methods—a review, Journal of Materials Processing Technology, Vol. 88, pp.195–202.

Shokrani, Dhokia, V., Newman, S.T., Imani-Asrai, R. (2012), An initial study of the effect of using liquid nitrogen coolant on the surface roughness of Inconel 718 nickel-based alloy in CNC milling, Procedia CIRP, Vol. 3, pp. 121–125.

Song, X.Y., Zhao, J. (2008), Wear mechanism of tools when cutting Inconel 718, Tool Technology Vol. 42, pp. 9–12.

Soo, S.L., Hood, R., Aspinwall, D.K., Voice, W.E., Sage, C. (2011), Machinability and surface integrity of RR1000 nickel-based super alloy, CIRP Annals-Manufacturing Technology, Vol. 60, Issue 1, pp. 89-92.

Sun, J., Guo, Y. B. (2009), A comprehensive experimental study on surface integrity by end milling Ti–6Al–4V, Journal of Materials Processing Technology, Vol. 29, pp. 4036–4042.

Thakur, A., Gangopadhyay, S., Maity, K.P. (2014a), Effect of cutting speed and CVD multilayer coating on machinability of Inconel 825, Surface Engineering, Vol. 30, pp. 516-523.

Thakur, A., Mohanty, A., Gangopadhyay, S. (2014b), Comparative study of surface integrity aspects of Incoloy 825 during machining with uncoated and CVD multilayer coated inserts, Applied Surface Science, Vol. 320, pp. 829–837.

Thakur, A., Gangopadhyay, S., Maity, K.P. (2014c), Effect of cutting speed and tool coating on machined surface integrity of Ni-based super alloy, 6th CIRP Conference on High Performance Cutting, HPC 2014 to be held at UC, Berkeley, Published in Procedia CIRP, Vol.14, pp. 541-545.

Thakur, A, Gangopadhyay, S, Mohanty, A. (2015a), Investigation on some machinability aspects of Inconel 825 during dry turning, Materials and Manufacturing Processes, Vol. 30, Issue 8, pp. 1026-1034.

Thakur, A, Gangopadhyay, S, Maity, K.P., Sahoo, S.K. (2015b), Evaluation on Effectiveness of CVD and PVD Coated Tools during Dry Machining of Incoloy 825, Tribology Transactions, *Accepted*.

Thakur, A, Gangopadhyay, S, Mohanty, A., Maity, K.P. (2015c), Experimental assessment on performance of TiN/TiCN/Al2O3/ZrCN coated tool during dry machining of Nimonic C-263, International Journal of Machining and Machinability of Materials, *Accepted*.

Thakur, A., Gangopadhyay, S. (2016), State-of-the-art in surface integrity in machining of nickel-based super alloys, International Journal of Machine Tools Manufacture, Vol. 100, pp 25–54.

Thakur, D.G., Ramamoorthy, B., Vijayaraghavan, L. (2009a), Study on the machinability characteristics of superalloy Inconel 718 during high speed turning, Materials & Design, Vol. 30, pp. 1718–1725.

Thakur, D. G., Ramamoorthy, B., Vijayaraghavan, L. (2009b), A Study on the parameters in high-speed turning of superalloy Inconel 718, Materials and Manufacturing Process, Vol. 24, pp. 497-503.

Thakur, D.G., Ramamoorthy, B. Vijayaraghavan, L. (2009c), Machinability investigation of Inconel 718 in high-speed turning, International Journal of Advanced Manufacturing Technology, Vol. 45, pp. 421–429.

Thakur, D.G., Ramamoorthy, B., Vijayaraghavan, L. (2010), Investigation and optimization of lubrication parameters in high speed turning of superalloy Inconel 718, International Journal of Advanced Manufacturing Technology, Vol. 50, pp. 471–478.

Thakur, D. G., Ramamoorthy, B., Vijayaraghavan, L. (2012a), Some investigations on high speed dry machining of aerospace material Inconel 718 using multicoated carbide inserts, Materials and Manufacturing Processes, Vol. 27, Issues 10, pp. 1066-1072.

Thakur, D. G., Ramamoorthy, B., Vijayaraghavan, L. (2012b), Effect of cutting parameters on the degree of work hardening and tool life during high-speed machining of Inconel 718, International Journal of Advanced Manufacturing Technology, Vol. 59, pp. 483–489.

Thamizhmanii, S., Rosli, Hasan, S. (2009), A study of minimum quantity lubrication on Inconel 718 steel, Archives of Materials Science and Engineering, Vol. 39, Issue 1, pp. 38-44.

Ulutan, D., Ozel, T. (2011), Machining induced surface integrity in titanium and nickel alloys: A review, International Journal of Machine Tools Manufacture, Vol. 51, Issue 3, pp. 250-280.

Umbrello, D. (2013), Investigation of surface integrity in dry machining of Inconel 718, International Journal of Advanced Manufacturing Technology, Vol. 69, Issues 9-12, pp. 2183-2190.

Vagnorius, Z., Sørby, K. (2011), Effect of high-pressure cooling on life of SiAlON tools in machining of Inconel 718, International Journal of Advanced Manufacturing Technology, Vol. 54, pp. 83–92.

Velásquez, J.D.P., Bolle, B., Chevrier, P., Geandier, G., Tidu, A. (2007), Metallurgical study on chips obtained by high speed machining of a Ti–6 wt% Al–4 wt% V alloy, Materials Science and Engineering: A, Vol. 452–453, pp. 469–474.

Veldhuis, S.C., Dosbaeva, G.K., Elfizy, A., Fox-Rabinovich, G.S., Wagg, T. (2010), Investigations of white layer formation during machining of powder metallurgical Ni-based ME 16 super alloy, Journal of Materials Engineering and Performance, Vol. 19, pp. 1031–1036.

Vigneau, J., Bordel, P., Léonarda, A., Geslot, R. (1987), Influence of the microstructure of the composite ceramic tools on their performance when machining nickel alloys, Annals of the CIRP, Vo1.36, Issue l, pp. 13-16.

Vincent, D., Andre, P., Gilles, D., Joel, A., Géraldine, P. (2010a), Impact of disturbed drilling conditions on the surface integrity of a Nickel-base superalloy, CIRP ICME'10 - 7th CIRP International Conference on Intelligent Computation In Manufacturing Engineering, 23-25 June, Capri, Italy.

Vincent, D., Andre, P., Gilles, D., Joel, A., Géraldine, P. (2010b), Links between machining parameters and surface integrity in drilling Ni-Superalloy, Advanced Materials Research, Vol. 112, pp. 171-178.

Wan, Z.P., Zhu, Y.E., Liu, H.W., Tang, Y. (2012), Microstructure evolution of adiabatic shear bands and mechanisms of saw-tooth chip formation in machining Ti6Al4V, Materials Science and Engineering: A, Vol. 531, pp. 155– 163.

Wang, C., Xie, Y., Zheng, L., Qin, Z., Tang, D., Song, Y. (2014), Research on the chip formation mechanism during the high-speed milling of hardened steel, International Journal of Machine Tools and Manufacture, Vol. 79, pp. 31–48.

Wardany, T. I. F., Mohammed, L.E., EL-Bestawi, M. A. (1996), Cutting temperature of ceramic tools in high speed machining of difficult-to-cut materials, International Journal of Machine Tools Manufacture, Vol. 36. Issue 5, pp. 611-634.

Wusatowska-Sarnek, A. M., Dubiel, B. , Czyrska-Filemonowicz, A., Bhowal, P. R., Ben Salah, N., Klemberg-Sapieha, J. E. (2011), Microstructural characterization of the white etching layer in nickel-based super alloy, Metallurgical and Materials Transactions A, Vol. 42, Issue 12, pp. 3813-3825.

Xue, C., Chen, W. (2011), Adhering layer formation and its effect on the wear of coated carbide tools during turning of a nickel-based alloy, Wear, Vol. 270, pp. 895–902.

Yazid, M.Z.A., CheHaron, C.H., Ghani, J.A., Ibrahim, G.A., Said, A.Y.M. (2011), Surface integrity of Inconel 718 when finish turning with PVD coated carbide tool under MQL, Procedia Engineering, Vol. 19, pp. 396-401.

Yildiz, Y., Nalbant, M. (2008), A review of cryogenic cooling in machining processes, International Journal of Machine Tools Manufacture, Vol. 48, pp. 947–964.

Zębala, W., Słodki, B. (2013), Cutting data correction in Inconel 718 turning, International Journal of Advanced Manufacturing Technology, Vol. 65, pp. 881–893.

Zhang, S., Li, J., Zhu, X., Lv, H. (2013), Saw-tooth chip formation and its effect on cutting force fluctuation in turning of Inconel 718, International Journal of Precision Engineering and Manufacturing, Vol. 14, Issue 6, pp. 957-963.

Zhang, S.J., Tob, S., Wang, S.J., Zhu, Z.W. (2015), A review of surface roughness generation in ultra-precision machining, International Journal of Machine Tools Manufacture, Vol. 91, pp. 76–95.

Zheng, G., Zhao, J., Gao, Z., Cao, Q. (2012), Cutting performance and wear mechanisms of Sialon–Si_3N_4 graded nano-composite ceramic cutting tools, International Journal of Advanced Manufacturing Technology, Vol. 58, pp.19–28.

Zhou, J. M., Bushlya, V., Avdovic, P., Stahl, J.E. (2012), Study of surface quality in high speed turning of Inconel 718 with uncoated and coated CBN tools, International Journal of Advanced Manufacturing Technology, Vol. 58, Issues 1-4, pp. 141-151.

Zhou, J. M., Bushlya, V., Peng, R. L., Johansson, S., Avdovic, P., Stahl, J. E. (2011), Effects of tool wear on sub surface deformation of nickel-based super alloy, Procedia Engineering, Vol. 19, pp. 407-413.

Zhou, J., Bushlya, V., Peng, R. L., Chen, Z., Johansson, S., Stahl, J. E. (2014), Analysis of subsurface microstructure and residual stresses in machined Inconel 718 with PCBN and Al_2O_3-SiCw tools, Procedia CIRP, Vol. 13, pp. 150 – 155.

Zhu, D., Zhang, X., Ding, H. (2013), Tool wear characteristics in machining of nickel-based superalloys, International Journal of Machine Tools Manufacture, Vol. 64, pp. 60–77.

Zhuang, K., Zhang, X., Zhu, D., Ding, H. (2015), Employing preheating- and cooling-assisted technologies n machining of Inconel 718 with ceramic cutting tools: towards reducing tool wear and improving surface integrity, International Journal of Advanced Manufacturing Technology, Vol. 80, Issue 9, pp. 1815-1822.

Zhuang, K., Zhu, D., Zhang, X., Ding, H. (2014), Notch wear prediction modeling turning of Inconel 718 with ceramic tools considering the influence of work hardened layer, Wear, Vol. 313, pp. 63–74.

Zou, B., Chen, M., Huang, C. (2009), An study on surface damages caused by turning NiCr20TiAl nickel-based alloy, Journal of Materials Processing Technology, Vol. 209, Issue 17, pp. 5802-5809.

Scholastic Achievements:

International journal

1. **Thakur, A.,** Gangopadhyay, S., State-of-the-art in surface integrity in machining of nickel-based super alloys, **International Journal of Machine Tools and Manufacture,** 100 (2016) 25–54.
2. **Thakur, A.,** Gangopadhyay, S., Influence of tribological properties on the performance of uncoated, CVD and PVD coated tools in machining of Incoloy 825, **Tribology International,** 102 (2016) 198–212.
3. **Thakur, A.,** Gangopadhyay, S., Dry machining of nickel-based super alloy as a sustainable alternative using TiN/TiAlN coated tool, **Journal of Cleaner Production,** 129, 2016, 256–268.
4. **Thakur, A.**, Mohanty, A., Gangopadhyay, S., Comparative study of surface integrity aspects of Incoloy 825 during machining with uncoated and CVD multilayer coated inserts, **Applied Surface Science**, 320 (2014) 829–837.
5. **Thakur**, **A.,** Gangopadhyay, S., Maity, K.P., Sahoo, S.K., Evaluation on Effectiveness of CVD and PVD Coated Tools during Dry Machining of Incoloy 825, **Tribology Transactions**, 2015, DOI: 10.1080/10402004.2015.1131350.
6. **Thakur, A.,** Gangopadhyay, S., Maity, K.P., Effect of cutting speed and CVD multilayer coating on the machinability of Inconel 825, **Surface Engineering**, 30 (2014) 516-523.

7. **Thakur, A.**, Gangopadhyay, S., Mohanty, A., Investigation on Some Machinability Aspects of Inconel 825 during Dry Turning, **Materials and Manufacturing Processes,** 30 (2015) 1026–1034.
8. **Thakur, A.,** Gangopadhyay, S., Maity, K.P., Mohanty, A., Experimental assessment on performance of TiN/TiCN/Al_2O_3/ZrCN coated tool during dry machining of Nimonic C-263, **International Journal of Machining and Machinability of Materials**, Accepted, 2015.
9. Koyilada B., Gangopadhyay, S., **Thakur, A.**, Comparative evaluation of machinability characteristics of Nimonic C-263 using CVD and PVD coated tools, **Measurement,** 85 (2016) 152–163.
10. Mohanty, A., Gangopadhyay, S., **Thakur, A.**, On Applicability of Multilayer Coated Tool in Dry Machining of Aerospace Grade Stainless Steel, **Materials and Manufacturing Processes,** 2015**,** DOI: 10.1080/10426914.2015.1070413.
11. Sahoo, S., **Thakur, A.,** Gangopadhyay, S., Application of Analytical Simulation on Various Characteristics of Hole Quality during Micro-Drilling of Printed Circuit Board, **Materials and Manufacturing Processes,** 2015, DOI: 10.1080/10426914.2016.1140189.

International conference

1. **Thakur, A.**, Gangopadhyay, S., Maity, K.P., Effect of cutting speed and tool coating on machined surface integrity of Ni-based super alloy, 6th CIRP Conference on High Performance Cutting, HPC 2014, UC, Berkeley, Published in **Procedia CIRP**, 14(2014) 541-545.
2. **Thakur, A.**, Dewangan, S., Y. Patnaik, Gangopadhyay, S., Prediction of Work Hardening during Machining Inconel 825 using Fuzzy Logic Method, ICAMME-2014, NIT Surathkal Published in **Procedia Materials Science**, 5 (2014) 2046–2053.
3. **Thakur, A.,** Mohanty, A, Gangopadhyay, S., Maity, K.P., Tool wear and chip characteristics during dry turning of Inconel 825, ICAMME-2014, NIT Surathkal Published in **Procedia Materials Science**, 5 (2014) 2169–2177.
4. **Thakur, A.**, Gangopadhyay, S., Maity, K.P., Study on effect of cutting parameters on the machinability of Inconel 825, International Conference on Surface Finishing for Research and Industrial Applications INTERFINISH- SERIA 2013, Rajalakshmi Engineering College, Chennai.pp.48-55.
5. **Thakur, A.**, Gangopadhyay, S., Maity, K.P. Experimental investigations on tool wear and chip characteristics of Inconel 825, International Conference on Smart Technologies for Mechanical Engineering (STME-2013), Delhi Technical University, Delhi, pp. 760-764.
6. **Thakur, A.**, Mohanty, A, Gangopadhyay, S., Maity, K.P., Performance Evaluation of CVD Multilayer Coating on Tool Wear Characteristics during Dry Machining of Nimonic C-263, AIMTDR-2014, IIT Guwahati from 12-14 December, 2014.
7. Azim, S., Gangopadhyay, S., **Thakur, A.**, Evaluation of chip characteristics of Inconel 825 during dry turning with uncoated and CVD multilayer coated tool, COPEN-2015, December 10-12, 2015, IIT Bombay.
8. M. Singh, **A**. **Thakur**, S. Gangopadhyay, Comparative evaluation on Machinability Aspects of Inconel 825 using TiN/TiAlN and Al2O3/TiCN coated tool, COPEN-2015, December 10-12, 2015, IIT Bombay.

Brief bio-data of the author

The author, Aruna Thakur, born on 07-Sept-1984, graduated in Mechanical Engineering from Institute of Engineering and Technology, Kanpur, India in the year 2006. She completed her Post-graduate study (M.Tech) in Mechanical Engineering with specialization in Design and Production Engineering from the GBPUA&T, Pantnagar, India in the year 2009. After completion of M.Tech programme, she joined as an Assistant Professor in the Department of Mechanical Engineering at ITGGU, Bilaspur, India and served for about 1.5 years. She joined CEC, Bilaspur, India, in the year 2011 as an Assistant Professor in the Department of Mechanical Engineering and served for about 1 year. She took admission in the Department of Mechanical Engineering, National Institute of

Technology, Rourkela in the year 2013 as a Research Scholar. The author is engaged in active research in the area of machinability of nickel-based super alloys since 2013. She has 6 research papers to her credit which have been published in various international journals of repute.